Application of EL CID to salient-pole electrical machines

by

Eur Ing George Kenneth Ridley

A thesis submitted in partial fulfilment of the requirements for the degree of

Doctor of Philosophy in Engineering

University of Warwick, School of Engineering

October 2017

Index for Thesis submitted for degree of Doctor of Philosophy

Appendices

Figures for Thesis submitted for degree of Doctor of Philosophy

Figures

Figures for Thesis submitted for degree of Doctor of Philosophy

Figures (Continued)

Figures for Thesis submitted for degree of Doctor of Philosophy

Figures (Continued)

Tables for Thesis submitted for degree of Doctor of Philosophy

Notation

Φ_m	Magnetic flux induced in an annular stator core
V_1	Voltage applied to the EL CID excitation winding
I_o	Excitation (Primary) winding current
E_1	emf induced in the excitation winding
E_2	emf induced in the equivalent secondary winding
I_e	Stator core magnetisation current
I_w	Current component supplying the core iron losses
I_2	Secondary winding current
I_1	Primary winding current
δ	Fault current circulating through adjacent laminations (delta)
I_c	Stator winding circulating current
P_e	Excitation amp: turns per stator slot
I_ℓ	Current equivalent of joint air gap leakage flux
I_R	Current equivalent of leakage flux between the stator and the rotor

<u>**Note**</u> The symbol δ is chosen to represent the fault current, merely on the basis that such current is small compared to other electrical current values. But typographically **"*delta*"** is usually preferred to $\boldsymbol{\delta}$**.**

Acknowledgements

Grateful thanks are expressed to Dr. David R. Bertenshaw for his interest and encouragement. Warm appreciation is also due to Mrs Rodica Zlatanovici, the widow and former close colleague of her husband, Professor Dan Zlatanovici, for permission to include the very positive Book Review by the latter, published in 2008 of the 3rd edition of the candidate's book "EL CID - Application and Analysis". The finite element analyses provided by Dr Tom Preston, and Mr Mike Tarkanyi are also readily acknowledged.

The debt owed to Professor Li Ran is acknowledged for his encouragement of the submission of this thesis, which recognises many years of contribution to Engineering Literature.

Finally, appreciation is thankfully expressed for the recognition by the candidate's mother, Clara Annie Ridley, of his potential for higher education, when none others did.

DECLARATION

No portion of the work referred to in the thesis has been submitted in support of an application for another degree or qualification of this or any other university or other institute of learning.

Abstract

Sutton introduced EL CID in the 1970's. This thesis records the development of EL CID theory, with particular reference to its application to large, salient-pole, water-turbine driven, electrical machines, known as hydrogenerators. Factors are identified and clarified which otherwise may cause misunderstanding of hydrogenerator stator core interlamination insulation condition..

Features discussed, with reference to their impact upon the detected EL CID signal, are alternative forms of excitation winding of the stator core, its constructional features, including core build bars (or key bars), core segmentation, proximity of ferrous components, plus ancillary matters such as the location of brake/jack units, the degree of machine assembly, whether in or out of the operational situation, the extent of the machine enclosure, and the presence of the stator winding and rotor-mounted salient poles.

Although satisfactory application of EL CID to turbogenerators was achieved in the 1970's, anomalies arose when applied to salient-pole machines, due to shorter stator winding end-overhang, its multi-parallel circuits, and also the disincentive of realignment of the rotor if removed, making access to the stator bore and accurate location of the excitation cable more difficult. When present, joints in very large hydrogenerator stator frames and cores, for transportation, made analysis of EL CID results particularly difficult.

The problem presented by core joints arose in the initial factory demonstration of application of EL CID to hydrogenerators. The solution recognises the interdependence of the two orthogonal EL CID signal components, which indicate EL CID as analogous to a transformer, with two short-circuited secondary windings; one for interlamination fault current (designated "***delta***"), the other being the stator winding, when present. In order to draw the phasor diagram with reference to the secondary side of the analogous transformer, the direction of the excitation phasor is reversed, since the fault current is detected in a secondary circuit. Application of standard transformer theory produces an appropriate EL CID phasor diagram, in various forms, depending upon the particular test circumstance. In this context, the significant concept of a line for which interlamination fault current (***delta***) is zero (i.e. a *zero* ***delta*** *line*) was introduced.

The two orthogonal EL CID signals, designated *PHASE* and *QUAD*, are plotted on equal scales; unless related appropriately by a technique described, which takes the difference into account, to ensure the highest accuracy.

Evaluation of delta indicates the effectiveness of core repairs, which supports the usefulness of the EL CID technique when applied to hydrogenerators, as well as turbogenerators. At core joints, the detected maximum fault current ($\boldsymbol{delta_{max}}$) is usually appreciably greater than the traditional acceptance criterion of 100 mA. This is discussed, and the conclusion drawn that the distribution of ***delta*** along the core length provides an adequate indication of any weak region of interlamination insulation.

The practise of routinely resetting the Phase Reference for an EL CID test is examined, and found to be not acceptable, unless the results are subsequently referred back to the basic reference.

As a final demonstration of the EL CID technique usefulness, the analysis of results from a core joint, where there was an imposed artificial fault, identifies the location concerned.

Chapter 1 - Introduction

1.1 The essential need for extending experience of application of EL CID from turbogenerators to hydrogenerators.

EL CID is an acronym for the full name of "Electromagnetic Core Imperfection Detection". The EL CID technique and associated equipment are discussed in this thesis. The full name identifies the purpose of EL CID as detecting circulating current arising from degradation of stator interlamination insulation, resulting in a short-circuit between adjacent laminations. The fault current is induced in a largely resistive electrical circuit comprising the metallic contact between adjacent laminations, the adjacent stator laminations themselves and the build bars (also sometimes called keybars) which short the laminations at their outer periphery. In some cases, there may also be water carrying cooling tubes fitted through the stator core.

This chapter introduces a) the basic EL CID technique[1,p.8], b) the effectiveness when applied to turbogenerators[2,3], and c) anomalies encountered with hydrogenerators[1,p.29et seq]. The analysis for hydrogenerators requires several discrete steps p.82 et seq.. Electromagnetic Testing (EMT) of stator cores, and particularly EL CID[2], is used worldwide, assuming that the test results can be relied upon to predict the thermal risk of stator core faults. But, despite more than 30 years' experience of EL CID with both turbogenerators and hydrogenerators, the test, when applied to the latter, remains relatively little studied in terms of its efficacy and accuracy. Industrial confidence in the technique stems much more from experience than analysis. Bertenshaw[2] researched and quantified a number of sources of error in certain circumstances relating to turbogenerators, so as to improve the reliability of result interpretation. The research is inevitably specific to the EL CID test due to its dominance in the industry. Many results can be read across to alternate EMT techniques with little difficulty. Bertenshaw has communicated privately that these are covered in his doctoral thesis.

Differences between turbogenerators and hydrogenerators [p.38] are identified, e.g. the length to diameter ratio, which results in a long stator winding overhang for the former, compared to the latter. That affects the disposition of the EL CID stator core excitation winding relative to the stator core, with consequences to the EL CID trace [p's 52, 53].

Another practical factor, for some hydrogenerators, is the form of excitation which can be applied. Constraints may arise due to civil work foundations, machine steel support structure and the desirability not to remove the rotor of vertical shaft type hydrogenerators, to avoid interfering with the line-out.

When present, other physical features, which produce falsely high EL CID results, are rotor salient poles [p.59] and stator core annular airgaps [p.47]. This latter feature arises when large diameter machines are factory tested.

The thesis shows that circulating fault current, arising from degraded interlamination insulation, may be identified by regarding the EL CID set-up as analogous to a transformer [p,65 et seq] with two secondary windings. It will be seen that several stator magnetic flux patterns may apply, depending upon the particular features present (Figure 19). For each of these, there is an equivalent electrical circuit diagram (Figure 20), and a corresponding phasor diagram, replacing the very simple phasor diagram[1,p.11] applicable to turbogenerators.

The complexity, of the magnetic field at core joints, is recognised by identifying that a single criterion, for the fault circulating current (**delta**), is not always sufficient. It is found that the relative distribution of **delta,** along the length of the core, can be more applicable p.[99]. This depends upon the basic assumption that the **delta** value will not be unacceptable throughout the core length.

This general research area is offered as a significant contribution to the maintenance of large power generation utilities, which is of the utmost importance for modern society, both industrially and socially. The unexpected loss of such facilities causes major distress domestically, and places high risk upon many industrial processes. Therefore, the importance of resolving anomalous EL CID results, and their interpretation is identified.

1.2 – EL CID basic theory

The basic theory of EL CID, illustrated by Figure 1, is well-known[3] and understood, but for completeness a summary is provided.

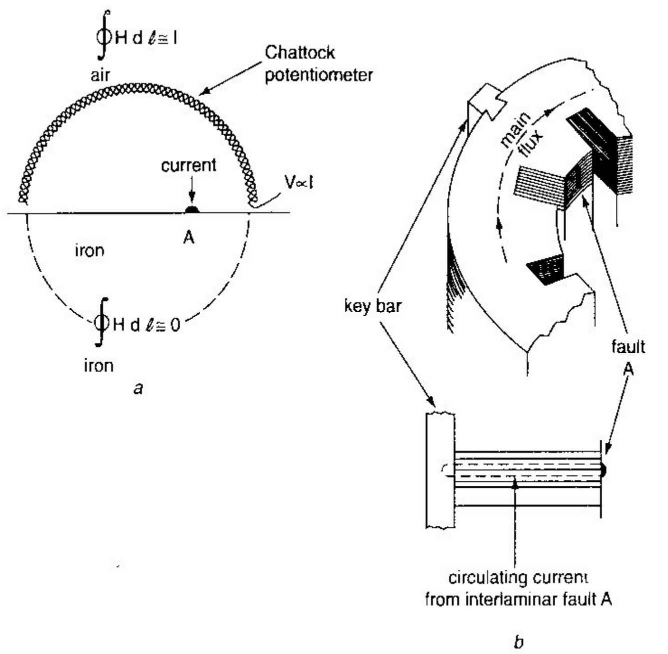

Figure 1 **Basic EL CID principles**

AC excitation of an annular stator core produces a pulsating circumferential magnetic flux to link with a largely resistive electrical circuit as identified in Section 1.1. above. This induces circulating current. The resultant magnetic field at the stator bore (core inner periphery) is detected (Figure 2) by a Chattock Potentiometer[4] (or Rowgowski coil[5]). The mathematical justification of this proposition was established by Sutton[6], the inventor of EL CID, basically by a simple application of Ampére's Law. Sutton also discusses further ramifications, which are not of concern here.

The **purpose of this present thesis is to justify its application to large salient-pole rotating electrical machines,** not to defend the basic concept of EL CID, which is already well established and well tried[7]. Briefly, therefore, the output from the EL CID sensor, whether called a Chattock Potentiometer or a Rowgowski coil, is connected to an electronic package, called a Signal Processor Unit (SPU)[3].

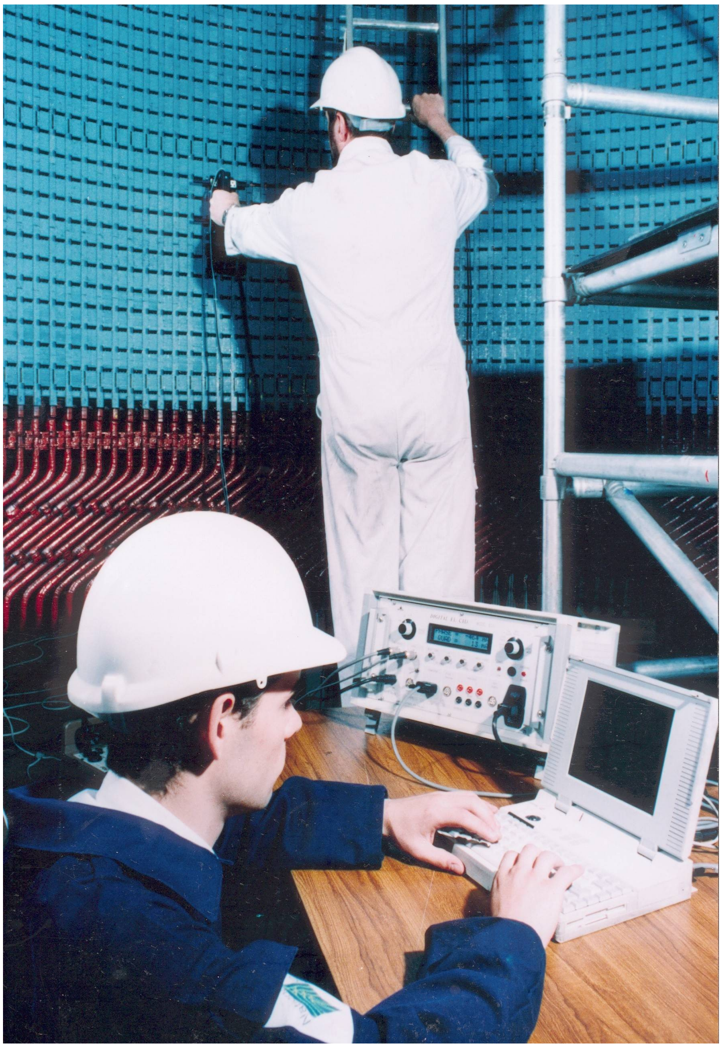

<u>Figure 2</u> EL CID test on a hydrogenerator

The SPU incorporates an electronic phase sensitive detector to produce two orthogonal current components. The one in phase with a reference signal (now provided from the excitation current) is called PHASE, the other is named QUAD. Further details on the electronic operation of EL CID may be found in Reference 2, Ch: 3, p. 52 et seq. In particular, on page 63 of that Reference, an EL CID functional block diagram, Figure 3.11 is provided. The PHASE and QUAD components are fed to a computer (see Figure 2), which produces a graphical display, which is immediately viewed on the computer screen, and is then normally also printed. Originally, the SPU output was recorded by a graphical printer on paper. The modern SPU, based on digital technology, produces a simultaneous output of both PHASE and QUAD values. For methods of applying excitation, see Figure 5 (p. 40) below.

When EL CID was applied to turbogenerators, the phasor diagram adopted consisted simply of the PHASE signal and, orthogonal to it, the QUAD signal, as reproduced, both by the candidate[1,p.11,Fig:5] and by Bertenshaw[2,p.57,Fig: 3.5]. It was considered that the PHASE signal would be essentially constant[6], and that the QUAD signal would indicate, therefore, the mainly in-quadrature current circulating in the fault circuit of adjacent laminations. Such fault current would be large compared to any other deviations arising from relatively minor inherent stator core permeability variations (Figure 3)[1,p.29].

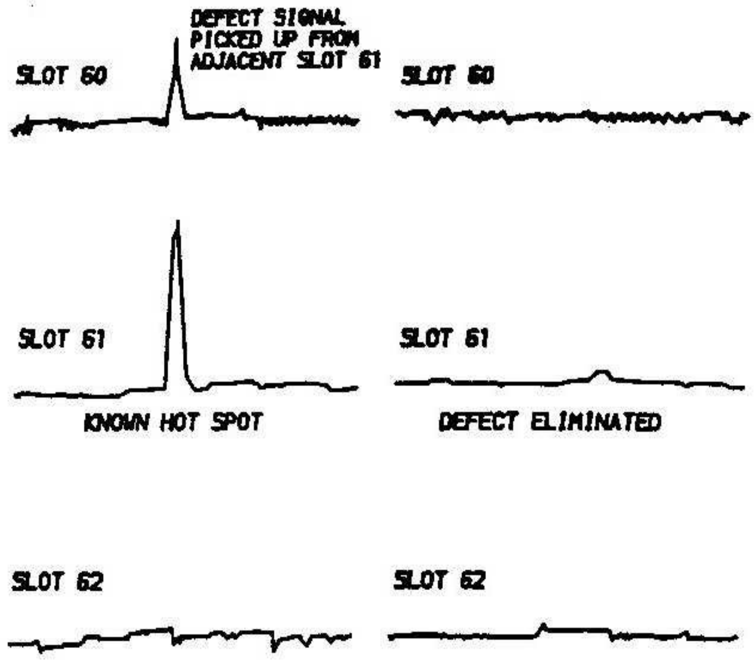

Figure 3[1,p.29,Fig:13] A normal EL CID trace (before and after rectification)

EL CID was first encountered by the candidate as only an observer of its application, demonstrated by John Sutton[3], to a large hydrogenerator stator core in the machine manufacturer's factory. The result was good, except where core joints (provided for shipping purposes) existed. The solution, suggested by Sutton, was simply to transfer the reference (initially provided by an air cored coil) to the core joint. Although the signal magnitude was considerably reduced, it was still much higher than the normal acceptance value of 100mA[6,p.17]. When applied to salient-pole hydrogenerators, the EL CID technique came to be regarded, therefore, with considerable suspicion by operators of such machines generally, and the application was abandoned; at least by some.

1.3 - Anomalous EL CID results encountered

EL CID is still widely used, in the context of hydrogenerators, for checking core regions considered to be beyond the influence of core joints. Nevertheless disconcerting anomalies in the results, arose[1], the full range being as follows:-

1. Incorrect magnetic induction level.
2. EL CID trace axis tilt.
3. EL CID trace tails.
4. EL CID trace axis curvature
5. Circumferential EL CID peaks and troughs,
6. Changes to QUAD signal values generally.
7. Increased QUAD signal values near salient poles.
8. QUAD signal ripples.
9. Negative PHASE indications.
10. Significantly increased QUAD signal values near core joints.

1.4 General steps in the solution of anomalies of Section 1.3

These problems were initially referred to others, both of high academic and of high industrial standing, who were considered best qualified to deal with them. This proved negative, as none had any clarification to offer.

The candidate has endeavoured, therefore, to determine the validity[7] of the EL CID technique when applied to hydrogenerators. The bulk of the work was undertaken after retirement without support financially or technically, apart from three valuable finite element analyses (prompted by the candidate) - two contributed by Dr. Tom Preston[8,9], and one by Mr. Mike Tarkanyi[10].

The various problems, identified above, arose intermittently, according to circumstances. The candidate's interest in validating the EL CID technique with reference to hydrogenerators has persisted, nevertheless. In this activity, the candidate has had the interest and encouragement of Dr David Bertenshaw, one time CEO of the EL CID manufacturing company (originally Adwell Industries Ltd., subsequently ADWEL International Ltd and finally IRIS Power LP), who, after retirement, also pursued research into the electromagnetic field at the bore of large stator cores[2].

This present thesis identifies the following steps in the analysis:

1. Correct excitation level. Originally it was assumed by technician staff that the approximate setting advised in the Instruction Book of that time, could be used for hydrogenerators. It has, however, to be calculated for each particular machine (Ref: Appendix 3). It should be noted that if the excitation is not set precisely on the value required to produce the recommended 4% of rated stator magnetic flux, it is permissible[6,p.8] to make a pro-rata correction to the resulting values of PHASE and QUAD.
2. Awareness of several categories of EL CID trace distortion (Section 2.6.5)

3. Association of the anomalies with particular circumstances:

    (i) excitation type

    (ii) impact of stator winding

    (iii) effect of salient-pole rotor

    (iv) proximity to stator core joint

    (v) general state of assembly

4. Recognition of various forms of EL CID set-up with appropriate analogous transformer situations (Figures 19[p.69] and 20[p.70]).

5. Alternative solutions of the identified problems

    (i) direct comparison of the evaluated fault value (***delta***) to the recognised criterion[6,p.17]

    (ii) assessment of the distribution[p's99,116] of fault values along the core length

1.5 The advantages of EL CID

The first advantage of EL CID is that it provides the means of putting the monitoring of stator core interlamination insulation on a new and more convenient basis than had been provided by the long established High Flux Ring Test (HFRT).

The HFRT procedure involves several difficulties:

1. A significantly large a.c. power is required to provide the required excitation, which is not always readily available, particularly in Hydro Power stations.

2. The cabling involved has to be heavily insulated to match the relatively high voltage required.
3. The cabling is also of considerable cross-section to meet the current rating involved.
4. Such cable is not easily handled, therefore the activity is labour intensive.
5. Adequate access is required by which to apply the excitation cable.
6. The high magnetic flux level required is likely to exacerbate the degradation already present of the interlamination insulation.
7. Appreciable time is required, both to mount an HFRT, and to execute it,
8. The results are susceptible to changing ambient conditions.
9. There is lack of a sound quantitative basis for assessing the results[2].

It is unsurprising, therefore, that correlation of EL CID results with those from an HFRT is difficult, and depends largely upon the experience of those involved. An attempt to correlate EL CID results from hydrogenerators with those of an HFRT was initiated by the candidate and reported[11] to the Biennial Session of CIGRE in Paris in 2002.

Initially, it appeared that EL CID results were little better than the HFRT, as a basis for establishing an assessment of stator core interlamination insulation condition. This was due to misunderstanding of how to set the excitation level, lack of awareness of local features which could modify EL CID results, incorrect conclusions from the results obtained, failure to take account of the effect of the manner of applying the excitation winding, and complete ignorance of the effect of core discontinuities produced by core joints (i.e. circumferential gaps).

EL CID was soon established as a valuable aid for comparing locally damaged or repaired core material, with other undamaged regions in the vicinity. It was also soon recognised that EL CID could provide a valuable basis, or foot print, from which to judge later tests, thus assessing the degree of degradation suffered in the course of service operation.

Unfortunately, one major stumbling block existed, for the removal of which no-one appeared to have an answer. That was the effect of core joints, required when such physically large machines were specified by the customer to be tested in the place of manufacture, and then shipped to the site where the machine would operate.

It was widely reported (e.g. from USA, Australia, New Zealand) that, at core joints, EL CID indicated alarming deterioration, which was not confirmed when machines were kept in service. In fact, they continued to perform satisfactorily for many years, and EL CID became largely discredited by hydrogenerator operators. The candidate's research into the state of such situations was stimulated purely by the desire to achieve a true understanding: either EL CID worked, or it didn't! Whilst Bertenshaw[2] has researched this correlation, his work did not extend to core regions in the locality of core joints. This thesis records the candidate's success in resolving the problem presented by stator core joints.

1.6 The work covered by this PhD thesis

This is summarised as follows:

(i) Recognition of the need for and the consequences of different forms of excitation set-up[Section 2.6.1].

(ii) Awareness of the environmental electromagnetic field[Section 2.62].

(iii)The significance of PHASE and QUAD signal variations, both independently and mutually[Section 2.6.3.1 to 4].

(iv) The impact of stator core joints[Section 2.6.4].

(v) The cause and significance of circulating current in the stator winding[Section 3.2.2].

Chapter 2 - Review of Previous Work

2.1 – Initial need for the development of EL CID

In the 1970's a major step upwards took place in the specific rating of steam-driven turbo-generators, due to the introduction of direct water cooling, i.e. the primary coolant (water) was put into direct contact with the high voltage stator winding copper, with the result that heat dissipation was vastly improved. Normally, intimate contact between the conductor (copper) of high voltage electrical machine windings and coolant water is unacceptable. The cooling water used for direct cooling of these highly rated turbo-generators is very pure (conductivity being 2 to 5 microSiemens per centimetre). In a thermal power station, condensate from the steam turbines provides a ready source. In hydropower stations such ready access to very low conductivity cooling water is not available, but the candidate has had excellent experience[12] in designing and commissioning a purification system for the UK's first direct-water-cooled hydro-generator/motor. In practice, the system achieved 0.13 microSiemens per centimetre, or less[12]. This illustrates the possibility of the specific rating of hydro electrical machines being raised equally as high as turbo-generators, with similar consequent problems.

The means of checking repairs to the interlamination insulation, in the early days of interlamination insulation failure, due to the increased specific rating, was the well established High Flux Ring Test[11] (HFRT) method. That involved exciting the stator core to near normal magnetic flux. The chosen method of inducing this relatively high magnetic flux in turbogenerator stators was usually of the Figure 5c (Ref: page 39) form, since the rotor was normally removed to allow access for personnel carrying out the repair to the core.

A radical new method of checking the progress of the repair work, which would overcome all the foregoing problems involved with the HFRT, was needed.

2.2 - Application to round rotor steam turbine driven generators[13]

When the early increased specific rated designs of turbogenerators were commissioned, unexpected problems began to develop, in terms of hot spots in the stator cores, built from thin steel laminations. Figure 4[1,p.3](provided by Adwel Industries Ltd, original manufacturer's of EL CID) shows a photograph taken by a heat sensitive camera of a stator core undergoing a high flux test.

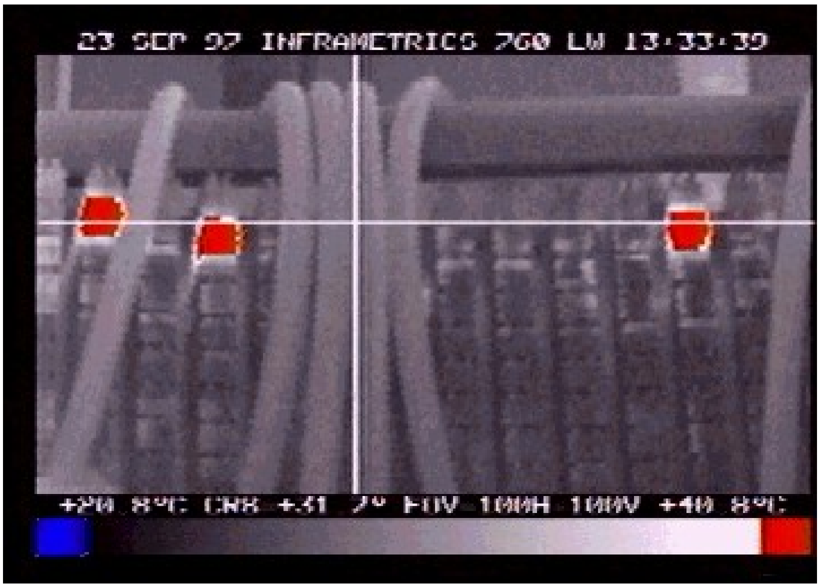

Figure 4 [1,p.3] Stator core hot spots during a High Flux Ring Test on a turbogenerator

When the original development of electrical machines began, it was realised that the alternating magnetic field would produce significant circulating current between the stator laminations, unless they were insulated from each other. Suitable insulation was applied, therefore, to these laminations, and the problem appeared to have been avoided.

Unfortunately some designers, of the early direct water-cooled machines with significantly increased specific rating, overlooked that the increase in output, also increased the electromagnetic field, to the extent that the interlamination voltage exceeded the ability of the insulation to withstand that applied voltage. Consequently break-down occurred and the circulating current between affected laminations led to intense hot-spots (See Figure 4[p.30]) above. The subsequent burning of the laminations caused unacceptable damage, and an outage of the machine. Such outages were, of course, extremely expensive[3,p.1] for the operating management and also for customers, both domestic and industrial.

The first step was to assess the damage and consider the possibility of a repair. Access to the bore of such machines is not easy, usually necessitating removal of the rotor – quite a major activity. Generally, a repair strategy could be undertaken, but the question arose as to when the repair had been sufficiently achieved. The method was well known, and conveniently referred to as the High Flux Ring Test (HFRT)[11], consisting of applying a high voltage excitation cable toroidally round the stator, to induce a near normal operating magnetic flux in the stator iron. This had several associated difficulties. Primarily, a suitable power source was not always immediately available. As already identified (in Section 2.1), the cable required was necessarily of substantial diameter, and it required a team of personnel to handle it. This was also time consuming, during which the machine was absorbing huge amounts of money[3,p.1] through loss of revenue, and the cost of repair work. The unplanned outage was additionally causing severe disruption of processes dependent upon a reliable source of electrical energy. In addition, this form of investigation may exacerbate the damage caused by the insulation failure. The reliability of power generation is an aspect becoming ever increasingly important throughout the world. Reference to it in the news media is almost a daily occurrence.

2.3 A brief over-view of the EL CID system providing a simpler way to test the interlamination insulation of stator cores

An easier way than the HFRT to check stator cores became a vital necessity. A physicist, John Sutton, of the CEGB's research establishment, called CERL, found himself tasked with solving this problem. Consequently, he invented an Electromagnetic Core Imperfection Detector[3], for which the acronym EL CID was coined. The equipment involved is described basically in Reference 6. It comprises a Chattock potentiometer sensor, connected to a Signal Processor Unit, which provides simultaneous orthogonal signals, known as PHASE and

QUAD to a computer. This both displays the results on a screen for immediate inspection, and also permits a printed copy to be obtained.

Briefly the operation of the EL CID test is as follows. The interlamination circulating (fault) current (*delta*) flows in a largely resistive circuit, comprising contact between adjacent laminations, the laminations themselves, and core structure features (usually building bars – or key bars, and, if present, cooling water tubes). It was argued that the circumferential magnetic field induced in an annular stator, would be modified by a component in quadrature to it. It was only necessary, therefore, to detect such a combined field and separate the orthogonal components. John Sutton found that the Chattock Potentiometer[4] could be applied as the required sensor. This sensor is highly sensitive, so that a much lower magnetic induction was required than that for normal operation. The signal from the sensor was then passed through an electronic Signal Processor Unit (SPU) to produce the PHASE and QUADRATURE (known simply as QUAD) components relative to the main core flux. Experience showed that the QUAD component was less than 100 mA for a healthy core[6,p.17], and was the main part of the circulating current. It was recognised that the path of the circulating current is not perfectly resistive, and therefore, a small component would exist in phase with the basic magnetic field, but that was considered of secondary significance.

Consequently, checking for the adequacy of a core repair became very much simpler, and quicker[3]. Moreover, the supply power required for the excitation winding was considerably less than for the HFRT[3,p.1]. This meant that a suitable cable was more flexible, readily obtainable and could be handled quite easily. Instead of a team of half a dozen or so personnel, the test could be made in a relatively short time, say a day, by a couple of people.

There were one or two teething problems, but nothing serious, and the advent of EL CID was regarded as a great success. It so happened that the convenient power supply available when introducing EL CID produced about 4% of normal flux, and that was adopted as the standard, for which the corresponding QUAD value was not more than 100 mA[6,p.17]. This became the acceptance criterion. Since it appeared that there was not a great variability in the electromagnetic parameters of turbo-generators, a standard excitation set-up (in terms of volts per unit length) was conveniently incorporated in the original Instruction Book.

2.4 Application to large diameter salient-pole water turbine driven generators (typically, hydrogenerators)[1]

After the success achieved with the application of EL CID to turbogenerators, the next logical step was its application to hydrogenerators. This was demonstrated in the factory of a British manufacturer of large machines in the early 1980's. The demonstration, carried out by John Sutton, was very positive, except in the region of core joints, which had been introduced to allow shipment of such very large stator units. At that time an "air-cored coil" was used to provide the reference of the main circumferential flux. The Reference Coil was held on the stator core bore by a magnetic base, with the plane of its turns in line with the longitudinal (or axial shaft) direction. Consequently, **leakage flux from the core, which is circumferential in direction, linked with the Reference Coil turns.** It was suggested, therefore, that the problem, caused by the **extra large leakage flux at a core joint**, could be alleviated by re-siting the Reference Coil close to the joint. This changed, in effect, the PHASE Reference of the EL CID set-up, which will be shown to be undesirable, unless appropriate compensation is made (See Section 8.3.3).

This strategy proved inadequate. Even the introduction of a current transformer, fitted on the excitation cable, and the improved ability of the EL CID kit to cope with very much higher circulating current values, did not solve the core joint problem. The thesis identifies the solution later (See Chapter 5).

In the course of further use of EL CID in connection with hydrogenerators, a number of anomalies in the results arose, as identified in Section 1.3 (p.23). Clearly, for reliable use of the EL CID technique, it is essential that the evaluation of the outcome should be accurate and unambiguous. Whilst maintenance in service of large turbogenerators is important for a reliable electrical power system, good serviceability from renewable energy powered hydrogenerators contributes additional ecosystem value. The purpose of this submission is to present the considerable volume of work published by the candidate in order to provide an adequate understanding of the theory behind EL CID, and hence to facilitate comprehensive analysis of EL CID results. There is no other such study known (App: 7). For example, a theoretical study, by Müller et al[14], demonstrates a very interesting application of 3-D finite element modelling, involving advanced mathematics, but the work does not apply to the practical situations encountered in actual electrical machines. Also, Bertenshaw has completed a PhD submission[2] on the competence of EL CID or any comparable electromagnetic test, compared to the HFRT thermal test, other than anecdotally. His undoubtedly valuable work, which is not yet released into the public domain, seeks to establish confidence in this correlation. The test model employed by Bertenshaw related primarily to turbogenerators. The electromagnetic field of a hydrogenerator core joint situation was not included.

2.5 – Design differences between the two basic types of rotating electrical machine in electrical power production (i.e. turbogenerators and hydrogenerators)

In view of the prior highly successful application of EL CID to turbogenerators, the need to consider separately the application to hydrogenerators is of interest. This arises from significant differences in the design of these two basic types of large rotating electrical machine employed in the electrical power production industry throughout the world, Therefore, before considering in detail the application of EL CID to hydrogenerators, these design differences are set out in Table 1 below. These features have to be determined by a pre-test survey of the machine. Their significance was only appreciated in the course of developing the work covered by this thesis.

An aspect of setting up for an EL CID test on hydrogenerators which cannot be closely predetermined, is the electrical power supply required. Whilst this is significantly less that for an HFRT[3,p.33], allowance for the magnetic flux absorbed by the massive stator frame is indeterminate because it is a significantly large feature, which varies considerably for different situations. Although this affects the setting up of an EL CID test overall, it is only the resultant electric field in the stator (in terms of volts per unit length of core) which determines the level of fault current.

Turbogenerator(TG) design features	Hydrogenerator(HG) design features	Impact on EL CID Test
1. Large air gap between stator and rotor may permit application of motorised EL CID without rotor removal.	1. Space between salient poles may allow access without rotor removal, or by removal of only one or two salient-poles.	1. Pole proximity effect arises in HG's(Sect: 3.2.3. p.59)
2. Cylindrical rotor needs removal, if work on stator bore is required, to allow access for personnel.	2. Removal of the rotor is undesirable for vertical machines to avoid realignment. Removal of rotor poles, spider and rim may be possible, but leaves the shaft in-situ.	2. Major dismantling of TG's is needed. Excitation winding is difficult to apply for HG's, with shaft in-situ, even with poles, rim and spider removed. EL CID traces may have tails & sloping axes (Sect:2.6.1, p.43).
3. Stator core cooling usually involves longitudinal ventilation ducts	3. Air-cooled hydro machines normally have radial stator ventilation ducts	3. Stator radial vent ducts of HG's affect EL CID signals. (Sect: 2.6.3.2 (ii),p.45)
4. A pressurised hydrogen cooling system is usually provided in additon to direct-water cooling of stator winding.	4. Some of the larger HG's may employ direct-water cooling, but a hydrogen atmosphere would be exceptional.	4. In practise, preparaton of either for application of EL CID is similar.
5. TG stator endwinding extention beyond the ends of the stator core is relatively long.	5. HG winding overhangs are relatively short, and space at the bottom of vertical machines may be limited by supporting structure.	5. Proximity to core ends of HG's excitation cable may affect EL CID trace. (Sect: 3.1.4 p.53)
6. The number of stator winding parallel circuits is limited to two in TG's	6. HG's may have a relatively large number of parallel circuits.	6. Disturbance of HG EL CID trace greater than for TG's (Sect: 3.2.2 p.57)
7. TG stator cores are of relatively small diameter, compared to most HG's, and have always been built as a complete annulus.	7. Stator cores of large HG's may be built in sections resulting in small, but significant, radial air gaps in the core.	7. Core joints in HG's create complexity in the electromagnetic field.(Sect: 2.4 p. 35; Sect:4.2.4 p.77)

<u>Table 1</u> Basic design differences between turbogenerators and hydrogenerators affecting application of EL CID.

2.6 Introduction to the detail of the work submitted

2.6.1 - Application of excitation to stator cores of salient-pole machines for the EL CID test.

EL CID was initially applied to round rotor steam-turbine-driven large electrical machines[13]. Removal of the rotor was required in order to provide access for remedial work on the stator core. It was most convenient, therefore, to apply the excitation winding in the form of a group of turns along the axis of the core (Figure 5c). The strength of excitation was given in Reference 6[p's 3,8,11,17], and repeated in the original Instruction Book, as a standard value, in terms of trace turn voltage, of 5Vrms/metre of stator core length, since it was considered that most turbogenerators had similar electromagnetic characteristics.

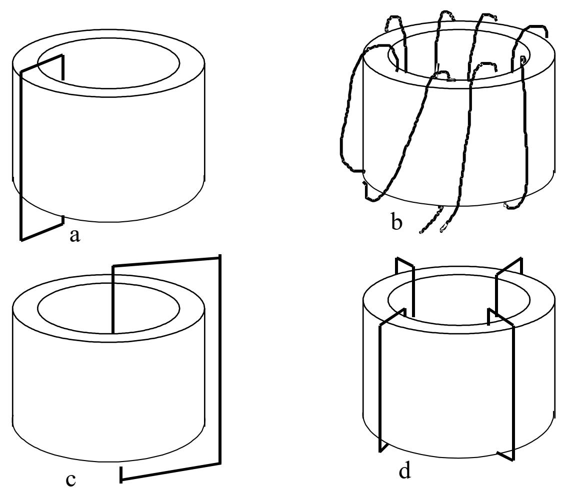

Figure 5 Alternative forms of EL CID excitation winding

The first EL CID test on a hydrogenerator in its work-site was made in order to check remedial work on the ends of the stator core in a few locations. The excitation winding was applied as a group of turns, wound close to the stator bore, between the salient-poles local to the remedial work (Figure 5a). The strength of the excitation adopted was as given in the Instruction Book. Although this was later shown to be erroneous for salient-pole machines, it was of little consequence at that time, since the checks were of a comparative nature and made only in relatively few limited positions around the stator bore. Nevertheless, this practise demonstrates the need for EL CID tests to be made under the close supervision of an engineer qualified to check the work[6,p.7], rather than only a technician, with a limited understanding of the work and the situation.

Excitation of this form (Figure 5a) is theoretically acceptable, as shown by Moullin[15]. His work, however, related to a steel annulus situated remotely from any source of magnetic leakage. In the practical situation of a machine in a hydro-electric power station, significant magnetic leakage arises from various ancillary structures, i.e. bearings, brakes, stator frame, machine enclosure, etc. If the test is in the machine maker's factory, environmental factors such as steel flooring can be significant.

When EL CID was first applied globally to a stator, the previous experience regarding excitation level was adopted by the technician appointed to the task. This immediately produced abnormally high EL CID signals. As the candidate chanced to be on site for other purposes, and being the only design engineer present, the results were referred to him. Although not previously directly involved with EL CID tests, the candidate quickly identified that, for salient-pole hydrogenerators, it is necessary to evaluate the excitation level appropriately for the specific machine concerned, as given in Appendix 3. The candidate had been responsible for the refurbishment design[16]. From memory of that design, it was possible, therefore, to calculate the required excitation volts per turn close to that required for magnetisation of the core to the standard level[6,p.3] of 4% of the operational value, as had been adopted previously.

The EL CID test then proceeded appropriately. But in the region of the core joints (or splits), apparently unacceptably high signals were evident. It was recalled by the candidate, from memory of witnessing the factory demonstration of EL CID by John Sutton, that in the similar situation on that occasion, it was suggested that the reference coil should be moved to the joint region, thus resetting the Phase reference. This action was recommended, therefore, to the EL CID operator. Although the level of EL CID signal was significantly reduced, it was still abnormally high in comparison to the acceptance standard of 100mA[6,p.17], for interlamination insulation in good condition. The electromagnetic field at core joints was not, at that time, understood. The anomalous results from such situations were the last to be analysed, despite having been referred to several electrical machine experts, from both university and industry.

In this event, it was decided, by the customer, that the machine, and its five sister machines, should have their stator cores renewed as part of the refurbishment and enhancement in hand. It is interesting to note that the major French electrical power utility (EDF) had already adopted such action as its standard policy[17].

The form of the excitation coil is decided according to the circumstances. Reference has been made already to Moullin's justification of the Figure 5a type, but only in a rather theoretical situation. Figure 5b illustrates excitation turns wound toroidally, or helically, close to the stator bore. In Figure 5c, the excitation winding comprises a group of turns wound along the axis of the stator. Appendices 1 and 2 show that both Figure 5b and 5c forms of excitation respectively establish a uniform circumferential magnetic field in an annular core. Figure 5d is only an extension of Figure 5a, but the added groups provide compensation for possible flux leakage.

When the rotor is removed, the excitation is applied most easily in the way generally adopted for EL CID testing of turbogenerators, (Figure 5c), i.e. the required number of turns are located as a group along the axial centre-line, then returned over the core ends. This was found to be very satisfactory for turbogenerators, but when applied to hydrogenerators the results contained anomalies, which were traced to subtle differences between the two types of machines, such as the greater length of winding overhang for turbogenerators. Although the hydrogenerator rotor-mounted salient-poles can be sometimes removed as an integral unit with the laminated rotor rim, leaving the shaft in-situ, the remaining shaft influences the results. The Figure 5c form of the excitation in these circumstances may cause trace axis tilt (Section 3.1.4) and trace tails (Section 3.1.5). Removal of the shaft is undesirable, as such action introduces a significant delay during re-assembly for renewal of the line-out of the generator and turbine shafts.

Where the hydrogenerator rotor is not removed, the only alternative form of excitation winding is as a toroidal coil spread evenly around the stator (Figure 5b). This form has particular merit, if it is desired to establish EL CID results for a core, whether new or not, as a basic footprint to be compared with later EL CID results. To remove the rotor for such a purpose would probably be impractical. Use of the toroidal form of excitation winding, however, raises its own problems. Firstly, care is necessary not to work too closely to the winding turns. This requires sufficient slack in the turns at the back of the stator core to allow easy movement during the test. A restriction on this requirement sometimes arises due to the limited access available through the machine foundations and/or top structure. Of course, the circumferential location of the EL CID axial traverse of the core relative to salient poles has an impact on the EL CID results, in the form of curvature of the trace axis (See Section 3.2.3, page 60), whatever the form by which excitation is applied.

2.6.2- Environmental electromagnetic field

Although not usually a problem, the sensitivity of the EL CID sensor is such that occasions have been identified when a change to the background electromagnetic field has been detected. This arose when other machines were started-up or shut-down in the power station during the course of an EL CID test.

2.6.3 - The significance of PHASE and QUAD signal variations

2.6.3.1- Identification of perturbations arising from an interlamination insulation fault and those produced otherwise.

The fundamental concept of EL CID for a fault free core, was that the sensor would produce an approximately flat trace (i.e. to within 50 mA)[6,p.13] for both PHASE and QUAD detected signals. Where a fault was detected, the QUAD trace would show a very significant excursion (See Figure 3), but the PHASE signal would be largely unaffected, and equal to the magnetic potential difference (mpd) established by the applied excitation. For turbogenerators, this was the normal experience. For hydrogenerators, however, the EL CID results were usually much different, although initially the focus was on QUAD values.

2.6.3.2 – QUAD value variations from other than defective interlamination insulation.

(i) The Effect of the form of excitation winding

Several of these have been identified in the discussion (Section 2.6.1) of the form of excitation applied to a stator core for an EL CID test, i.e. trace axis tilt, trace tails and trace axis curvature (See also Sections 3.1.4 and 3.1.5).

(ii) The impact of ventilation passages

Historically, ventilation of hydrogenerators has been mainly by means of air as the primary coolant, whether for the "open" type of machine, or the "closed" type, employing water for the latter as a secondary coolant. In each case, the heat generated by machine losses is dissipated by air circulating through the machine. For this, radial air passages along the core have usually been provided. These constitute a discontinuity in the permeability of the core, which is reflected in a reduction of the longitudinal signal of the EL CID sensor.

(iii) An additional source of QUAD signal variation

This was reported in Reference 18. At the time of the tests to which these results are mainly referred, understanding of the application of EL CID to hydrogenerators was considerably lacking, and the attempted analysis left much to be desired. There was, however, some indication of correlation with the number of slots per core plate segment, and the location of key bars (or core building bars), which previously had not been noted. The former cause of trace variation is now considered most likely to have been a stator winding circulating current effect (See Section 3.2.2).

2.6.3.3 - PHASE variations.

Initially, little or no interest was taken in PHASE values, except to check, at locations remote from core joints, that the magnetic potential difference (i.e. mpd), given by excitation ampere turns divided by the number of teeth, or slots, was as desired.

It was found, however, that when the PHASE signal from hydrogenerators was recorded, it could have a wide variation in both the axial and circumferential directions.

(i) Negative PHASE values circumferentially

Circumferential (i.e. from slot to slot) PHASE variations were particularly notable, in so far as they sometimes became negative Fig:[10,p.58]. This appeared to have a very special significance, as identified later (Section 3.2.2).

(ii) Correspondence of longitudinal *PHASE* and *QUAD* values

The axial *PHASE* variation was found to be matched, approximately, by that of the *QUAD* signals, which also indicated some particularly special significance. This is taken into account later (Section 3.2.1).

2.6.3.4 - *PHASE* and *QUAD* variations together.

(i) Further consideration of circumferential variations will be given later.

(ii) The matching *PHASE* and *QUAD* longitudinal variations arise fundamentally from variation in permeance along the length of the core.

Dukshtau et al[19] have noted that "The stator of a hydro-electric generator is a large, complicated structure subject to diverse loads of electromagnetic, vibration and thermal origin when in operation." In other words, stator cores of such machines are not at all homogeneous, which is reflected strongly in EL CID results. It is no surprise, therefore, that EL CID results are far from the theoretical form often assumed and expected. The matching of variations in *PHASE* and *QUAD* values along the core length is indicative of a very important connection to be discussed later (Section 3.2.1).

2.6.4 - The impact of stator core joints

At or close to stator core joints, the EL CID signals indicated a serious deterioration in the condition of the interlamination insulation. But experience, voiced by hydrogenerator users at international engineering forums, did not support such a conclusion, and cast doubt on the reliability and value of the EL CID technique. This erroneous perception may be dispelled by application of recent work by the candidate in successfully[p. 82,90 et seq.] analysing the situation.

4. 2.6.5 - Summary of problems (other than arising from fault conditions) encountered when applying EL CID to salient-pole electrical machines[7,10]:-

Problem	Cause
1. Higher signal values than normal	1. a)Incorrect excitation level. b)Sensor too close to excitation cable turn.
2. Sloping signal trace axis	2. Misalignment of excitation cable with the machine axis.
3. Signal trace tails	3. a) Excitation cable too close to core end. b) Magnetically sensitive component(s) in the vicinity.
4.Trace axis curvature	4.Salient-pole proximity to traverse of sensor.
5. Trace ripple along the core length	5. a) Ventilation ducts b) Core construction features (e.g. core build (or key) bars, core segmentation gaps).
6. Significantly low signal values	6. a) Incorrect excitation level b) Deeply embedded fault
7. Major cyclic signal circumferential variations	7. Stator winding circulating current
8. Alarmingly high localised signals	8. Proximity to stator core joint.

Chapter3 - Detail of the initial phase of the work submitted

3.1 - Application of excitation to stator cores of salient-pole machines for the EL CID test.

3.1.1 - The form of excitation winding to be applied (Section 2.6.1, Figure 5)

It has been identified that there are four basic forms[7] by which to apply the excitation winding for an EL CID test :-

a) A single multi-turn group wound closely to the stator bore (Figure 5a).

b) A toroidal application of the excitation winding turns (Figure 5b).

c) A single multi-turn group wound along the longitudinal axis of the machine (Figure 5c).

d) Several (often four) groups of turns wound at evenly spaced locations around and close to the core (Figure 5d).

The Form 5a excitation winding is useful when it is only necessary to apply local magnetisation of the core. Although Moullin has shown[15] that this form of excitation can theoretically produce a uniform magnetic field around an annular steel construction, this is only feasible when there are no leakage paths. But, when access is very limited, this form can be useful.

The Form 5b excitation is shown in Appendix 1 to produce a magnetic field in the annular stator which is principally circumferential, other components being negligible.

The Form 5c excitation is shown in Appendix 2 to induce a relatively high flux density in the iron annular stator compared to that produced in the air.
The Form 5d excitation is merely an extension of Form 5a). Form 5d overcomes the tendency of leakage flux to diminish the circumferential magnetic field.

3.1.2 – The strength of excitation to be applied

The hydraulic conditions of hydro-electric schemes are far from standardised. This is reflected in the highly variable electromagnetic characteristics of the associated large salient-pole electrical machines. Standardisation of the strength of excitation to be applied to the stator core of such machines for an EL CID test is virtually impossible. Consequently the voltage per turn of the excitation winding, as detected by a trace turn, needs to be calculated as laid out in Appendix 3. As the characteristics of the stator core steel magnetic properties are not well defined at the low intensity of magnetic field employed in an EL CID test, it is necessary to set the excitation ampere-turns by some measure of trial and error. This can be refined from experience, although some difficulty remains in pre-test assessment of the excitation supply requirements.

Although the standard 4%[6,p.3] of normal operational stator core magnetic field strength is recommended, it is not absolutely essential to achieve this figure, as the strength of the signal obtained from the EL CID kit may be adjusted pro-rata with magnetic field within a limited range.

3.1.3 – Avoidance of being too close to excitation turns

Application of excitation forms b and d (Figure 5) requires care in the provision of adequate slack to permit moving the turns sufficiently to provide about a metre distance between the EL CID sensor and the nearest excitation turn. This is in order to avoid undue interference of the excitation current electromagnetic field with that of fault current. A metre is considered good practise, based on experience, although not an absolute rule from theory.

3.1.4 – Care required when applying the Figure 5c form of excitation winding

Before discussing the EL CID traces arising when this form of excitation was applied, it is necessary to identify the significance of variations exhibited in any case. If a stator core consisted of a truly homogeneous mass of steel, the trace of an EL CID signal would be a perfectly straight line, there being no variation in permeability, and no varying fault current. It is necessary, however, to use insulated laminations as the stator core material to inhibit inherent circulating current. This introduces two factors which impact upon the EL CID trace. First, there is a variation in permeability along the length of the core, causing a reduction in the EL CID signal. Secondly, there is imperfection of the interlamination insulation, causing a further variation in the EL CID signal. Also, as noted in Section 2.6.3.2(ii)[p.45], ventilation ducts reduce the core permeability, and hence, the EL CID signal.

Thus variation in the EL CID trace indicates some measure of circulating current. Complete elimination of circulating current is, of course, impossible. For the purpose of assessing the degree of slope of the EL CID trace, it is necessary to exercise judgement regarding the general level of signal.

When the EL CID sensor was moved circumferentially, with the Figure 5c form of excitation applied, it was noted that at the end of the trace, there were sometimes exceptionally high values.

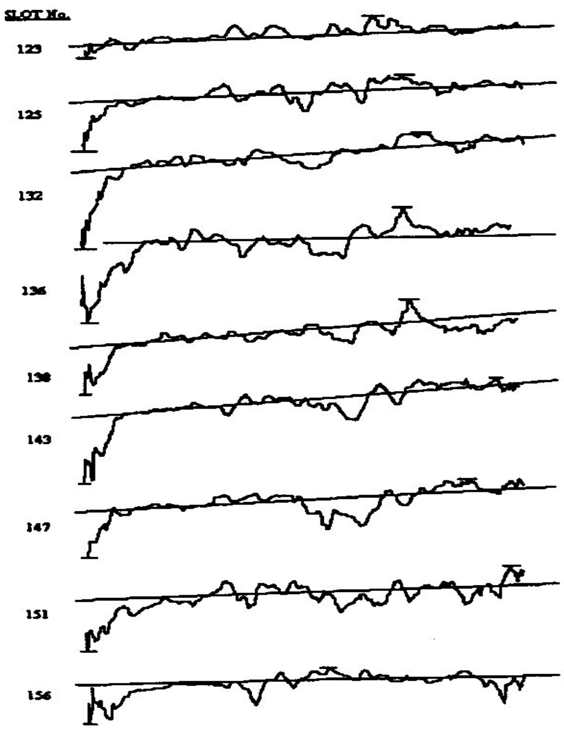

<u>Figure 6</u> EL CID results, along the stator core length, exhibiting trace axis slope and significant deviations at one end of the stator core.

The significance of the trace slope is dealt with in Section 3.1.5[p.55].

The high values at the end of the trace appeared indicative of interlamination insulation degradation at the core ends. This could sometimes result from filing the ends of the stator slots as an aid to fitting the stator winding. Examination of the core usually eliminated such a cause. The high end trace values formed a pattern, however, relative to the radial arm of the excitation cable crossing the core end[10].

This provided a clue to an item by Carter[20 [p.142,Sect:7.12(a)]] relating to the effect of a current carrying conductor above a magnetic surface. This was not developed by Carter but the candidate has shown[10], as reproduced in Appendix 4, that the field intensity in the steel surface, in this situation, varies dramatically in the region close to the conductor (Figure 7).

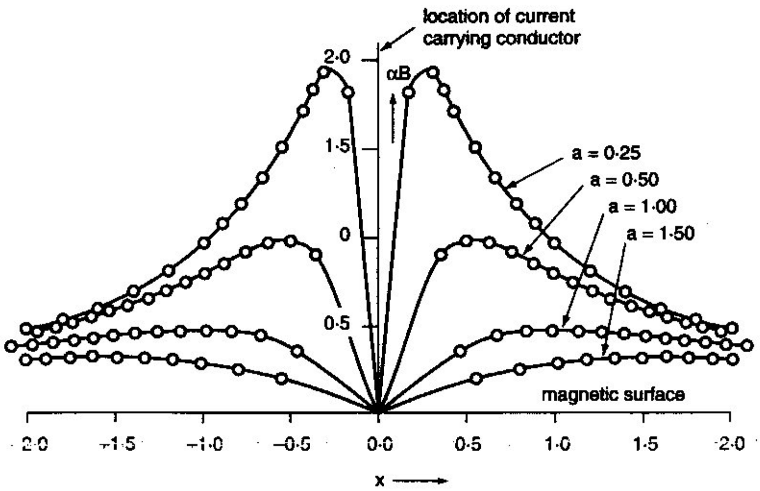

<u>Figure 7</u> Theoretical variation of Flux Density (*B*) in a magnetic surface due to a current carrying conductor above and parallel to it.

The conclusion was reached, from this development, that for a Form 5c type of excitation winding, it is desirable to run the radial arm at least a metre away from the end of the core. Although this is not always possible, particularly at the bottom of a vertical machine, this awareness provides a warning with regard to interpretation of the results.

3.1.5 – Misalignment of the excitation Form 5c within the stator bore

A further distortion of the signal picked up by the EL CID sensor, in the form of a slope of the trace axis (Reference Figure 6), arises from misalignment of the axial leg of excitation winding Form 5c with the axis of the machine[7,10]. Such misalignment may be twofold, i.e. at an angle to the machine axis, and also offset. This is readily illustrated in Figure 8 resulting from a finite element analysis. It is noted that if the shaft has been left in-situ, an offset of the excitation winding through the stator bore is inevitable.

In order to analyse the effect of misalignment of the Form 5c excitation cable through the stator bore the field intensity at the stator bore is considered for a given degree of off-set, thus representing a particular cross-section of the situation. Figure 8 is the result for one particular such off-set of 10%. Additional studies, for different values of off-sets, to simulate slope of the cable, showed that the flux density is essentially inversely proportional to the distance of the cable from the bore[1]. Saturation effects may be neglected at the low level of magnetic induction involved.

The variation[1,21] of the EL CID trace axis slope round the bore indicates the position of the excitation cable, if it has not been reported clearly. The need for attention to detail, of such as the excitation winding application, again highlights the need for an adequate understanding of the EL CID technique for application of EL CID.

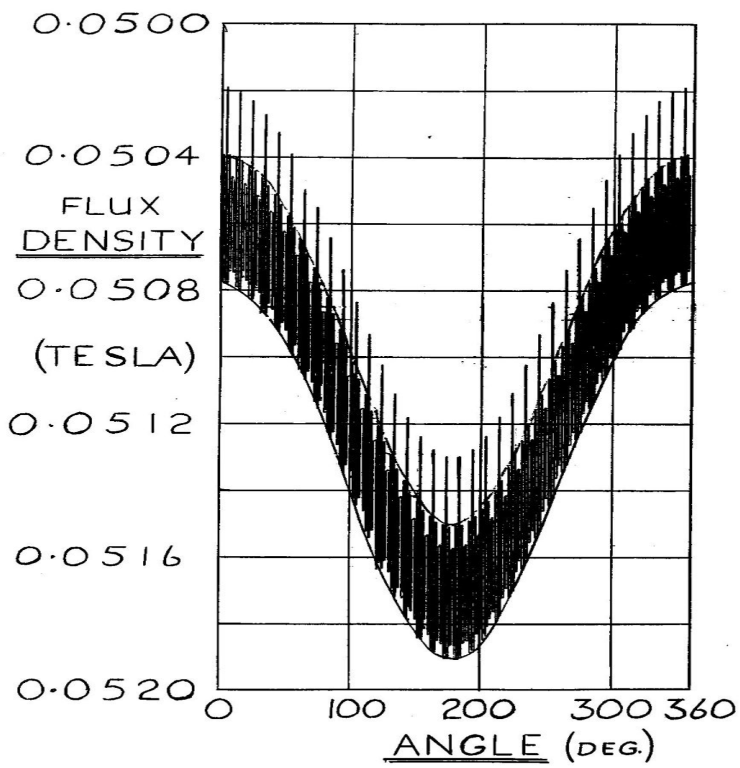

Figure 8 – **Finite element analysis of cable attitude**

3.2 Variations of *PHASE* and *QUAD* values unrelated to fault conditions

3.2.1 – Corresponding *PHASE* and *QUAD* variations

As has been stated earlier, initially *PHASE* values (traces) were largely disregarded, as it had been the experience in relation to turbogenerators that they were relatively constant. When, however, *PHASE* traces were recorded for hydrogenerators, it was found that variations along the core length could be quite marked. It was noted in Section 2.6.3.4 above that stator cores are far from homogeneous constructions. Moreover, it was observed that resulting variations were reflected in corresponding *QUAD* traces[22]. Figure 9 records this at a core joint, where the the *QUAD* values were particularly significant.

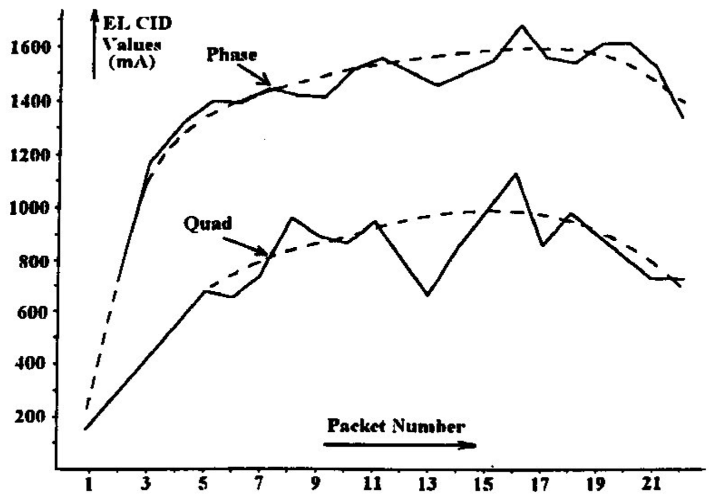

<u>Figure 9</u> – Corresponding *PHASE* and *QUAD* values at a core joint

Whilst the correlation of *PHASE* and *QUAD* values in Figure 9 is not immediately striking, it is evident that there is evidence of it to some degree. Moreover, it has to be recognised that these results were not obtained using the latest version of EL CID, which electronically records both *PHASE* and *QUAD* at the same time. In addition, paper traces, used earlier, suffered from some lack of precision in the recording of the values relative to their disposition along the stator core. The general trend can, however, be seen.

3.2.2 – The impact of stator winding circulating current on *PHASE* records[9]

Figure 10 records a major departure from the expected uniform value of mmf circumferentially. Particularly noteworthy was the excursion into the negative region in the case the *PHASE* trace of one of the two machines illustrated.

The significance of these records was not immediately recognised, until it was realised, in discussion, that a negative value of *PHASE*, i.e. essentially mmf, pointed to a driving electrical current. This led to an examination of the possible effect by the stator winding, if present, during an EL CID test. It was found that if all the phases and parallel paths of the stator winding were shorted, the circulating current would have the same distribution pattern as the upper *PHASE* values in Figure 10, as seen in Figure 11. The same result was obtained for the lower PHASE values in Figure 10 by again taking account of stator winding circulating current.

A fuller discussion is given in Reference 1. An important confirmation of this aspect of the work was provided by Bertenshaw and Sutton[23].

As a supporting check, Dr. Preston applied a finite element analysis technique, using a SLIM package, with the result given in Figure 12.

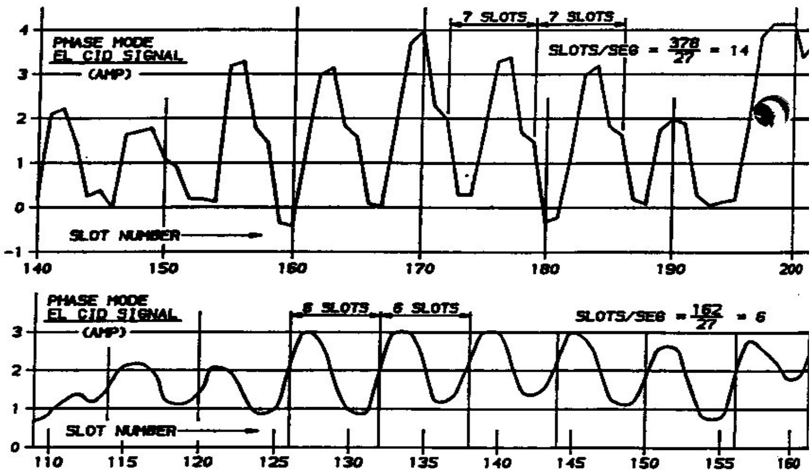

<u>Figure 10</u> - Circumferential variation in *PHASE* value

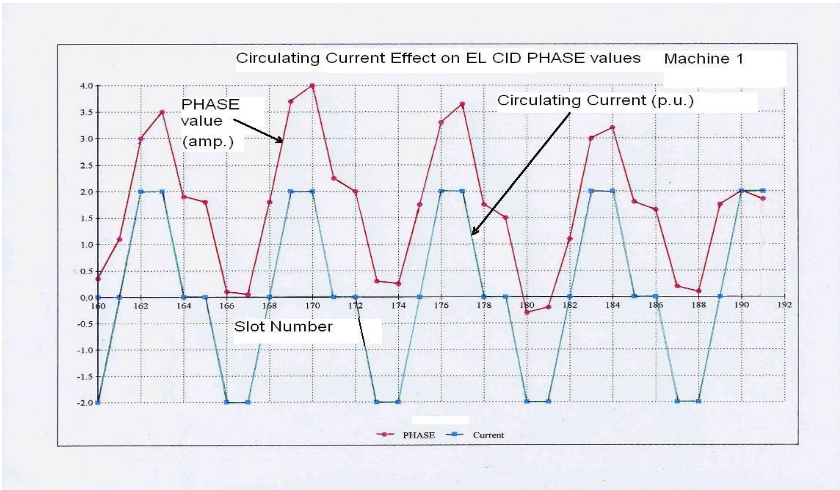

<u>Figure 11</u> - Circulating current effect on EL CID values

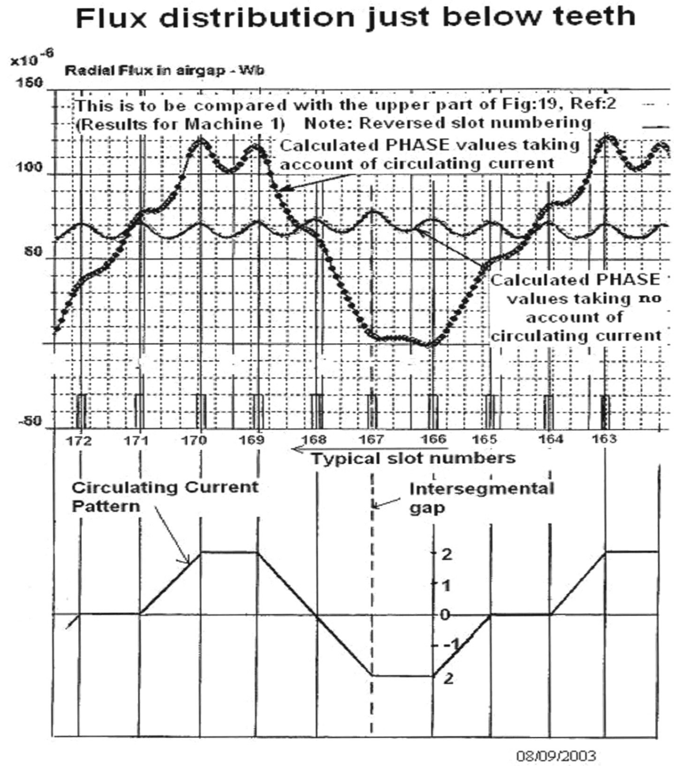

Figure 12 – **Finite element analysis calculation of *PHASE* values with and without circulating current in the stator winding**

3.2.3 – The proximity effect of salient poles on EL CID traces[8]

In general, the space (air gap) between the stator bore and the surface of salient-poles is small for hydrogenerators, particularly those of early vintage, which are most likely to suffer from degradation of stator core interlamination insulation. In order to carry out a monitoring check during an in-service period (although not operationally active), it is not worth dismantling a machine to the extent of removing the rotor to provide the EL CID operator with access, nor is the air gap usually large enough to permit an EL CID remote controlled trolley (tractor) to travel through it. At best, therefore, sufficient access is usually made available by removing only one, or maybe two, of the salient poles.

In the case of an early application of EL CID to check the stator core insulation condition, the resultant *QUAD* trace obtained was that identified as Curve A in Figure 13. Initially, it appeared that the insulation towards the ends of the stator core was defective. But upon turning the rotor to allow access to another part of the stator bore, it was found that the results for the same slot had become Curve B. It was recognised that the essential characteristic of the trace, which included a pronounced blip near one end, had not changed, but the axis had been flattened. This raised awareness of the possible effect of salient poles on EL CID results.

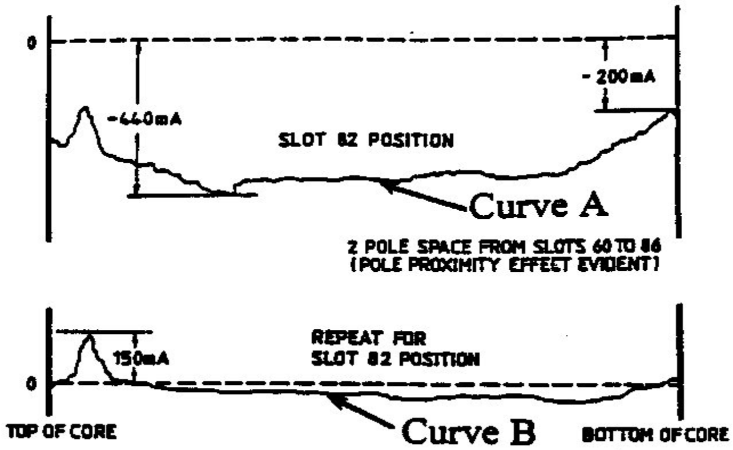

<u>Figure 13</u> – EL CID trace curvature due to Pole Proximity effect

The question was also raised as to the circumstances in which a pole-proximity effect might be expected. An earlier test on another machine, for which no poles were removed, was thought (erroneously, as it was later proved [p.'s61,62]) to indicate the absence of such an effect.

An in-depth study of this phenomenon was undertaken[8]. It included three-dimensional Finite Element Analysis models for two machines, such as shown, for only one of them, in Figure 14. Figure 15 shows the geometry for both.

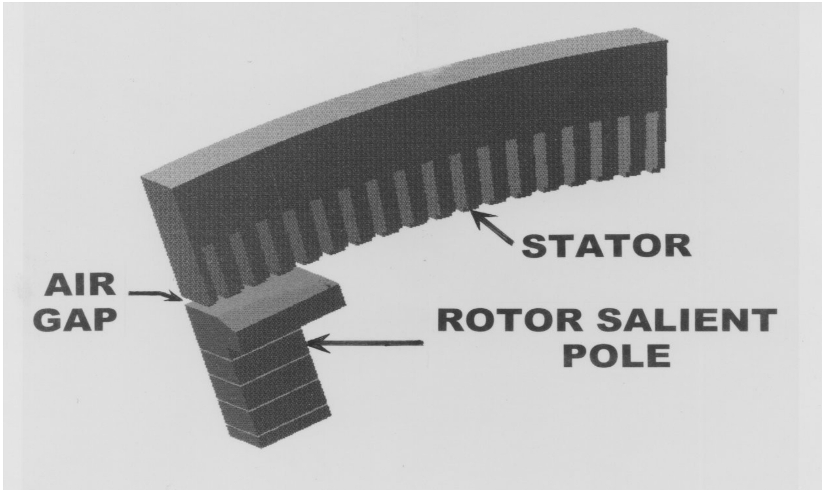

<u>Figure 14</u> - Three-dimensional finite element analysis model

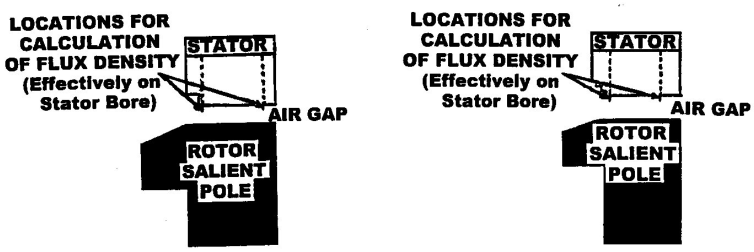

<u>Figure 15</u> Longitudinal sections for two machines investigated for pole-proximity

Details of this study of pole proximity during an EL CID test are given in Reference 8. In the light of this, a re-examination of results, which initially appeared not to show a pole-proximity effect, found that such did exist, although of varying degree, as reported in detail in Reference 8. The conclusion was that a pole-proximity effect will always be present where there are salient-poles.

3.2.4 Brief analysis of EL CID results from a remote site[21]

An important point illustrated here is that application of EL CID needs to be under the control of engineers who understand all that this dissertation covers, as indicated by Sutton[6,p.7].

EL CID results reported from a distant site were received for comment. Questions raised were not referred back to the data source, although requested. Consequently, progress with analysis was deferred. The reported EL CID results were unusual, as they referred only to the end packets of laminations, rather than the length of an entire tooth (or slot).

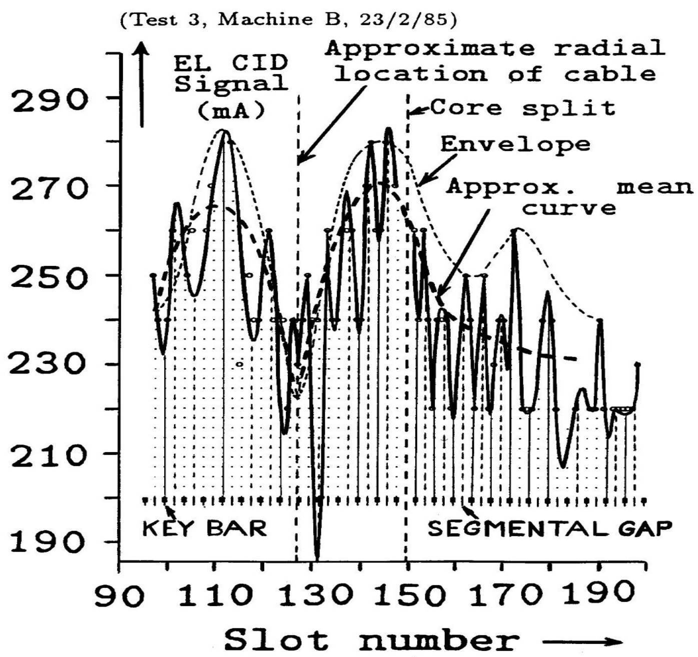

Figure 16 A plot of top-end core packet EL CID QUAD signal results

The comprehensive suite of EL CID vector diagrams (Reference Section 4.2p.68) had not been developed, but understanding already gained indicated the analysis of results as shown in Figure 16. For instance, the theoretical form of EL CID signal values identified in Figure 7, arising from too close a proximity of the excitation cable to the core end, is seen also in Figure 16. In the appendices of Reference 21 it is deduced that there was a tilt of the excitation cable as it passed through the stator bore, such that the EL CID signal distribution might be greatest to the right of the indicated location of the cable. This is suggested by the approximate mean curve drawn. Although the relationship to construction features is uncertain, there is clearly some correlation.

From Figure 16 it is considered that the recorded maximum *QUAD* value of 280mA is falsely inflated(if an indication of core condition) as follows:-

From results elsewhere around the core, the base signal was indicated as 68mA. The signal in this region of slots 100 to200 affected by the excitation cable and core joint is considered to level off to about 228 mA, i.e. an increase of 160 mA, possibly due to stator winding circulating current. There is also the apparent effect of proximity to the core end, estimated as 38 mA. The 4 mA difference between results each side of the cable position is considered to be due to tilt. A further increase of 10 mA is ascribed to the segmentation of the core laminations. Finally, the core was judged to be over-excited by [(4.90 / 2.69) - 1] 100% = 82%. Thus, the recorded maximum QUAD value of 280 mA is reduced to (280 -10 – 4 – 38 – 160) (2.69/ 4.9) = **37mA**, indicating a very acceptable core condition. In fact, the machine performed good service over many further years. This was confirmed by the candidate's personal visit. The need for comprehensive reporting of the test set-up and results is nevertheless strongly indicated, for a reliable analysis.

Chapter 4 – The major development in the work submitted - based upon identification of EL CID as a transformer

4.1 The basic EL CID phasor diagram[24]

The accumulated evidence indicated that PHASE and QUAD values were closely inter-related, and it was concluded that consideration of the EL CID set-up as a transformer, with two short-circuited secondary windings, closely represented the situation. The standard phasor diagram for this is shown in Figure 17[25]. The identification of the symbols used is given in the Notation (p. 13).

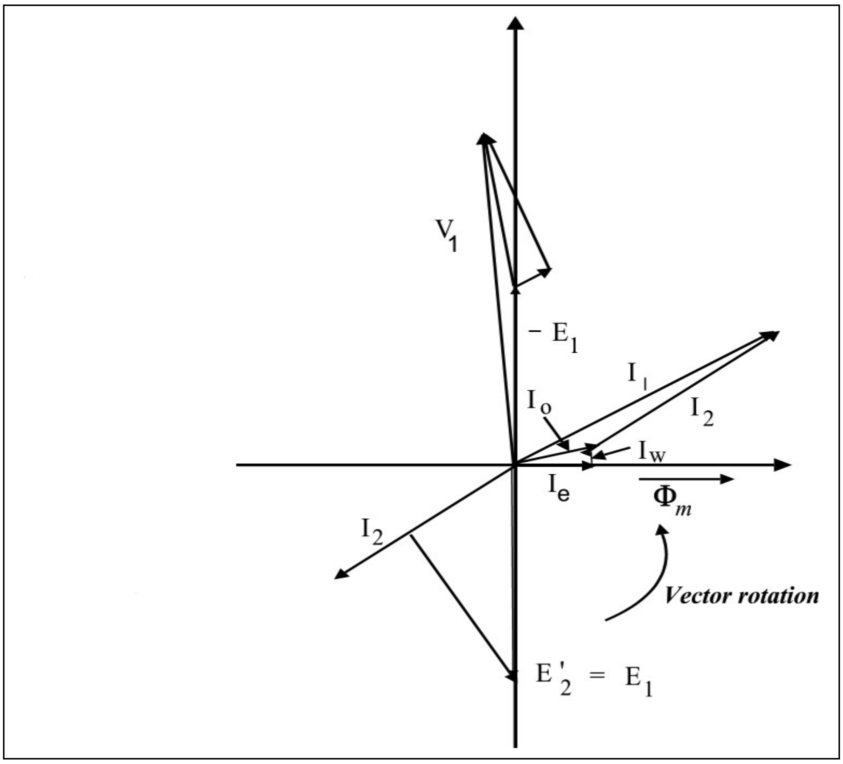

<u>Figure 17</u> The phasor diagram for a transformer with shorted secondary

Since the EL CID sensor detects the effect of current in the secondary circuits comprising a) the fault, and b) the stator winding, it is necessary to view the excitation circuit (i.e. the normal primary circuit) from a secondary winding point of view. The phasor diagram is re-drawn below, therefore, with reference to the secondary side of the EL CID set-up regarded as a transformer. It is to be noted also, that the Signal Processor Unit (SPU) of the EL CID equipment, reverses the *Phase* values[26,p.3]. The result is shown in Figure 18, where only current phasors are included.

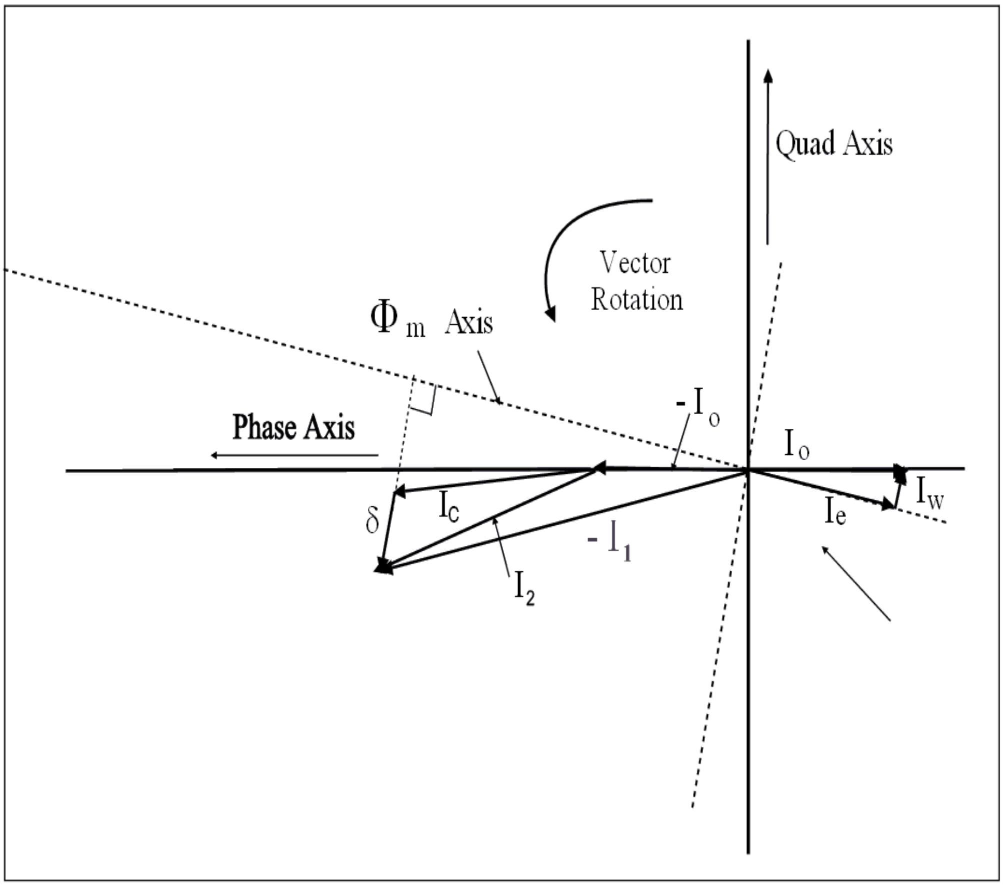

<u>Figure 18</u> The basic EL CID phasor diagram, including Circulating Current (I_c) and PHASE axis reversal; current phasors only shown; all components referred to the secondary side)

Figure 18 is essentially as produced by Bertenshaw[26] from basic electromagnetic theory of the induction of a magnetic field in the stator core, including current in a fault path (due to degradation of interlamination insulation). The diagram is extended for current in the stator winding (if present). Bertenshaw does not develop the phasor diagram to match the various different electromagnetic situations which may be encountered in practical situations. The effect of the presence of a rotor is neglected until later.

4.2 Development of a suite of EL CID phasor diagrams to match different electromagnetic conditions[24]

4.2.1 Introduction

When the EL CID test is applied to the annular stator core of a salient-pole large electrical rotating machine, such as a hydrogenerator, a number of conditions may apply. These are illustrated in Figure 19. As indicated earlier[p.65], it is considered that the EL CID set-up may be regarded as a transformer. For this purpose, a comprehensive equivalent circuit is presented in Figure 20, deduced as shown in engineering literature[25]. It covers all the various alternatives. Interlamination insulation degradation (i.e. a fault), with its associated fault current (***delta***) is assumed to be present in each case, and is not shown in Figure 19.

This diagram is a very simplified version of the magnetic flux paths set up by the conditions identified as “a”, “b” and “c”. Stator slots and rotor salient-poles are only shown where necessary to illustrate the effect of different machine conditions.

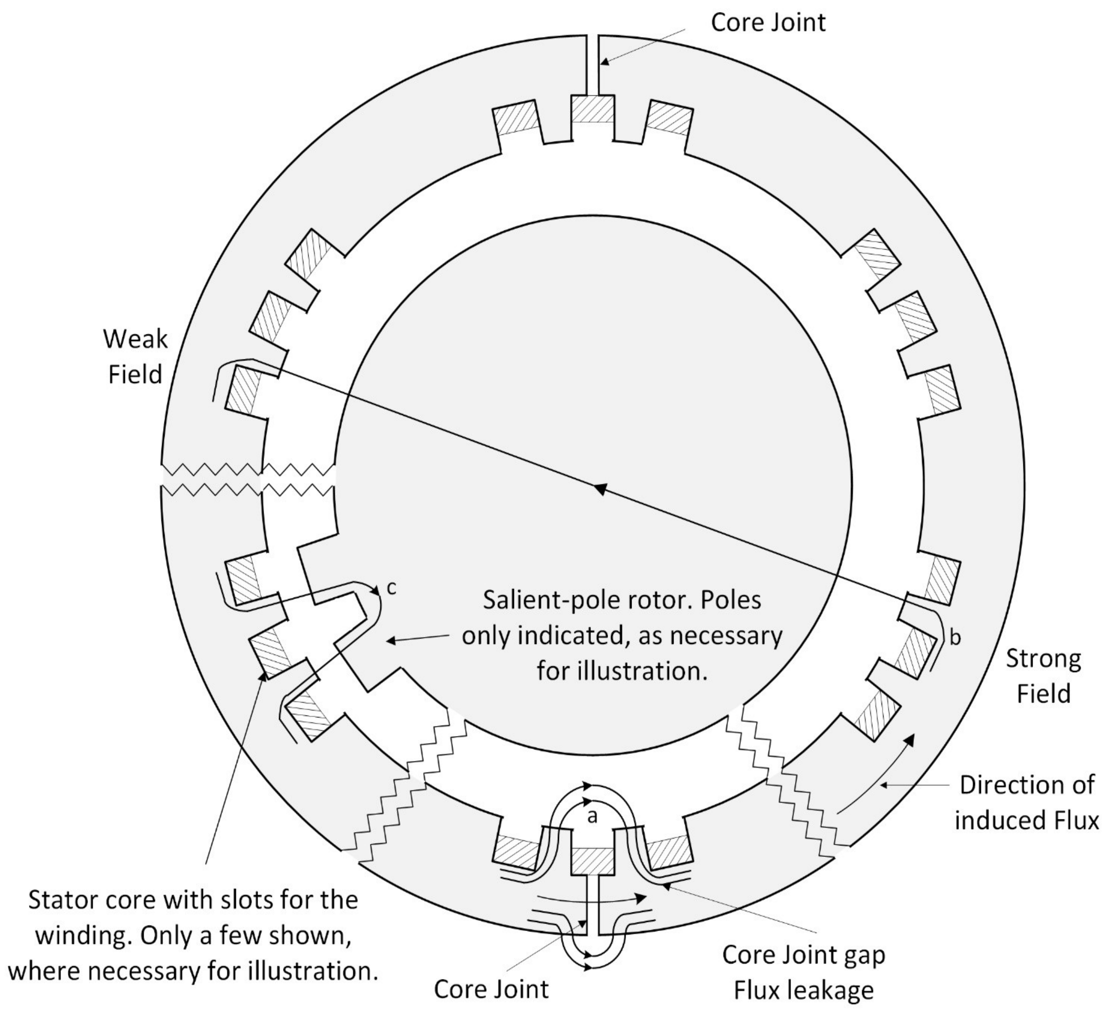

<u>Figure 19.</u> Flux paths during an EL CID test for various cases

Three different flux conditions are identified in Figure 19, by text and by illustration, as:

a. air gap leakage flux at stator core joints (Ref: Figure 24)

b. an unbalanced excitation winding (Ref: Sect: 3.1.4 & 3.1.5; Figures 22 & 23)

c. leakage flux between the stator and rotor (Ref: Figure 25)

All three situations may arise at one time or be established separately. For clarity an example of each situation is illustrated individually. Each condition produces an imbalance to the magnetic field. If a shorted stator winding is present, with two or more parallel paths, the magnetic imbalance gives rise to circulating current in the stator winding, which is an extra item to be included in the phasor diagram (See Ch: 4, p.65 et seq).

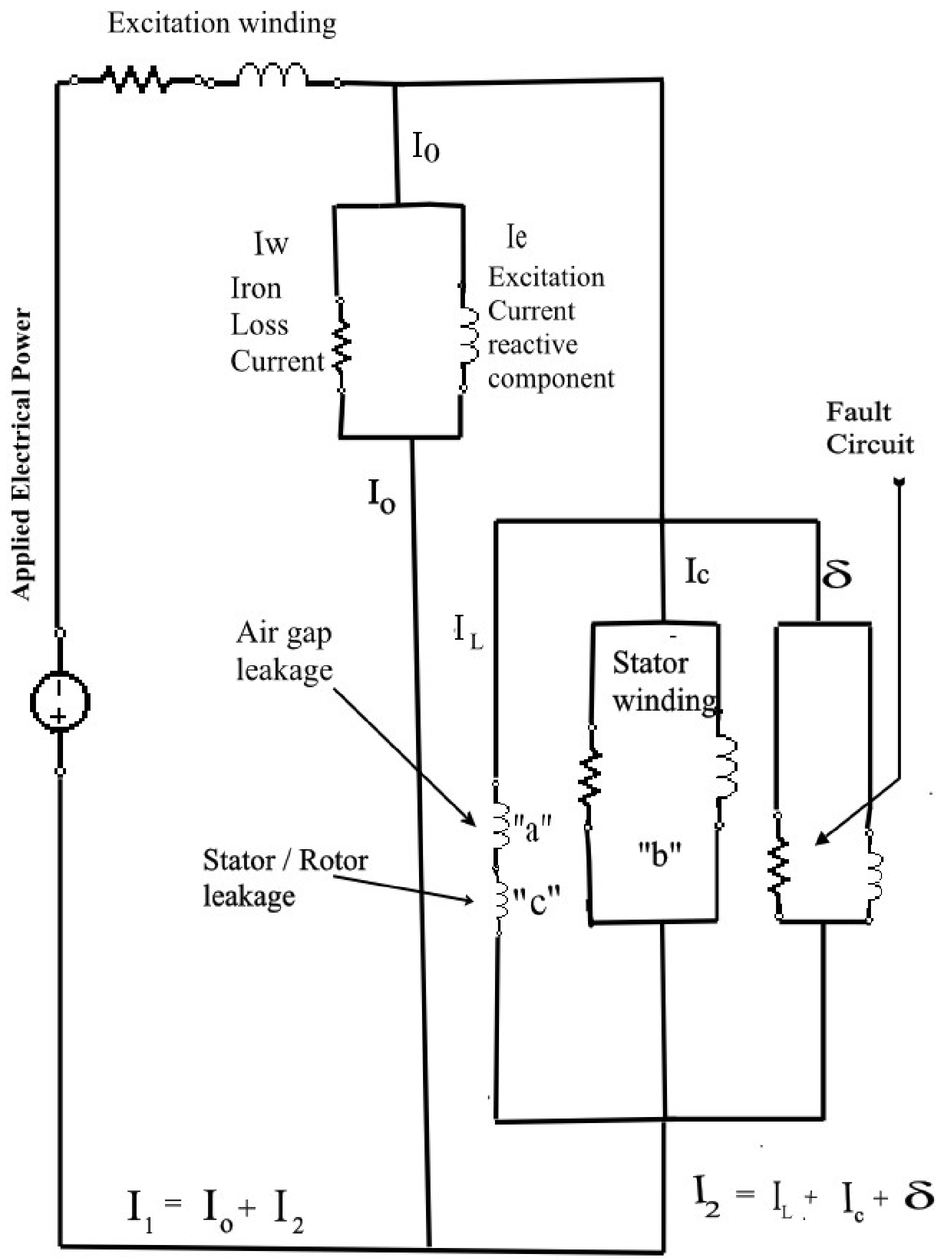

<u>Figure 20.</u> Equivalent transformer circuit diagram for various cases

The objective is to evaluate ***delta*** from the results of an EL CID test. To achieve this, it is very important that EL CID operators, and subsequent analysts, have sufficient understanding of the physical conditions existing, and also the electromagnetic situation at the time of the test. ***For any one test, therefore, the appropriate features in Figures 19 and 20 are selected, and the corresponding choice made from the suite of phasor diagrams developed below. It may be necessary to develop new ones which are most appropriate for different situations.***

It is fundamental to the analysis to accept the basic EL CID theory, as set out in the thesis, with reference to Figure 1. The immediate extension to that is awareness that the EL CID sensor (Chattock Potentometer) detects whatever magnetic field is present at the inner periphery of the annular core for a particular case. Detailed consideration of several cases follows. In this discussion of each of the conditions identifed, reference is made only to those features of Figure 19 and 20 which apply in the particular case under consideration.

Excitation of the annular stator core is applied in one of the four forms shown in Figure 5. In ideal circumstances, Moullin[15] shows that Form 5a would induce a uniform magnetic field in the iron of the stator core. It is shown in Appendices 1 and 2 of this Thesis that Forms 5b and 5c, for equally ideal conditions, would also induce a uniform magnetic field. Inevitably conditions are not ideal, with the consequence that there is flux leakage, as illustrated in Figure 19 for different circumstances of the stator core assembly and state of erection. Excitation Form 5d produces an acceptably practical uniformity of flux induction, but must clearly be associated with a significant degree of flux leakage.

4.2.2 Case 1. No stator winding fitted, no rotor in-situ, no core joints.

For this case, none of the features a, b, and c, illustrated in Figures 19 and 20, are present.

It is to be noted that, as in Sutton's original work in developing EL CID, the phasor diagram is rotated clockwise through 90 degrees from the angular position in the general diagram given in Figure 18.

Thus the relevant phasor diagram comprises only the current (I_o) in the excitaton winding (drawn in the reverse direction to match the view from the secondary winding), plus the fault current (*delta*, drawn orthogonally to the direction of the flux induced in the annular stator core) to give the resultant secondary current (I_2), as shown in Figure 21.

This is virtually the same as the original simple phasor diagram proposed by Sutton, except that it is drawn in the 4th quadrant. Due to the power loss associated with the stator iron, the magnetic flux direction is out of phase with the PHASE axis, the direction of which is identified as that of the excitation current. As generally assumed in initial EL CID tests, whilst ***delta*** is seen to be approximately equal to the *QUAD* value, it is evident that it also has a small *PHASE* component.

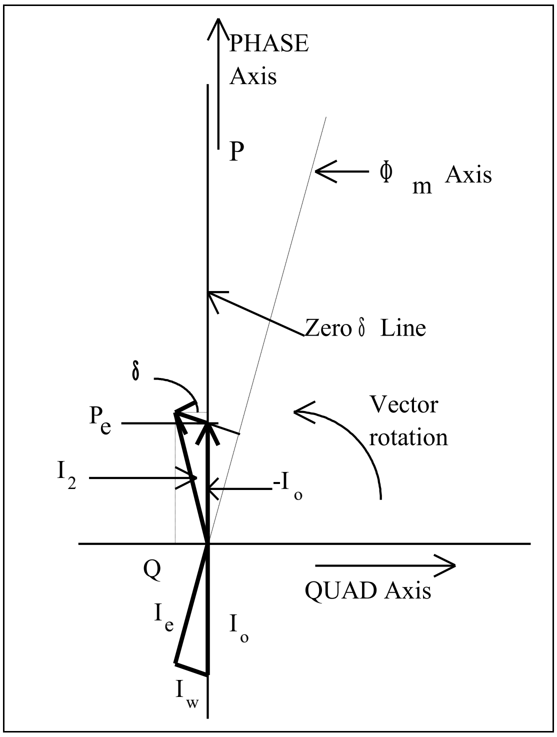

<u>Figure 21</u>   EL CID phasor diagram in the absence a stator winding.

It is to be recognised that the relevant version of the phasor diagram, applies strictly to the conditions encountered at a particular position at the core bore, circumferentially and longitudinally. If the stator winding is present in the stator, the associated circulating current is constant along the length of the particular slot position under examination, but the stator core permeance may vary for a variety of reasons, and hence also the apparent mpd, directly related to the effective excitation current (I_o), This appears as a variation in the detected PHASE value.

Consequently, if ***delta*** is zero and the PHASE value varies, the operating point moves along the PHASE axis. In this case the PHASE axis is defined as the **zero delta line**. Its significance will be seen more clearly in other cases.

4.2.3 Case 2. Stator winding present and its terminals short-circuited, no rotor in-situ, no core joints.

The relevant feature here in Figures 19 and 20 is b). As identified by Bertenshaw[25], when a stator winding, comprising parallel circuits, is in place with its terminals short-circuited, the unbalanced magnetic field of the stator core, arising from the disposition of the magnetising winding, provides flux leakage linking the stator conductors to induce current in them. Added to the phasor diagram of Figure 21, therefore, is the component of stator circulating current (I_c), in parallel with the interlamination fault, in which delta circulates, to form Figure 22.

For any one slot position the stator winding current is constant, thus if the *PHASE* value varies, the ***delta*** phasor moves along a line parallel to the PHASE axis passing through the tip of the stator circulating current phasor. This line is the reference line along which delta is zero, and defines the **zero delta line** for this case.

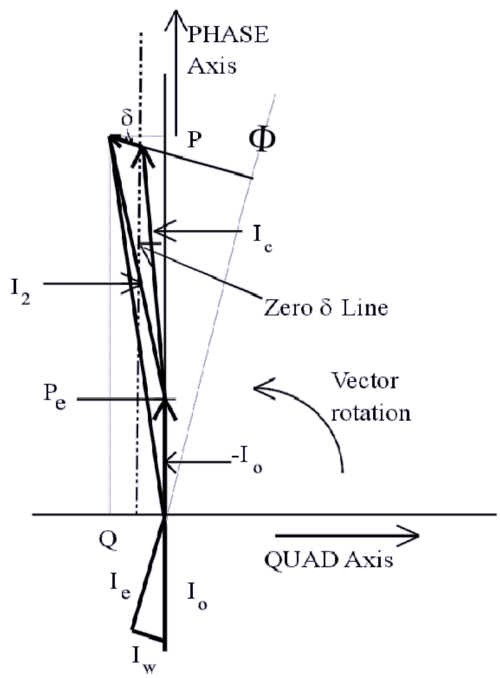

<u>Figure 22</u> EL CID phasor diagram for a location remote from a core joint, but including a shorted stator winding

Throughout the winding the current must balance out to zero. Therefore, whilst for any one slot position the stator winding current is constant, there is variation, circumferentially (i.e. from slot to slot, including phase reversal), as illustrated in Figure 23.

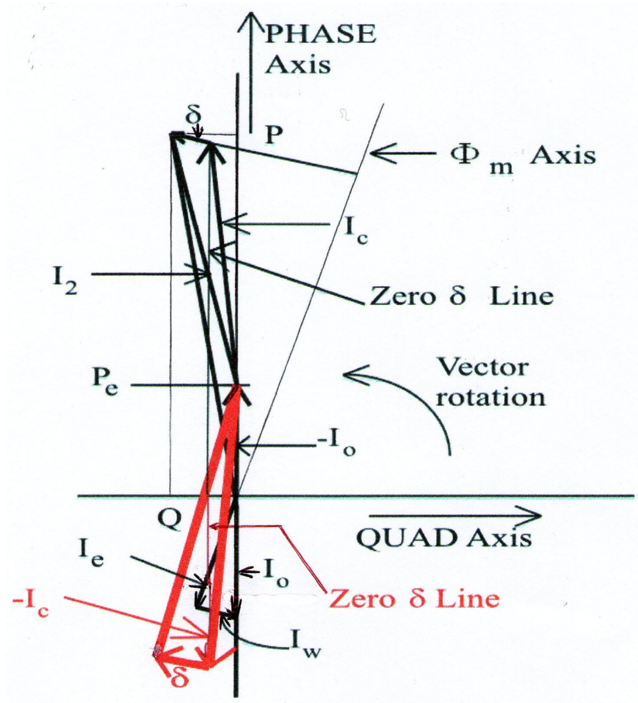

<u>Figure 23</u> **Phasor diagram for a location remote from a core joint, including reversed stator winding circulating current ($-I_c$)**

4.2.4 Case 3 Stator winding present (as in Case 2), rotor not in-situ (as in Case 1), core joints present (to facilitate transportation).

This very important case remained unsolved until all other EL CID phenomena had been analysed. Figure 24 applies.

The relevant features for this case in Figures 19 and 20 are a) and b).

The presence of core joints introduces a major degree of flux leakage, i.e. a relatively large phasor component (I_ℓ **),** which is aligned to the direction of the main magnetic flux Φm. To I_ℓ is added the stator winding current (I_c). The direction of I_c is such as to oppose the local leakage flux, but due to the winding resistance the direction of I_c is slightly out of direct phase opposition to the leakage flux's equivalent current phasor. Bertenshaw[26] has shown that the phase difference is not far from 180 degrees. The presence of resistance tends to produce an anti-clockwise rotation relative to the leakage flux. This rotation is exaggerated in Figure 24 for clarity. Although the symbols in this figure are as defined in the Notation, it is important to observe the following:-

Ie represents the excitation current, required to magnetise the stator core.

Io represents the total current required in the excitation winding, when account is taken of Iw, the current drawn by the losses in the core iron.

Ic, Io and Iw are essentially primary side values, which are reversed due to the diagram being drawn from the perspective of the secondary side, to correspond to the current values detected by the EL CID sensor. Thus **-**Io is the base for the rest of the diagram.

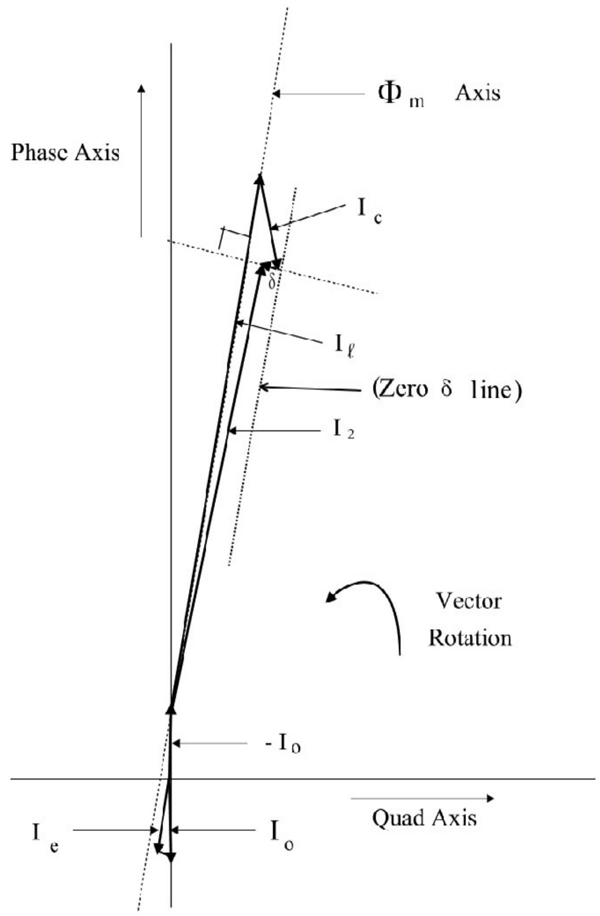

<u>Figure 24</u> The EL CID vector diagram, including leakage flux from a core joint, and stator winding circulating current.

The final phasor component contributing to the total current detected by an EL CID sensor is the fault current (***delta***). i.e. the current circulating in (a) the short between laminations, (b) the laminations themselves, and (c) the short effected by building bars, and/or sometimes cooling tubes. This ***delta*** component produces heating in the defined circuit, particularly in the relatively high resistance short between laminations. As this is a loss component, it is directed in the phasor diagram at right angles to the direction of the leakage flux inducing it. This flux is from the core, and has the same phase as the main flux (*Φm*).

4.2.5 Case 4 Stator winding present, the salient-pole rotor in situ, no stator core joints.

The relevant features in this case in both Figures 19 and 20 are b) and c).

The phasor diagram (Figure 25) is essentially the same as Figure 22, with the addition of the current phasor I_R corresponding to the leakage flux crossing the machine air gap from the stator iron to that of the rotor. The direction of this additional phasor is parallel to the main stator magnetic flux phasor, as it is leakage from the latter. With the rotor present, allowance has to be made for the phasor I_R.

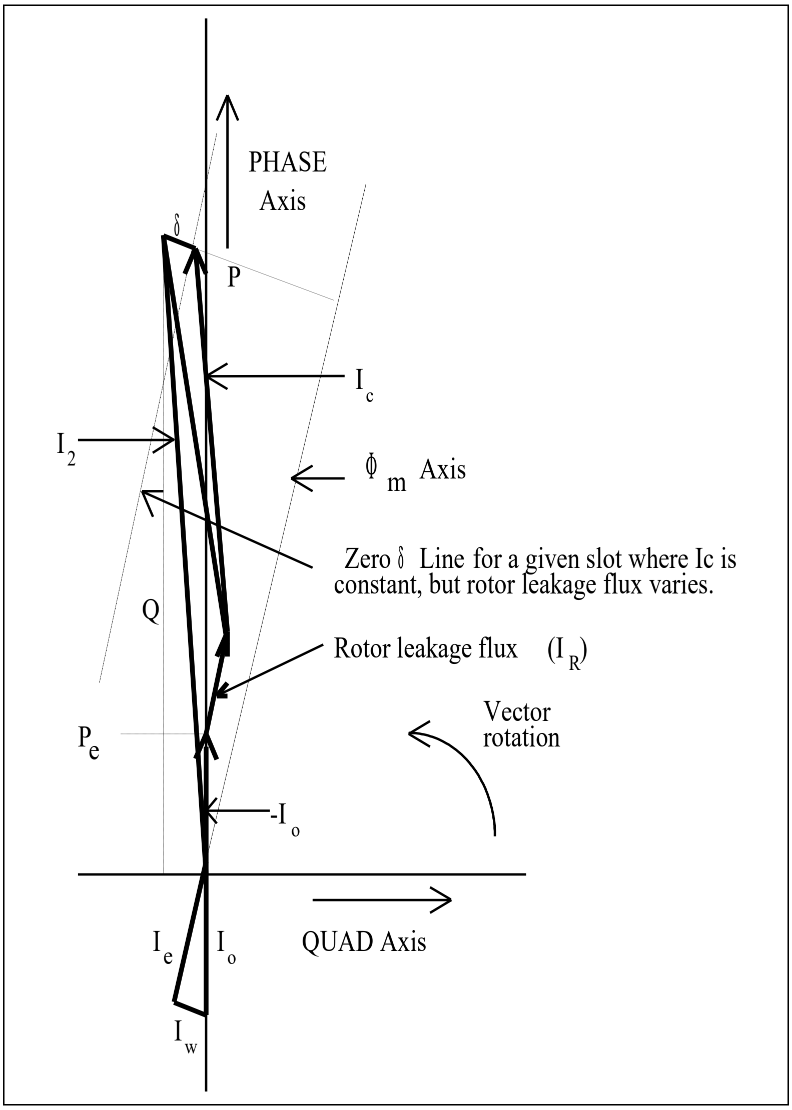

<u>Figure 25</u> The EL CID phasor diagram for a location remote from a core joint, but including stator winding circulating current, plus the effect of a salient-pole rotor in situ.

4.3 Justification of the various forms of the EL CID phasor diagram

A check that the phasor diagrams developed are applicable to EL CID results, as obtained for defined situations, has been detailed for several cases in Section 6.6 of Reference 1[(p. 95 et seq.)].

Locations considered include:-

a) Remote from a core joint, no stator winding, no rotor present[1,p.94,95].

b) Two slots away from a core joint, no stator winding, no rotor present[1,p.94,96].

c) Two slots away from a core joint, stator winding current circulating, rotor in-situ[1,p.93,97].

d) At a core joint, stator winding current circulating and rotor in-situ[1,p.91,98].

After establishing the various forms of the EL CID Phasor diagram, they were checked that they matched appropriate plots of *PHASE / QUAD* values[1,24]. The phasor diagrams exhibited above are not necessarily a perfect match for the EL CID results obtained in practise, but they provide a basis and pointer for what to expect. At two slots away, a core joint, perhaps in most cases, may have very little impact upon the detected EL CID results, whereas in some cases the core joint effect can be still evident[1,p.28,Fig.12] at a considerable circumferential distance from such a feature.

Chapter 5 Evaluation of *delta* at a core joint

This chapter sets out the procedure for evaluating *delta*, thus providing the opportunity of identifying specific interlamination insulation failure locations.

5.1 - The 1st step in the process of evaluating *delta* is obtaining the EL CID traces

EL CID signal traces are first obtained, in the form as recorded in Figure 26, as output from the computer in the EL CID set-up. Only the *QUAD* trace is shown here, as the *PHASE* trace is of similar form, but with much higher recorded values. To allow the scale to be increased for clarity, an offset (the so-called DC offset) from zero is selected and removed by the computer for convenience (i.e. values to be measured are reduced, but the Phase Reference is not affected).

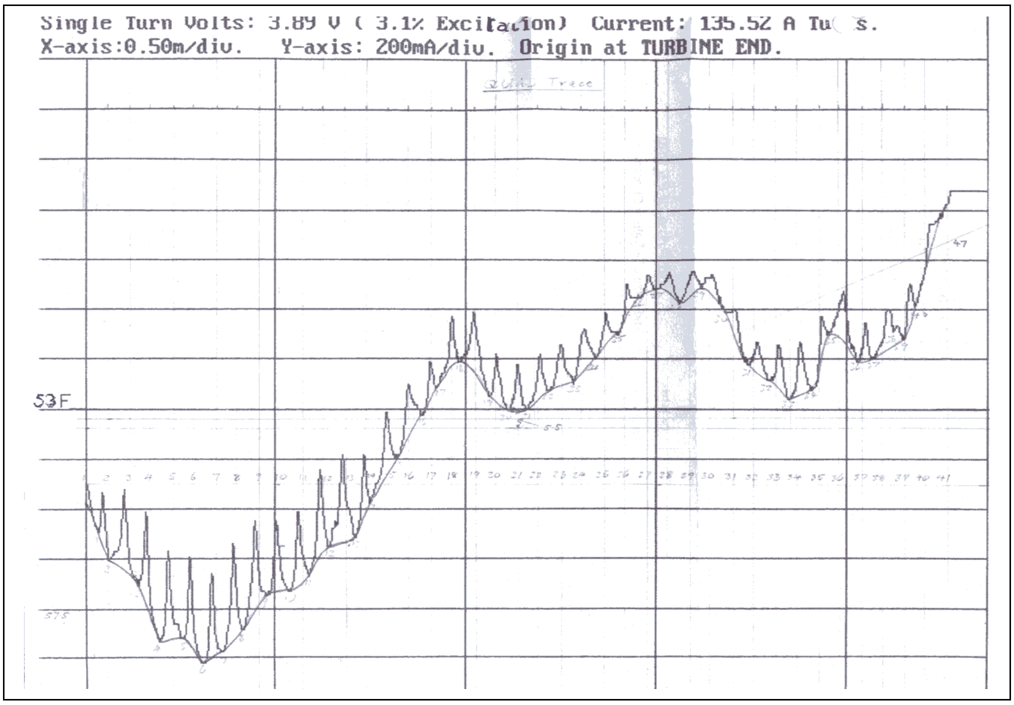

Figure 26[32,Fig;2] *QUAD* trace at a core joint, with the DC offset removed

5.2 2^{nd} step in evaluating delta is plotting *PHASE / QUAD* points

QUAD and *PHASE* values have to be read off the traces by which to plot points on a *PHASE / QUAD* diagram (Figure 27). It is necessary to decide which values to read off the traces at corresponding longitudinal positions. There are four possibilities:-

a) the actual trace, b) a minimum envelope, c) a mean curve, or d) a maximum envelope.

As discussed in Section 2.6.3.2(ii), it is considered that the variations along the traces, caused by vent ducts, arise from reduced magnetic permeance. Therefore, the deviation must be an excursion towards zero and the true value would be that given if there were no such deviations. It is argued[28], therefore, that the envelope touching the maximum values are those which are to be selected for drawing the *PHASE / QUAD* diagram (Figure 27). *PHASE* and *QUAD* scales are the same in this Figure.

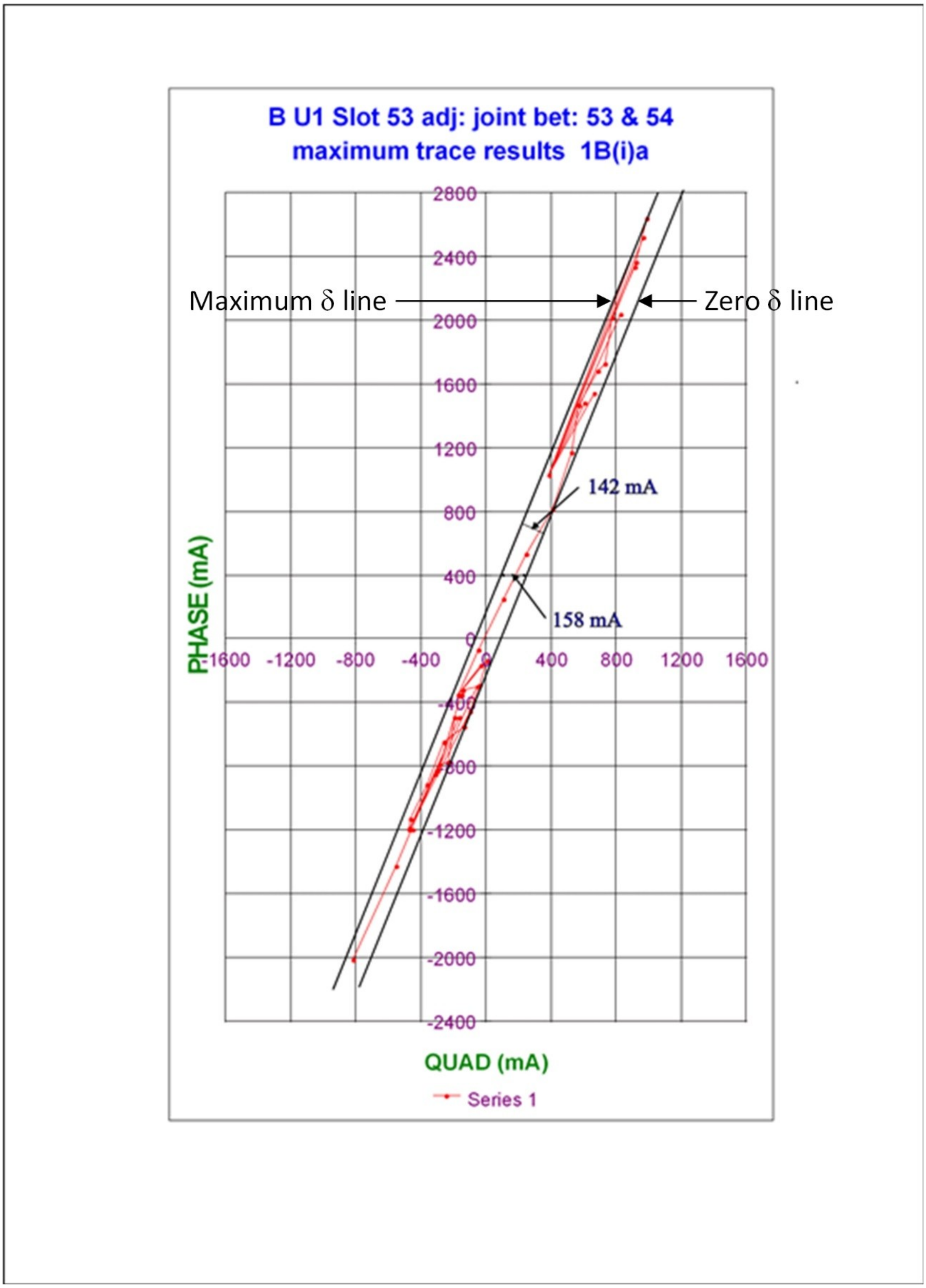

<u>Figure 27</u> ***PHASE / QUAD*** **plot of EL CID results adjacent to a core joint with offset removed**

5.3 3rd step in evaluating delta is determining the "zero delta line"

From knowledge of the phasor diagram of Figure 24, it is recognised that the line, which touches the right-hand side of the plotted points, is the "zero delta line". Occasionally, a difficulty arises when there are too few outstanding points to provide a confident reference for the "zero delta line". It may be necessary to try more than one position for the "zero delta line", but this is exceptional.

The method of determining ***delta*** for any other electromagnetic condition is the same as for this case (i.e. proximity to a core joint), except that the reference phasor diagram has to be identified appropriately.

5.4 4th step in evaluating *delta* is final determination of the *delta* value

A line parallel to the "zero delta line" is drawn in Figure 27 to touch the left hand side of the points. The orthogonal distance between these two lines gives the maximum value of ***delta*** **(i.e. $\boldsymbol{delta_{max}}$)**. A value of $\boldsymbol{delta_{max}}$ less than the criterion of 100mA[6,p.17] indicates an acceptable condition of the intersegmental insulation. If $\boldsymbol{delta_{max}}$ exceeds the criterion, it is desirable to identify where the insulation is degraded (i.e. ***delta*** is high) by evaluating each individual value. This requires measurement of the orthogonal distance from each plotted P,Q point to the "zero delta line". Such measurement appears likely to be subject to error. This is addressed in Section 7.3 (p.92).

Chapter 6 Repeatability of EL CID results after a significant interlude

6.1 Comparison of EL CID results after a 12 year interval

Figure 28 is the record of ***delta*** values obtained in 2007 for a particular large hydrogenerator, and Figure 29 is the comparable record obtained in 1995 for the same machine.

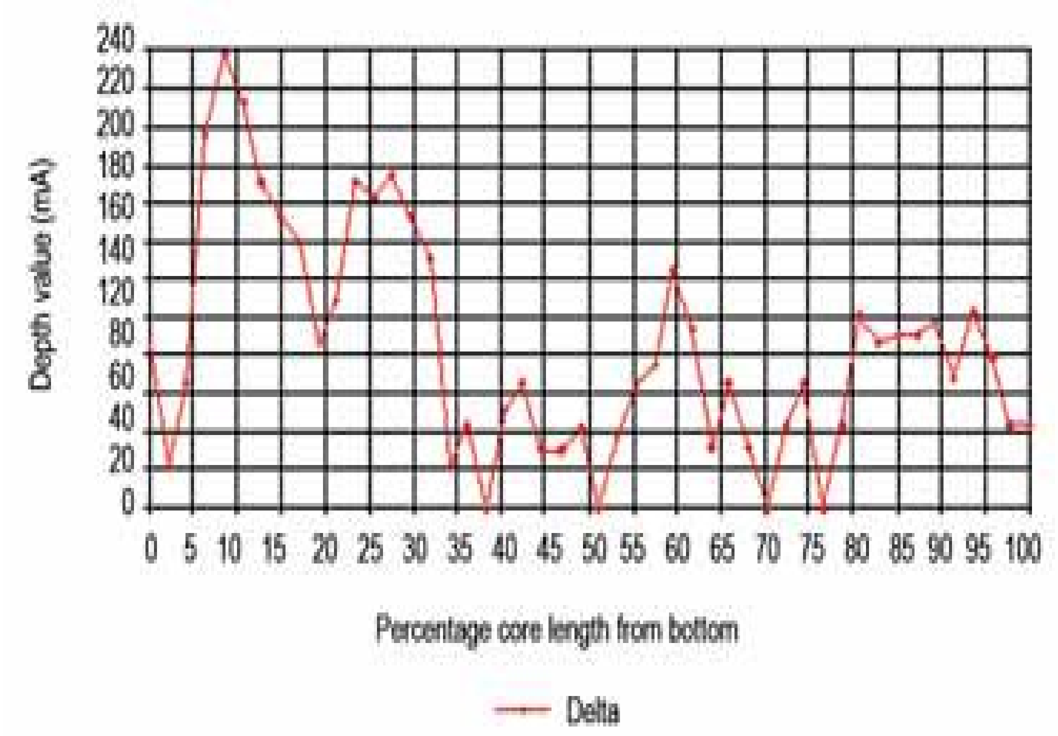

Figure 28 ***delta*** **values from an EL CID test in 2007 for the same machine as Figure 29**

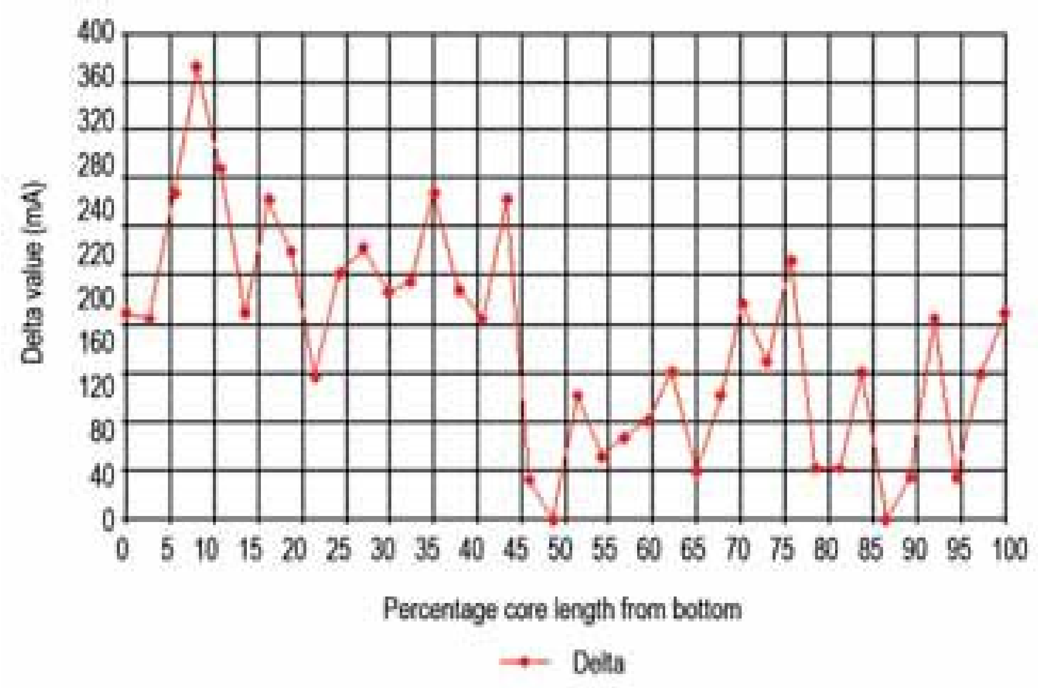

<u>Figure 29</u> ***delta*** **values from an EL CID test in 1995 for the same machine as Figure 28**

It is significant that the maximum ***delta*** value occurs at the same location along the stator core length for both tests.

The general distribution of ***delta*** values is comparable, confirming the repeatability of an EL CID test. This is significant with regard to the use of EL CID as a condition monitor.

It might have been expected that the value ***delta*** would have increased over a 12 year period of service, whereas the indication generally is of a reduction. Some possible reasons are judged to be that a) the core had become better consolidated, b) the modern version of EL CID equipment may have performed with greater accuracy, c) any slight off-set of the excitation coil through the stator bore from the machine centre-line originally may have been corrected.

6.2 Further discussion of the results shown in Figures 28 and 29

It is observed that the values of ***delta*** indicated by the analysis of *PHASE*, *QUAD* values recorded over a large portion of the core length in Figures 28 and 29 are greater than the normal acceptance criterion of 100mA[6,p.17]. The integrity of the core insulation is not doubted, since the relevant machine has had many years of good service, without remedial attention to the core. This raises yet another problem requiring a solution in connection with EL CID.

. This is discussed in Reference 26. Briefly, attention is focused upon the possible effect of the cut edges which are exposed at a core joint. Various measures have been applied by different manufacturers with a view to insulating these vulnerable lamination edges. In one case, the practise has been to apply varnish insulation to cover both the main surfaces (top and bottom sides) together with the edges. Core joint faces, however, are particularly vulnerable to the relative movement which undoubtedly occurs in service. Other manufacturers have endeavoured to protect against such movement by inserting sheets of insulation material, but experience has shown that it is very difficult to maintain these in place.

Experience indicates, therefore, that, even in a sound core, detection of higher than normal circulating current values between adjacent laminations at core joints may be expected. This may be so, because current paths between laminations are envisaged as being well distributed along the radial edge of laminations at a joint. This is understood as follows:- There are no perfect insulators. Slight circulating current must develop along the radial depth of the stator core. Without any of this becoming unacceptable, the total may add to a greater value than is usually detected. Although the bulk of the current is buried in the radial depth of the core, it is known that EL CID can detect electric current which is quite far distant from the surface of the stator **bore**[28]**.**

Determination of an acceptable criterion at core joints remains to be undertaken, but it will be shown in Section 7.6 that the lack of such a criterion is not necessarily a major difficulty.

Chapter 7 Correlation of EL CID results with a deliberately imposed fault in the interlamination insulation[29,30].

This is the culmination of the candidate's work being submitted, with a view to greater general understanding of the EL CID technique, giving increased confidence in using and accepting its results.

References 29 and 30 are the published results of the analysis of EL CID test results at a core joint, where a fault had been deliberately created in the interlamination insulation. Both papers are identical except for their titles. Subsequent to the publication of Reference 29, it was regarded by the editorial staff of Dam Engineering, who claim only to publish "International papers of technical excellence", as appropriate for them to request permission to include Reference 28 in their journal. The candidate agreed[30].

Although Chapters 5 and 6 give actual values for EL CID results, these can only be used as an indication of their validity, since the core condition was not known absolutely. The results evaluated in this section actually pinpoint where a fault had been deliberately imposed.

The opportunity for this exercise arose from the work reported by Paley et al[31]. As 4 inches of the upper end laminations of the core of the machine concerned were due to be replaced, after an HFRT check, artificial faults (by screw compression of a short copper strip into the laminations[31]) were imposed in selected locations, prior to an EL CID test. The results showed good correlation between fault locations identified by EL CID, and the known locations, except at core joints. The report in Reference 31 stated that EL CID results at core joints were ***useless*** due to the disturbed electromagnetic conditions produced by the small air gap inherent at a core joint.

It seemed most appropriate, therefore, as a final confirmation of EL CID as a valid technique, to analyse the results, which fortunately were available in Reference 30. The several steps in this task are basically the same as those in Chapter 5, as briefly repeated below, plus an extension.

7.1 1st step of the analysis, i.e. obtain corresponding P & Q values

At corresponding distances along the stator core trace axis, mark off ordinates to the recorded *PHASE* and *QUAD* traces (Figure 30) to obtain corresponding *PHASE* and *QUAD* values. Tabulate these on a spread sheet. Note: the original caption above Figure 30 labelled the *QUAD* results ***incorrectly*** as “unusable”.

7.2 2nd step of the analysis, i.e. plot *P,Q* points

Plot the tabulated points on a *PHASE / QUAD* diagram (Figure 31). The appropriate values are determined as discussed in Sections 3.1.4. and 5.2. In view of a procedure introduced to enhance accuracy[32], it is desirable to rotate the QUAD axis clockwise through 180° , and then the whole diagram through 90° clockwise[31]. This brings the QUAD axis to be vertical on the page.

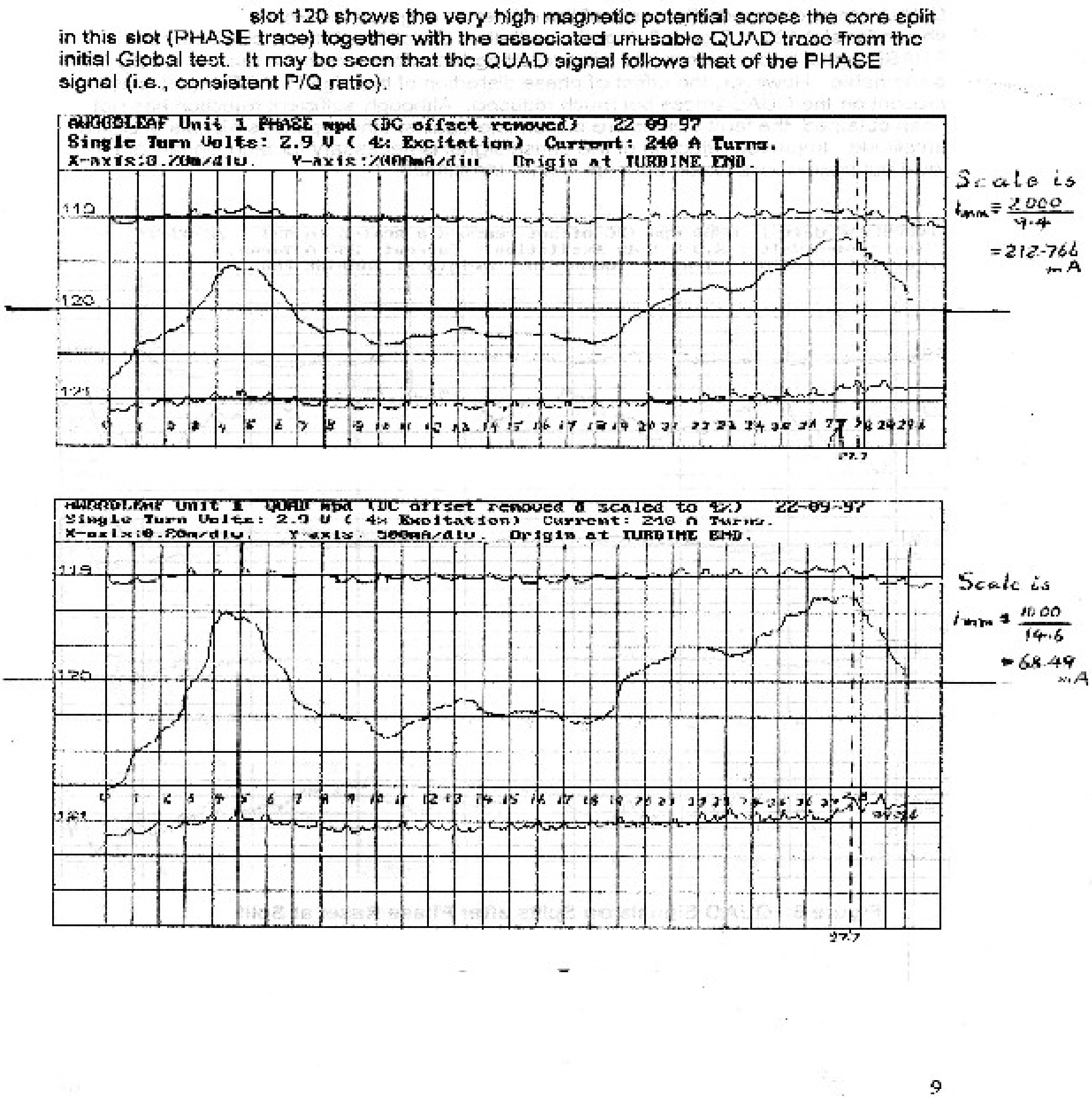

Figure 30 ***PHASE*** **and** ***QUAD*** **traces from EL CID test at joint slot 120 after insertion of an artificial fault (Reprinted from Reference 31, also 29 & 30)**

7.3 3rd Step of the analysis - Determine the "zero delta line"

From the various alternatives of the phasor diagram, Figure 24 is identified as appropriate. The "zero delta line" is determined accordingly. The accuracy of the determination of ***delta*** depends upon two factors:- i) the location of the **"**zero ***delta*** line**",** ii) the accuracy of measurement of the distance (i.e. the length of a "***delta*** line") of the relevant P/Q point from the **"**zero ***delta*** line**".** When equal P and Q scales are used, ***delta*** values are given by the **<u>orthogonal</u>** distance from a given P / Q point to the "zero ***delta*** line".

Since P values are so much greater than Q values, it can be seen that error may be introduced in determining the length of the ***delta*** line, both regarding the position of the "zero ***delta*** line" and the measurement of the ***delta*** line itself. In order to achieve maximum accuracy, a special routine was developed as reported initially in Reference 32, and repeated substantially in References 29, 30 & 33. This involves increasing the scale for plotting *QUAD* values, as shown in Figures 31, for which, as mentioned above (p.91), it is most convenient to have the QUAD axis vertical on the page. This is to suit computer work.

Two benefits accrue from this technique:- a) The "zero ***delta*** line" can be located more accurately. b) The length of the ***delta*** lines can be measured more precisely.

For clarification, Figure 31 is repeated in Figure 32, with the same orientation of the axes.

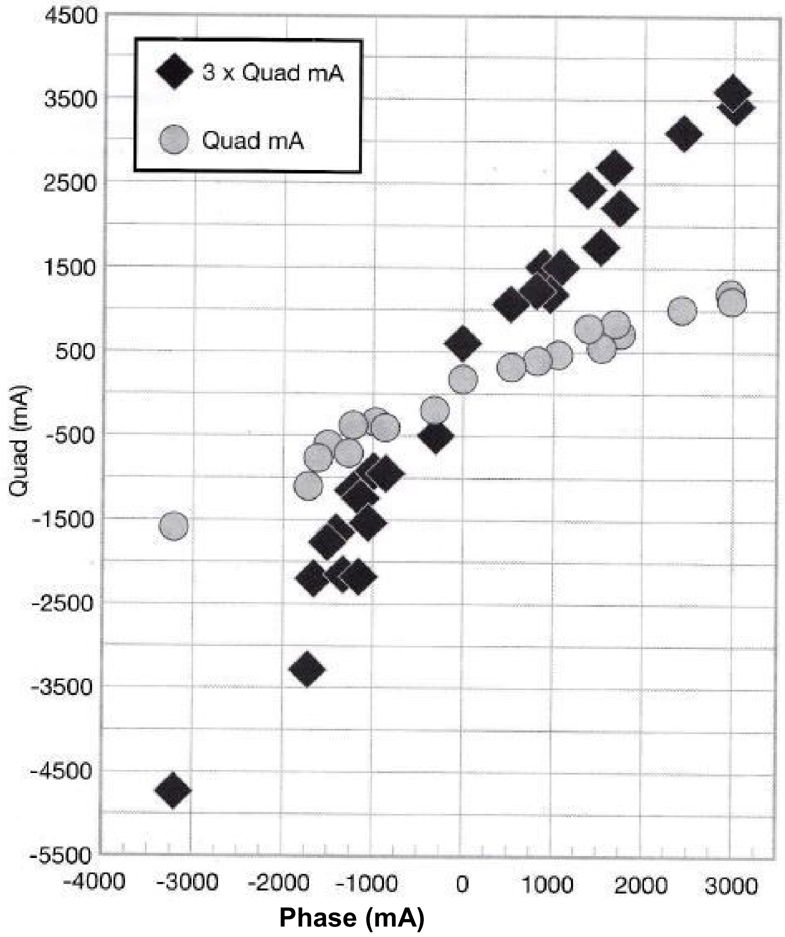

Figure 31. Spread sheet plot of recorded *PHASE* and *QUAD* values at a core joint

Location of the "zero ***delta*** line" is initially with reference to the plot of *P/Q* values (Figure 32) with the enhanced QUAD scale. It can then be readily transferred to refer to the plot of *P/Q* points with equal scales, by proportioning the position of the "zero ***delta*** line" according to the different scales. If the new "zero ***delta*** line" does not have a good fit with the plot of P/Q values with equal scales, it is necessary to adjust the position relative to the plot of *P/Q* values having an enhanced QUAD scale.

7.4 4th Step of the analysis. Determining *delta* values

The next problem is to determine the direction of the ***delta*** lines, since it is not the simple matter of drawing lines orthogonally to the "zero ***delta*** line". The method of compensating for unequal *PHASE* and *QUAD* scales originally set out in Reference 32, repeated in References 29, 30 & 33, involves construction of trapezoid AA'BB' (See Figure 32). Briefly, the starting point is A on the "zero **delta** line" for the P,Q points with the increased Q scale. The line AA' is drawn parallel to the QUAD axis to A' on the "zero ***delta*** line" for *P,Q* points having equal scales. The line A'B' is then drawn orthogonally between the boundary lines for the *P,Q* points having equal scales. From B', a further line is drawn parallel to the Q axis to cut the boundary line of the *P,Q* points with the increased Q scale at B. The line BA provides the required direction of the "***delta*** lines", i.e. the lines from which the magnitude of ***delta*** values are derived.

The required ***delta*** values are evaluated from the length of the "***delta*** lines" drawn from each P,Q point to the "zero ***delta*** line" in the direction determined. There are alternative ways of making this measurement:-

i) direct ruler measurement and a simple division by the increased QUAD scale factor, This is useful for achieving a quick result.

ii) use of endpoints given by the computer grid, plus application of the Pythagoras theorem, and then simple division by the QUAD scale factor, Theoretically slightly better than i) above, but no real difference in practice.

iii) as ii), except for division of the *QUAD* values by the scale factor before applying Pythagoras. This is the most accurate measurement of ***delta.***

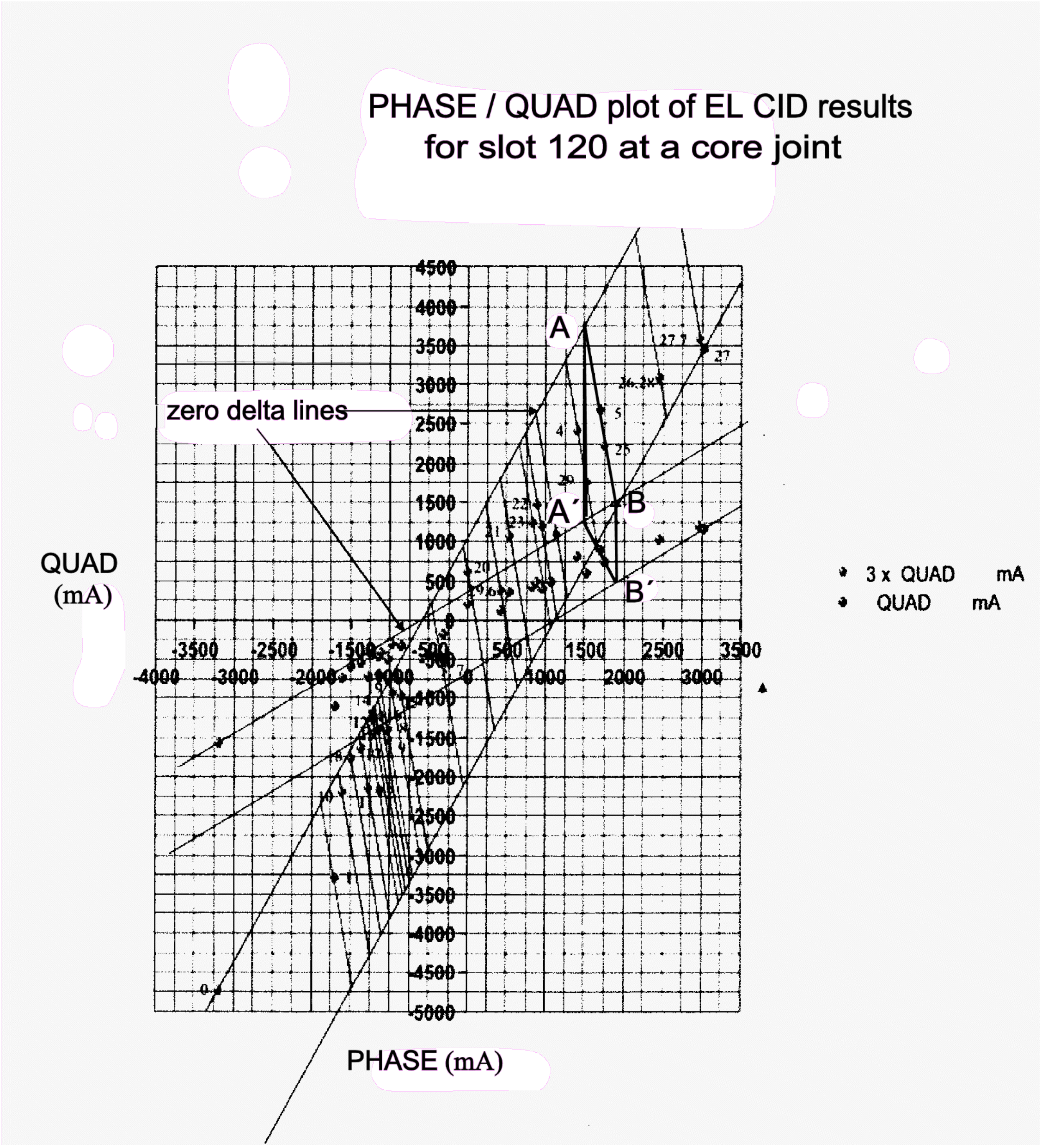

<u>Figure 32.</u> Plot of *PHASE* and *QUAD* values with delta lines added

<u>7.5 Identify the location of a pre-established fault at a core joint</u>

The result of the determination, by all three methods set out above, of ***delta*** values for this case of a pre-established interlamination insulation fault at a core joint, is plotted in Figure 33. The pronounced spike of ***delta*** values is located less than 2½% of the core length different from the reported 4 inches (approximately 100 mm) from the top of the stator core. But it is not known how precise the reported 4 inches was. It is noted that conversion alone from inch units to mm incurs over 1% difference. Moreover, from other EL CID traces in Reference 31, there is doubt regarding the consistency in the length of trace, which puts doubt on the exact correspondence of the length of trace with the core length. It is considered, therefore, that Figure 33 clearly identifies the position of the deliberately imposed interlamination insulation fault. This demonstrates, when the method is adequately understood, the validity of the EL CID technique in this most difficult of electromagnetic field situations,

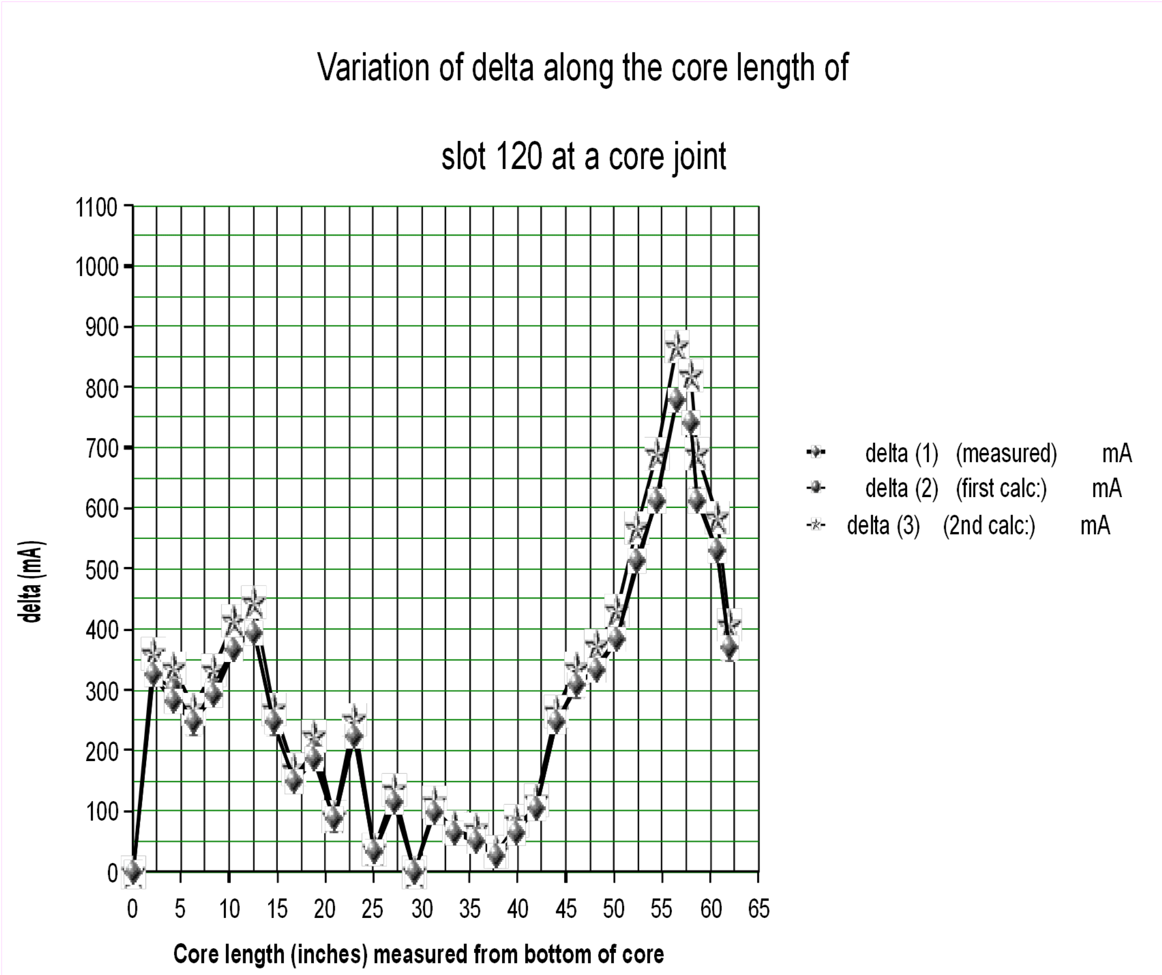

<u>Figure 33</u> Variation of *delta* along the length of the core at a joint slot

7.6 Further discussion of the results shown in Figure 33

It is observed that the ***delta*** values generally in Figure 33 are significantly higher than the normally acceptable criterion of 100mA[6,p.17]. This feature of core joint EL CID results was discussed in Section 6.2. The important factor in the assessment of EL CID results at core joints, therefore, is the distribution of ***delta*** along the core, i.e. in the longitudinal direction.

Whilst it is evident that there is significant degradation of the interlamination insulation where the fault was deliberately imposed, the question arises regarding the integrity elsewhere as values of about 400mA are observed. But it had already been concluded that such values might be expected[26] at core joints. Also, no data is recorded regarding the condition of the interlamination insulation other than in the upper part of the vertical core. Since, however, after the HFRT check, remedial action was only considered necessary for the top 4 inches, the indication is that the condition of the remainder was judged to be adequate.

It is concluded that EL CID is well able to identify stator core interlamination insulation degradation ***in every situation for a salient-pole machine***, as well as for round rotor machines.

Chapter 8 PHASE reference reset[34]

8.1 The need for Phase reference reset

In the early days of applying EL CID, relatively high values encountered at core joints promoted the practise of resetting the PHASE reference. The motive for this is clearly illustrated by Figure 34 where the *QUAD* values are very much less than in Figure 31. But the magnitude of *QUAD* values at core joints is not a problem for the modern version of EL CID equipment. That is not to be confused with removal of the "DC" value (See Figure 31), which is a built-in feature of the modern EL CID package.

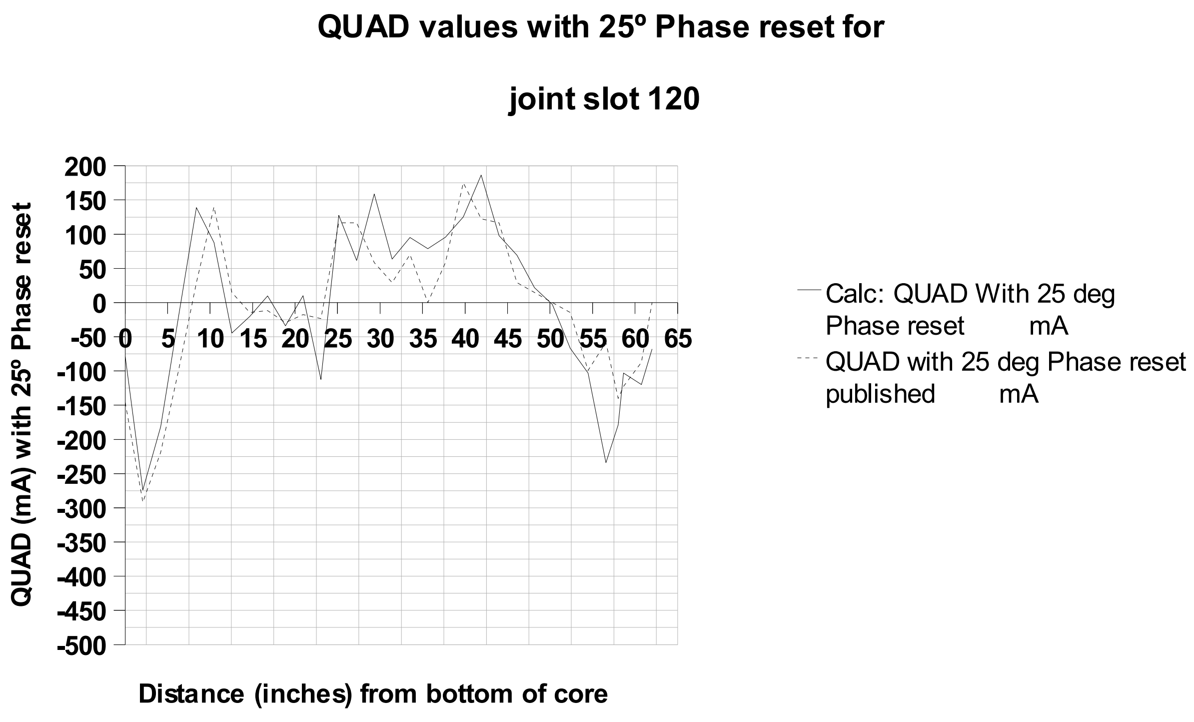

Figure 34 ***QUAD* values with the PHASE reference reset for the case analysed in Chapter 7**

(Note:**"Calc: *QUAD* with 25° Phase reset"** values are calculated, assuming 25° Phase reset, from *QUAD* signals recorded without Phase reset.
And **"*QUAD* with 25° Phase reset published"** values are as published[31] with an unrecorded degree of reset, but deduced from other information to have 25°.)

8.2 The consequence of resetting the *PHASE* reference[29,30]

It is immediately evident, from Figure 34, that the plotted *PHASE / QUAD* values do not identify the location of the artificial fault, when the PHASE reference is reset. The significance of the *QUAD* values has been lost. In general *QUAD* values in themselves are clearly insufficient for fault identification. Only in the circumstances for which Figure 21 applies (i.e. no core joint, stator winding or rotor) would the *QUAD* values be approximately significant themselves.

If, for some reason, it should be considered necessary to reset the *PHASE* reference when making an EL CID test, then the values obtained need to be referred back to the basic axes[1,p.103]. This can be readily achieved using the appropriate geometrical equations[34,p.88].

8.3 Further examples, of "*delta*" evaluation, for which the *PHASE* reference is reset and also when not reset

It is demonstrated below that if EL CID results, obtained with *PHASE* reset, are not referred back to the basic axes, the result will be ***delta*** values which are inaccurate, and/or their distribution distorted along the length of the core.

8.3.1 *“delta”* evaluation at a stator core location remote from any core joint, with no stator winding in the core and no rotor in-situ.

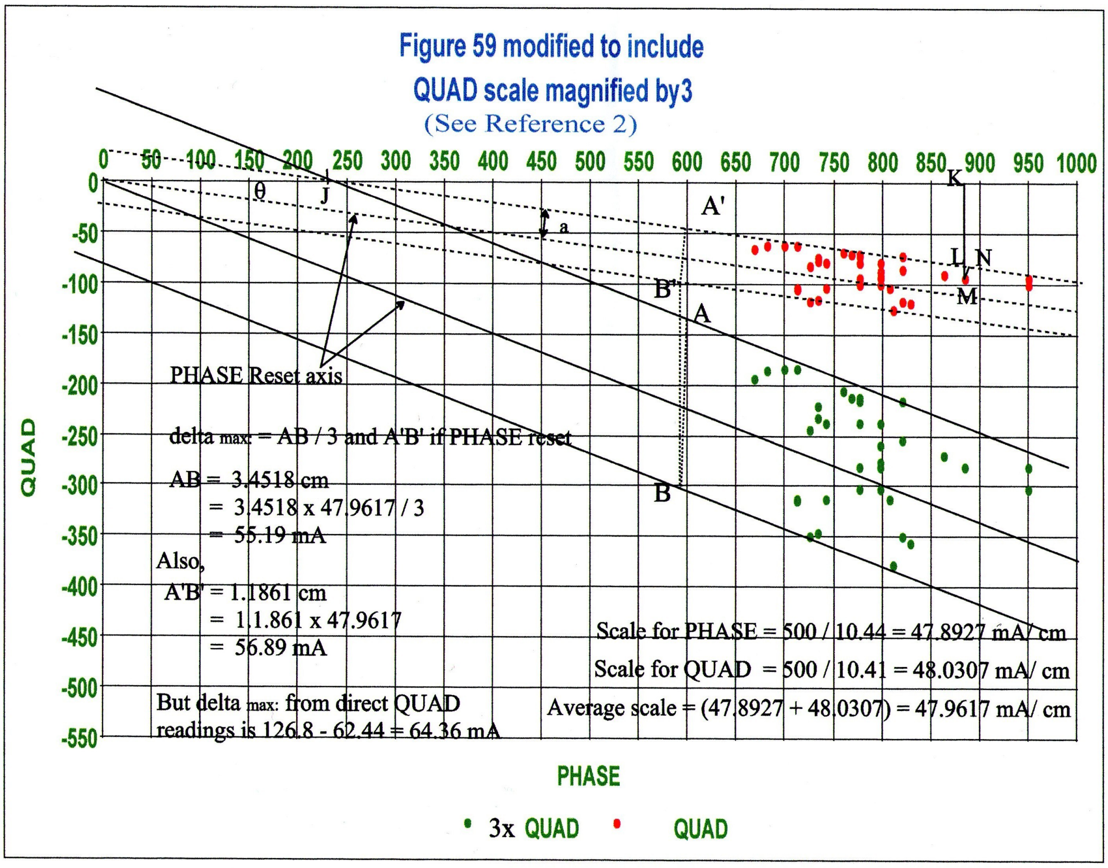

Figure 35 (Figure 3 of Reference 34) *PHASE/QUAD* plot of EL CID results for a slot remote from a core joint, with no stator winding in the core and no rotor in-situ

In Figure 35, as identified in Reference 34, the theoretical zero delta line is the PHASE axis. It is evident that there is an offset from the theoretical zero delta line. The reason is not known, although discussed in Reference 34, where it is not considered significant. Evaluation of ***deltamax*** is derived, for no *PHASE* Reset, by subtraction of the offset (i.e. the minimum *QUAD* value) from the maximum value. Evaluation of ***delta*** throughout the core length is obtained similarly by subtracting the offset value from each of the *PHASE/QUAD* points.

The result is displayed in Figure 36 by the red line.

The effect of resetting the PHASE axis is investigated by drawing a PHASE Reset axis through the estimated centroid of the group of *PHASE/QUAD* points produced by the EL CID test. Although results from an EL CID test with the PHASE reference reset were not obtained directly, they were simulated by taking the angle (θ) by which the PHASE reference was reset, and calculating revised $\boldsymbol{delta}_{reset}$ values from the equation[33] derived as follows:-

$$\boldsymbol{delta}_{reset} = \text{LM} \cos\theta$$

$$= (\text{KM} + \text{KL}) \cos\theta$$

$$= \text{KM} \cos\theta + (\text{OK} - \text{OJ}) \tan\theta . \cos\theta$$

$$= \text{KM} \cos\theta + (\text{OK} - [\text{a} / \sin\theta]). \tan\theta . \cos\theta$$

$$= \underline{Q\cos\theta + P\sin\theta - a}$$

where P, Q and θ are referred to the basic axes, and a = the orthogonal distance between the **PHASE** reset axis and the parallel line enclosing the minimum *P, Q* points. The result is displayed by the green line in Figure 36. This provides the results for a further example[34] of evaluation of ***delta***, both when the PHASE reference is reset and when not reset.

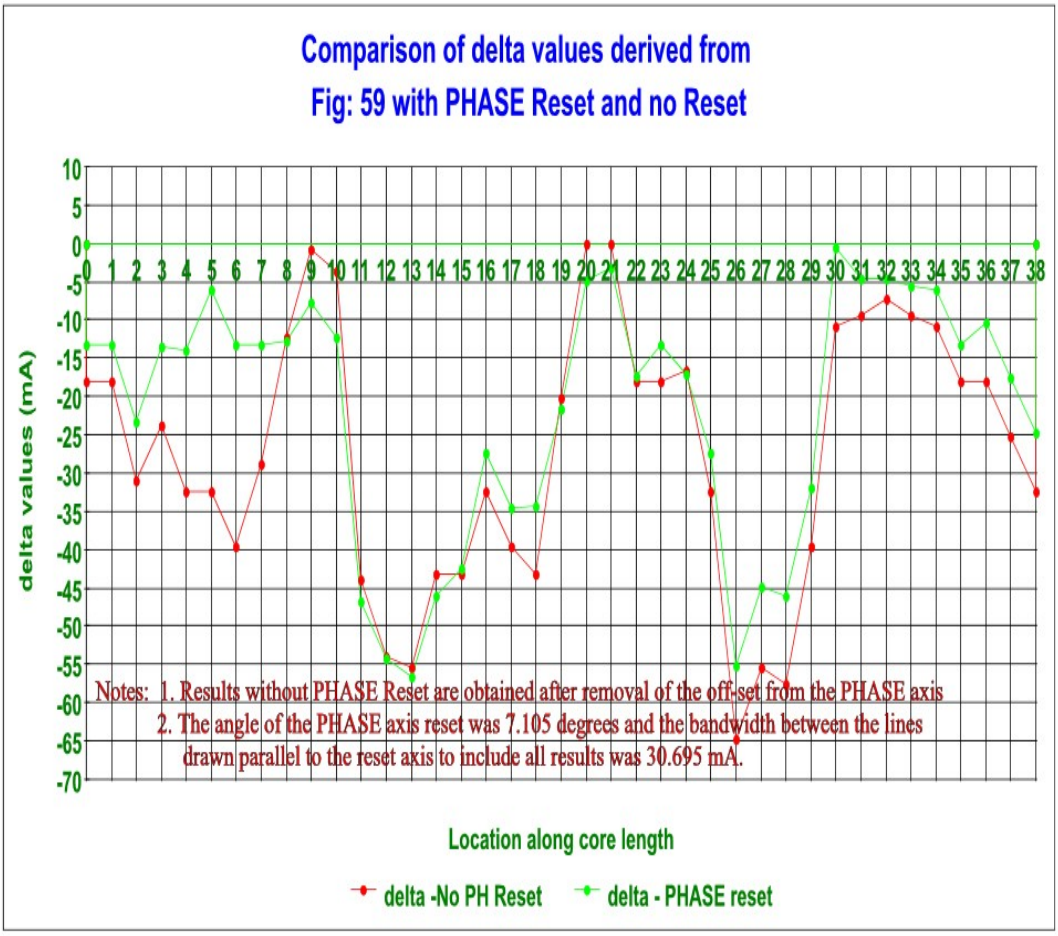

Figure 36 [Figure 4 of Reference 34] Comparison of delta values with and without PHASE reference reset

For the most part of the core length, Figure 36 shows that there is close agreement between the *P,Q* points for which the PHASE reference is not reset and also for which it is reset. But in part of the core there is significant difference. This is undoubtedly due to the choice of reset angle (θ), which indicates that there is an inherent weakness involved in resetting the PHASE reference.

8.3.2 "*delta*" evaluation close to a stator core joint, with both stator winding and rotor present, and no PHASE reference reset

Results for this situation are plotted in red in Figure 36.

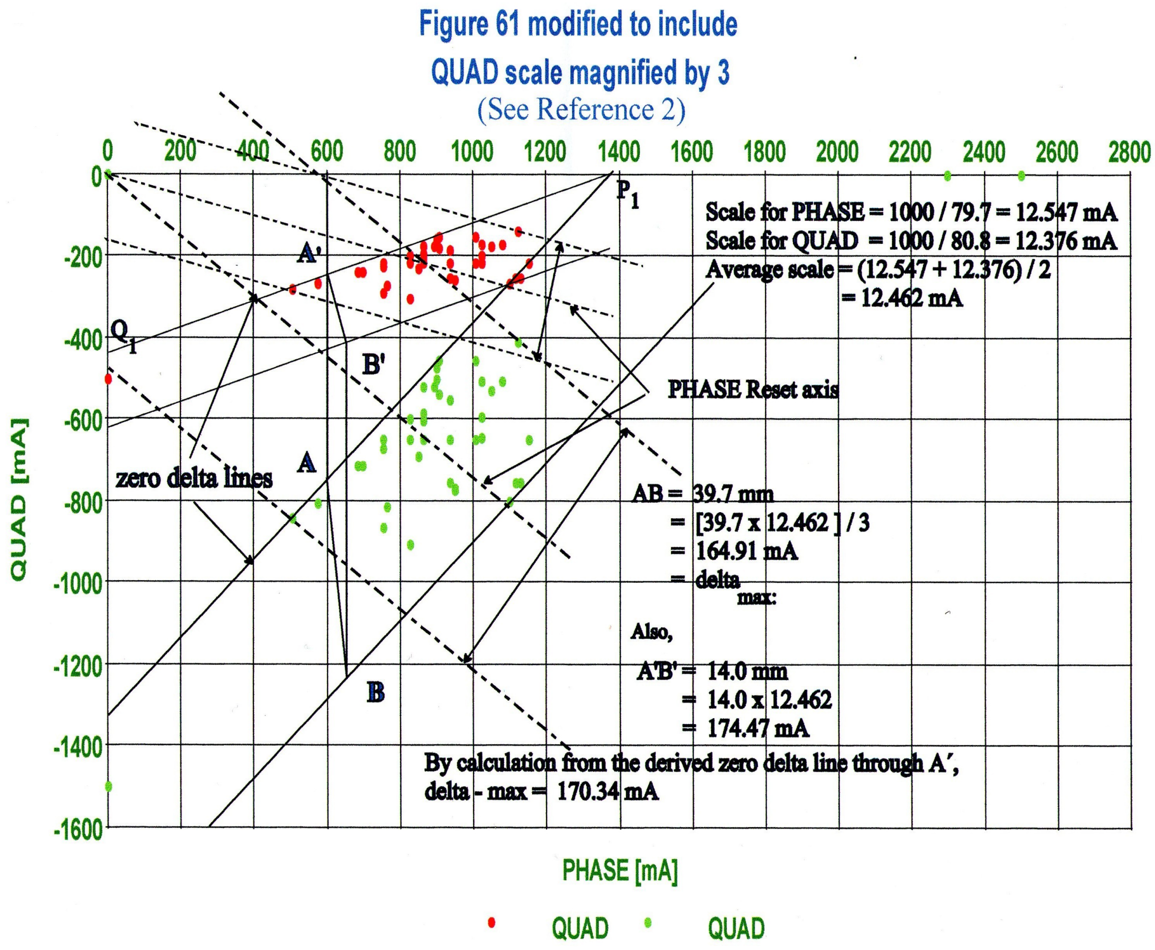

Figure 37 **(Figure 5 of Reference 34)** ***PHASE/QUAD*** **plot of EL CID results for a slot near to a core joint, with both stator winding and rotor in-situ**

Evaluation[34] of $delta_{max}$, including that by application of the procedure described in Chapter 7 (i.e. introducing an increase in the QUAD scale) produces $delta_{max}$ values as in table 2. The several steps involved are set out below.

a) (i) The first step (before introducing unequal scales) is to establish the "zero delta line" for *PHASE(P), QUAD(Q)* points plotted on axes having equal P and

Q scales. From this "zero delta line", the parallel line embracing the largest "delta" value can be drawn.

(ii) In many cases the plot of *P,Q* values will readily indicate where the "zero delta line" is to be found and drawn. If this is not the case, it is necessary to consider which phasor diagram applies. Typical cases have been illustrated in various publications, particularly Reference 1. Not all cases are covered, of course, which possibly necessitates the creation of a new version by considering how the case under consideration may be expected to modify the nearest existing example. It may be necessary, however, to return to basic principles, with occasional reference to someone of greater experience.

(iii) The case in hand is not fully covered already by any published phasor diagram, but the starting point is considered to be that of Figure 25. Account is taken there of stator winding circulating current, and the presence of a salient-pole rotor, it is, however, remote from a stator core joint. The proximity of a core joint introduces further leakage flux, which is in the same direction as the flux leaking from the stator to the rotor. But the influence of core joints does not usually extend very far. Hence, Figure 25 essentially includes all the phasor components required for the case under consideration, with some change in the magnitude of the phasor I_R.

The phasor diagrams are not produced to scale, therefore, it is permissible to assume a diagram essentially similar to Figure 25. That view might need reconsideration in the light of actual *P,Q* values obtained from EL CID signal records.

(iv) In this instance it is evident from the Plot in Figure 37 of *P,Q* values that the above view is valid. The *P,Q* values plotted as "red" points are those obtained directly from the EL CID output, plotted with equal scales.

b) In order to check for possible error in locating the "zero delta line", the routine of increasing the Q scale is employed. The subsequent *P,Q* points are plotted in Figure 36 as "green" points. It is evident that a line can be reasonably applied to the upper points nearest to the PHASE axis, which is the relevant "zero ***delta*** line" as already defined by Figure 25. It is identified from the plot of the "green" points for greatest clarity of its position, and is then transcribed to lie with reference to the "red" points by proportionality, taking account of the increased Q scale.

The validity of the chosen "zero ***delta*** line" is confirmed by it lying in the same proximity to the "red" points, as it did when applied to the "green" points.

c) As identified in a) above, the parallel line to embrace the largest "*delta*" value is drawn relative to the "zero ***delta*** line" produced by either set of *P,Q* points.

d) By identification in the basic EL CID phasor diagram, for equal *P* and *Q* scales, the length of the line drawn orthogonally from the "zero ***delta*** line" to any particular P,Q point represents the relevant value of ***delta*** for that axial location along the stator bore.

e) With reference to the plot of P and Q values for which the scales are unequal, it is evident that delta lines are not orthogonal to the "zero ***delta*** line". It is necessary, therefore, to deduce the angle required. The candidate has evolved and published a routine in Reference 32, and incorporated into References 29 and 30, whereby the required direction of the delta lines can be determined.

In Figure 37, the orthogonal direction, identified by line $A'B'$, applicable when equal scales are used, is converted by the routine mentioned above to line AB. After establishing the direction of one delta line, those for all other P,Q points, plotted with unequal scales, are given by lines parallel to AB.

f) The value of ***$delta_{max}$***, or, in fact, delta for any P,Q point, may be determined finally by five ways, as identified below.

i) A ruler measurement of the delta line. In the case of the plot of P,Q points with equal scales, the $delta_{max}$ line is the orthogonal line between the "zero delta line" and the parallel line embracing all points. "d***elta***" for individual points is obtained by measuring the relevant orthogonal distance to the "zero ***delta*** line".

ii) A ruler measurement of the length of ***delta*** lines constructed as referred to above, (Section 8.3.2e), with increased QUAD scale. This line is not orthogonal to the two parallel lines. Division of this measurement by the QUAD axis scale factor provides a value of delta, which is slightly approximate. See below in **v)**.

iii) Accurate ruler measurements are difficult. Therefore, it is better to use the computer grid to determine the end points of a particular ***delta*** line for the plot of P,Q values using equal scales, and then calculate the length using the Pythagoras theorem.

iv) The same technique of measurement as in iii) above may also be applied to delta lines obtained from the plot of P,Q values involving an increased QUAD axis scale. A value of delta is then obtained by dividing by the QUAD axis scale factor, as in **ii)** above, with the same caveat.

v) In later papers[29,30], it was clarified that, strictly, the *QUAD* value of the end points of the delta line should be divided by the scale factor, before being combined with the corresponding PHASE values using the Pythagoras theorem.

It has been found that the values of delta obtained by the different methods are not greatly different. In a particular case the variation was only +2.4% to -3.8%.

Method	**"$delta_{max}$"** in mA
Ruler measurement of AB	164.91
Ruler measurement of A´B´	174.47
Grid determination of AB	164.26
Grid determination of A´B´	174.82
Calculation for A´B´	170.68

Table 2 Summary of the evaluation of *$delta_{max}$* by the methods identified in Section 8.3.2 without applying PHASE reference reset.

8.3.3 Close to a stator core joint, with both stator winding and rotor present, and PHASE reference reset applied

The choice of the PHASE reset angle is a matter of opinion. It is normally chosen so that the revised axis passes through the region where it is thought that ***delta*** will be least, after a preliminary scan. This is difficult to determine, and in Figure 37 it so happens that the PHASE reset axis passes through the location along the core where **delta** is a maximum. Inspection of Figure 37 indicates that, without referring the PHASE reference back to the basic axis (assuming that it had initially been obtained with the PHASE reference reset), the value of **delta** indicated by the lines parallel to the reset axis is 295.3mA, which is far different from the values in Table 2 above.

It is evident, therefore, that resetting the PHASE reference, without referring the results back to the basic axes, produces an incorrect analysis, indicating that the magnitude of fault circulating current (***delta***) and its distribution along the longitudinal length of the core is distorted.

Chapter 9 Conclusions

9.1 The original need for EL CID

A major rise in the specific rating of large steam-turbine-driven round rotor generators in the 1970's due to the introduction of direct-water- cooling resulted in a severe increase in the electrical stress on the stator core interlamination insulation. Due allowance for this was not always incorporated in new generator designs, leading to failure of the insulation.

An urgent need arose for a means of checking the effectiveness of remedial work on stator cores subjected to such failures, which would be less time consuming than the traditional High Flux Ring Test (HFRT). The Central Electricity Research Laboratory (CERL), the research arm of the British Central Electricity Generating Board (CEGB), was tasked to develop such a new facility, with the result that John Sutton, a physicist on the staff of CERL, invented an Electromagnetic Core Imperfection Detector (EL CID)[3], which was a much simpler and easier means than HFRT.

9.2 Problems arising when EL CID was applied to hydrogenerators

The success of EL CID in its initial application to turbo-generators naturally promoted the idea of its application to water-turbine driven salient-pole generators, and similar large machines. This was demonstrated, with considerable success on an appropriate machine in the manufacturer's factory. The only indication of a problem was extremely large signals arising from encounter at the core joints with a major disturbance of the electromagnetic field, although not due to fault conditions. The suggested solution at the time was to move the reference coil to the core joint, in effect resetting the Phase axis.

When EL CID was subsequently applied on site, the core joint problem was again encountered, and the resultant signals were not reduced to acceptable proportions by the recommended tactic. This remained a major stumbling block causing wide spread lack of trust in the reliability of EL CID in the hydro-electric field, and subsequent discarding of EL CID in that context.

EL CID continued to be used on hydro-electric machines as a valuable monitoring device for the major part of their stator cores. There were, however, other EL CID result phenomena encountered :- generally higher readings than appeared justified, traces of the EL CID output exhibited a slope, sometimes a curvature of the axis, plus unexpected and initially alarmingly high values at the ends of the stator core.

9.2.1 Solution of problems due to the form of excitation winding

Since it was usually required that the rotor was removed for access when remedial work was in hand, the form of the excitation winding for EL CID applications to turbo-generators was generally a group of turns down the centre-line of the stator(i.e.Figure 5c), necessarily passing over the core ends, Although this is applicable to hydro-generators when major refurbishment is being undertaken, in general an alternative is desirable, particularly if the object is primarily to establish a “footprint” of the core condition, i.e. a reference when carrying out subsequent comparative checks.

But each method of applying the excitation winding has presented problems which require understanding in order to eliminate their impact. Appropriate solutions have been demonstrated in this record of the candidate's investigations. Briefly:-

i) the required mmf should be calculated in terms of trace turn voltage;

ii) a note should be made of environmental factors likely to cause electromagnetic disturbance (e,g, operational state of nearby machines, magnetic materials in the area, the test machine's constructional features, including its state of erection);

iii) form 5c cable in the bore should be carefully aligned to the stator axis;

iv) the distance from the core ends should be not less than 1 metre, if possible;

v) an adequate distance should be maintained for the EL CID sensor from excitation turns.

9.2.2 Counteracting the pole-proximity effect

If the salient-pole rotor of a hydrogenerator is in-situ, removal of one, or possibly two poles may be necessary to provide access for the EL CID operator. In some cases, adequate physical access is available without removal of poles. The presence of salient-poles always has some “pole-proximity effect”, i.e. curvature of the EL CID trace axis, although for some configurations the effect may be slight. To minimise this, an adequate distance from the side of nearby salient-poles is required. Mainly, it is important to recognise that the effect may be present.

9.2.3 Analysis of the electromagnetic field at the stator bore

Originally, only a very simple vector diagram, comprising two orthogonal components, was proposed for the electromagnetic field arising from establishing a circumferential magnetic field in the stator iron, and the presence of circulating current between adjacent laminations due to imperfection of the interlamination insulation. The phasor components, known as *PHASE* and *QUAD*, were understood to represent the excitation mmf and the fault current, respectively.

Whilst such a simple phasor diagram was adequate, although not perfect, for EL

CID results from turbogenerators, it was soon evident that it did not represent the situation for hydrogenerators. The original phasor conception required development to a more complex approach. This was provided by regarding the EL CID set-up as a transformer with one or more shorted secondary windings. Whilst one basic phasor diagram was identified, several versions were developed to cater for different situations. One of these very importantly covered circulating current in the stator winding, if present and short-circuited. Other versions allowed for flux leakage between the stator and rotor. Perhaps most importantly, allowance was made for the leakage flux at stator core joints. This permitted the derivation of a solution of the problem encountered at core joints in the original application of EL CID to hydrogenerators having stator cores constructed from more than one part, as required for transportation.

9.3 Overall conclusion

The work described in this thesis covers a wide range of situations which originally were not understood, and resulted in loss of confidence in the EL CID technique for hydrogenerators as an adequate core condition monitor, although useful for checking the adequacy of remedial work, other than at core joints.

Importantly, every known electromagnetic situation at the stator bore has been encompassed satisfactorily. The EL CID results have been reasonably correlated with those produced by the HFRT, although more work in this context would be useful. It is considered that for absolute confidence in the core insulation condition as acceptable it should, in general, meet the 100mA criterion, except at core joints.

At core joints the circulating current evaluated is usually substantially greater than the normal acceptance criterion. Reason for this has been shown. Therefore, it is not considered essential that the actual value should meet the standard criterion. It has been demonstrated that the vital aspect of the circulating fault current, more than its absolute value, is its distribution along the length of the core. This outcome of the work by the candidate is **a most important conclusion**.

It is recognised that at core joints, an immediate analysis of EL CID results is not readily available, but the importance of taking time to achieve this should be seen as well worthwhile.

Finally, EL CID may be applied as a monitoring tool, not only as a check on interlamination core insulation deterioration due to normal service, but also after application of a quality control high voltage impulse test on a coil component of the stator winding. Sutton has shown[35] that such a test may apply a very high electric field to the stator core laminations at the bottom of a slot. This emphasises the need for high quality insulation of stator core laminations subjected to impulse testing. The reliability of EL CID in this context is clearly of first class importance. It should be noted that Sutton's paper has restricted access, but the candidate had approval to reproduce a version of it as Appendix 8.1 in his book[1].

Thesis References

1. Ridley, G. K., "EL CID – Application and Analysis", Ed. 3, Adwel International Ltd./IRIS Power LP, 2007. [Book submitted separately]

2. Bertenshaw, D. R., "Stator Core Interlamination Faults and their detection by Electromagnetic Means", Ph.D. Thesis, University of Manchester, Faculty of Engineering & Physical Sciences, 2014.

3. Sutton, J., "EL CID: an easier way to test stator cores", Electrical Review, Vol. 207, No 1, 1980, pp 33-37.

4. Chattock, A. P., "On a magnetic potentiometer", PHIL. MAG. 24. 1887, pp 94.

5. Rogowski, W. and Steinhaus, W., "Die Messung der magnetische Spannung", Arch. Electrotech 1, pp 141-150.

6. Sutton, J., "Procedures for use of Electromagnetic Core Imperfection Detector (EL CID), CEGB Report, 1981.

7. ***Ridley, G. K., "EL CID application phenomena", Proceedings of the 6th IEE International Conference on Electrical Machines & Drives, Publication No: 376, September 1993, pp 491-498.*** [Full Paper attached as Appendix 8]

8. ***Ridley, G. K., "Pole proximity effect on EL CID results", Proceedings of 8th IEE International Conference on Electrical Machines & Drives, September 1997, pp 346-350.*** [Full paper attached as Appendix 10]

9. Ridley, G. K., "The impact of stator winding circulating current on EL CID results", International Journal on Hydropower and Dams, February 2004, Vol. 11, Issue 1, pp 68-73. [Full paper attached as Appendix 11]

10. ***Ridley, G. K., "Electromagnetic field distortion effects on EL CID tests", Proceedings of the 7th IEE International Conference on Electrical Machines and Drives", Publication No: 412, September 1995, pp 187-193.*** **[Full Paper attached as Appendix 9]**

11. Ridley, G. K., “Hydrogenerator EL CID results referred to High Flux Ring Test Results” Proceedings of Session 2002 of CIGRE, August 2002, Paper 11 – 201.

12. Ridley, G.K.“An ultra-pure water system for a hydro-electric generator-motor” September 1991, Proceedings of the 5th IEE International Conference on Electrical Machines and Drives, pp: 285-289.

13. Klempner, G., Ridley, G. K., EL CID (Electromagnetic Core Imperfection Detector) Testing of Large Steam-Turbine-Driven Generators, CIGRE Journal "Electra", Technical Brochure No. 257, October 2004, pp 1-10.

14. Müller, G. L. et al,"Interlaminar short circuit detection modelling and measurement", COMPEL: Int: Journal for Computation & Mathematics in Electrical & Electronic Engineering, Vol. 31, Iss. 5, 2012, pp 1448-1457.

15. Moullin, E.B., "The principles of Electromagnetism", Oxford Clarendon Press, 1932, pp 164-168.

16. Ridley, G. K., Enhancement of major water power resources in Zimbabwe and Uganda Proceedings of Joint SAIEE/CIGRE Colloquium on Electrical Machines for Africa, October 1993, Paper No: 11.

17. Electricite de France (EDF), Direction de la Production et du Transport, Service de la Production Hydrauliques, "Justifications Economiques des Remplacements de Circuits Magnetiques lors des rebobinages d'Alternateurs" EDF Communication N°322, June1972.

18. Ridley, G. K., "Conducting an EL CID test on a hydrogenerator", International Journal on Hydropower and Dams, November 1994, Vol: 1, Issue 6, pp 113-119.

19. Dukshtau, Detenka and Pinskii , "Ways of improving Hydro-electric-generator stators", Elektroteknika, 1978, Vol: 49, No. 5, pp18-20.

20. Carter, G. W. , “The electromagnetic field in its engineering aspects” (Longmans, Green and Co., London, 1954.

21. Ridley, G. K., "Four hydrogenerator EL CID test analysis case studies", Proceedings of Water Power and Dam Construction's 5th International Conference on Uprating and Refurbishing Hydro Powerplants, October 1995, Vol: 3, Appendix 2.21.

22. Ridley, G. K. "Hydrogenerator stator core condition monitoring by EL CID", Proceedings of an EPRI International Motor & Generator Predictive Maintenance & Refurbishment Conference, November 1995.

23. Bertenshaw, D., Sutton, J., "Application of the EL CID Test with Circulating Currents in Stator Windings", Inductica, Berlin, June 2004, pp 128-134.

24. ***Ridley, G. K., "Further development of the EL CID vector diagram", International Journal on Hydropower and Dams, July 2007, Vol. 14, Issue 4, pp 96-101.*** [Full paper attached as Appendix 12]

25. Say, M. G., "The Performance and Design of Alternating Current Machines", Sir Isaac Pitman & Sons, Ltd. 1948

26. Bertenshaw, D. R., "Analysis of stator core faults – a fresh look at the EL CID vector diagram", Proceedings of HYDROPOWER 2006, October, 2006 (on CD).

27. Ridley, G. K., "Evaluating interlamination circulating current at core joints in large machine stators", International Journal on Hydropower and Dams, 2008, Vol: 15, Issue 6, pp 106-114.Ridley, G. K..

28. Sutton, J., "Theory of electromagnetic testing of laminated stator cores", Insight, Vol. 36, No: 4 April1994, pp 246 – 251.**27.**

29. Ridley, G. K. "Analysis of EL CID results at stator core joints", International Journal on Water Power & Dam Construction, July2014, Vol:,

pp 32-37.

30. Ridley, G. K. "Correlation of EL CID results with a Stator Core Joint Interlamination Insulation Fault, Dam Engineering, October 2014, Vol: XXV, pp 3-17. [Full paper attached as Appendix 14]

31. Paley, D., McNamara, B., Mottershead, G., Onken, S. C., "Verification of the effectiveness of EL CID on a hydrogenerator core", ADWEL International Ltd., Canada & UK, June 1998

32. Ridley, G.K., "Increased accuracy in determining interlamination fault current at stator core joints", International Journal on Hydropower and Dams, 2009, Vol: 16, Issue 6, pp 104-107.

33. Ridley, G.K., “Evaluation of interlamination circulating current at core joints in large machine stators”, Proceedings of the Lisbon “HYDRO 2010” conference, International Journal on Hydropower & Dams, September 2010, Paper 29.06.

34. ***Ridley, G. K. "Consequences of resetting the PHASE reference for EL CID tests", International Journal on Hydropower and Dams, 2012, Vol: 19, Issue 4, pp 84-88.*** [Full paper attached as Appendix 13)

35. Sutton, J., “On the possibility of motor winding impulse test increasing stator core losses”, CEGB Report (Copy held by the British Library, Copyright Div: London), June 1986.

Author's Bibliography (additional to Thesis References)

1. “Digital Computer applied to Design of salient-pole synchronous machines”, The Engineer, October 1960, pp 705-710.

2. “Designing with a digital computer”, Engineering, August 1962, pp 198-200.

3. “An electronic digital computer, applied to engineering design”, Proceedings of Rugby Engineering Society, 1962, pp 136-163.

4. “Computer analysis of open circuit magnetic noise in synchronous machines,” AEI Engineering Supplement – Computation in engineering, October 1963, pp. 29-35.

5. “Tokke III hydro-electric power station”,AEI Engineering, March/April 1965.

6. “Site testing of hydro-electric a.c. Synchronous Machines”, AEI Engineering, November / December 1966.

7. “140 MVA waterwheel generator site testing”,Electrical Times, February 1969, Volume 155, No: 7 pp 54-59.

8. “Discussion on:- Synchronous starting of motor from generator of small capacity”, IEEE Transactions on Power Apparatus and Systems, April, 1969.

9. "Dinorwic generator-motor units", GEC Journal for Industry, February 1979, Volume 2, No;3, pp132-139.

10. "Direct water-cooled machine for Cruachan", Electrical Review, June 1982, pp 32-33

11. **"**UK's first direct water-cooled pumped-storage generator-motor", Proceedings of the IEE International Conference on Electrical Machines, July 1982, pp 168-173.

12. "Uprating and rewinding hydro- generators", International Water Power and Dam Construction, September 1982, pp 31-34

13. "The UK's first direct water-cooled pumped-storage generator-motor", IEE Electrical Power Journal, October 1982, pp 676-681.

14. "Performance tests on UK's first direct water-cooled generator-motor". Proceedings of IEE 2nd International Conference on Electrical Machines, September 1985., pp:21-26.

15. "Refurbishment & up-rating of large hydro-generators", Proceedings of IEE/IMechE International Symposium on Performance, Economics & Operation of Generation, September 1986, pp1/1-8.

16. "The case for refurbishing & uprating hydro-generators",Proceedings of Water Power & Dam Construction's International Conference on Up-rating & refurbishing hydro-power plants, October 1987, pp:130-147.

17. “The case for refurbishing & uprating hydro-generators", GEC Review, 1988, Volume 4, No:2, pp:83-93

18. “Refurbishment & uprating of hydro-generators”,Proceedings of IEE International Conference on Refurbishment of Power Station Electrical Plant, November 1988, pp165-169.

19. “Hydrogenerator refurbishment by replacement” (short presentation), Water Power & Dam Construction 2nd International Conference on Uprating & refurbishing hydro powerplants, October1989.

20. “An ultra-pure water system for a hydro-electric generator-motor”, Proceeding of the 5th IEE International Conference on Electrical Machines and Drives, September 1991, pp 285-289.

21. “Hydro generator design for refurbishment”,International Water Power and Dam Construction's Journal, May 1992, pp 29-32.

22. “Widening horizons in hydro- generator enhancement”,Proceedings of IEA, OECD & UNIPEDE International Conference on Hydropower, Energy & the environment, Session 4, June 1993.

23. “Enhancement of major water power resources in Zimbabwe and Uganda”, Proceedings of Joint SAIEE/CIGRE Colloquium on Electrical Machines for Africa, October 1993, Paper No: 11.

24. **“**Hydrogenerator enhancement confirmed by calorimetry”, Proceedings of the 4th Water Power & Dam Construction International Conference on Up-rating and Refurbishing hydro power plants, December 1993, pp: 289**-**300.

25 “Bearing Design & Performance for Large Hydrogenerators (i.e. 50 MVA and above)”, CIGRE Journal “Electra”, December 1996, pp:42-56.

26. “EL CID test evaluation, 1984 – 96”, IEE Power Engineering Journal, February 1997, pp 21-26.

27. “Application of EL CID with salient-pole rotor in-situ”, Uprating & Refurbishing Powerplants International Conference Proceedings, International Water Power & Dam Construction, October 1997 pp 339-346.

28. “EL CID as a core condition monitor”, Proceedings of 3rd CIGRE Southern Africa Regional Conference – New Technologies for Effective Power Systems, May 1998, Paper 46.

Appendices

Appendix 1 - The magnetic field induced by a toroidal coil around the core

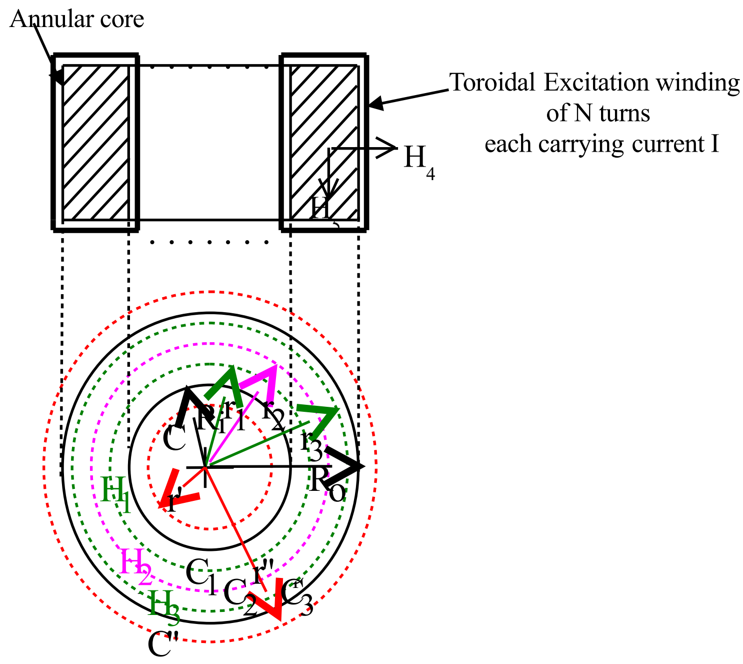

Figure 38 Arrangement of excitation winding as in Figure 5b

A homogeneous annular steel ring of inner radius R_i and outer radius R_0 is magnetised by a closely wound toroidal coil of N turns (i.e. the successive turns are close to each other) carrying I amperes. Flux paths in the steel are identified in length by the letter C, with an appropriate subscript, and in radial location by the letter r, with a corresponding subscript, i.e. C_1 , r_1 ; C_2 , r_2 ; etc. Flux paths in air are identified in length by the letter C, with an appropriate superscript, and in radial location by the letter r with a corresponding superscript, i.e. C', r' ; etc.

1. Considering flux paths C_1 , C_2 , C_3 , within the steel core, which are all

linked by the excitation winding having NI ampere-turns, then

By Ampère's law, $NI = \oint_C H_S.ds$

Thus NI $= \oint_{C1} H_1.ds = \oint_{C2} H_2.ds = \oint_{C3} H_3.ds$

$$H_1 . 2\pi . r_1 = H_2 . 2\pi . r_2 = H_3 . 2\pi . r_3$$

Hence, $H_2 = H_1 \frac{r_1}{r_2}$ and $H_3 = H_1 \frac{r_1}{r_3}$

If R_1 and R_0 are great compared to $(R_o - R_1)$,

$$H_2 \simeq H_3 \simeq H_1 \simeq H \text{ (say)}$$

2. Considering a flux path C' internal to the annulus, it is seen that it does not link any current,

therefore $\oint_{C'} H'. ds = 0$,

and $H' = 0$

3. Considering a flux path C'' external to the annulus, it is seen that it links equal and opposite values of NI,

therefore $\oint_{C'} H''. ds = 0$

and $H'' = 0$

4.It is shown by Carter[20], that both H_4 and H_5 are small in comparison to H. This implies that the magnetic field is principally circumferential and other components may be neglected.

Appendix 2 - The magnetic field set up by a concentrated coil along the core Axis.

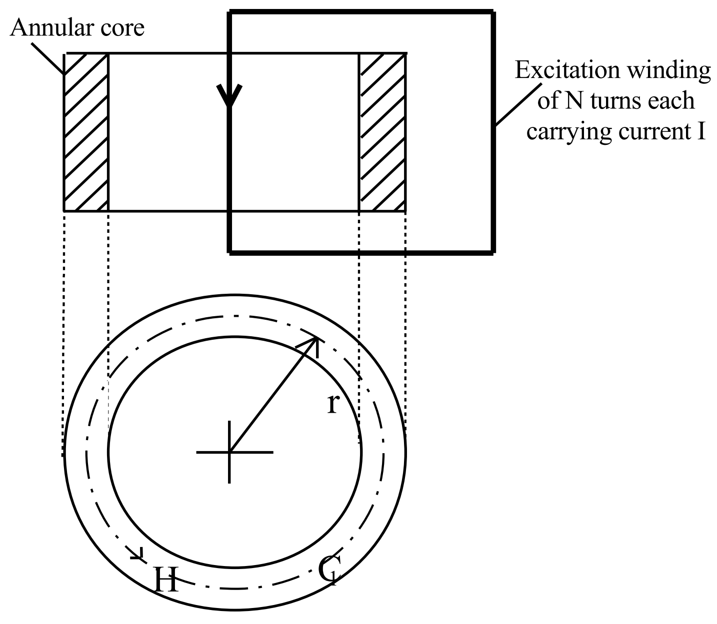

Figure 39 Arrangement of excitation winding as in Figure 5c

Application of Ampère's Law (alternatively known as the Magnetic Circuit Law) to the path C_1 in a homogeneous annular iron ring gives

$$NI = \oint_{C'} .H_s . ds$$

$$= H . 2 . \pi . r$$

$$\text{Therefore } H = \frac{NI}{2\pi r}$$

The value of H is given everywhere by the above equation, whether within or outside the iron core. But the Flux Density B depends upon the permeability of the medium, which is much greater for iron than for air.

Thus, a relatively high flux density is induced in the iron compared to that produced in the air.

Appendix 3 - Calculation of EL CID trace turn voltage

Let Φ = sinusoidal circumferential flux induced in an annular stator core

$= \Phi_m . \sin(2 . \pi . f . t)$

where

Φ_m = maximum value of the above flux in Webers

f = frequency in Hz of sinusoidal variation

t = time in seconds

Then, the voltage induced in a turn round the stator core, enclosing the above cyclic flux, is given by Faraday's Law as:

$$V_t = \frac{d\Phi}{dt} = -2 . \pi . f . \Phi_m . \cos(2 . \pi . f . t)$$

The r.m.s. value is:

$$v_t = \frac{2 . \pi . f . \Phi_m}{\sqrt{2}} = 4.44 . f . \Phi_m$$

since Φ_m is in Webers.

However, $\Phi_m = \Phi_a / 2$ (that is, flux per pole crossing the air gap divided by two) therefore:

$$v_t = \frac{\pi . f . \Phi_a}{\sqrt{2}} = 2.22 . f . \Phi_a$$

Appendix 3 - Calculation of EL CID trace turn voltage (Cont:)

For 4 per cent of normal flux crossing the air gap, the EL CID trace turn voltage is equal to:

$0.0888\ f\ .\ \Phi a$ volts r.m.s.

$4.44.\ \Phi_a$ volts r.m.s. for $f = 50$

$5.33.\ \Phi_a$ volts r.m.s. for $f = 60$

But electrical machine air gap flux (Φ_a) in Webers is given as:

$$\Phi_a = \frac{\frac{V_L}{\sqrt{3}}}{4.44\ .\ K\ .\ T_{ph}\ .\ f}$$

where,

V_L = Rated Line Voltage (Y connected),

K = Combined spread and chording factor of the winding

T_{ph} = Series turns per phase

Therefore, at 4 per cent flux,

$$v_t = 0.0888 f \frac{\frac{V_L}{\sqrt{3}}}{4.44\ K\ T_{ph}\ f}$$

$$v_t = 0.04. \frac{V_L}{\sqrt{3}\ .\ K\ .\ 2\ .\ T_{ph}}$$

as given in the EL CID Handbook.

<u>Appendix 3</u> <u>- Calculation of EL CID trace turn voltage (Cont:)</u>

Note: If V_L is in kilovolts, and a typical value of K of 1/1.08 = 0.926 is adopted, then

$$v_t \approx 12.5\left[V_L / T_{ph}\right]$$

Appendix 4 - The effect of the excitation cable crossing the core end.

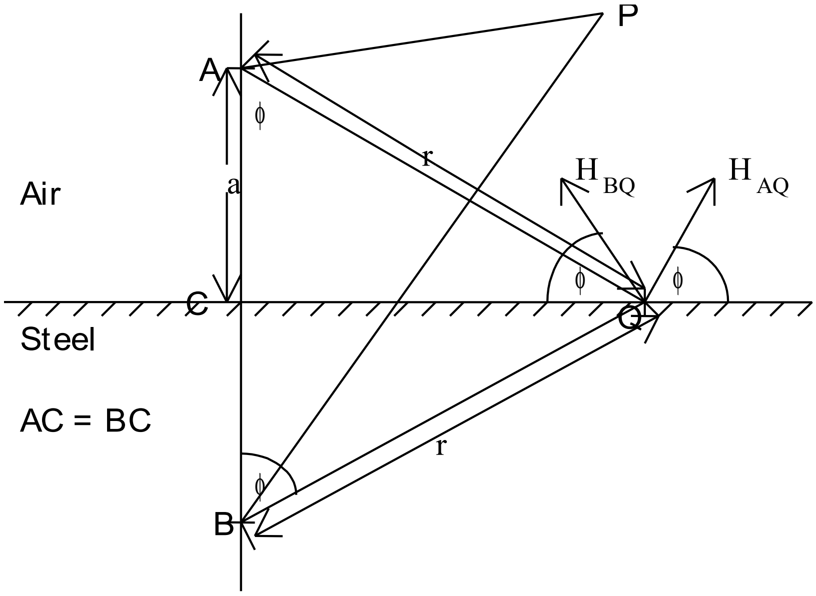

Figure 40 The field of an electrical current in the presence of an iron block

The problem is to determine the flux density at the surface of a steel block arising from the field of current in a straight conductor above and parallel to the steel surface.

Point A, in Figure 39 above, identifies the position of a conductor carrying current I at a distance AC = a, above the surface of a block of steel.

The solution is obtained by application of the proposal given in Reference 20, pages 141 and 142. This comprises the use of an ***image current***. In this, the steel block is replaced by a second conductor located at Point B, at a distance BC = a, directly below Point A, and carrying current I, which produces an equipotential plane of corresponding position to the original iron surface.

Appendix 4 - The effect of the excitation cable crossing the core end. (Cont:)

Applying Ampère's law to any Point P, distant r from Point A,

$$\mathbf{I} = \oint_c H_s \, . ds$$

$$\mathbf{I} = \oint_{2\pi r} H_s \, . ds$$

$$= H_{AP} \, . \, 2 \pi r$$

$$\text{Therefore, } H_{AP} = \frac{I}{2 \pi r}$$

Hence, at any Point Q on the steel surface,

$$\text{from current I at Point A, } H_{AQ} = \frac{I}{2 \pi r}$$

$$\text{and from current I at Point B, } H_{BQ} = \frac{I}{2 \pi r}$$

It is shown in Reference 20, that the Magnetising Force (H) is perpendicular to the radius joining the current carrying conductor to the point of observation (i.e. Q), and in accordance with a right-handed screw rule relative to the current direction.

From geometrical considerations, it is clear that both H_{AQ} and H_{BQ} are inclined at an angle ϕ to the steel surface.

Thus, the resultant magnetising force at Point Q is $H = \dfrac{2 I \sin\phi}{2 \pi r}$

$$= \frac{I \sqrt{r^2 - a^2}}{\pi r^2}$$

Appendix 4 - The effect of the excitation cable crossing the core end. (Cont:)

and, the required Flux Density (B) $=$ η_o H

$$\text{i.e.} \quad B = \frac{\eta_0 \, I}{\pi} \frac{\sqrt{r^2 - a^2}}{r^2}$$

where η_o = the primary magnetic constant $= \frac{4\,\pi}{10^7}$

in the rationalised MKS system.

$$\text{Consequently,} \qquad B = \frac{4\,I}{10^7} \frac{\sqrt{r^2 - a^2}}{r^2}$$

where B is in weber per sq: metre, I is in amperes, r and a are in metres.

It is clear from the above formula for **B** on the iron surface, that

1. when r = a, then B = 0, and

2. when a = 0, then B = $\frac{1}{10^7} \cdot \frac{4\,I}{r}$

The above general expression for Flux Density (*B*) is plotted for several values of "*a*" in Figure 7

Appendix 5 - An independent assessment of the candidate's work

A "Book Review" by Professor Zlatanovici and published in "Hydropower and Dams" Issue 1, 2008.

The third edition of G.K. Ridley's book "EL CID – Application and Analysis"[1] represents a complete revision compared with the previous two. The book deals with the very particular field of determining the magnetic stator core condition of rotating electrical machines, using the method of low flux density: about 4 per cent of the rated flux density. The author has made an important contribution to the development of this method, which is already widely known as the EL CID method.

In the first part of the book (chapters 1 to 4) the basic principles and practical application of EL CID are presented, including the factors which influence test results. Some test results and a comparison with the classical high flux ring test (HFRT) are also given. In the second part (chapters 5 to 7), the theoretical fundamentals of the method are presented, and in the third part (chapters 8 to 9), details are provided about why, where, when and how to use the EL CID method.

In this third edition of the book, starting from the theoretical basis developed in the previous editions and having an extensive experimental base consisting of results from tests carried out on various types of generators, the author presents in the 6th chapter a new theoretical approach. This is based on a complete vector diagram, including all the electro - magnetic phenomena accompanying the EL CID test. To develop this complete vector diagram, the author presents the analogy of the EL CID phenomena with those existing in a transformer having one or more secondary circuits. The author applies standard transformer theory, and considers the basic electromagnetic theory of the magnetic flux induced in the stator core, the flux leakage at joints built into the core, the current induced in a fault path caused by degradation of the interlaminar insulation and, if present, the current induced in the stator winding. Fault current and, when present, stator winding circulating current, are thus both seen to be induced in secondary circuits of the equivalent transformer.

The author focuses attention particularly on the phenomena in the region of the core joints. Application of the vector diagram in the core joint zones, such as presented in the 6th chapter, is now very importantly able to explain fully the results obtained from EL CID tests. The vector diagram contributes to a comprehensive understanding of all other phenomena appearing in the EL CID tests, arising from variable conditions of the core, both along its length and around its circumference, and also caused by perturbations provoked by the measuring system itself. This full understanding of all phenomena is the necessary basis for a correct assessment of the stator core condition.

Another very important contribution of the vector diagram developed by the author is the inclusion of a component representing leakage flux between the stator and a salient-pole rotor, when the test is carried out without complete removal of the rotor, or at least of only a couple of poles.

In conclusion, by the procedures now incorporated in this third Edition, it is now possible to solve that most difficult case of stator core condition: the one encountered at a core joint. This is a most important contribution, and one for which users of EL CID have waited a long time. I consider that the book is of a high level, both scientifically and in practical application, explaining all of the phenomena and their theoretical justification, which proves the superiority of the EL CID method and contributes to its generalization. - Prof. Dan Zlatanovici, Scientific Secretary of Icemenerg, Bucharest, Romania.

Appendix 6 Extracts from References and Bibliography in IEEE

P1719 (Draft version – R44, Nov: 2015)

(Permission given on 12.02.17 by G. Mottershead, P1719 Working Group Chairman)

F4.7 References include:

1. Ridley, G.K., Site testing of large hydro-electric a.c. synchronous machines. November/December 1966, AEI Engineering.

2. Ridley, G.K., 140 MVA waterwheel generator site testing, February 1969, Electrical Times, Vol: 155, No: 7, 54 – 59.

5. Ridley, G.K., EL CID - Application and Analysis, Ed: **3**, ADWEL International Ltd., 200**7**.

6. Ridley, G.K., Increased accuracy in determining fault current at stator core joints. Hydropower & Dams, Vol: 16, Issue 6, December 2009, 104 – 107.

8. Ridley, G.K., Hydro generator design for refurbishment, May 1992, Water Power & Dam Construction, Vol. 44, No. 5, 30 – 33.

12. Ridley, G.K., Analysis of El-Cid Results at Stator Core Joints, International Water Power & Dam Construction Conference, July 2014, pp 32-37

F.4.7 Bibliography includes:

[B1] Ridley, G.K., Site testing of large hydro-electric a.c. synchronous machines. November/December 1966, AEI Engineering.

[B2] Ridley, G.K., 140 MVA waterwheel generator site testing, February 1969, Electrical Times, Vol: 155, No: 7, 54 – 59.

[B5] Ridley, G.K., EL CID - Application and Analysis, Ed: 2, ADWEL

International Ltd., 2004

[B8] Ridley, G.K.. Hydro generator design for refurbishment, May 1992, Water Power & Dam Construction, Vol. 44, No. 5, 30 – 33.

Appendix 7 – Correspondence

A communication in 2010 in support of a nomination (unsuccessful) as Fellow of the IEEE from Prof. Dan Zlatanovici (deceased), formerly Scientific Secretary of Icemenerg, Bucharest, Romania. [Original held by Mrs Rodica Zlatanovici, Professor Zlatanovici's widow and former professional colleague as Head of Electrical Machines in Icemenerg]. Mrs Zlatanovici is one of the two referees required by the University of Warwick for this submission.

………
………

In 1994 I assisted at a test on a large turbo-generator (330 MW, Rovinari - Romania), performed with the instrument called EL CID, used to detect stator core defects. Then, I read some of the Mr. Ridley's papers in international journals or conference proceedings, dealing with this subject. As a result, the EL CID method was accepted in Romania instead of the classical method.

In 2000 I met Mr. Ridley personally at a CIGRE meeting in Paris and after that and till today we had a constant change of opinions and information about this subject.

"I read almost all Mr. Ridley's papers and the 3 editions of his book "EL CID – Application and Analysis" and I see the progress made by the author in understanding and explaining all the phenomena appearing in the EL CID tests, arising from variable conditions of the core, and also caused by perturbations provoked by the measuring system itself.

The book entitled "EL CID – Application and Analysis" 3rd Edition July 2007 is a comprehensive record of the theory and practice of the electromagnetic technique for assessing the condition of stator core inter-lamination insulation in large electrical machines, with particular reference to hydrogenerators. The book represents an extraordinary development beginning from the theoretical base and finishing with practical application in the field.

The application of EL CID for the analysis of the condition of interlamination insulation of stator cores, particularly for the more difficult case of hydrogenerators, recorded in Mr. Ridley's numerous papers & his book, entitled "EL CID - application and analysis" has been pursued entirely independently. This body of work is not known to be paralleled elsewhere, and is, therefore, a unique contribution to engineering literature. Most recently, the determination of absolute values of interlamination fault current at core joints, reported in papers published in 2008 and 2009, has been a major advance, and has solved a long standing problem. Mr. Ridley is the foremost authority on the use of this electromagnetic technique."

Dan Zlatanovici

- Ph. D. in Electrical Engineering from "Politechnica" University Bucharest in 1987

- Univ. Professor at the "Valahia" - Targoviste University in 1998 – 2005

- Scientific Secretary and senior researcher at the Energy Research and Modernizing Institute – Bucharest, Romania (www.icemenerg.ro), employed by

Icemenerg from 1969 till present time.

- Member (on behalf of Romania) of the CIGRE - Study Committee A1 – Rotating Electrical Machines in 1996 – 2006

- Member of the staff of the Study Committee A1 – CIGRE from 2006 till present

- Reviewer of the review “Electra”.

- Awarded with the CIGRE Technical Committee Award in 2005

Appendix 8

El CID APPLICATION PHENOMENA

G K RIDLEY

GEC Alsthom Large Machines Ltd, England

INTRODUCTION

The Electromagnetic Core Imperfection Detector (El CID) was invented in the late 1970's (Sutton, 1) as an additional tool in the field of condition monitoring. It is more convenient than the traditional full flux ring test for checking stator core interlaminar insulation. Initial application was to large turbogenerators but it is equally straight forward for industrial sized multipolar machines with one piece cores built in a continuous ring of segmental laminations (Figure 1).

Anomalous results were obtained, however, when El CID was applied to large diameter, split stator cores which are typical of hydrogenerators. A range of the problems encountered are presented and it is shown how they may be understood, or, if possible, avoided. An exhaustive theoretical treatment is not attempted. The large number of illustrations necessitates only brief comment on each.

The fundamentals of the El CID theory are illustrated in Figure 2. See (1) for more detail. Only 4% of rated voltage flux is induced, consequently the excitation cable is of light section. The Chattock coil sensor output is indicated by a milliammeter or used to drive a trace pen. The main core leakage flux and the magnetic field of the fault current are virtually out of phase by 90°. Thus a Reference Coil, sensitive to the former, is used to separate the two flux components.

ALTERNATIVE EXCITATION WINDINGS

Experience has been gained with 5 different forms of excitation winding (Figures 2 and 3). The initial choice arose primarily from particular circumstances. Alternatives were sought in the light of problems. Merits and demerits are identified by the discussion.

EXCITATION LEVEL

Sutton (1) unambiguously recommended a flux level of 4% of that corresponding to rated voltage. This was equated for convenience to an electric field strength of 5 volts per metre which was typical for large turbogenerators, but not for other machines.

Although it is the electric field strength which has to be withstood by the interlaminar insulation, the test objective is to indicate machine performance at rated conditions. A standard flux level relative to those conditions (ie 4%) is therefore the relevant criterion.

El CID RESULTS WITH A SINGLE CONCENTRATED, CLOSE-WOUND EXCITATION WINDING

The first major use by GEC Alsthom Large Machines Ltd of Rugby of the El CID technique was to check a 7.85 metre bore stator core which had been stripped prior to being rewound. Figure 4 is a plot of minimum and maximum signal values obtained along the core length for each of the 378 slots.

Relatively constant results, which would be expected from Moullin (2), occur only in the half of the core furthermost from the magnetising coil. The signal level rises as the excitation source in slot 39 is approached. At stator joints, there are marked discontinuities. These were exceedingly high values, until the Reference Coil was placed at the core splits.

The results on the Left Hand Side of Slot 39 were clearly affected by the core joint between Slots 6 and 7. On the Right Hand Side, however, an acceptable envelope is provided, until the next core joint effect, by a curve based on the magnetic field decay being inversely proportional to the distance from a current carrying conductor (Reference standard theory). At a metre distance from the excitation coil, the effect has reduced to about 20% of the apparent initial additional El CID signal due to the excitation coil's proximity. This supports the rule of thumb that the excitation cable should be maintained at a metre distance from any location where it may have potential influence.

The results of Figure 5 were obtained, with the above configuration of excitation coil, to check the effect of introducing the rotor into the stator. Two poles were removed for convenience of access. The insignificant effect indicated the possibility of El CID tests without major dismantling.

El CID RESULTS WITH A TOROIDAL EXCITATION WINDING

Initial experience of an El CID test with minimal dismantling encountered severe flux attenuation round

Appendix 8

the core when excited by a concentrated excitation winding. Clearly the top bearing assembly provided added leakage paths. This prompted the use of a toroidally wound coil.

Pole Proximity Effect

Figure 6 shows the effect of pole proximity, which is overcome by turning the rotor. A minor defect is evident in both cases. Distortion became pronounced, for the machine concerned, at less than 6 slots from the pole side. Although the entire signal level was raised by the pole proximity, the distortion is apparently an end effect. This is considered to be due to the machine geometry, which is compared in Figure 7 to that of the previous machine. Use of a special Chattock Sensor lying flat on the stator bore mitigated the pole proximity effect.

El CID RESULTS WITH A CONCENTRATED EXCITATION COIL DOWN THE CORE AXIS

Whilst a toroidal winding ensures a uniform flux, the turns need to be moved frequently. In cases where the rotor has been removed, the coil form shown in Figure 3a appeared desirable. The results (Figure 8), however, were initially perplexing, there being high end values and a tilting of the trace axis relative to that of the core.

Restriction of the traversed area of the core to a sector some 120° from the plane of the coil (Figure 9) gave more expected results. Those for Slot No. 1 obtained with two different coil positions (Figures 10a & b) show dissimilarities. That these are coil proximity effects was demonstrated by the additional investigation using a short-span or mini-Chattock (Figure 10c, d and e).

This led to maintaining the excitation coil at least a metre from the core ends as it passes over. Figure 11 illustrates the benefit.

DISCUSSION OF El CID TRACE AXIS TILT

Figure 11 still shows some degree of axis tilt. To investigate this a Finite Element study was made of the effect of a tilted coil leg as it passes through the bore. The results are very briefly displayed in Figure 12, which shows that the flux density varies in a manner expected to tilt the axis of an El CID trace.

Not all the results appeared immediately to conform to this theory, but a careful analysis indicated that a $\Theta = 0$ position was identifiable. The tipping of the two traces in Figures 10a and b for Slot 1 implies a change in coil attitude. This is most likely, since the shaft remained in-situ, thus impeding access.

BRIEF COMMENT ON El CID TAILS

In addition to the effect of the cable in proximity to the core ends, noted already, cases have arisen where end abnormalities persisted despite every care being taken with coil positioning. Careful consideration revealed that other factors such as a steel flooring or components like a bearing bracket and brake/jack units could have been significant.

El CID RESULTS WITH SYMMETRICALLY DISPOSED, CLOSELY WOUND, CONCENTRATED COILS

Figure 3c is now the recommended form of excitation winding. Typical results are shown in Figure 13. A minor blemish is identified clearly both before and after winding the stator coils into the core. The small irregularities mainly correspond to ventilation ducts.

El CID, RESULTS WITH FOUR SYMMETRICALLY PLACED CONCENTRATED EXCITATION COILS WOUND DOWN THE CORE AXIS (Figure 3d)

Relatively smooth El CID traces were obtained in this case, except at core joints, to be discussed later. Figure 14 shows, however, the presence of disturbing factors already identified. Although the influence of the excitation coil can be minimised by moving it, such action is not necessarily justified. Figure 14 shows that only in the joint regions are the signal levels of possible concern.

The tilt in the distribution of values plotted indicates some eccentricity of the common bundle of excitation conductors in the bore. A reasonable analysis of the total distribution is achievable in terms of the several field influencing features encountered elsewhere.

STATOR CORE JOINT EFFECT

Briefly, although correction for the additional flux leakage at a joint is primarily by placing the Reference Coil at the split, this is not always adequate. Moreover the distortion is usually not uniform along the core length.

The relationship of main field to the potential fault signal is illustrated in Figure 15 for a slot remote from a joint. The Quad: Reading (ie fault indication) could be accepted immediately as indicating a satisfactory condition as the variation is only 90 mA. Upon taking account of the tilt, however, the variation is not more than ± 30 mA, indicating a very good condition. The general correspondence between Phase and Quad: Readings is clear. At a core split, the general variation of Phase and Quad: Readings is again similar (Figure 16a) but the level of variation is over 1.5 amp. Investigation for real faults with the mini-Chattock

Appendix 8

(Figure 16b to e) showed that there was little variation along the slots either side of the split and the variation for the split tooth is of the same general pattern in both Quad: and Phase modes. Thus most of the disturbance is due to the joint effect. A disparity between Phase and Quad Mode readings of -350 to +550 mA indicates, however, concern for the long term integrity of the core.

EVIDENCE OF VALIDITY OF El CID INDICATIONS

This may be summed up as:-

1. correlation with observable core damage.
2. confirmation was obtained, on dismantling a core, that lack of a fault indication despite indentation was correct.
3. correspondence, when the core was stripped, between a poor condition of insulation near core joints and previous El CID warning signals.

VARIATION OF MMF ROUND THE CORE

Experimental observation, by the Phase Mode application of El CID, shows non-linearity of MMF along the inner periphery of the Core (Figure 17). Both Sutton (1) and Moullin (2) indicate this, but only as a relatively small variation.

In both Figure 17a and 17b, the periodicity of the MMF variation is clearly a function of the number of slots per segment arising from peaks and troughs of leakage flux produced by inter-segmental gaps. The indication is that in one case the intersegmental gaps every half lamination were detected. This corresponded to thinner laminations. Also a different sensor was used.

A peripheral variation is not significant for the El CID fault indication readings. Axial variation, as at joints, will tend to cause confusion.

CONCLUSIONS

Causes of distortion identified are:-

1. excitation winding turns less than 1 metre from the working area.
2. excitation cable less than 1 metre from core ends.
3. misalignment of inner leg of cable with core axis.
4. proximity of poles or other ferrous components.
5. joints between core sections.
6. gaps between core lamination segments.
7. a non-standard flux level.

The most favourable conditions are:-

1. a closely wound, concentrated excitation winding, sub-divided into several symmetrically spaced series connected sections, ie Figure 3c.
2. a flat Chattock Sensor
3. location of the Reference Coil where the main flux is representative of the area traversed.
4. compensation, so far as possible, for the magnetic field detected by the Reference Coil.
5. on-site involvement of a qualified engineer to monitor the test conditions and analyse the results.

Applications of the El CID technique are:-

1. monitoring of remedial work
2. investigation of core condition with minimal dismantling of the machine.
3. finger printing of a new core for later comparisons.
4. checking that no damage has occurred during winding.

Overall, the conclusion is that the El CID technique, when applied under adequate supervision and taking account of the several factors which may adversely affect the results, is a reliable and useful tool in the field of condition monitoring.

ACKNOWLEDGEMENTS

The author acknowledges with thanks the permission of the Directors of GEC Alsthom Large Machines Ltd to publish this paper.

REFERENCES

1. Sutton, J., July 1980, Electrical Review, Vol: 207, No.1, "El CID: an easier way to test stator cores", 33 - 37.

2. Moullin, E.B., 1932, "The Principles of Electromagnetism", Oxford Clarendon Press, 164 - 168.

Appendix 8

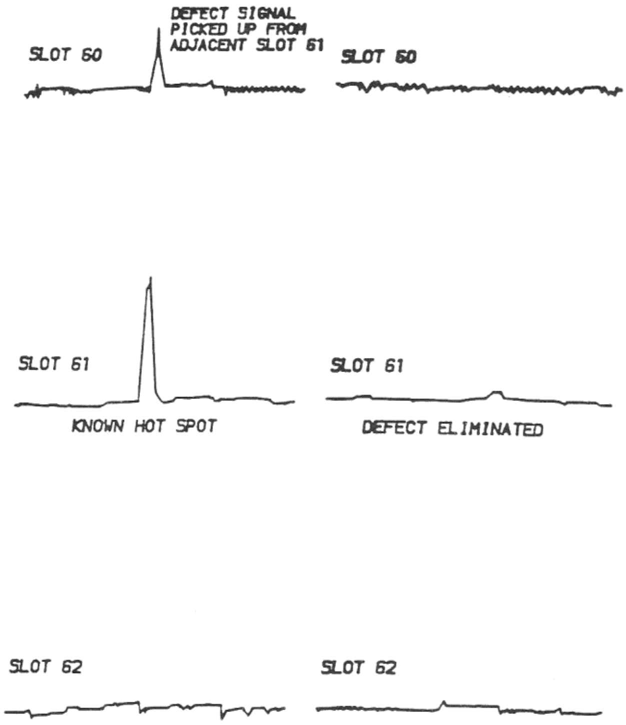

Figure 1. EL Cid results for one piece core.

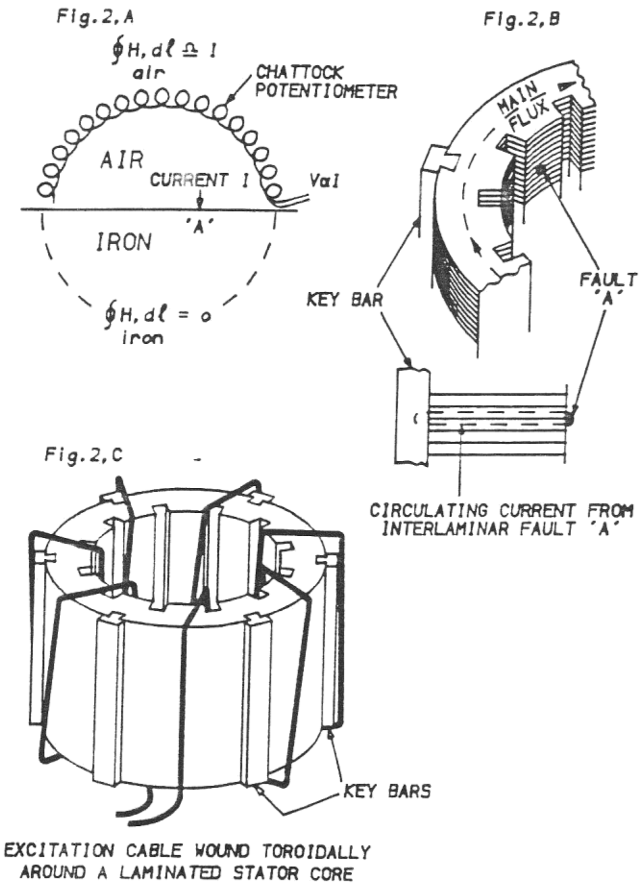

Figure 2. EL Cid core test basic principles.

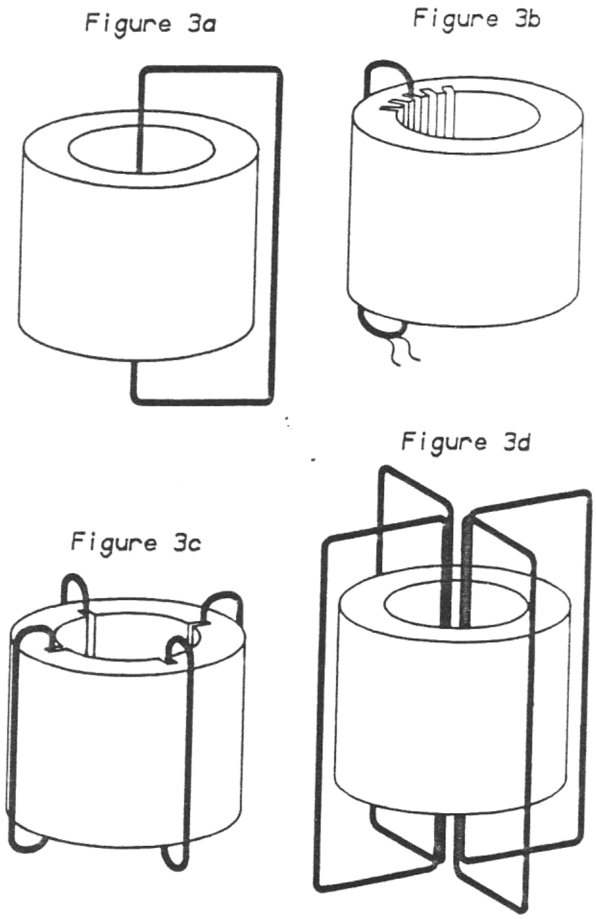

Figure 3. Four alternative forms of excitation winding.

Appendix 8

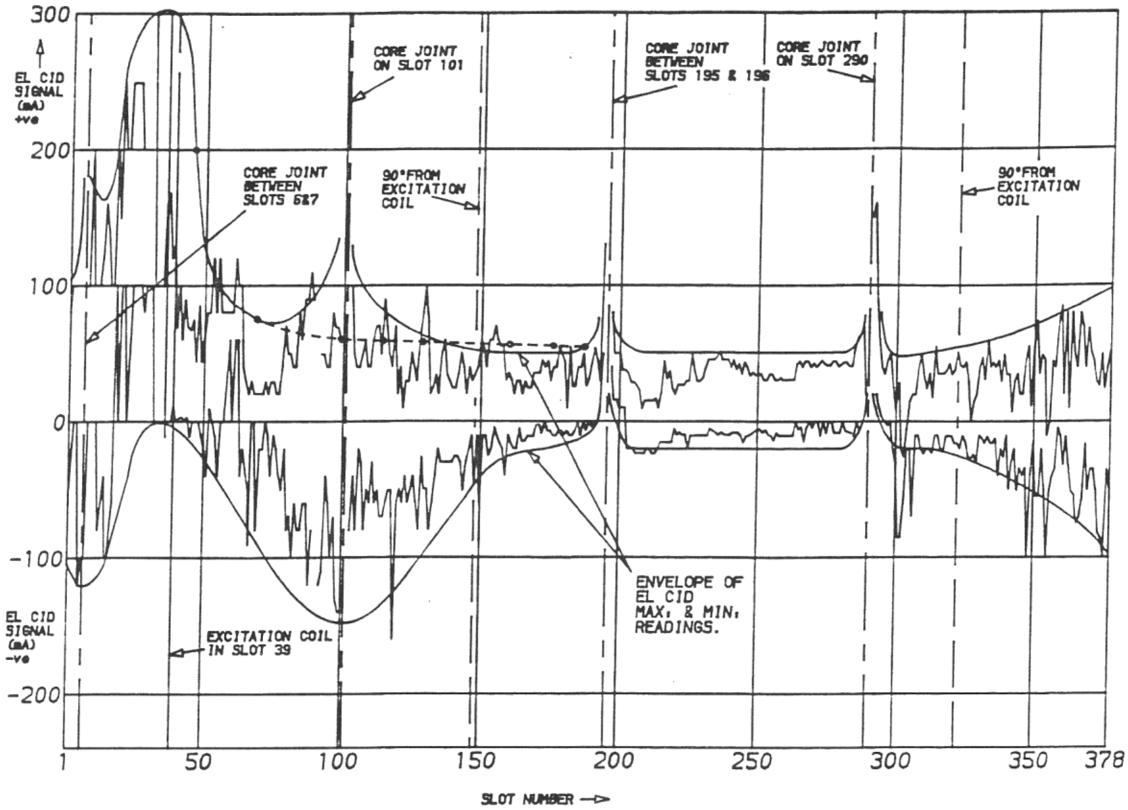

Figure 4. EL cid results for a core magnetised by a concentrated coil.

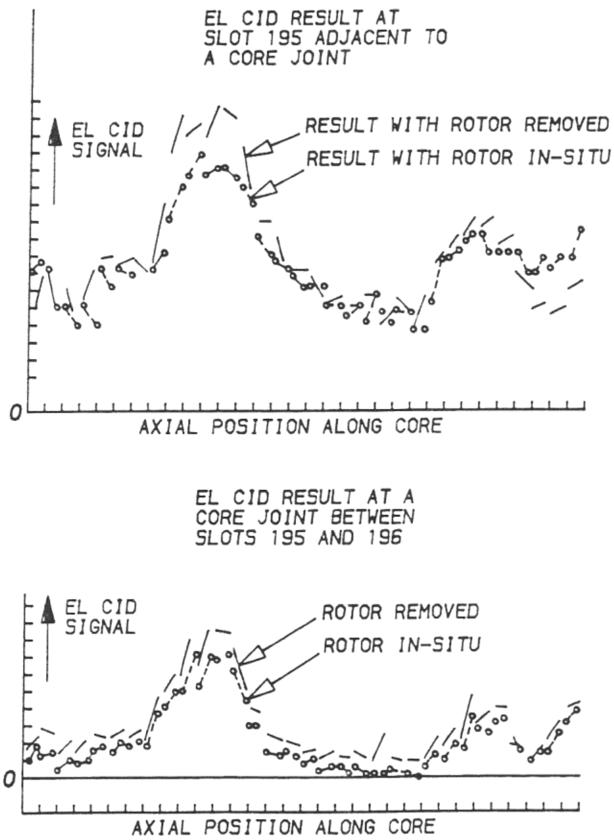

Figure 5. Comparison of EL Cid, results for Machine 1, with and without the rotor in-situ.

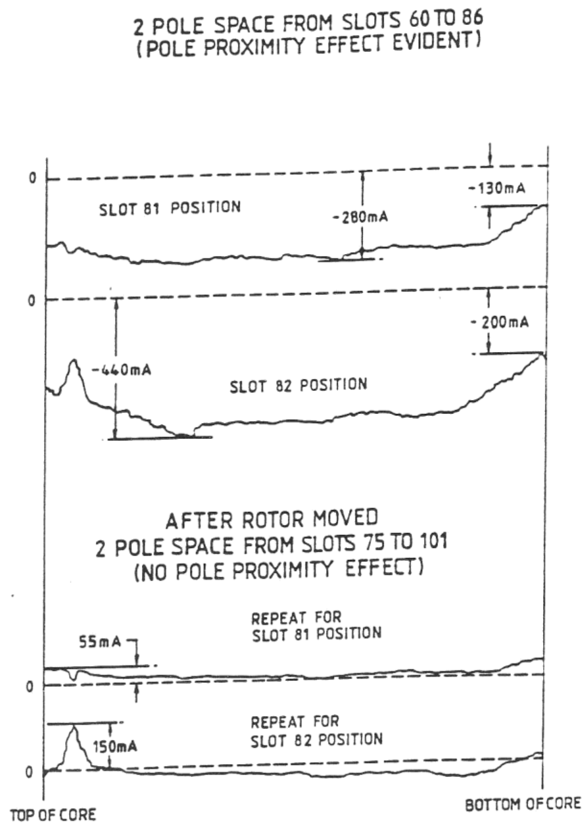

Figure 6. Pole proximity effect for Machine 2.

Appendix 8

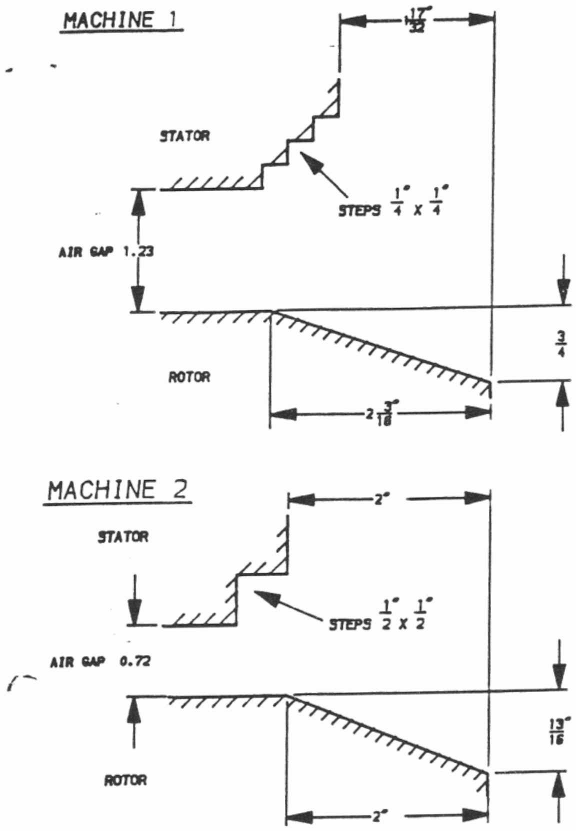

Figure 7. Machine 1 and Machine 2 geometries.

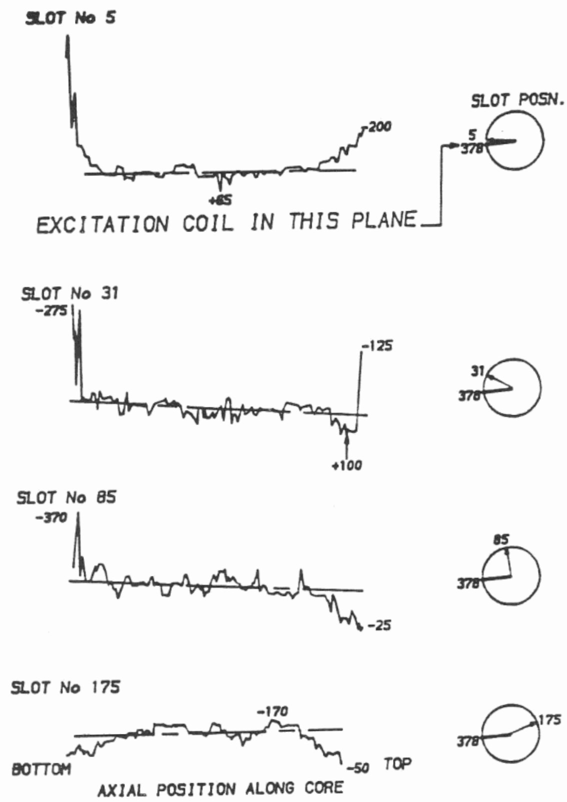

Figure 8. El Cid results for a core excited by a concentrated coil along the axis, as Fig. 3a.

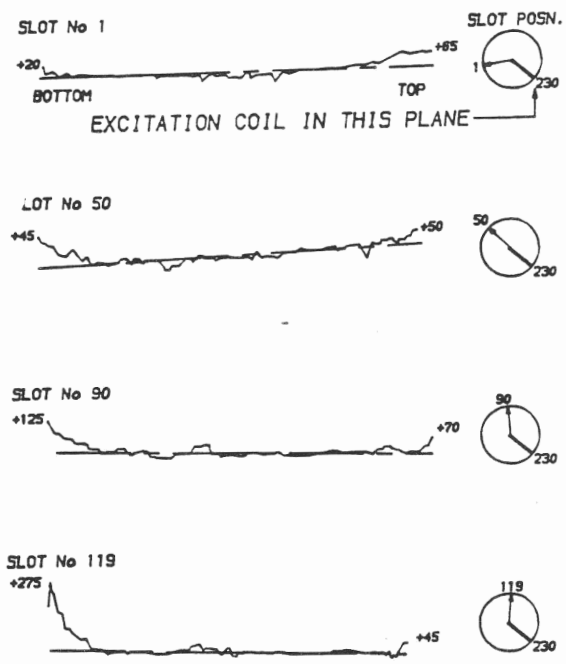

Figure 9. El Cid results restricted to a core sector not less than 120° from the excitation coil.

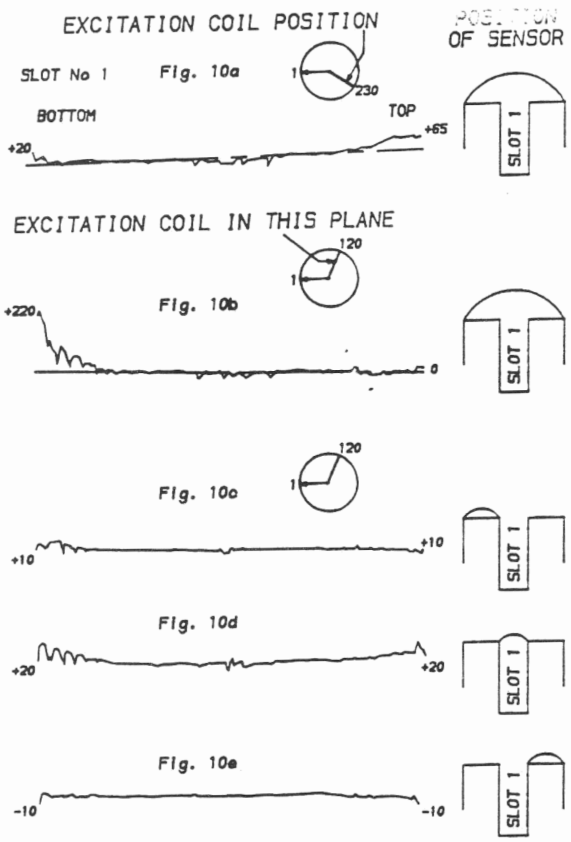

Figure 10. Results for a given slot for alternative excitation coil positions.

Appendix 8

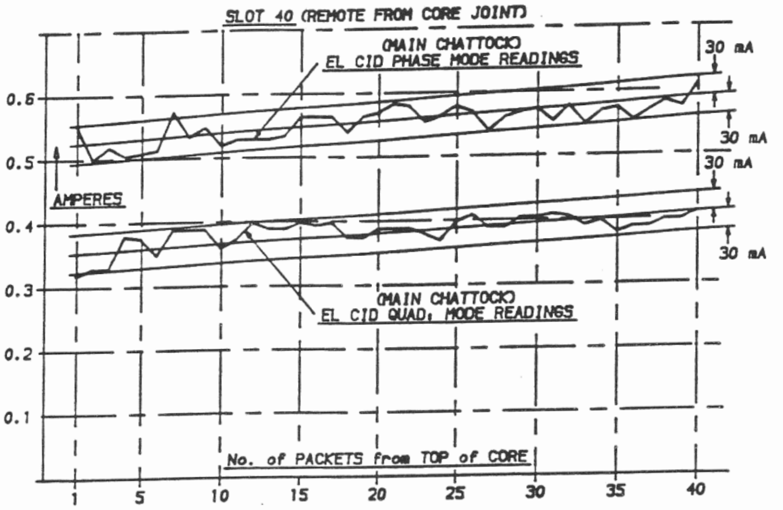

Figure 15. Phase and Quad EL Cid results
remote from a core split.

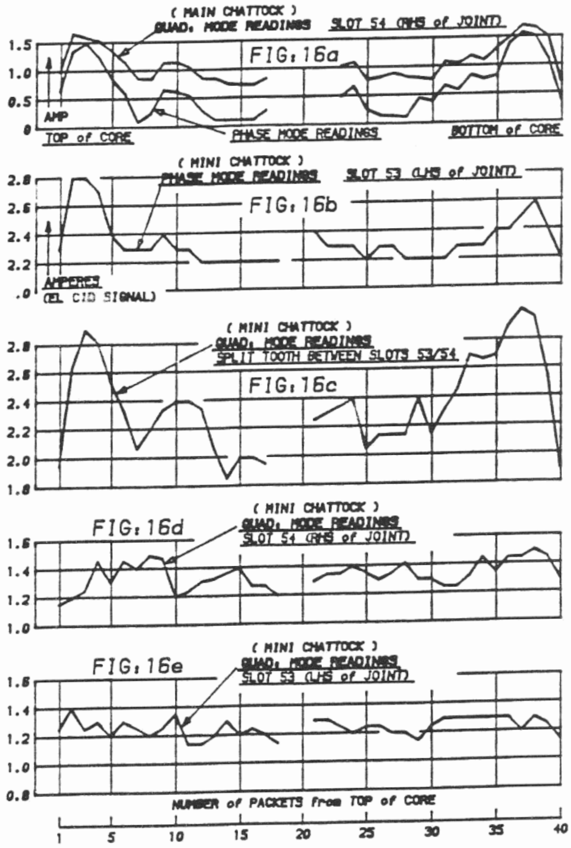

Figure 16. Phase and Quad EL Cid
results at a core split.

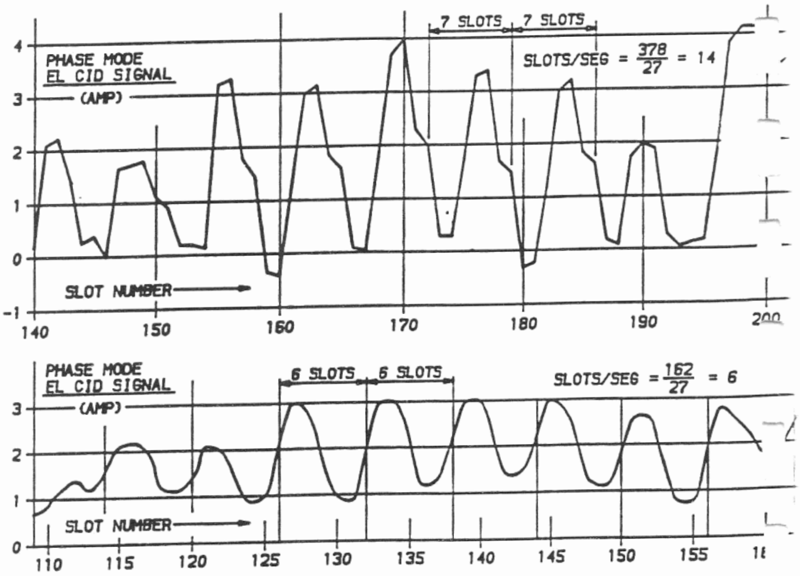

Figure 17. Variations in MMF round a core.

Appendix 8

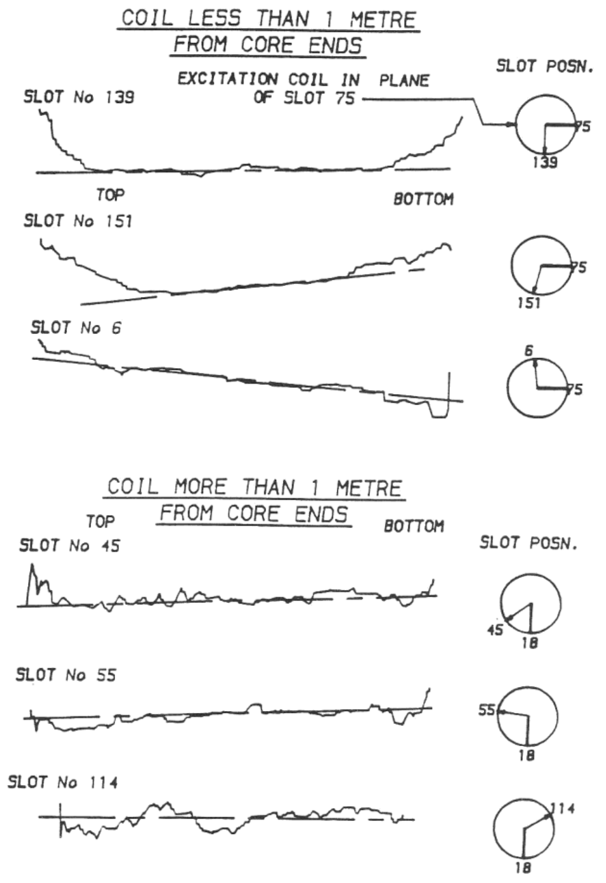

Figure 11. Comparison of EL Cid results with and without excitation coil a metre from the core ends.

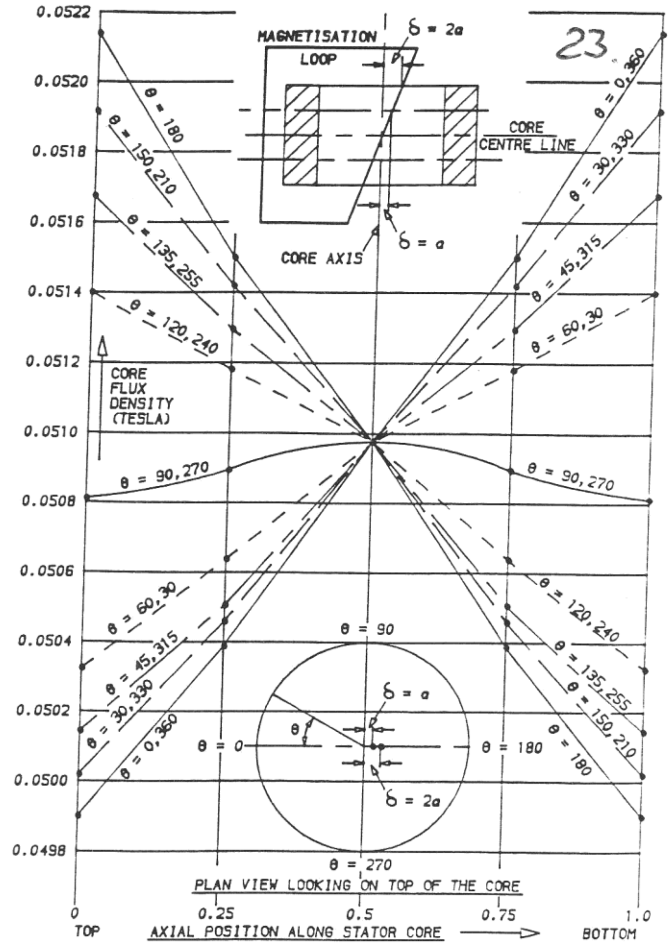

Figure 12. Tilting effect on EL Cid trace caused by inclination of the inside leg of excitation coil.

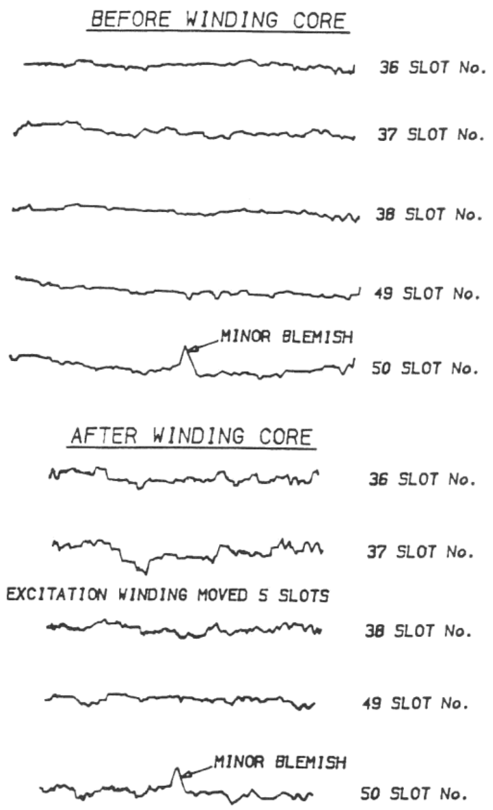

Figure 13. EL Cid results with four concentrated close-wound excitation coil sections.

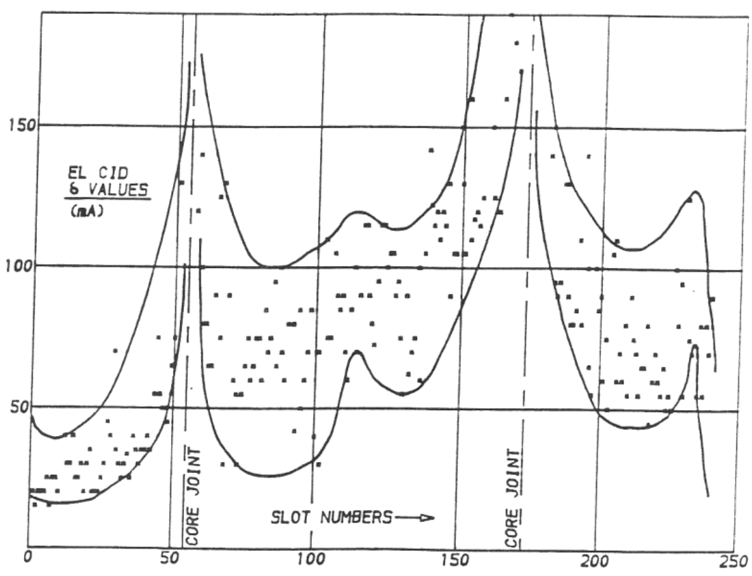

Figure 14. Minimum to maximum values (б) with four symmetrically placed concentrated coils, wound along the core axis.

Appendix 9

ELECTROMAGNETIC FIELD DISTORTION EFFECTS ON EL CID TESTS

G.K. Ridley

Private Consultant to Adwel Industries Ltd., U.K.

INTRODUCTION

EL CID (Electromagnetic Core Imperfection Detector) monitors the condition of large a.c. rotating machine stator cores. Applications cover turbogenerators, industrial-sized machines and hydrogenerators. The basic principle is that of detection by a Chattock potentiometer of the electromagnetic field set-up by circulating current from interlaminar insulation defects. Detailed theory is given by Sutton(1).

The test provides an indication of core insulation faults, remedial work progress, a satisfactory condition before, and after winding, and also on-going service condition (as a guide to the necessity for core renewal). Alternative EL CID forms are described by Shelton, Fischer & Paley(2).

SERVICE EXPERIENCE

EL CID, developed by Sutton(4), and used since the early 1980's, is well established world-wide. Application to turbogenerators was straight-forward. Unexpected phenomena, identified qualitatively by Ridley(3), arose when EL CID was applied to hydrogenerator sectionalised cores, as indicated in Table 1.

TABLE 1 Review of previous qualitative analysis

EL CID signal distortion sources	CAUSE of distortion
1. Magnetic circuit discontinuities:- a. Core splits (3), b. Segmentation gaps (3) c. Vent ducts (5).	Core permeance non-uniformity.
2. Core building bars (5) (See note below)	Variation in circulating current path resistance.
3. The excitation coil (Figure 1) approximately one metre away (3).	Magnetic field of the current.
4. Bearing brackets, etc. of a minimally dismantled machine, when excited as Figure 1.	Significant leakage paths attenuate magnetising force around core (3).
5. The excitation cable (3), when wound as in Figure 2, and passing within a metre over the core end.	The flux is significantly reinforced by the electro-magnetic field (Figure 3).
6. (i) Rotor poles (3) near the sensor with the rotor in-situ. (ii) Other ferrous components (3), such as brake/jack units, steel flooring etc.	The magnetic material of the poles, or other ferrous items, may distort the flux (depending on the geometry).
7. Inclination of cable inner leg (3) when the excitation is as Figure 2.	Core flux depends on cable distance from the core.

Note. Uninsulated core building (or key) bars are standard at the back of hydrogenerator stator cores. Figure 4 clearly shows the correlation between this constructional feature and EL CID results obtained recently by Ridley (5). The disturbing mechanism is deduced as a variation in the circulating current path resistance.

'Electrical Machines and Drives', 11–13 September 1995, Conference Publication No. 412, © IEE, 1995

Appendix 9

CALCULATION OF MAGNETISING FORCE (H)

Calculation of the EL CID H value is given in (5). Complications arise from :- a) core slotting, b) inaccuracy of B-H Curves in the range involved and c) additional magnetic circuits. The last can be most significant. Calculated and test values of H, tabulated in (5), indicate 1.3 as an appropriate multiplying factor. This may be inadequate if the excitation cable embraces a large amount of supporting steel.

MAGNETIC FIELD OF CURRENT CARRYING CONDUCTOR

Ampere's Law, applied to the electromagnetic field set up by an electric current in air, eg. Ref: Carter(6), shows that the flux density (B) is inversely proportional to the distance r metres (SI units) from the current. Figure 5 shows that, at 1 metre in air from the excitation cable, B is only one tenth of its value at 0.1 metres.

Figure 6 shows that EL CID signals, near a concentrated, closely wound cable, follow an inverse function of distance from the cable. At one metre from the cable, the EL CID reading approaches a steady value.

The recommendation (3) to maintain a closely wound excitation cable (Figure 1) at least a metre from the EL CID sensor is thus confirmed quantitatively.

ELECTROMAGNETIC THEORY OF THE EFFECT OF THE EXCITATION CABLE PASSING OVER THE CORE END

Figure 3 indicates a strengthening of the magnetic field at the core ends, by an excitation cable of the form shown. Appendix 1 provides a quantitative analysis. Figure 7 shows that, when the cable is a metre or more above the core end, the effect on the induced flux is minimal. This flux distribution was unexpected, but earlier results (Figures 8 & 9) confirm it.

The general EL CID signal level is relatively high in the case of Figure 9. These results are for the bottom end of a core, supported not far above a steel floor. That is expected to produce higher values. It should be noted that the results do not decrease to zero directly under the cable, due to the test flux in the core.

FINITE ELEMENT ANALYSIS APPLIED TO THE MAGNETIC FIELD CREATED BY THE SLOPE OF THE INTERNAL LEG OF THE EXCITATION CABLE WHEN WOUND AS A SINGLE LOOP

FE results, only mentioned previously (3), are given in Figure 10 as envelopes of magnetic field distribution round the core when the inner leg of the excitation cable is parallel to, but radially offset from, the core axis. Results are for different degrees of eccentricity, which is related to axial position along a sloping inner cable leg. The values e = 0, a and 2a are chosen to correspond to the cable eccentricity at the centre, quarter core length and core end positions. This provides flux variation over one half of the core. Reversal for e = a and 2a completes the analysis for the full core length.

AN ALTERNATIVE GEOMETRIC APPROACH

A comparable result to the above FE analysis, but with different scaling, is obtained from simple geometrical considerations. The upper part of Figure 11a shows the excitation cable arrangement relevant to Figure 10 with an additional cable offset relative to the core axis. An inverse plot of cable leg distance from the core bore (Figure 11a) is comparable to the flux distribution shown in Figure 10. Only core end curves are shown for clarity, but a complete family can be obtained.

A plot of the reciprocal distance, from cable to bore, relative to core length at particular values of core peripheral position produces Figure 11b, which is comparable to EL CID results. This shows that the slope of the trace axis changes with the core peripheral position (Figure 11c). The significance of this is shown later. Zero values of slope do not occur at θ = 90 Deg. and 270 Deg.

This geometrical approach gives slightly different results, for the same disposition of the cable, to those of the FE analysis; as expected from non-linearity of the core material magnetic characteristic. The form, however, is basically the same.

ANALYSIS OF EL CID RESULTS

Figure 12 shows EL CID traces, obtained in 1986, which initially caused concern. Recognition of trace axis tilt identified significantly high values at one end of the core. Application of the foregoing theory (Figures 13 & 14) to these results reveals, however, recognizable features of the test situation.

Figure 13 shows the characteristic effect (Figure 7) of the excitation cable crossing the core end. The cable position was only recorded as being between slots 120 and 160. It is identified now as slot 138.

Appendix 9

Figure 14 shows the trace slope variation round the core. Slope values are not highly accurate as the position of the axes is subjective. EL CID equipment cannot produce a base for each trace, since its operation assumes a symmetrically located excitation source. Also, signal variations inevitably occur and may obscure the true axis position. A technique, which works relatively well in this type of situation, is application of an envelope to "clouds" of results (3). On this basis Figure 14 is examined for an indication of the plane of the cable tilt relative to the stator slot numbers.

Figure 11b defines the maximum positive slope as at $\theta = 0$ in Figure 10. In figure 14, therefore, $\theta = 0$ is at about slot 151. This implies that the inner cable leg sloped from about slot 70 (there being a total of 162 slots) at the top of the core towards slot 151 at the bottom. Weakening of the flux may be expected, therefore, at the top of the core in the region of slot 151. A reduction in EL CID values to the right of the deduced cable position (slot 138), compared to values on the other side, is in fact observed (Figure 13). Thus the analysis is consistent.

CONCLUSION

A quantitative analysis of some unusual EL CID results, further confirms the soundness of the EL CID technique. A competent technician may perform the test (5). Adequate analysis of the results requires, however, knowledge of electromagnetic theory. The analyst needs full details of the test situation. This is best achieved by attending the test.

Acknowledgements

Thanks are gladly expressed to the Directors of Adwel Industries Ltd. and GEC Alsthom Large Machines Ltd, UK. for secretarial assistance.

REFERENCES

1. Sutton, J., April 1994, INSIGHT, 36, No:4, "Theory of electromagnetic testing of laminated stator cores", 246 - 251.

2. Shelton, J.W., Fischer, M.W. and Paley, D.B., April 1994, 56th AMERICAN POWER CONF: PROC:, "Introduction and qualification of digital electromagnetic core imperfection detector (EL CID) test equipment and associated robotic delivery and inspection systems".

3. Ridley, G.K., September 1993, IEE ELECTRICAL MACHINES and DRIVES INT: CONF: PROC:, Pub: No: 376, "EL CID application phenomena", 491 - 498.

4. Sutton, J., July 1980, ELECTRICAL REVIEW, 207, NO:1, "EL CID: an easier way to test stator cores", 33 - 37.

5. Ridley, G.K., Nov: 1994, HYDROPOWER and DAMS, 1, Iss: 6, "Conducting an EL CID test on a hydrogenerator", 113 - 120.

6. Carter, G.W., 1954, "THE ELECTROMAGNETIC FIELD IN ITS ENGINEERING ASPECTS", Longmans, Green and Co:, London.

APPENDIX

Analysis of the effect on EL CID test results arising from part of the excitation cable passing over the end of the stator core, when the inner leg of the cable lies along the core longitudinal axis.

By Carter (6), "The field of a current in the presence of an iron block is solved by replacing the effect of the iron block by that of an image current" ie. the image current , equal to that of the 1st current, produces an equipotential plane of corresponding position to the original iron surface. Thus, the iron surface is simulated.

Let there be two conductors, each carrying I amperes, at A and B, each "a" metres above and below the iron surface, respectively. Therefore, at any point Q in the plane of the iron surface, where the distance from A and B is equal to "r" metres, the magnetising force from each conductor is

$$H_{AQ} = H_{BQ} = \frac{I}{2\pi r} \text{ in magnitude,}$$

directed at right angles to the line joining the relevant conductor to Q.

The resultant flux density (B) at Q is, therefore,

$$B = \eta_0 H = 2\eta_0 \cdot \frac{I}{2\pi r} \cdot \frac{\sqrt{r^2 - a^2}}{r} \quad \alpha \frac{x}{r^2}$$

Appendix 9

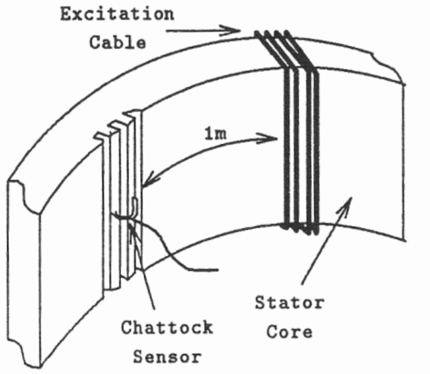

Figure 1 Recommended minimum distance between excitation cable and work area

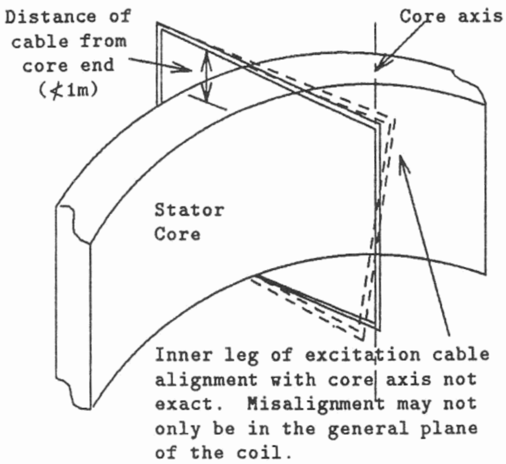

Figure 2 Recommended minimum distance of the excitation cable from the core end, when inner leg wound along core axis

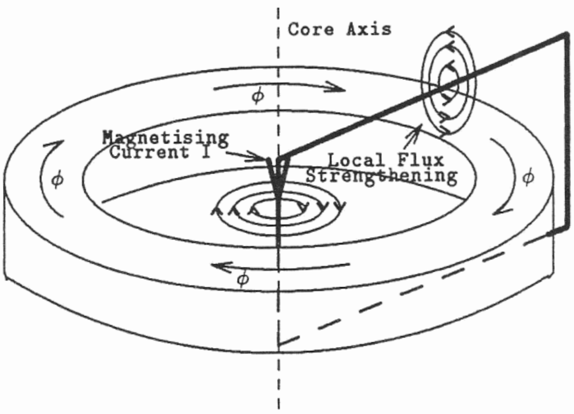

Figure 3 Diagramatic illustration of core end flux reinforcement by electromagnetic field of the radial section of the excitation cable

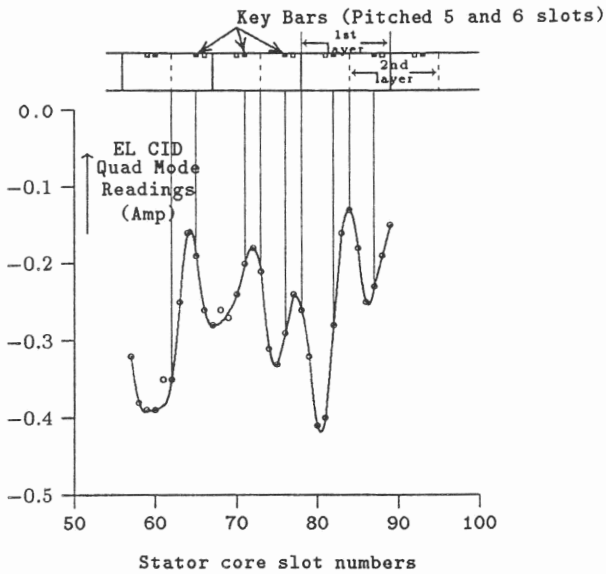

Figure 4 Correlation of EL CID signal with core-build features (Ref:5 for details)

Appendix 9

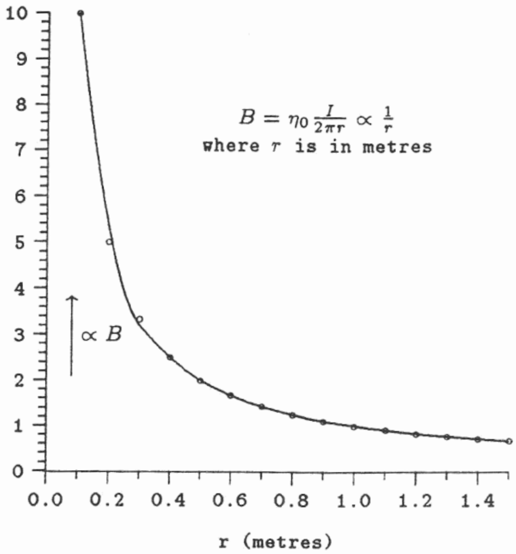

Figure 5 Decay of electromagnetic field in air arising from a current carrying conductor

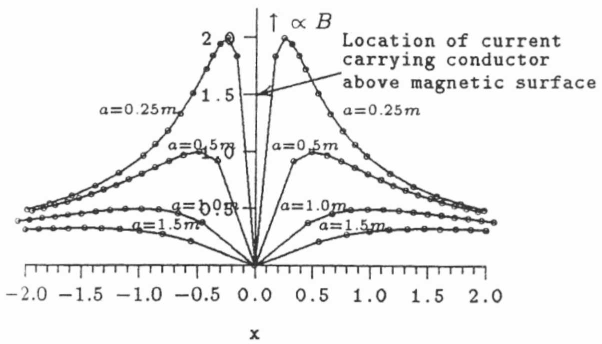

Figure 7 Theoretical variation of flux density (B) in a magnetic material surface due to a current carrying conductor above it

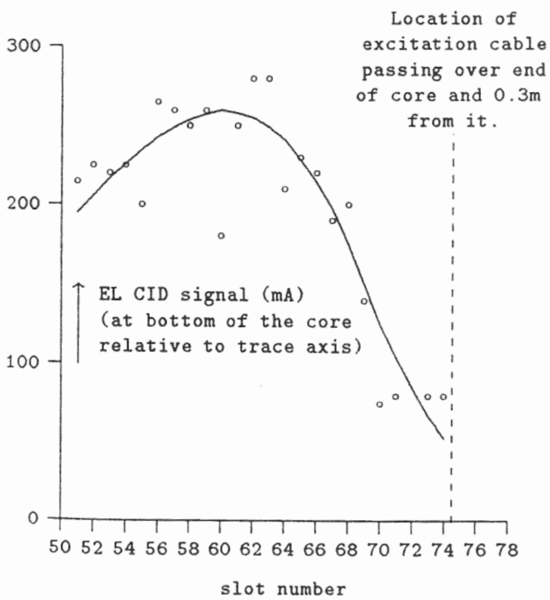

Figure 9 EL CID signal variation at a core end over which the excitation passes (Machine 2, July 1987)

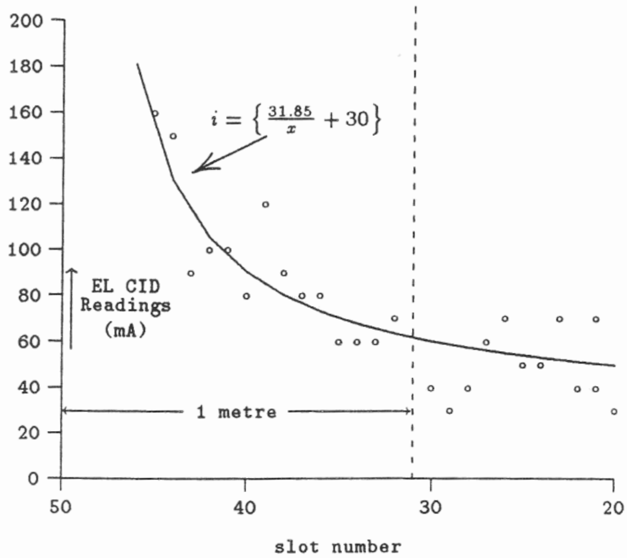

Figure 6 Correlation of EL CID test results with the reciprocal of distance from the excitation cable

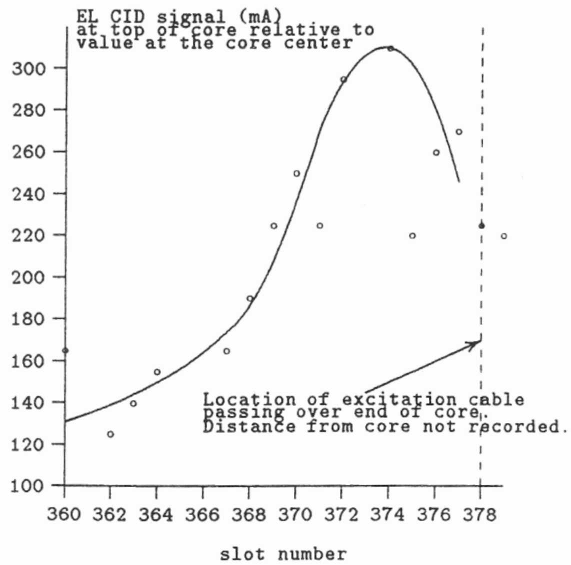

Figure 8 EL CID signal variation at a core end over which the excitation cable passes (Machine 1, Jan 1987)

Appendix 9

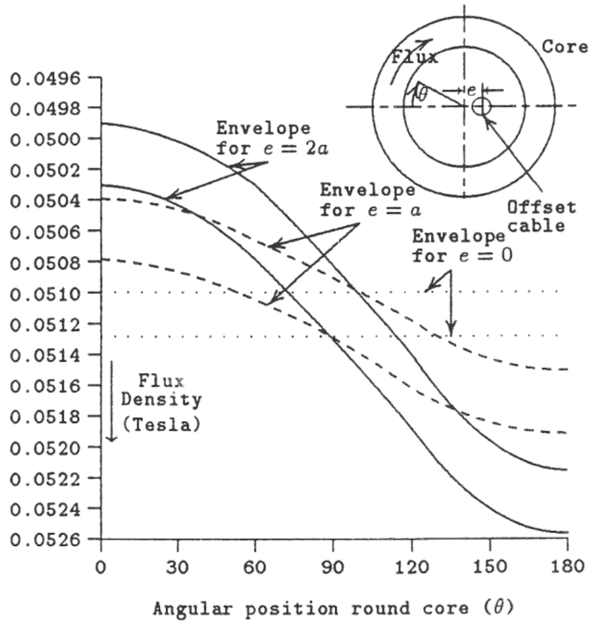

Figure 10 Finite element solution of magnetic field produced by excitation cable located eccentric to the core axis

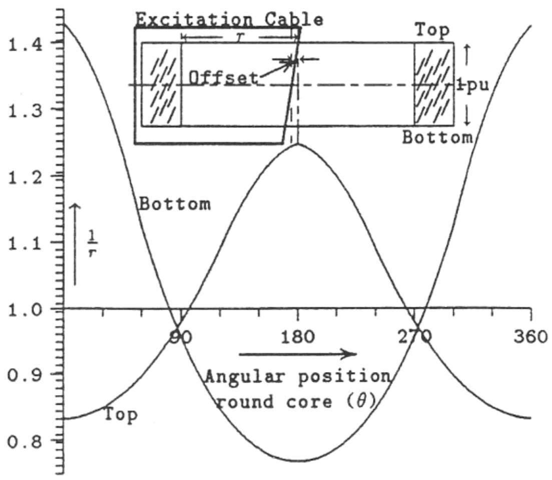

Figure 11a Geometric arrangement of excitation cable and reciprocal distance from cable to stator bore as a function of angular position round core

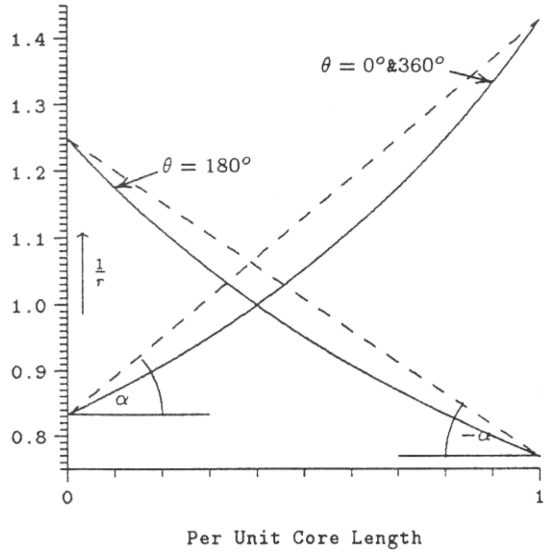

Figure 11b Reciprocal distance from cable to stator core bore as a function of core length

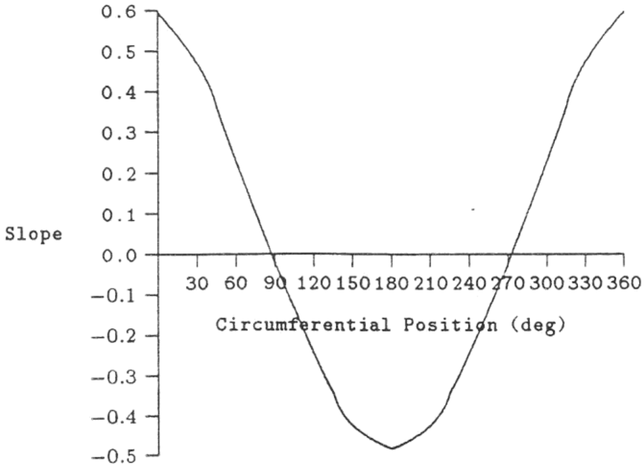

Figure 11c Slope as a function of circumferential position

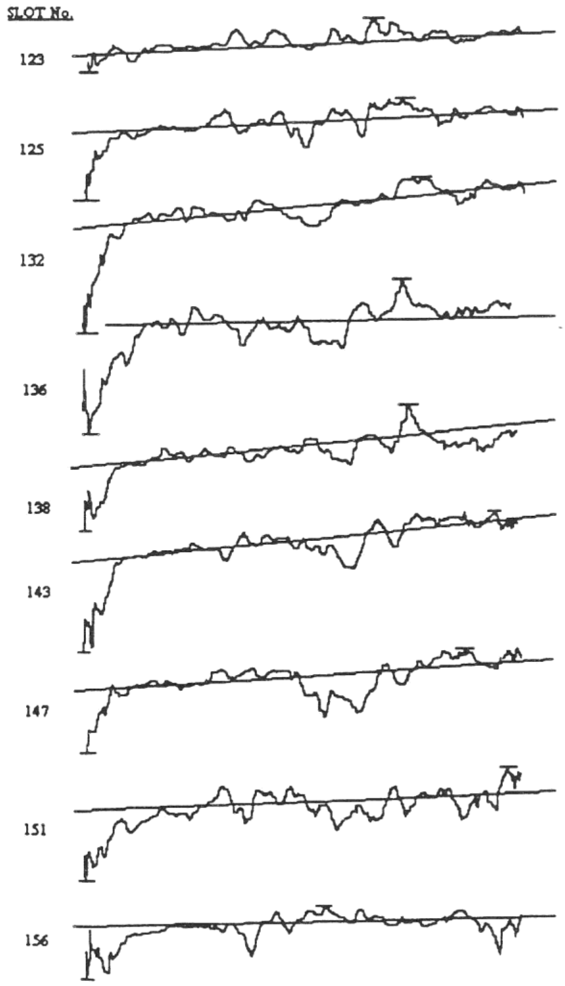

Figure 12 EL CID traces illustrating
a) a tilt of trace axis.
b) a significant deviation at the TOP of the core.
(Machine 3, October 1986)

Appendix 9

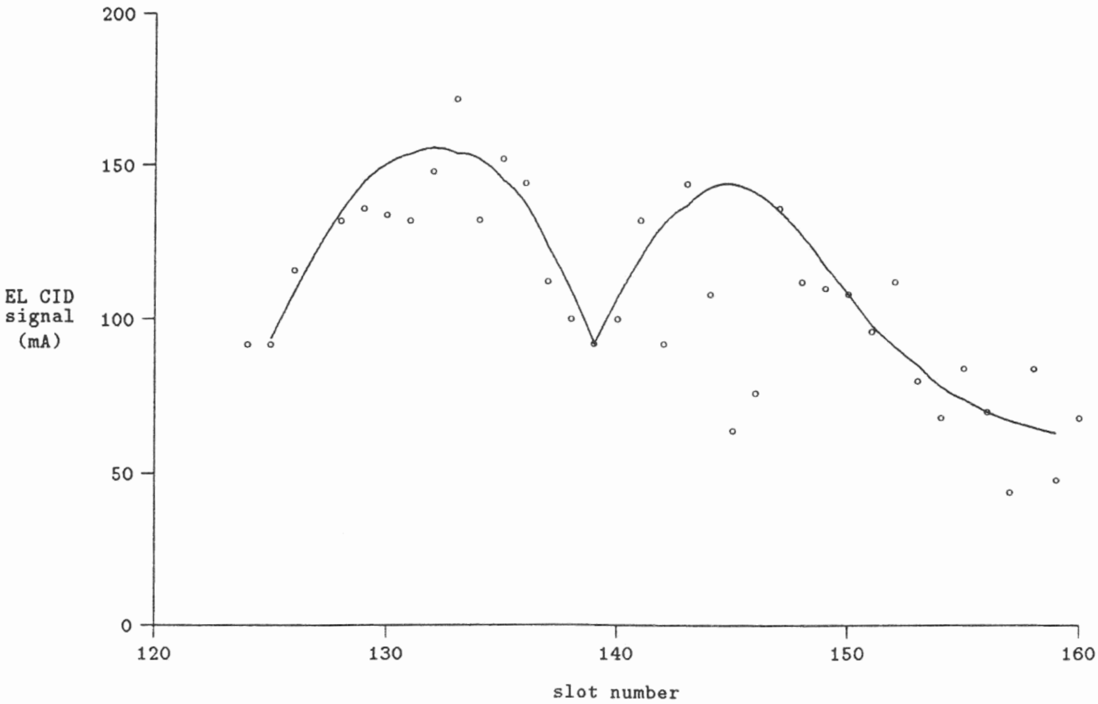

Figure 13 EL CID signal variation at the top of the stator core (Machine 3, Oct 1986)

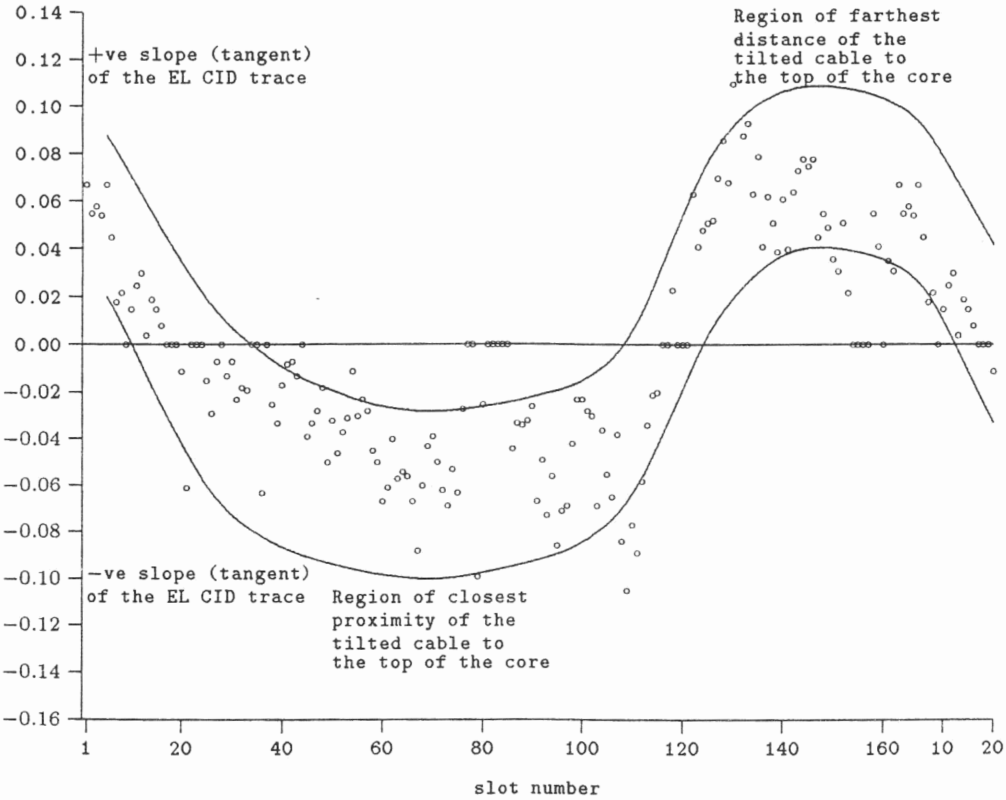

Figure 14 Envelope of EL CID trace slope (Machine 3, Oct 1986)

Appendix 10

POLE PROXIMITY EFFECT ON EL CID RESULTS

G. K. Ridley

Private Consultant, ADWEL International Ltd.,Canada

BRIEF BACKGROUND TO EL CID

The dielectric stress imposed on the stator core interlaminar insulation by the stator electrical field of the very large rotating machines being commissioned in the 1970's, sometimes incurred break-down and very expensive outages. To minimise these, EL CID (Electromagnetic Core Imperfection Detector) was developed by Sutton (1), as a more convenient core condition monitor than the normal high flux ring test.

The essence of the EL CID technique is the detection, by a Chattock Potentiometer, of the magnetic potential difference at the stator bore. The detected signal is converted to a current value by a Signal Processor Unit (SPU), which also resolves it into two orthogonal components, called PHASE and QUAD. Since the interlaminar electric current component (δ) flows in a mainly resistive circuit, it is virtually 90 degrees out of phase with the general magnetic field component. It is normally small, and equal, very nearly, to QUAD.

EL CID was applied initially to turbogenerators. Little difficulty was encountered in interpreting the results and the EL CID technique became well accepted. Problems arose, however, upon application to large hydrogenerators, which present a different electromagnetic topography, usually including split stator cores for ease of transportation from the factory to the construction site. Over the last 12 years these have been comprehensively investigated by Ridley (2).

POLE PROXIMITY EFFECT

This was observed early in the experience of EL CID testing of hydrogenerators, but later tests on another machine apparently did not indicate the effect. The solution, briefly introduced recently in (2), is now presented in detail.

Curve A (Figure 1) shows test results with the rotor-mounted, salient-poles of hydrogenerator No:1 initially close to the work area. The relatively high values at the ends of the stator core were identified as a pole proximity effect, by moving the nearby pole to a more remote position to produce Curve B. This shows the same general characteristic as Curve A, but without the upward curve of the trace axis at the ends. The cause was understood, therefore, to be additional leakage flux at the ends of the machine.

This phenomenon was not identified in an earlier test on machine No:2. The results (Figure 2), with the rotor out and also with the rotor in the stator, appeared insufficiently different to suggest a pole proximity effect. The difference in geometry, of the airgap between the stator and rotor and of the end structure of the two machines (Figures 3 and 4), indicated a possible cause for this discrepancy. A three-dimensional finite element analysis was applied when an approximate geometrically based analysis showed no great difference.

THREE DIMENSIONAL FINITE ELEMENT ANALYSIS

Figure 5 illustrates the three dimensional, finite element mesh modelling employed.

Results from the analysis were selected at a location unaffected by the end leakage (ie. effectively at the longitudinal centre-line of the stator core), plus two other locations, one near the end of the stator core and an intermediate position (see Figures 3 and 4).

An EL CID sensor is applied to the stator bore and traversed along the core length for each stator slot position. Interest, therefore, is in the comparative distribution of radial flux density along the bore surface for the selected longitudinal positions. A plot of flux density, for one such position, is given in Figure 6. It is for machine No:1, near the core end. This results from the magnetic field between the stator and rotor in three dimensions, thus taking account of the contribution from the ends. The case considered was that in which two salient-poles, adjacent to the one included in the study, are removed from the rotor to permit physical access to the stator bore with the EL CID sensor.

The evaluation of the magnetic field is limited by a) the definition of the finite element mesh and b) the effect of the stator slots.

3D-FE ANALYSIS RESULTS

To simplify the assessment, comparison at the three longitudinal locations for each machine was based on the flux density envelopes (eg. Figure 6). The reference value is taken as the flux density (due to magnetic flux between the stator and rotor) at the common stator and rotor longitudinal and radial centre-lines; this being virtually unaffected by the end magnetic fields. The relative increase in flux density, along the circular distance on the stator bore from the salient-pole centre-line, is shown in Figure 7. This is rationalised, for the two machines, by assigning 1 p.u. as the distance of the pole shoe edge from the pole centre-line. A relative scale is included to identify the number of stator slot pitches from the pole shoe edge in each case.

As expected from the geometry, machine No:1 has the greater leakage flux in the airgap between the stator and the rotor. This predominance, however, only extends beyond the side of the pole shoe at the outermost axial location and within one stator slot pitch.

The relative increase in leakage flux along the core length for increasing slot positions from the pole shoe side is shown in Figure 8 for machine No:2. A similar set of curves applies for machine No: 1. They are of the same form as trace A in Figure 1. This satisfactorily confirms the early diagnosis that the phenomenon detected for machine No:1 in the vicinity of a salient-pole is due to distortion of the magnetic field by end leakage flux. It does not, however, confirm the apparent difference in the results for the two machines as being due to geometrical differences.

MACHINE NO: 2 RESULTS RECONSIDERED

Figure 2 was published previously by Ridley (3) as indicative of the minimal effect of the presence of the rotor on EL CID results. It represents EL CID ammeter readings taken at the ends of each packet of laminations along the core length.

The results of Figure 2 relate to a core joint region, which accounts for their considerable variation. The joint effect is removed by taking the difference between the readings with the rotor in-situ and those with the rotor removed (Figure 9). Machine 2 is thus revealed to have a clear end-effect due to the presence of the rotor, despite being 11 stator slot pitches from the nearest pole. This had been masked by the predominant core joint disturbance.

To confirm the presence of a pole-proximity effect for machine No: 2, further results are examined, although few were obtained after reassembly of the rotor, due to priority being given to recommissioning the machine. The significance of comparing results for the two conditions is illustrated by results some 8 slot pitches from the rotor pole side. A plot of their difference in Figure 10, clearly has the pole proximity characteristic.

A set of results was also obtained immediately adjacent to the pole side. Although Figure 11 shows the influence of the nearby pole, this was not recognised initially because the absolute values were well within the normal acceptance criterion of 100 mA. A small span- or mini-Chattock sensor was used for these further tests, which meant that less of the background magnetic field was detected.

CONCLUSION

A three dimensional finite element analysis of the magnetic field between the stator and rotor of salient-pole hydroelectric generators has shown quantitatively that end leakage flux produces distortion of EL CID results, which are obtained relatively close to the side of a pole piece. The conclusion is in agreement with results obtained from two test cases. This was expected for machine No:1, but a careful reappraisal of the test results for machine No:2 was required to establish a correlation with the 3D-FE analysis, as a pole proximity effect had not been obvious initially.

The further conclusion is that EL CID results obtained with the rotor in-situ would inevitably be subject to distortion due to the pole proximity effect. Recognition of this permits it to be taken into account.

Acknowledgements

Thanks are gladly expressed to the Directors of ADWEL International Ltd. for their financial support and to the Directors of GEC ALSTHOM Large Machines Ltd., U.K. for facilities provided. Thanks are due also to Dr. Tom Preston, Head of the Electromagnetics Group of the GEC ALSTHOM Research Laboratory, Stafford, for his assistance with the three-dimensional finite element modelling.

References

1. Sutton, J., 1980, "EL CID: an easier way to test stator cores", Elec: Review, 207, No:1, 33 - 37.

2. Ridley, G.K., 1996, "Why, When and How to apply EL CID to Hydrogenerators", Proc: 2nd Hydro Power and Dams - Modelling, Testing & Monitoring for Hydro Powerplants International Conference 293 -301.

3. Ridley, G.K., 1993, "EL CID Application Phenomena", Proc: 6th IEE Electrical Machines & Drives International Conference , Pub: 376, 491 - 498.

Appendix 10

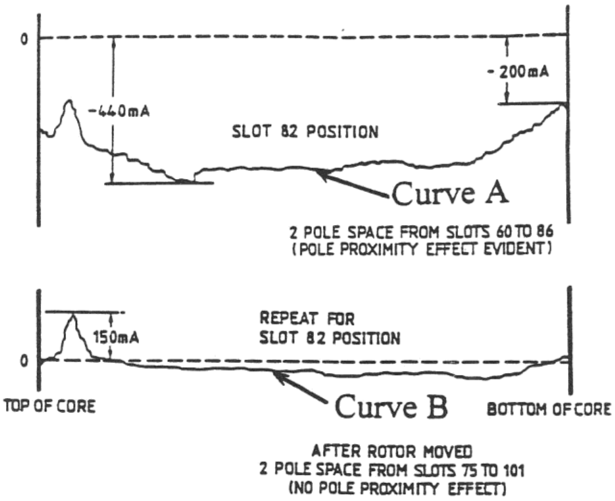

Figure 1. Machine No:1 EL CID values for slot 82 with and without rotor in-situ

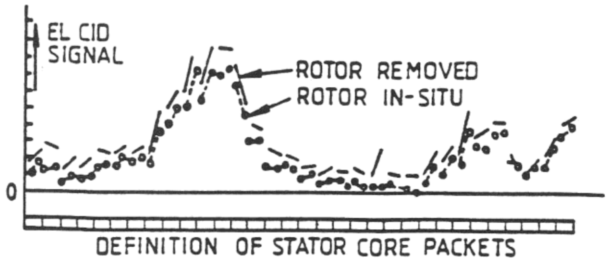

Figure 2. Machine No:2 EL CID values for split tooth 195/196 with and without rotor in-situ

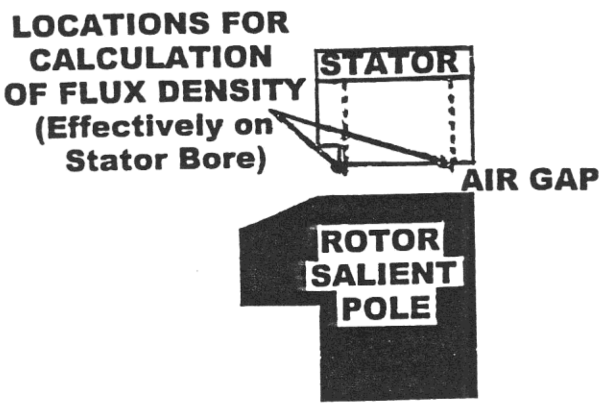

Figure 3. Longitudinal Section of Machine No:1 stator and rotor

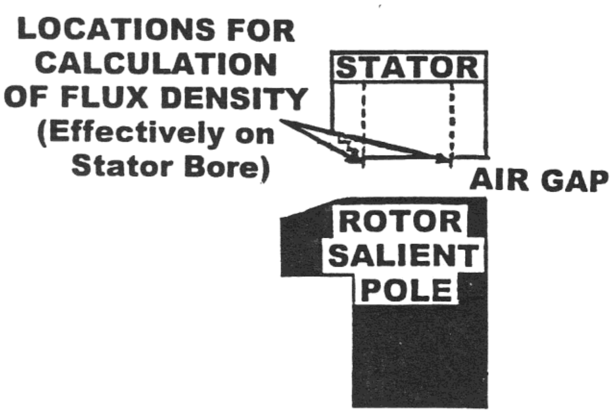

Figure 4. Longitudinal Section of Machine No:2 stator and rotor

Appendix 10

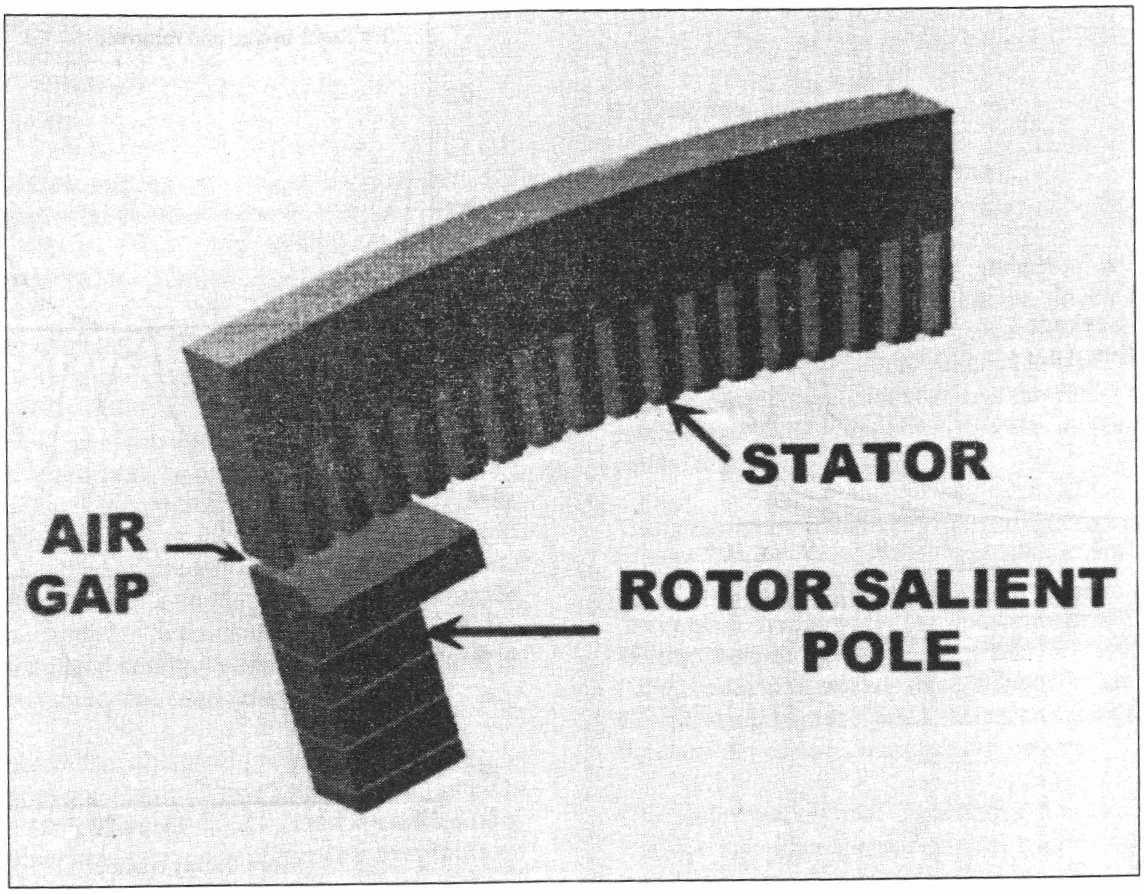

Figure 5. Three Dimensional Finite Element Analysis Model

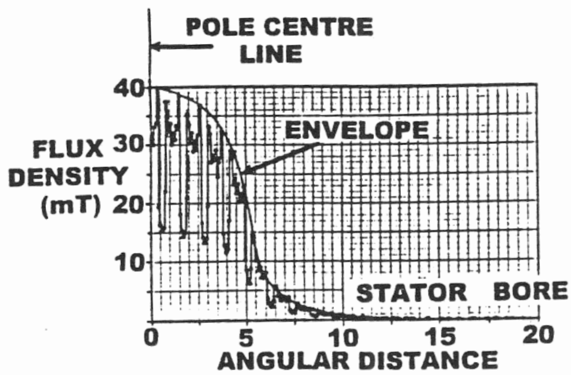

Figure 6. "3 - D" F.E. Analysis of leakage flux due to Pole Proximity Effect

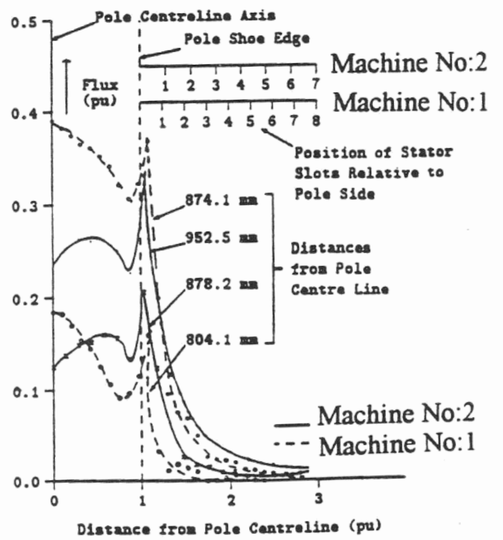

Figure 7. Additional leakage flux relative to that opposite the centre of the pole face

Appendix 10

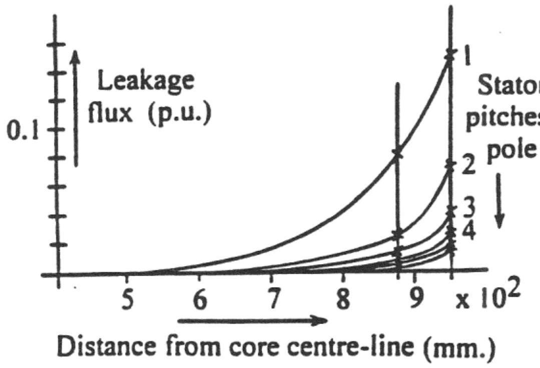

Figure 8. Increase in leakage flux for Machine No:2 relative to the value at the centre of the pole

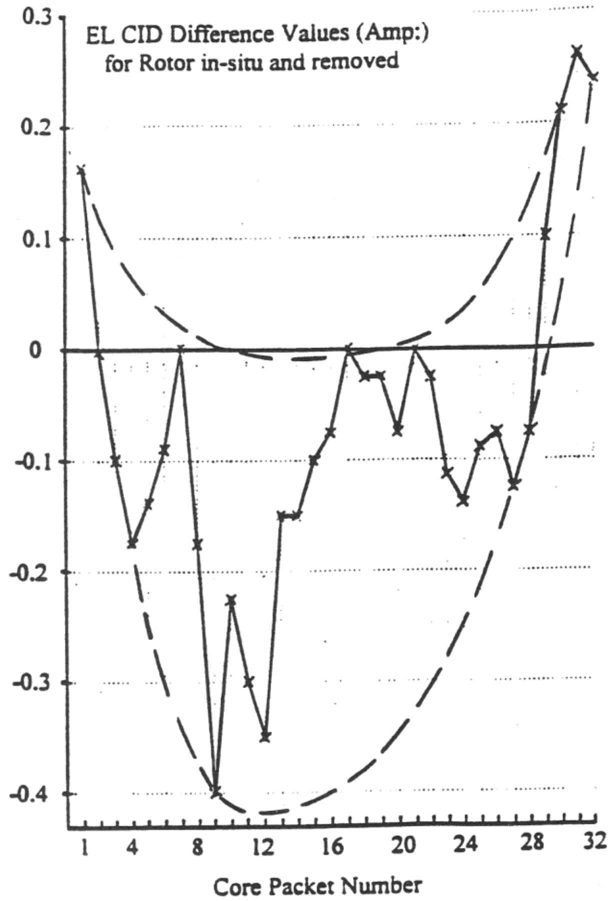

Figure 9. Difference in Figure 2 EL CID values with and without the rotor in-situ

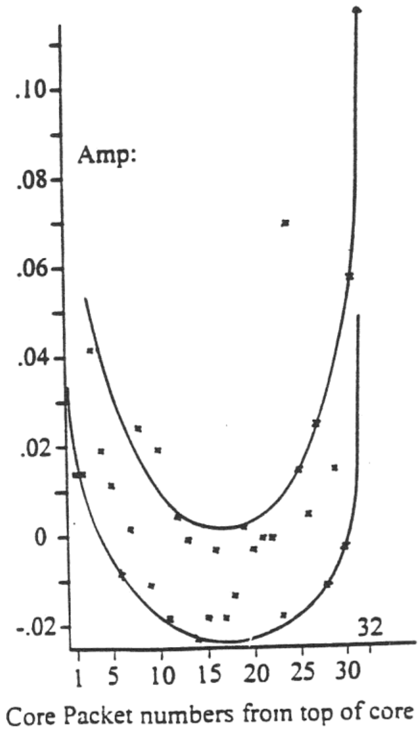

Figure 10. Difference in EL CID values 8 slot pitches from the pole side with and without the rotor in-situ

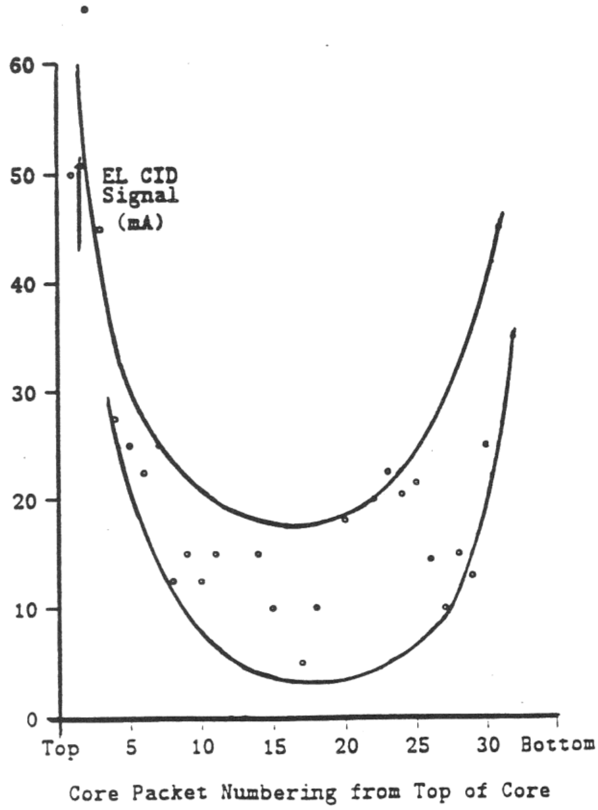

Figure 11. EL CID values close to a Machine No:2 pole

Appendix 11

The impact of stator winding circulating current on EL CID results

G.K. Ridley, UK

An unexplained phenomenon in the results of EL CID tests on generator stator cores, particularly in the case of hydro generators, was the cyclical circumferential variation in PHASE signal values. Recently, attention has focused on the existence of circulating currents, where parallel circuits exist in the stator winding. Analysis of these currents from a knowledge of the winding diagram has shown that they produce a magneto-motive force pattern corresponding to the observed PHASE variation. Thus a further significant solution in the analysis of EL CID results has been achieved, and a formula has been deduced for the wave length of the repetitive pattern of circumferential PHASE variation.

The basic principle of the EL CID test on interlaminar insulation of large electrical machine stator cores is well known [Sutton, 1980[1]]. Essentially, a circumferential magnetic field is induced in the stator iron by AC excitation, and the excitation magneto-motive force (MMF) is adjusted [Ridley 2000[2], Appendix 2.1] to produce a magnetic field strength of 4 per cent of the value required for normal operation. A Chattock potentiometer (or Rogowski coil) detects the magnetic field at the stator bore, and the signal received is resolved into orthogonal components (designated PHASE and QUAD) by an electronic phase discrimination circuit. The PHASE component is a measure of the induced magnetic field (or magnetic potential difference, that is, MPD) in terms of the applied MMF. It was assumed originally to be constant around the core periphery, on the basis of an approximately constant circumferential permeability. This value (Pe) is given by the excitation ampere turns (AT) divided by the number (S) of slots (or teeth), that is AT / S.

The first applications of EL CID were to turbogenerators. As expected, an approximately constant value of PHASE was found in most cases. On applying the technique to hydro generators, some anomalous results were observed. Explanations for most of these have been given by Ridley [2000[2]]. One anomaly, that is, cyclical circumferential variation of PHASE values at locations remote from core joints, was previously unexplained.

Core joints are introduced into the construction of many large diameter hydro generators, when originally built in the manufacturer's factory, to permit shipment in sections. These introduce a major disruption of permeance. The problem of cyclical PHASE variaton is now addressed.

Evidence of PHASE variation

Initially, the basic interest in the PHASE value was to check the working of the EL CID equipment by a spot check that the value of the detected signal in the PHASE mode was as anticipated. The QUAD signal was expected to be an indication of fault current arising from defective interlaminar insulation, and flowing in a mainly resistive circuit, that is, a circuit comprising the short circuit fault between adjacent laminations, the lamination steel and the back of the core building bars (or keybars).

One factor, noted early in the application of EL CID to hydro generators, was a variation in the general level of the QUAD signal from one slot position to another. The reason was not evident. It was usually

Fig. 1. Circumferential variation in PHASE value.

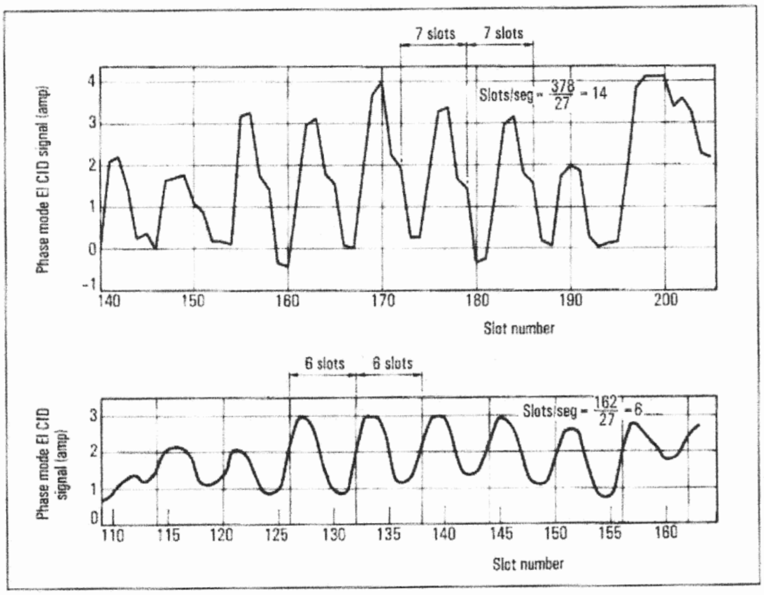

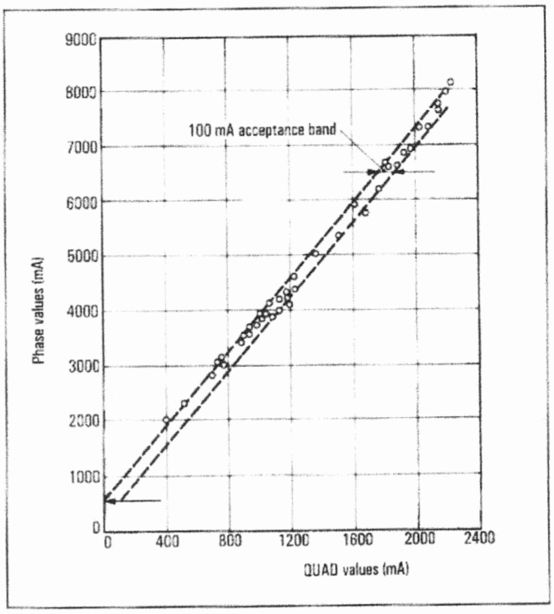

Fig. 2. EL CID PHASE/QUAD plot at a core joint.

Appendix 11

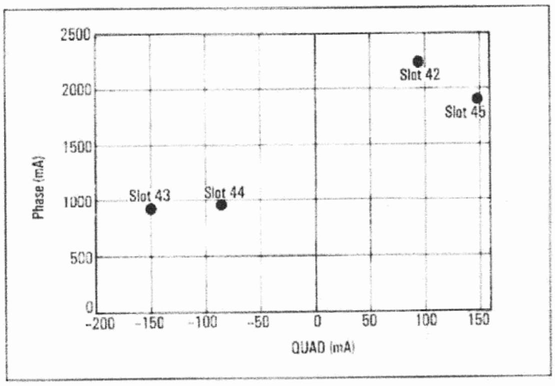

Fig. 3. PHASE / QUAD values at a given longitudinal position.

considered that the significant value was the deviation along the core length, rather than the absolute value. Nevertheless, this base variation resulted in frequent re-setting of the equipment, which incurred extra time.

As a result of this phenomenon, interest developed in the PHASE value. A record was occasionally made, therefore, of circumferential PHASE values, such as in Fig. 1 (Fig. 19 of Reference 2), and reproduced again later in Fig. 6. However, the significance of the variation remained obscure.

The much greater deviation of PHASE values observed when core joints were encountered was not unexpected. The inevitable existence of an air gap between the section faces, although small, clearly results in a significant local increase in flux leakage, representing a corresponding increase in MPD, or concentration of MMF. It was noticed that the QUAD signal had also increased considerably, despite there being no grounds to suspect the existence of a fault, either from physical observations or temperature recordings.

For a particular case, both PHASE and QUAD readings at a core joint were recorded and plotted, as shown in Fig. 2 (Fig. 39 of Reference 2). This was seen to demonstrate an essentially linear relationship. Since it was reasonable to assume that not all locations along the core joint had any significant defect, it was assumed that the straight line upper boundary represented zero fault current (δ). This line has become known as the 'zero δ line'. It will be seen below that the form of the 'zero δ line' is modified, depending on:

- the set-up of the EL CID test; and,
- whether or not the core is wound.

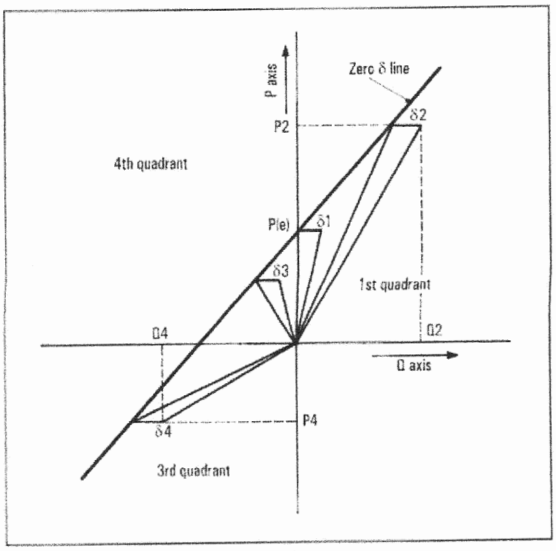

Fig. 4. Extended EL CID vector diagram.

Deviations from this line, therefore, are an indication of fault current. When the QUAD values lie between the upper 'zero δ line' and another lower and parallel line, whereby the separation is no more than 100 mA, it is reasonably concluded that the core condition at the joint faces is acceptable.

Thus, a relationship between PHASE and QUAD signals was highlighted. This suggests that, at locations remote from a core joint, PHASE variation is matched by a corresponding variation in QUAD, even if there is no fault condition. Support for this view is shown in Fig. 3 below (Fig. 43 of Reference 2). The importance of recording PHASE variation, as well as noting QUAD readings, is thus identified.

This conclusion led to an extension of the EL CID vector diagram, as is shown in Fig. 4 above (Fig. 44 of Reference 2).

The importance of PHASE variation, such as that given for two cases in Fig. 1, can now be seen. Recognition of this fact and its impact on QUAD values allows for a more accurate evaluation of the true δ value, rather than assuming that QUAD = δ. For instance, the assumption mentioned earlier that deviation in QUAD readings was an adequate indication of core condition when the general base changed from slot to slot is now understood not always to be correct. The magnitude of such deviations may result more from changes in the PHASE value than to core condition.

Evidence for stator winding circulating current

Since PHASE variation is an important factor in successful application of EL CID, especially in the case of hydro generators, it is important to show that the source of cyclical circumferential PHASE variation is understood.

The flux induced in the annular stator core during an EL CID test is in the circumferential direction. Clearly, therefore, it cannot link directly with the turns of the stator winding to produce circulating current. The EL CID sensor essentially detects leakage flux [Ridley, 2000[2], Sections 5.2 and 5.3] from the stator bore, resulting from the vector sum of the main circumferential flux induced by the excitation and the electromagnetic field arising from any interlaminar fault current. As the variation in PHASE values was observed to relate to the number of slots per core segmental lamination, the implication seemed initially to be that of a direct connection with leakage flux arising from the interlaminar gap between adjacent core segments in any one layer.

In Fig. 1, however, negative PHASE values are recorded. Since a negative magnetic field requires a negative magnetizing current, there must be a source of excitation capable of opposing the applied excitation. This pointed to the presence of circulating current in the parallels of the stator winding; the line terminals being open-circuited. Recently, stator winding

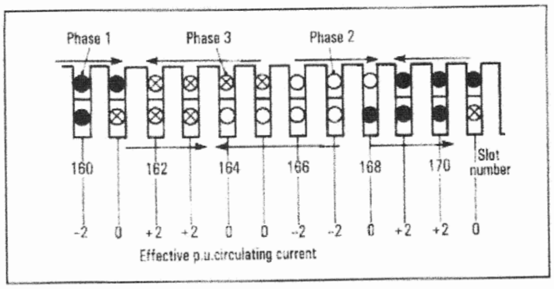

Fig. 5. Machine 1 Phase groups from stator winding connection diagram.

Appendix 11

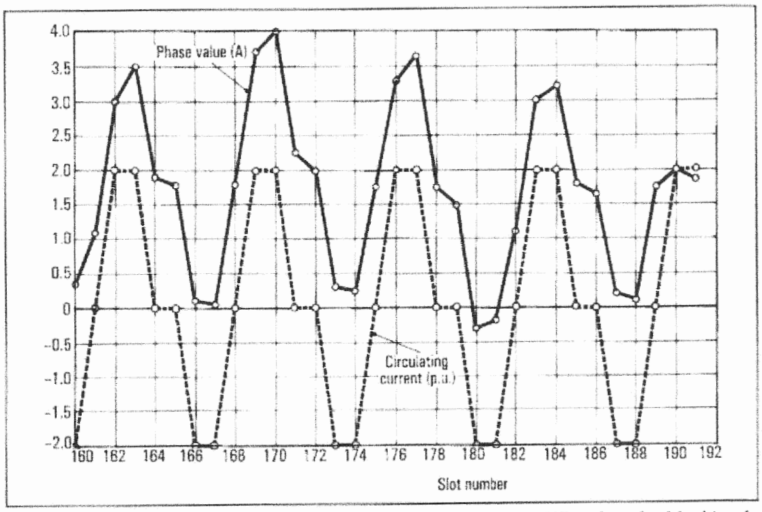

Fig. 6. Circulating current effect on EL CID values for Machine 1.

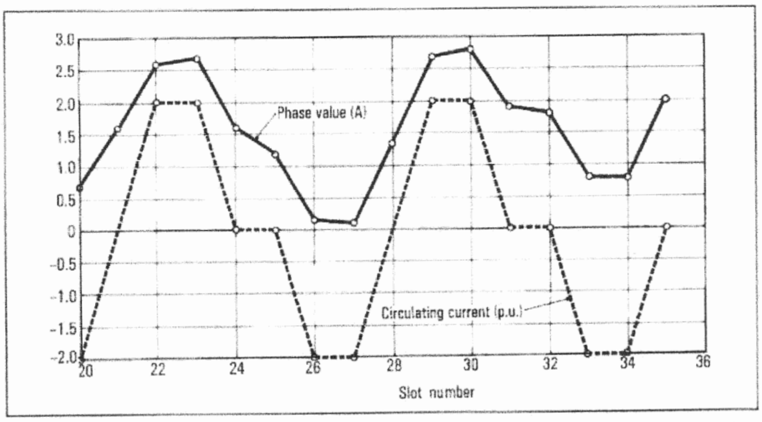

Fig. 7. Circulating current effect on EL CID PHASE values for a duplicate of Machine 1.

circulating current was reported as being detected in a machine for which a service organization had unexpectedly found significant PHASE variation remote from a core joint, similar to that recorded by Ridley (Fig. 1). This indicated interaction between stator winding parallels and radial leakage flux at the stator bore, to produce a significant impact on PHASE values.

Examination of the relevant stator winding connection diagram

The evidence of stator winding circulating current during EL CID tests prompted an examination of relevant stator windings for correspondence of circulating current effect with the observed cyclical PHASE variation.

This required identification of the winding coil groups. From the connection diagram of the machine (say, Machine 1) corresponding to the upper part of Fig. 1, the distribution of the coil groups is given in Fig. 5 for a portion of the winding corresponding to slots numbered 160 to 171. The connection diagram also shows the direction of progression of the groups through the winding. This is identified by the arrows in Fig. 5.

The mechanics of the production of circulating current are somewhat complex, and an analysis of this is not considered here, as it is not necessary to make a detailed evaluation of the circulating current. It can be seen from Fig. 1 that, although there is some variation in the magnitude of PHASE variation, the pattern of variation is fairly constant. Therefore, the assumption is made that the current in each circuit over a localized portion of the core may be assigned a value of 1 p.u.

The effective ampere-conductors in each slot depend on the direction of current in each of the top and bottom halves of the slot. Note is taken that the current direction in the top and bottom of a coil side is opposite when viewed in the slots. The distribution of the groups of turns which arises for a normal three-phase winding produces the pattern of effective ampere-conductors tabulated below each slot number in Fig. 5. For this purpose, no account needs to be taken of the number of turns per coil. For comparison purposes, it is sufficient to reckon that there is only one effective turn per coil.

Comparison of the EL CID PHASE distribution and the circulating current distribution

The upper part of Fig. 1, plus the distribution of circulating current ampere conductors, as produced when the core is excited by an excitation winding connected to a single-phase supply, is plotted in Fig. 6. The form of the excitation winding may be any one of those illustrated in Fig. 9 of Reference 2.

In Fig. 7, the same exercise is shown for a duplicate machine.

A further identical exercise applied to the machine (say, Machine 2) for which the PHASE values in the lower part of Fig. 1 are drawn, produces Fig. 8.

Correspondence of the two patterns for all three machines is clear, thus illustrating that circulating current is undoubtedly the source of the observed EL CID PHASE variation. As the circulating current effect has both positive and negative excursions along the core bore, it is obvious that it is possible for PHASE values to be driven negative. This will not always be the case, as it depends on the relative value of the electromagnetic fields set up by both the main excitation and the circulating current.

The relationship of the measured PHASE values to the deduced p.u. circulating current ampere conductors is not constant, as expected in view of the assumption of constant circulating current and the previously observed variation in magnitude of the pattern of PHASE variation. This is not important from the point of view of establishing a general principle.

Calculation of PHASE variation by finite element technique

This was applied by T. W. Preston for the upper PHASE values of Fig. 1, using a SLIM software package. The result in Fig. 9 shows good agreement once again between the form of PHASE variation and that of circulating current.

Fig. 8. Circulating current effect on EL CID PHASE values for Machine 2.

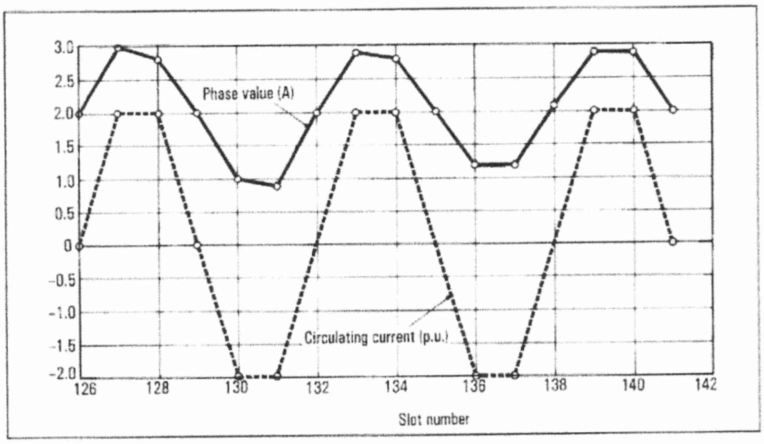

Number of stator slots for which circulating current pattern repeats

For a balanced N phase winding, the conductor pattern must repeat every $(2\pi / N)$ radians electrical angle.

The electrical angle covered by each slot position is $(P\pi / S)$, where P = number of poles, and S = number of slots.

Then, the conductor pattern repeats every:

$(2\pi / N) / (P\pi / S) = (2S / NP)$ slots
= number of slots per pole pair per phase.

For Machine 1, the above number is:

$378 / (3 \times 18) = 7$

For Machine 2 it is:

$162 / (3 \times 9) = 6$, as seen in Fig. 1.

Further implications for EL CID results of circulating current

Identification of the presence of circulating current in the parallel circuits of a stator winding, when the core is subjected to an EL CID test, has promoted interest in the vector diagram applicable to the test set-up when considered as a transformer with a shorted secondary winding.

Figs. 10 (a) and (b) shows the relevant vector diagrams, as deduced from the standard form given in any appropriate text book [Say, 1949[3]], with modification as identified below. They assume that the EL CID equipment is adjusted so that the PHASE setting is set to resolve PHASE and QUAD components strictly against the reference, without any offsetting for core loss, and so on.

There are two possible situations to be considered. In the first case, the PHASE reference is obtained from an air-cored reference coil mounted on the stator bore,which was the original standard method. But the EL CID sensor cannot identify separately leakage flux from the main flux (ϕ) and that from the circulating current electromagnetic effect. The component of excitation current required to establish the core loss is not detected by the sensor, as there is no associated magnetic flux. On the assumption that a location is found where there is no fault current ($\delta = 0$), the PHASE and QUAD axes are defined, therefore, as P' and Q', for any location A' on the stator bore, where the circulating current is $I_{CA} = P_eA'$ as shown in Fig. 10a. The PHASE and QUAD values, when fault current exists, are obtained as at location A.

The PHASE reference obtained as above is particular to the value of circulating current at A'. Therefore, for another location B, for which the circulating current effect ($I_{CB} = P_eB'$) is different, if the reference is not reset, then the QUAD value BD contains a portion caused by the circulating current. Nevertheless, a 'zero δ line' is identifiable on the assumption used

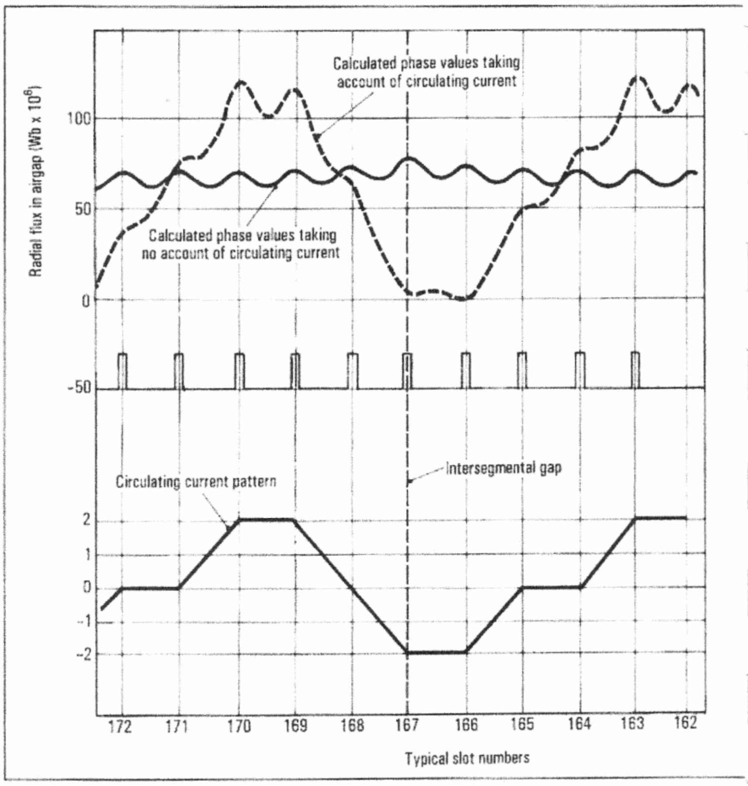

Fig. 9. Finite element analysis calculation of PHASE values for Machine 1, without and with circulating current being taken into account.

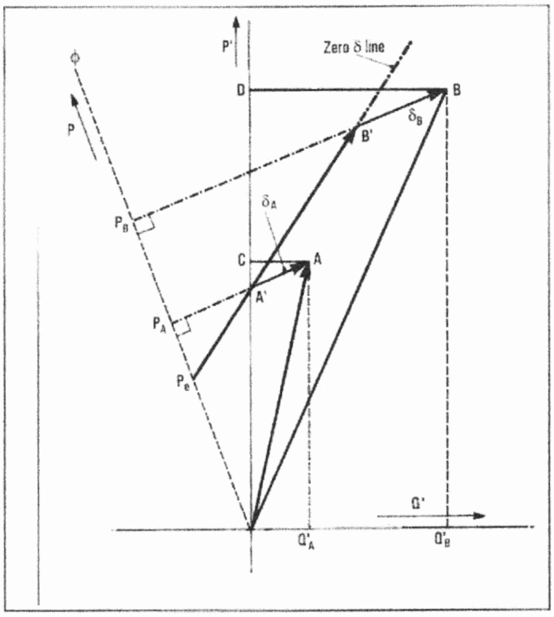

Fig. 10a. EL CID vector diagram taking account of circulating current with the PHASE reference set to the leakage flux.

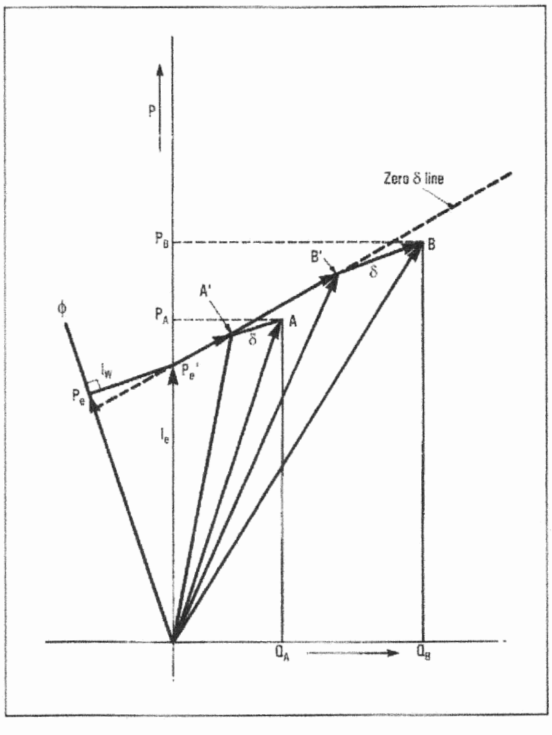

Fig. 10b. EL CID vector diagram taking account of circulating current with the PHASE reference set to the excitation current.

Appendix 11

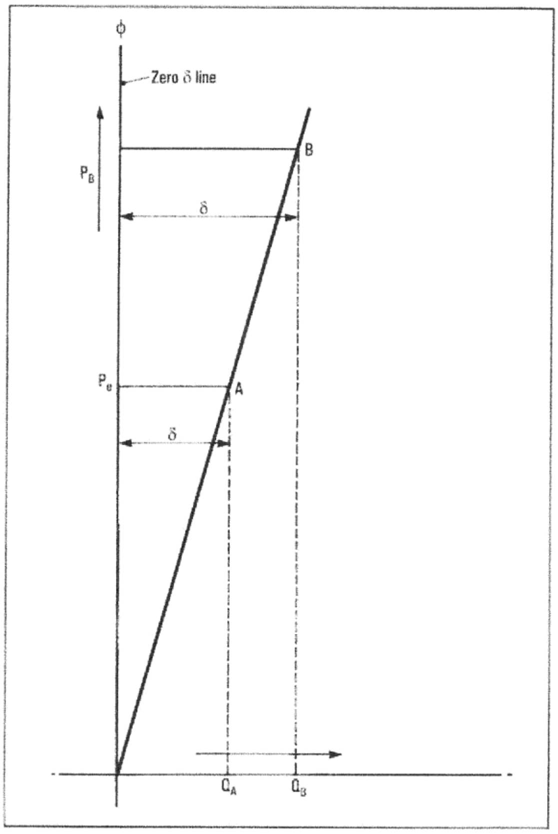

Fig. 11a. EL CID vector diagram with no circulating current and the PHASE reference set to the leakage flux.

previously that not all portions of the core contain significant faults. Thus, Fig. 10a shows essentially the same feature as Fig. 4, and justifies its previous empirical derivation, although the 'zero δ line' does not pass through P_e on the identified PHASE axis.

The second case is when the PHASE reference is established by a current transformer round the excitation cable. The circulating current form presented in Figs. 5, 6, 7 and 8 indicates that there is no net circulating current. As the assumption of 1 p.u. circulating current may not be true throughout the winding, it is possible that there may be some net circulating current to be provided from the excitation. Any net fault current will also contribute to the excitation current (I_e) detected by the current transformer. In Fig. 10b, the PHASE and QUAD axes are drawn on the assumption that the PHASE reference is again established for a zero δ value (that is, δ does not contribute to the electromagnetic field when setting the PHASE reference). PHASE and QUAD values are also indicated for two positions on the stator bore. As in the previous case, the QUAD values do not provide a direct indication of δ values. The 'zero δ line' can, however, be established as before, although located rather differently. Thus Fig. 10b also justifies the empirical establishment of Fig. 4.

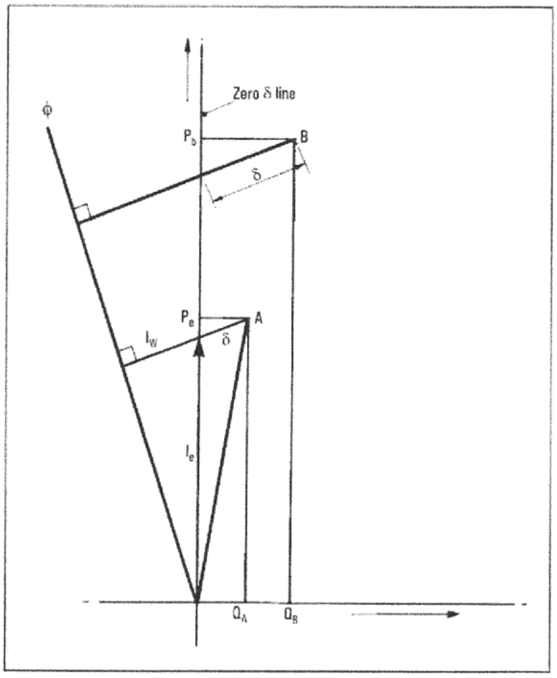

Fig. 11b. EL CID vector diagram with no circulating current and the PHASE reference set to the excitation current.

Significance of the absence of a stator winding

The foregoing discussion of the effect of a stator winding on EL CID results raises the question of the situation when there is no stator winding. This condition is that of a transformer with the secondary winding open-circuited, there being no secondary winding present. Fig. 11 shows the relevant vector diagrams as deduced again from a standard text book [Say, 1949[3]].

In Fig. 11a, the PHASE reference is that given by an air-cored reference coil on the stator bore, which detects the leakage flux. Again, the excitation current component required by the core loss does not contribute to the reference set-up. Although there are no circulating currents to vary the PHASE value, it may vary for other reasons. Consequently, the locus of the current when δ is zero (that is, the 'zero δ line') is the PHASE axis and the QUAD value is the true fault current (δ), neglecting any inductance component.

Fig. 11b shows the situation when the PHASE reference is obtained from the excitation current by a current transformer. Although the loss component (I_W) appears as part of the excitation current detected by the current transformer to establish the reference, the appropriate 'zero δ line' is again the PHASE axis. The QUAD value in this case is only approximately equal to the fault current (δ).

Conclusion

It is considered that the circumferential cyclical PHASE signal variation detected on EL CID tests has been shown to be caused by the presence of circulating current in parallel circuits of a stator winding. A long-standing problem is consequently solved. The basis of the repetition of the PHASE variation pattern has been established from basic electrical machine theory.

Furthermore, the justification of the previously detected 'zero δ line' characteristic can now be seen. The relative position of the 'zero δ line' depends on:

- the presence or otherwise of a stator winding with parallel circuits; and,
- the means by which the PHASE reference is established.

When there is no stator winding, the δ value is given almost directly by the QUAD signal.

This further, very important, understanding of anomalies encountered in the EL CID test strengthens confidence in the technique, and helps in the accurate evaluation of fault current level, whereby the condition of the core interlaminar insulation is assessed.

Appendix 11

PHASE variation is usually much less significant for turbo-generators, but it has been reported in cases where there are parallel circuits. It is noted that such machines generally have fewer stator parallel circuits than hydro generators. Detailed correlation of parallel circuit number and the degree of PHASE variation is beyond the scope of this paper. ◊

Acknowledgements

Grateful thanks are expressed to Dr. T. W. Preston for helpful comments regarding evidence of opposing MMF and for his finite element analysis using the SLIM package. Appreciation is acknowledged also to ADWEL International Ltd for the reported detection of circulating current during recent EL CID tests and useful discussions with its staff.

References

1. **Sutton, J.**, "EL CID an easier way to test stator cores", *Electrical Review*, Vol. 207, No. 1; 1980.
2. **Ridley, G.K.**, "EL CID application and analysis", ADWEL International Ltd; 2000.
3. **Say, M.G.**, "The Performance and Design of Alternating Current Machines", Sir Isaac Pitman & Sons, Ltd., Second Edition; 1949.

Eur. Ing. G.K. Ridley was a designer of large electrical rotating machines, mainly hydro generators, for a period of nearly 40 years with BTH, Rugby, UK, and its successors, concluding his career as Design Manager. He has been a registered engineer with FEANI since 1990. He became a Chartered Engineer in 1960, subsequently achieving the status of FIEE (1970) and FIMechE (1992). More recently he has been accepted as a Member of the IEEE. He has been an active member of CIGRE since 1992, having undertaken worldwide surveys of bearing design and practice for large vertical hydro generators, and also the comparison of EL CID and High Flux Ring Test (HFRT) results. He was invited to present a 'preferred subject' paper on the latter topic at the biennial meeting of the CIGRE Session in Paris in 2002. Mr Ridley has had 35 papers published, either in internationally recognized engineering journals, or in the proceedings of international conferences, and he authored a book in 2000 entitled 'EL CID - Application and Analysis'. Since nominal retirement in 1994, Mr Ridley has served as an independent consultant on hydro generators, with a special interest in EL CID result analysis.

11 Hoskyn Close, Hillmorton, Rugby, Warwickshire CV21 4LA, UK.

G.K. Ridley

Appendix 12

Further development of the EL CID vector diagram

G. K. Ridley, Consultant, UK

The EL CID vector diagram developed previously was limited by being derived with reference to the primary of an equivalent transformer and applying only to stator core bore locations remote from core joints. The reversal of PHASE values by the EL CID processor was undocumented and hence unknown. Recent work [Bertenshaw, 2006[1]] has provided a valuable insight into the electromagnetic process of the EL CID equipment, and provides support, from fundamental electromagnetic theory, for the constituent vector elements of a comprehensive EL CID vector diagram. An overall vector diagram was not produced, however. This present work identifies the different forms of the vector diagram, each of which apply for specific test conditions, and the particular location on the stator bore under examination.

The EL CID technique, devised by Sutton [1980[2]], is now a well known means of checking the interlaminar insulation of the stator core of large electrical rotating machines. The vector diagram representing the results from an EL CID test was envisaged initially as comprising two orthogonal vectors, known as PHASE and QUAD respectively. PHASE was defined as the reference vector derived from the electromagnetic field applied to the stator core by an appropriate excitation winding. QUAD was considered to be the detected signal arising from current which was allowed to circulate between adjacent core laminations by defective interlaminar insulation. Various phenomena in QUAD values were observed. These have been extensively identified and analysed by Ridley [2004[3]], thus allowing correction to be made of the EL CID results obtained.

One of these features of EL CID results was the extremely large QUAD values at core joints, such as are sometimes introduced into large machine design, mainly for purposes of transportation. This prompted interest in the PHASE/QUAD relationship, which was found to be essentially linear, initially at a core joint (Fig. 1). Subsequently the relationship between PHASE and QUAD values was explored, and the same basic relationship was found to exist elsewhere. Fig. 2 records such results for a particular position along the core length around the whole core periphery. While the relationship is generally as indicated previously, the band width along the QUAD axis is much greater, at around 400 mA, as compared with less than 150 mA in Fig. 1. It is emphasized that the Fig. 2 results are not for one peripheral position (that is, for only one slot), but for one core length position at different peripheral slot positions. Consequently, Figures 1 and 2 are not directly comparable, but illustrate that the PHASE and QUAD values are not entirely independent generally.

Subsequently, the vector diagram was extended [Ridley, 1997[4]] from the 1st quadrant into the 4th and 3rd quadrants of the geometric plane. This appeared to be well supported by results [Ridley, 1997[4]] appearing in the 4th quadrant. This version of the vector diagram has been maintained until now without further justification for some years.

In 2004, a significant advance in understanding the EL CID vector diagram took place when Ridley [2004[5]] demonstrated, from a study of the stator winding connection diagram, that circulating current in the stator winding accounted for the significant variation around a stator core reported many years before, while Bertenshaw and Sutton [2004[6]] showed that such variation can be predicted. Ridley [2004[5]] also developed the vector diagram further, including stator winding circulating current, on the basis of the EL CID test set-up being essentially that of a transformer with one or possibly two shorted secondary windings. The resultant form of the vector diagram corresponded to that previously developed empirically.

Re-appraisal of the transformer model

The transformer model for this vector diagram did not include, however, a feature analogous to core joints, thus leaving a question regarding more general application.

Recently, Bertenshaw [2006[1]] undertook an alternative development of EL CID vector diagrams, in which the EL CID test set-up is considered from a fundamental electromagnetic field point of view. His analysis shows:

Fig. 1. EL CID PHASE/QUAD plot at a core joint.

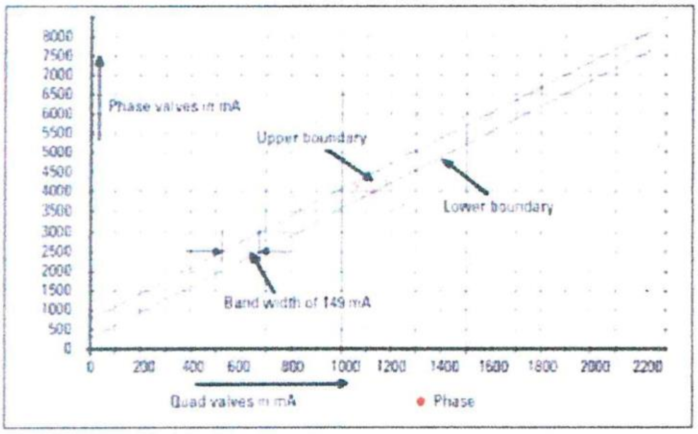

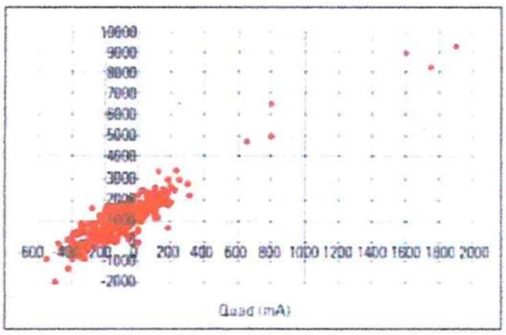

Fig. 2. Global PHASE/QUAD results at the core centreline (results for stator slots around the core periphery).

Appendix 12

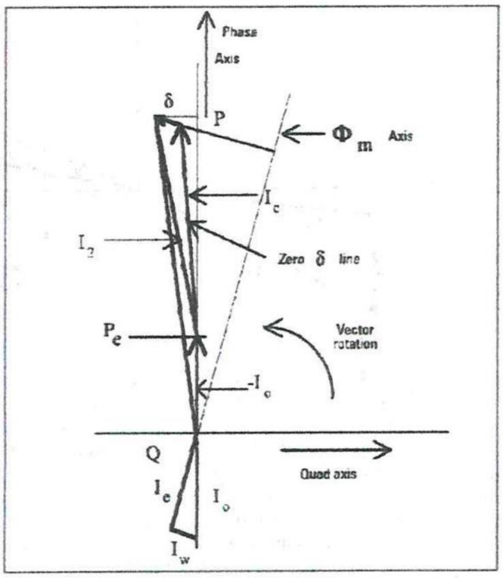

Fig. 6. Vector diagram for a location remote from a core joint.

QUAD signal, since it was considered to be independent of the PHASE values and, therefore, only its magnitude needed to be considered. When the QUAD values were recognized as undoubtedly negative, some doubt initially arose regarding the accuracy of the record, as there was no doubt that QUAD values at core joints were positive. The reason for this is identified below, but first a comment is made on setting the phase reference.

Phase reference

In the early application of the EL CID technique, the phase reference was established by the use of an air-cored coil mounted on the stator bore. The modern equipment incorporates a current transformer which is fitted round the excitation cable to provide the required phase reference. Undoubtedly the magnetic field at the stator bore comprises the electromagnetic field established by the excitation winding, as well as leakage flux from the stator bore, as has been discussed by Ridley [2004[3], Section 5.3 of the book]. It has now been established, however, from unpublished results, obtained both from tests by Bertenshaw, and also an approximate finite element analysis carried out by Preston, that the leakage flux from the stator, when there is no rotor present, is only about 3 per cent. As such it can be safely ignored for all practical purposes. Consequently, there is no need for different vector representation, whichever source of phase reference is used. In both cases it is taken as the excitation current (I_o), which is slightly out of phase with the magnetic flux (φ_m) induced in the stator core due to the inaccessible iron loss component (I_w).

Direction of the stator winding circulating current

Fig. 6 includes the stator winding circulating current vector drawn as it arises naturally as a result of transformer action. This applies primarily where the electromagnetic field is distorted for some reason. One such reason for this is the occurrence of stator leakage flux at core joints. Another reason may be an unsymmetrical location of the excitation cable relative to the stator core. The phenomenon of stator winding circulating current has been discussed in detail elsewhere by Ridley [2004[5]] and by Bertenshaw and Sutton [2004[6]]. A significant factor for the vector diagram is that the circulating current will be in the reverse direction at some slot locations, since it must balance out throughout the short-circuited winding. In this case, the voltage driving the current in the stator winding will lead the excitation current by 90°, which is in the opposite direction to that induced previously by transformer action. The current will lag the driving voltage by the same angle as applied previously. As illustrated by Bertenshaw, this reversed current is added into Fig. 6 as shown in Fig. 7, thus indicating the possibility of PHASE/QUAD results in either the 2nd or 3rd quadrants.

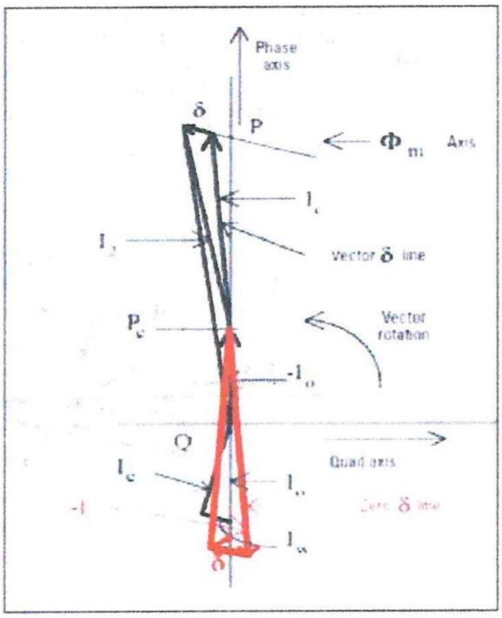

Fig. 7. Vector diagram for a location remote from a core joint, including reversed stator winding circulating current (-I c).

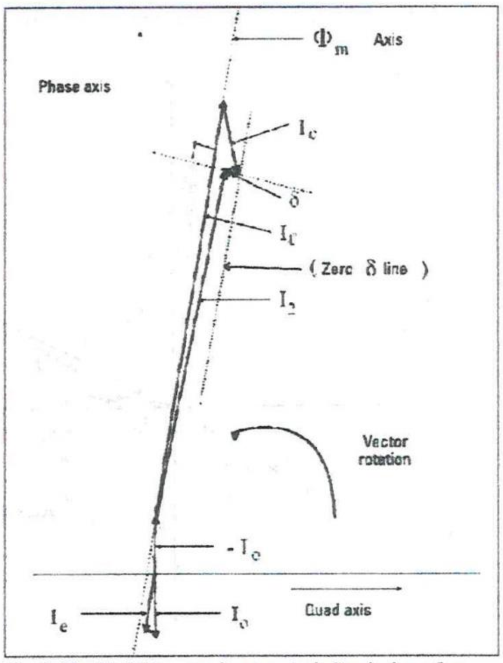

Fig. 8. The EL CID vector diagram, including leakage flux from a core joint, and stator winding circulating current.

Appendix 12

Symbols used in the EL CID vector diagrams	
Φ_m	Magnetic flux induced in an annular stator core
V_1	Voltage applied to the EL CID excitation winding
I_0	Excitation (primary) winding current
E_1	emf induced in the excitation winding
E_2	emf induced in the equivalent secondary winding
I_e	Stator core magnetization current
I_w	Current component supplying the core iron losses
I_2	Secondary winding current
I_1	Primary winding current
δ	Fault current circulating through adjacent laminations
I_c	Stator winding circulating current
P_c	Excitation amp: turns per stator slot
I_j	Current equivalent of joint air gap leakage flux
I_g	Current equivalent of leakage flux between the stator and rotor

- the importance of taking account of the iron loss in the stator core;
- the different methods by which circulating current is induced; and,
- the vector representation of the resultant detection.

It also demonstrates how the recommended test technique greatly minimizes the effect on the EL CID result of the disturbance of the magnetic field produced by the large drop in mmf at a core split. He also reported that the EL CID signal processor unit (SPU) has a previously undocumented feature which reverses the PHASE signal. An overall vector diagram, however, is not produced; preference being given to an understanding of the contribution to PHASE and QUAD of each signal. This provides a valuable insight into the electromagnetic process of the EL CID test, but does not permit an immediate correlation of the EL CID results with the test situation and identification of the interlaminar insulation condition.

Ridley [2005[7]] had noted that the form of the vector diagram deduced previously from transformer theory required reversal of the vector rotation from the standard direction, to achieve correspondence with the earlier extended vector diagram. Moreover, the vector diagram had been drawn with reference to the primary side of the transformer model, whereas the QUAD signal is detected, by the EL CID Chattock sensor, as a secondary circuit current, whether it is in the stator winding, or a path arising from defective interlaminar insulation.

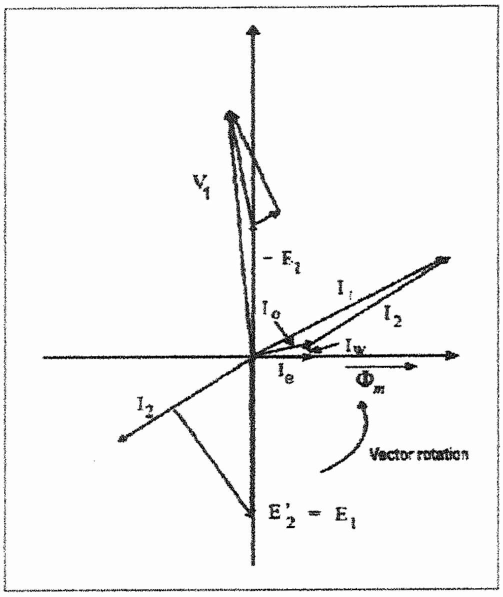

Fig. 3. The vector diagram for a transformer with a shorted secondary winding.

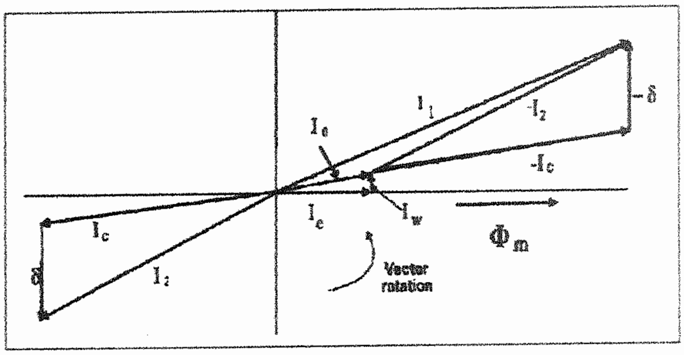

Fig. 4. Circulating current (I_c) included in the EL CID vector diagram (current vectors only are shown).

These factors have now been taken into account in a re-assessment of the previously developed EL CID vector diagram; as is shown step by step below. The symbols used are listed in the Table.

Fig. 3 is the standard vector diagram (reference any standard text on electrical machines) for a transformer, with a short-circuited secondary winding.

Fig. 4 is derived from Fig. 3, by the addition of stator winding circulating current (I_c), and the omission of voltage vectors. A further development is shown in Fig. 5, where the diagram is referred to the secondary side by the reversal of the excitation current, and the SPU reversal of the PHASE signal is taken into account by reversal of the PHASE axis.

Fig. 6 is Fig. 5 rotated through 90° to give the conventional orientation of the EL CID vector diagram for tests carried out at locations remote from core joints. This version of the vector diagram is essentially the same as the extended form published previously, except that it appears in the 4th quadrant of the current vector plane. The circulating current vector, although constant for a given slot location, varies for other locations, and is clearly the 'zero delta line', as previously defined by Ridley [1997[4]], that is, the locus of P,Q points for which there is no fault current (δ). This diagram shows that for normal anti-clockwise phase rotation and positive PHASE signal values, the QUAD signal detected will be negative for a fault within the span of the Chattock sensor. For many years, little attention was paid to the 'sign' of the

Fig. 5. Phase reversal of excitation current (I_0) included in the EL CID vector diagram.

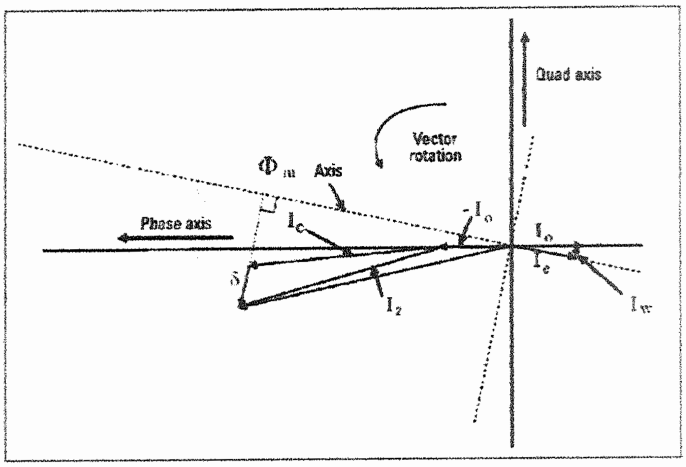

Appendix 12

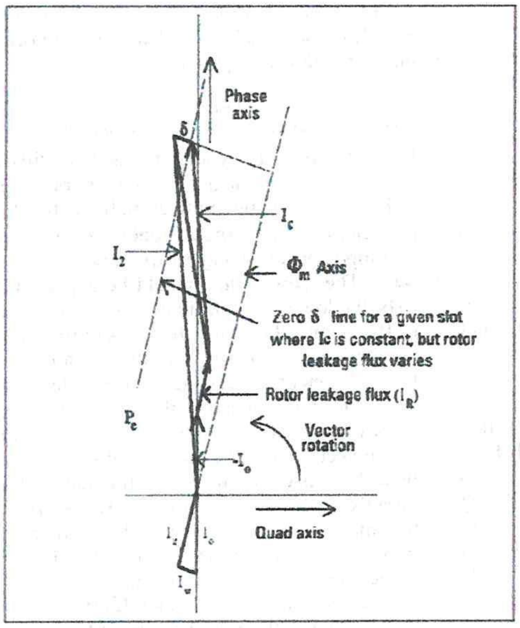

Fig. 9. EL CID vector diagram for a location remote from a core joint, including stator winding circulating current and flux leakage to the rotor.

The EL CID vector diagram at a core joint

At a core joint, the inherent air gap is of varying magnitude, because of the inevitable slight shuffle of the laminations in the course of stacking the core. This air gap produces a significant leakage of flux from the core, and absorbs a relatively large proportion of the excitation mmf. The leakage flux, being directly from the core, is of the same phase as the core flux (φ_m). It is represented in the vector diagram as an equivalent current component (I_L), which adds vectorially to the excitation current (I_o) in the direction of the vector φ_m. But this leakage flux links the stator winding in the opposite direction to the main core flux, as shown by Bertenshaw [2006[1]]. Thus the voltage induced in the stator winding is in the opposite direction to that arising from normal transformer action. The consequent stator winding circulating current is drawn as in Fig. 8. It combines with the fault current (δ), the current (I_L) equivalent to the local leakage flux, and the excitation current (I_o) to produce the final P,Q point, which has a positive QUAD value, as observed from EL CID test results.

The effect of the rotor being in-situ

The discussion so far has been on the basis that the rotor has been absent. Ridley [1997[8]] reported in connection with the Pole Proximity Effect, that Preston's FE analysis confirmed that there is leakage of flux between the stator and rotor. Although there has been no comprehensive investigation of this leakage flux, the phase direction must be the same as the stator core flux (φ_m). From the above, this is also the direction of the core joint leakage flux (I_L). It is permissible, therefore, to introduce a vector component (I_R), as shown in Fig. 9, for a location remote from a core joint. This represents a very complicated situation. Not only is the leakage flux between stator and rotor varying along the length of the core, but the core permeance also varies. Both these components affect the PHASE value. The 'zero δ line', therefore, may move in parallel to itself.

Such an addition would apply also to Fig. 8, but in that case I_R would be adding directly in the direction of vector I_L.

The overall vectorial picture of EL CID results

Figs. 6, 7, 8 and 9 are the vector diagrams required to describe EL CID results comprehensively, that is, for all cases envisaged, making allowance for fault current (δ), stator winding circulating current (I_c) (arising either directly from magnetic field distortion, or balancing the current throughout the winding), leakage flux from core joints (I_L), and leakage flux between the stator and rotor (I_R).

It will be appreciated that if there is no circulating current, and the rotor is not in-situ, then at locations remote from a core joint, the vector diagram reduces essentially to the form envisaged originally by Sutton, except that the QUAD values are negative, that is, in the 4th quadrant.

Illustration of the deduced vector diagrams by EL CID results

To establish confidence in the EL CID vector diagrams as proposed above, an examination has been made of EL CID test results, obtained from a large hydro generator, with the rotor in-situ and also with it removed.

1st case : a test location remote from a core joint, there being no stator winding and the rotor having been removed.

Although the point on the PHASE axis where it is cut by the 'zero δ line' has been defined by Ridley[1996[9]] as the magnetizing current, and evaluated as [P_e = mmf (excitation amp turns) per slot], modification is required when there are joints in the stator core. For the particular EL CID test under discussion, the mmf available per slot is calculated as follows:

Effective P_e = [Total excitation amp turns – (number of core joints × mmf absorbed per joint)] / number of slots

= [357 000 – (3 × 35 000)] / 300 = 840 mA

Fig. 10 records appropriate EL CID results, which comprise a cluster of P,Q points with PHASE values ranging from 700 to 950 mA, averaging approximately 825 mA, which is quite comparable with the P_e value calculated above. PHASE values along a particular slot are not constant due to effects identified previously and published in the EL CID literature by Ridley [2004[3]].

For this particular case the relevant vector diagram is expected to be of the simplest form (that is, Fig. 6, with no I_c component) and this does fit the results. QUAD values range from about 60 to125 mA. It

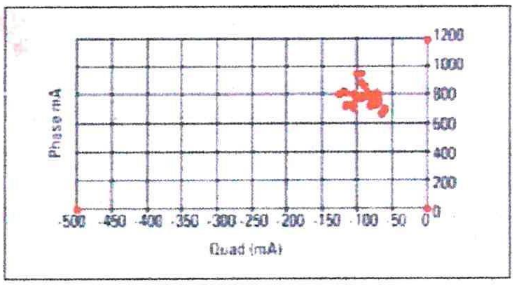

Fig. 10. EL CID results for a typical slot, remote from a core joint, without the stator winding or rotor.

Appendix 12

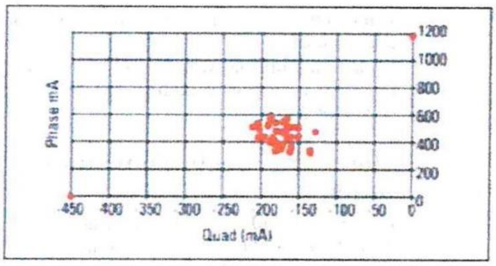

Fig. 11. EL CID results for a slot, located two slots from a core joint, without the stator winding or rotor.

should be noticed that the QUAD value is not precisely the fault current (δ), as the vector for the latter is not exactly orthogonal to the PHASE axis, but to the axis of the stator core flux (ϕ_m).

Although the maximum values might be rather more than the normal acceptance figure of 100 mA, they are clearly not exceptionally high. A High Flux Ring Test (HFRT) at 60 per cent flux applied to this core did not show a 'hot spot' at the slot location being considered. Results for an adjacent slot were only slightly higher, but the HFRT was judged to show a 'hot spot'. The surface temperature, relative to the core surface background temperature, was recorded as only 7°C, which is within the usual acceptance limit of 10°C, however.

2nd case : a test location close to a core joint, there being no stator winding and the rotor having been removed.

The location in this case was only three slots from a core joint. Fig. 11 records the relevant EL CID results. The appropriate vector diagram is the same as for the first case above. The QUAD values are in the range 132 to 220 mA, which indicates that the core joint effect diminishes quite rapidly with distance from the joint. Nevertheless, the values are relatively high, although the HFRT did not indicate a 'hot-spot' at this slot. As it is unlikely, in any case, that the whole slot location would be defective, it is considered that some off-set of the QUAD values had arisen because of the relative proximity of the core joint: the effect of which would be seen as reversed from that detected at the joint. The advantage is demonstrated, therefore, of the recommended technique of removing the mean or

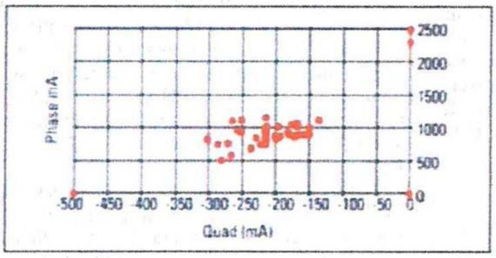

Fig. 12. EL CID results for the same slot as Fig. 11, but with the stator winding circulating current and the rotor in situ.

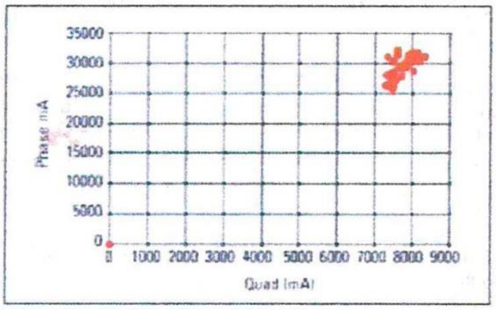

Fig. 13. EL CID results for a joint slot with stator circulating current and the rotor in situ.

'd.c.' value of the QUAD results, leaving a variation of only some +/- 45 mA, or a total value of 90 mA for δ at this slot, which is well within the normal criterion, and is thus acceptable.

3rd case : the same test location as for case 2, but with stator winding circulating current and the rotor in-situ.

Fig. 12 shows the result obtained for this case. The applicable vector diagram appears to be a combination of Figs. 7 and 9, the implication being that there is stator winding circulating current of reversed phase, plus a component of leakage flux between the stator and rotor. The 'zero δ line' would be expected, therefore, to be the lower, or right-hand side boundary of the plot of P,Q points, this being the locus of the end of the stator winding circulating current (I_c), in the direction of the component (I_R) arising from flux leakage between stator and rotor. Whether the P,Q points lie in the 2nd or 3rd quadrants depends on the relative magnitudes of the vectors. Fig. 12 indicates δ values of rather less than 150 mA, bearing in mind that δ does not lie directly in the direction of the QUAD axis. Two factors may influence the results. First, the relative proximity of the core joint; second, the Pole Proximity Effect. These results are for the same slot location as used as an example by Ridley [2004[3]] to demonstrate that by taking the Pole Proximity Effect into account the band-width of the P,Q points reduces from 150 mA to only 100 mA: the generally acceptable criterion.

Comparable results were recorded for another slot located four slots away from a core joint. In this case, the range of QUAD values was only about 100 mA, and the HFRT again showed no 'hot-spot'.

4th case: a test location at a core joint, with stator winding circulating current and the rotor in-situ.

Unusually, EL CID results, as recorded in Fig. 13, were obtained for a slot located at a core joint. Generally, the QUAD signals in such circumstances are well off-scale. The distribution of P,Q points in Fig. 13 is that expected from the vector diagram of Fig. 8, from which the 'zero δ line' is indicated as the lower boundary. This result supports Fig. 8 as the appropriate vector diagram.

However, the actual values indicated for δ, for this particular test on the same machine as the above cases already considered, are far in excess of the normal acceptance criterion, although no hot-spots were detected by the HFRT procedure. It is noted that the results in Fig. 1, for another machine, are for a comparable situation with that of Fig. 13, and the δ values derived in that case were within the normal acceptance limit, taking account of the true direction of δ. It is possible, of course, that a fault existed in the machine under consideration which the HFRT did not identify, since one of the advantages of the EL CID test is its ability to do so. The HFRT was carried out, however, after removal of the stator winding, which if present would otherwise shield any hot-spots on the slot surfaces from detection by a thermal camera.

There is no record of a problem being encountered at the core joint concerned, although the EL CID tests under discussion were undertaken some time ago, and there was no follow-up provided.

Nevertheless, there remains a question mark over the interpretation of these core joint results. While understanding of the electromagnetic conditions at core joints has much improved recently, there is scope for further investigation. It is noted that for another machine, similar very large QUAD values were recorded at its core joints by using the main-Chattock

Appendix 12

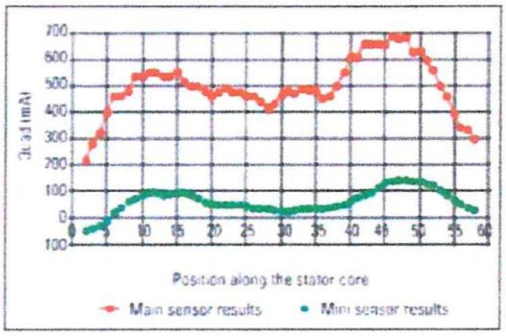

Fig. 14. Comparison of EL CID results obtained at a core joint from use of both the main Chattock sensor and also a mini-Chattock sensor.

sensor, but application of the mini-Chattock gave significantly reduced values, as shown in Fig. 14. The EL CID results at, or close to, a core joint are obviously dependent on the extent to which the leakage flux is enclosed by the sensor. This is confirmed by the results recorded in Fig. 15 for a slot adjacent to a core joint. The P.Q values are clearly much less than at the core joint of Fig. 13. This is expected, in any case, but the sensor is clearly enclosing a significant, but much reduced portion of the leakage flux, otherwise the signal would be reversed.

One of the factors is undoubtedly the way in which a core joint is formed during the core-build. For the machine in Fig. 1, the aim was to minimize the air gap at the joint by butting the joint faces together. It seems likely that for the machine in Fig. 13, a definite air gap was built-in and the joint space packed. Thus the leakage flux would extend relatively further from the joint. Increased P.Q results for a location affected by a core joint are fully anticipated, but it is not understood why the band width, which identifies δ values, should be affected.

Conclusion

The complete vector representation for EL CID results has been derived using essentially basic transformer theory. This generally provides an indication of the interlaminar circulating fault current δ, and a measure of the insulation condition.

It has been demonstrated that more than one vector diagram is required to represent EL CID results completely for a given stator core. The conditions for different slot locations have to be taken into account when selecting the appropriate form of vector diagram. Conversely, the plot of the results may indicate the relevant vector diagram, which thereby identifies the conditions which apply. Thus, the EL CID results

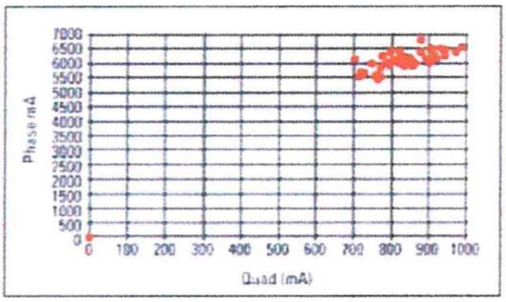

Fig. 15. EL CID results for slot 41, adjacent to a joint slot, with stator circulating current and the rotor in situ.

can be interpreted appropriately, and an indication obtained of the core insulation condition from the evaluated fault current δ

Although the situation at core joints is now described in vector terms, it appears that there are circumstances which are not yet fully understood, and require further investigation. ◊

Acknowledgement

Grateful thanks are expressed to David Bertenshaw, Director of UK Operations, ADWEL International Ltd., for helpful discussions in the preparation of this paper.

References

1. **Bertenshaw, D.**, 'Analysis of stator core faults – a fresh look at the EL CID vector diagram', Paper 15.02, *Proceedings*, HYDRO 2006 Conference, *International Journal on Hydropower & Dams*, October 2006, .
2. **Sutton, J.**, 'EL CID': an easier way to test stator cores', *Electrical Review*, Vol. 207, No 1, 1980.
3. **Ridley, G. K.**, 'EL CID application and analysis', Ed: 2, ADWEL international Ltd: 2004.
4. **Ridley, G. K.**, 'Application of EL CID with salient-pole rotor in-situ', *Proceedings*, Uprating & Refurbishing Powerplants *International Water Power & Dam Construction*, October 1997.
5. **Ridley, G. K.**, 'The impact of stator winding circulating current on EL CID results', *International Journal on Hydropower & Dams*, February 2004, Vol. 11, Issue 1.
6. **Bertenshaw, D. and Sutton,J.**, 'Application of the EL CID test with Circulating Currents in Stator Windings', *Inductica*, Berlin, Germany: June 2004.
7. **Ridley, G. K.**, 'A deeper insight into EL CID', *International Journal on Hydropower & Dams*, 2005, Vol. 12, Issue 4.
8. **Ridley, G. K.**, 'Pole proximity effect on EL CID results', *Proceedings*, 8th IEE International Conference on Electrical Machines and Drives, Cambridge, UK: 1997.
9. **Ridley, G. K.**, 'Why, when and how to apply EL CID to hydro generators', *Proceedings*, Modelling, testing & Monitoring for Hydro Powerplants II International, Lausanne, Switzerland: July 1996.

Bibliography

Say, M. G., 'The Performance and Design of Alternating Current Machines', Sir Isaac Pitman & Sons Ltd., 2nd Edition 1949.

This paper incorporates a correction published in issue Six, 2007.

Eur. Ing. G. K. Ridley was a designer of large electrical rotating machines, mainly hydro generators, for nearly 40 years with BTH, Rugby, UK, and its successors, concluding his career as Design Manager. He has been a registered engineer with FEANI since 1990. He became a Chartered Engineer in 1960, subsequently achieving the status of FIEE (1970) and FIMechE (1992). He is also a Senior Member of the IEEE. He has been an active member of CIGRE since 1992, having undertaken worldwide surveys of bearing design and practice for large vertical hydro generators, and also the comparison of EL CID and High Flux Ring Tests (HFRT) results. He was invited to present a 'preferred subject' paper on the latter topic at the biennial meeting of the CIGRE Session in Paris in 2002. Mr Ridley has had 39 papers published and in 2000 he authored a book entitled 'EL CID - Application and Analysis': the second edition of this was published in 2004, and the third edition is currently being printed. Since nominal retirement in 1994, he has served as an independent consultant on hydro generators, with a special interest in EL CID result analysis.

11 Hoskyn Close, Hillmorton, Rugby, Warwickshire CV21 4LA, UK.

K. Ridley

Appendix 13

Consequences of resetting the PHASE reference for EL CID tests

G. K. Ridley, Consultant, UK

The electromagnetic technique, generally known as EL CID, has been an important tool for checking the condition of inter-lamimation insulation in large rotating machines for more than 30 years. The implications of inaccuracies when resetting the PHASE reference are examined in the paper. It is reported that results after PHASE resetting should be referred back to the basic PHASE and QUAD axes.

EL CID (Electromagnetic Core Imperfection Detector) was invented in the 1970s [1980[1]]. The initial application to large round rotor generators, such as turbogenerators, has been highly successful, and permits a major reduction in the turnaround time and cost when the stators of these very large machines require repair. This is because the technique is a much simpler way of checking the adequacy of the repaired inter-lamination insulation than the previous high flux ring test (HFRT). The latter has a number of restrictions, and the relative merits of these alternative test procedures have been amply discussed by Ridley [2007][2].

In the early 1980s, EL CID was applied to typical hydro generators. These are often of large diameter, and, until fairly recently, were generally built in sections to permit transportation to their ultimate operational site. Experience soon showed that the significant physical differences between turbogenerators and hydro generators were reflected in EL CID test results. Although EL CID proved to be a very useful tool in many respects, new phenomena appeared, for which there was no ready explanation. These problems have been investigated, and the results, which were initially published in a series of papers, have mostly been collated by Ridley [2007][2].

The aim of the EL CID test is to allow evaluation of the current (delta) circulating between adjacent laminations in the stator core of large rotating electrical machines, as a measure of the adequacy of the inter-lamination insulation. Normal operation of such machines produces an alternating magnetic flux, which links with the electrical circuit formed by adjacent steel laminations, if they are shorted together. Inter-lamination insulation is provided to restrict this circulating current to acceptable proportions. When the insulation is defective, allowing the formation of a high resistance short circuit between adjacent laminations, the circulating electrical current causes a hot-spot to develop. This becomes the seat of high temperature damage of the affected laminations. A major fire may be instigated, producing deterioration not only of the stator steel, but also the stator winding insulation.

1. Fundamentals of the EL CID technique

In the early applications of EL CID[1], an elementary orthogonal relationship was assumed between the phase

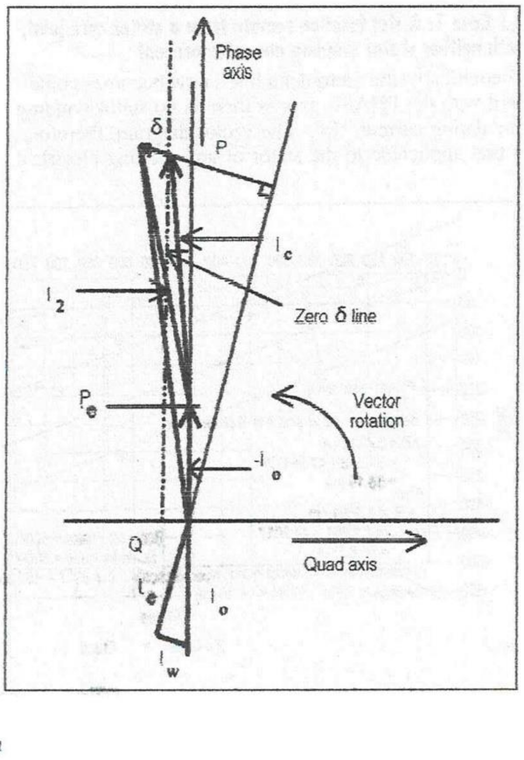

Fig. 1. The EL CID vector diagram, for a location remote from a core joint and including stator winding circulating current.

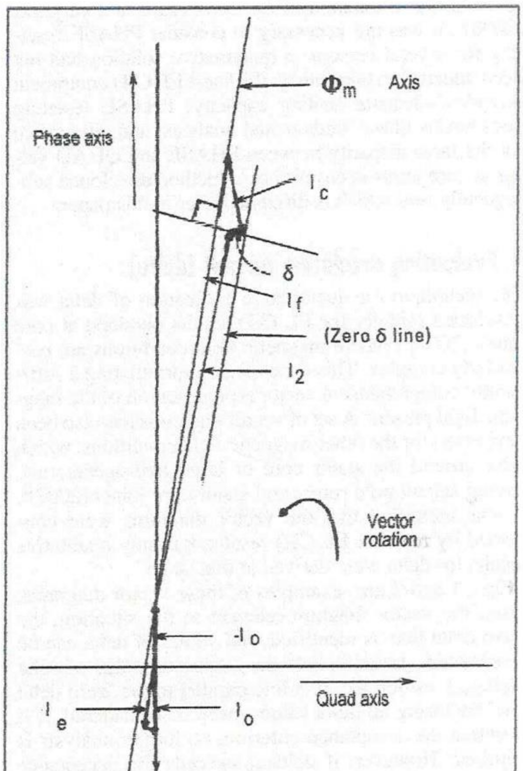

Fig. 2. The EL CID vector diagram, including both leakage flux from a core joint and stator winding circulating current.

Appendix 13

of the applied circumferential magnetic flux and that of the magnetic field produced by the circulating fault current. The EL CID equipment senses the combined magnetic field and resolves it into its two basic orthogonal components, identified as PHASE (P) and QUAD (Q), using the excitation current as the PHASE reference. On this basis, the QUAD component was considered to be the required circulating current arising from faulty interlamination insulation. In practice, as shown in Fig. 1, the induced circumferential field flux, in phase with the core magnetizing current (Ie), is offset from the reference axis provided by the excitation current (Io), by the small current component (Iw) supplying the core iron losses.

When relatively high Q values were indicated at hydrogenerator stator core joints, exceeding the initially available scaling in the QUAD mode, it was necessary to minimize such readings by resetting the PHASE axis, as illustrated in Fig. 3. Since PHASE resetting appeared to provide greater accuracy for QUAD values, this procedure became widely adopted for test locations throughout stator cores. Ridley [2007][2] noted that in such cases, a record should be made of the reset angle and that accurate results depend upon applying it. This has not generally been done when assessing the EL CID test results.

This paper investigates the validity of such practice, in two cases:

- Where there are no complicating influences from core joints, stator winding circulating current, nor leakage flux between rotor and stator.
- Where all these factors are present (see Fig. 2). Note that leakage flux between rotor and stator does not appear in Fig. 2 as a separate component, as it merely increases that corresponding to air gap leakage (I_l).

In the recent evaluation of EL CID results at core joints [2008][3], it was not necessary to consider PHASE resetting for several reasons: a quantitative solution had not been undertaken previously: the latest EL CID equipment provides adequate scaling capacity; PHASE resetting does not facilitate fundamental analysis; and, allowance for the large disparity between PHASE and QUAD values at core joints is covered by a method developed subsequently, and which is discussed later in this paper.

2. Evaluating circulating current (delta)

The technique for quantitative evaluation of delta was developed initially for EL CID results obtained at core joints [2007][4], where magnetic field conditions are particularly complex. This depended on formulating a sufficiently comprehensive vector representation of the magnetic field present. A set of vector diagrams has also been developed for the other magnetic field conditions, which arise around the stator core of large hydrogenerators, having salient pole rotors and stator core joints [2007][4]. It was identified that the vector diagrams were confirmed by relevant EL CID results, but only qualitative results for delta were derived at that stage.

Figs. 1 and 2 are examples of these vector diagrams. From the vector diagram relevant to the situation, the 'zero delta line' is identified, and values of delta can be determined. Initially, only the maximum value of delta ($delta_{max}$), as defined by a line parallel to the 'zero delta line' enclosing all delta values, need be considered. If it is within the acceptance criterion, no further analysis is required. However, if $delta_{max}$ exceeds the acceptance criterion, indicating that remedial work is needed, then delta along the whole length of the core needs to be evaluated, to define where degradation has occurred.

An important factor in quantitative evaluation of delta was recognition of the significance of plotting P, Q points using equal scales for both items, or being able to relate them to each other. Although Q values at core joints are relatively higher than elsewhere, they are still several orders less than the corresponding P values. This might cause significant error in the analysis. [2009 [5]] shows how a much larger scale can be used for plotting Q than P, but related to the P scale.

3. PHASE resetting

Ideally, the PHASE axis should be reset to lie along the 'zero delta line'. In this case all the PHASE/QUAD points detected would lie on one side of the 'zero delta line', as the required delta values would be essentially orthogonal to that new PHASE axis. The circulating current (delta) generates heat in the fault, thus drawing power from the supply, and, therefore, is mainly in quadrature with the flux. Fig. 1 illustrates this situation for a location remote from a core joint, with the rotor removed. Fig. 2 applies for locations at, or near to, a core joint. Ideal PHASE resetting, however, is generally not attainable.

It is noted that the EL CID Instruction Book recommendation is that PHASE reset is done before the start of a global EL CID test on a stator core, and not altered subsequently. The indication is that the PHASE axis should be reset to a location where it is confidently assumed that there is no deterioration of the core inter-lamination insulation. This implies that the PHASE axis is reset to where delta is zero, where PHASE/QUAD values obtained prior to PHASE reset identify a point on the 'zero delta line'. But until the EL CID scan has been undertaken, even for one slot position, it is a matter of chance that this recommended PHASE resetting can be achieved. The usual practice is to take a scan along at least one slot, and reset the PHASE axis to the approximate centroid of the cloud of PHASE/QUAD points (see Figs. 3 and 5).

3.1 Case 1: A slot location remote from a stator core joint, with neither stator winding nor rotor present

Theoretically, the 'zero delta line', now becomes coincident with the PHASE axis as there is no stator winding circulating current, 'Ic'. The vector diagram, therefore, is that applicable to the stator of any rotating electrical

Fig. 3. PHASE/QUAD plot of EL CID results for a slot location remote from a core joint.

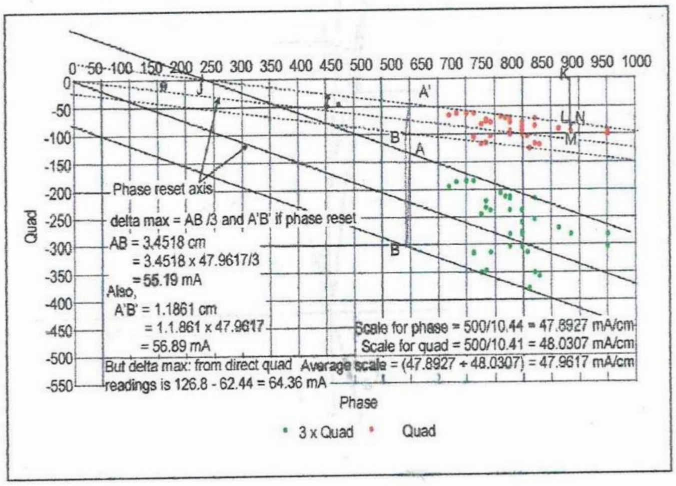

Appendix 13

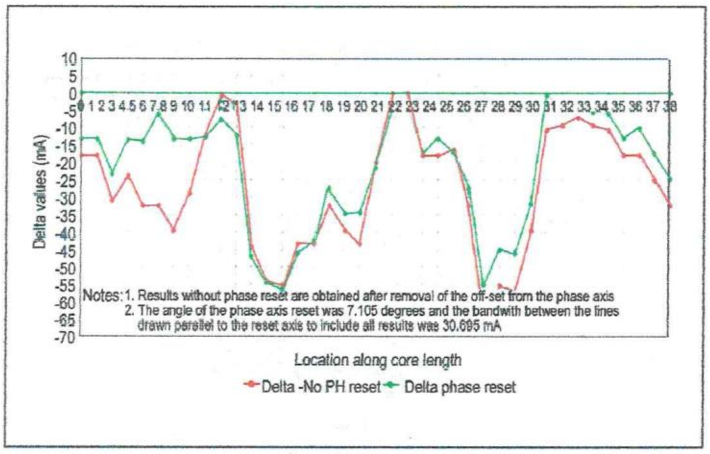

Fig. 4. Comparison of delta values with and without PHASE resetting.

machine, virtually as envisaged initially by Sutton[1], and the QUAD values would be expected to be the required delta values. Consequently, it appears that there is initially no need for PHASE resetting.

Before proceeding to discuss in detail the particular case recorded in Fig. 59 in [2007][2], it is desirable, for reasons which will appear later, to modify Fig. 59 [2007][2] by: (a) selecting equal scales for both PHASE and QUAD axes, and (b) first rotating the diagram through 90° clockwise and then the QUAD axis through 180°, to produce Fig. 3.

3.1.1 'delta' values derived without PHASE resetting for Case 1, from Fig. 3

For this particular case, where there is neither a stator winding nor a rotor in situ, it is evident from Fig. 3 that there is some offset of the delta values from the PHASE axis, the theoretical 'zero delta line'. This is inconsistent with the view, as generally held and applied, that it is unlikely that the core inter-lamination insulation is defective throughout the core length. The value of delta$_{max}$ is derived by subtracting the minimum QUAD value from the maximum value, which gives 64.7478 mA. This is negative, in accordance with the EL CID theory reported in [2007[2]].

The reason for the offset of the delta values from the 'zero delta line' is not known for certain. One possible reason may be that the discontinuities at the core joints are more far reaching than is usually appreciated. This was illustrated in Fig. 12 of [2007].

It should be noted, from Fig. 1, that the QUAD values are not absolutely true delta values. Since the losses in the stator core material produce an angular rotation of the internal flux (Φ) axis from the detected PHASE axis, the delta vector is not exactly orthogonal to the PHASE axis. The effect is generally regarded as insignificant. Since, it has always been present, it is an inherent feature of the long established acceptance criterion of 100 mA. Hence, the situation produces a set of results from the EL CID test for which it might be considered appropriate to consider PHASE resetting. The effect of this is considered below.

3.1.2 'delta' values derived from Fig. 3 with PHASE resetting for Case 1

As indicated above, the reset PHASE axis is drawn through the estimated centroid of the group of PHASE/QUAD points produced by the EL CID test, as shown in Fig. 3. Lines parallel to this reset PHASE axis are then drawn to enclose all the points plotted. On this basis, the orthogonal distance (A' B') between these parallel lines gives delta$_{max}$, the maximum value of delta. The value obtained, by reference to the end co-ordinates, derived very accurately from the computer screen grid, is 56.89 mA.

To reduce any inaccuracy arising from the significant difference in PHASE and QUAD values, the plot of PHASE and QUAD values has been modified, by increasing the scale of the QUAD axis. In this case, the increase by a factor of three is convenient for display on an A4 sheet (see Fig. 3). Therefore, by application of the technique published [2009][5], the distance AB is constructed. It is found, by use of the end co-ordinates, as above, to give a revised value of delta$_{max}$ of 55.19 mA, which is not markedly different from that obtained previously. The average of 56.04 mA is well within the usual criterion of not more than 100 mA for an acceptable condition of the inter-lamination insulation.

3.1.3 The location along the core length of 'delta$_{max}$' given by the two methods for Case 1

The above delta$_{max}$ values, derived with and without PHASE resetting, confirms the overall acceptable quality of the inter-lamination insulation. In general, however, it is also of vital interest to know the location where the inter-lamination insulation is weakest. It is important, therefore, to discover if these two values of delta$_{max}$ relate to the same location along the core. For this, the delta values need to be evaluated at all corresponding locations along the core length for both 'no PHASE reset' and 'with PHASE reset'.

There must be a common zero reference for delta values at every location. To obtain viable delta values, therefore, in the case of 'no PHASE reset', the minimum value of the QUAD signal is subtracted, giving the red line in Fig. 4, where delta values are plotted against core length location.

In the case of results with PHASE reset, the origin to which individual location values of delta refer has not been defined. As already stated, delta values must have a common zero reference at every location. Consequently, the line parallel to the reset PHASE axis nearest to the basic PHASE axis (the theoretical "zero delta line") must be the required practical "zero delta line".

This definition allows the determination of revised delta values, (delta$_{reset}$), along the core length. These could be obtained by direct measurement using a ruler, but it is quicker and more accurate to achieve the individual delta$_{reset}$ values by calculation from the co-ordinates (P, Q) referred to the basic axes, plus knowledge of the reset angle (q).

By application of simple geometry, it can be shown that the revised delta values required are given by:

$$\text{delta}_{reset} = LM \cos q$$

$$= (KM + KL) \cos q$$

$$= KM \cos q + (OK - OJ) \tan q . \cos q$$

$$= KM \cos q + (OK - [a / \sin q]). \tan q. \cos$$

$$= Q \cos q + P \sin q - a$$

where: P, Q and q are defined above and a = the orthogonal distance between the PHASE reset axis and the parallel line enclosing the minimum P, Q points (see Fig. 3). Note that the sign of Q is taken into account. The calcu-

4

Appendix 13

lated values of $delta_{reset}$ are plotted, in green, as shown in Fig. 4.

On the whole, the comparative plot of delta values in Fig. 4 shows a very close correspondence, except for locations 4 to 7 along the core length, although even the higher values determined from the 'no PHASE reset' method are not a matter of concern, in this instance.

Nevertheless, the lack of correspondence highlights a possible danger from the adoption of PHASE resetting, since there is the potential for incorrectly identifying the region where the interlamination insulation is most vulnerable. It is evident from the spread of (P, Q) points in Fig. 3, that the PHASE reset angle could result in some (P, Q) points, which are identified as relatively high without PHASE resetting, being located close to the revised "zero delta line". Thus indicating a better condition for the interlamination insulation than is justified.

3.2 Case 2: A slot location dose to the stator core joint, with both stator winding and rotor in situ

The results for this case are plotted in Fig. 5, with equal PHASE and QUAD scales and the axes processed as for Fig. 3.

From a study of the vector diagrams [2007][2] it is deduced that in this case the appropriate vector diagram is that of Figure 57 in [2007][2], but with varying leakage flux between the stator and rotor, and even reversal, as is demonstrated to be possible in Section 5.10 and Figure 56 in [2007][2].

The 'zero delta line' is determined by drawing a line to touch the P, Q points nearest to the origin. This is determined most accurately by re-plotting the QUAD values to a larger scale. This 'zero delta line' is then transferred back to the original plot of P, Q points, by reducing QUAD values on the 'zero delta line' by the relevant factor (3 in this case). This new 'zero delta line' should fit well with the original P, Q points. If not, the original 'zero delta line' needs review. The construction to identify $delta_{max}$ (AB in Fig. 5) from the revised plot is undertaken, as before, in accordance with the procedure in [2009][5].

$delta_{max}$ has been determined in five ways: measurement of AB and A´B´ by ruler; by reading the co-ordinates of the end points of AB and A´B´ on the computer display grid; and by the calculation shown below (see table).

Calculation of A´B´ ($delta_{max}$) referred to the ends of the "zero delta line" derived from that obtained by increasing the QUAD scale.

Let the relevant 'zero delta line' cut the P and Q axes at P_1 and Q_1 respectively.

For convenience, positive values of Q are assumed.

Then the equation of the 'zero delta line' is given by $Q = (P_1 - P)\,(Q_1 / P_1)$, since (Q_1 / P_1) is the tangent of the line to the P axis, and the value of delta, for any P, Q point given by the EL CID results, is readily written as:

$$delta = [Q - (P_1 - P)\,(Q_1 / P_1)] \times \cos\{\tan^{-1}(Q_1 / P_1)\}$$

Summary of the evaluation of '$delta_{max}$'

Method	'$delta_{max}$' in mA
Ruler measurement of AB	164.91
Ruler measurement of A´B´	174.47
Grid determination of AB	164.26
Grid determination of A´B´	174.82
Calculation for A´B´	170.68

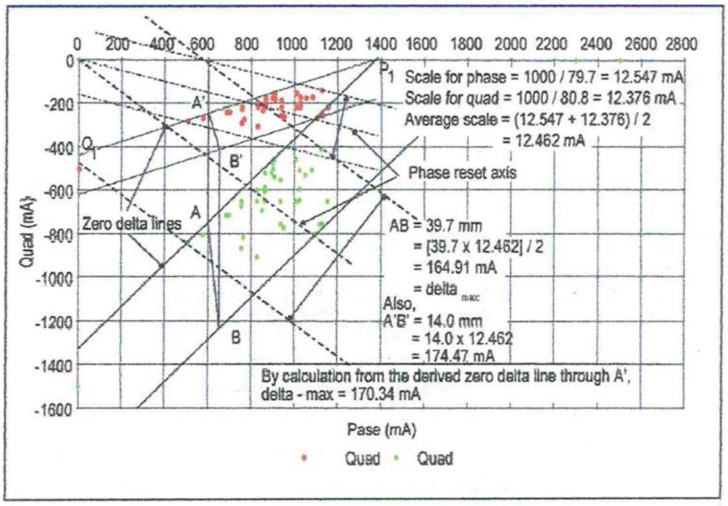

Fig. 5. PHASE/QUAD plot of EL CID results for a slot location near to a core joint.

$$= Q\cos\{\tan^{-1}(Q_1 / P_1)\} - (P_1 - P)\sin\{\tan^{-1}(Q_1 / P_1)\}$$

This equation permits the plot of delta relative to core length, as shown in Fig. 6.

By inspection, it is found that "$delta_{max}$" occurs where Q = 266.55 (adopting a positive value) and P = 1100.71. Thus "$delta_{max}$" is calculated as follows:

By use of the computer grid, Q_1 and P_1 are found to be 439.35 and 1373.90 mA respectively.

Let $\alpha = \tan^{-1}(Q_1 / P_1) = \tan^{-1}(439.35 / 1373.90) = 17.73$ degrees, for which $\sin\alpha = 0.30459$ and $\cos\alpha = 0.9525$.

Then:

$$delta_{max} = (266.55 \times 0.9525) - (1373.9 \times 0.30459) + (1100.71 \times 0.30459)$$

$$= 253.89 - 418.48 + 335.27$$

$$= 170.68 \text{ mA}$$

4. Case 2 results not referred back to the basic axes

As in the first case considered above, it is of interest to examine the effect of PHASE resetting which is not referred to the basic axes. Possible PHASE resetting is indicated in Fig. 5.

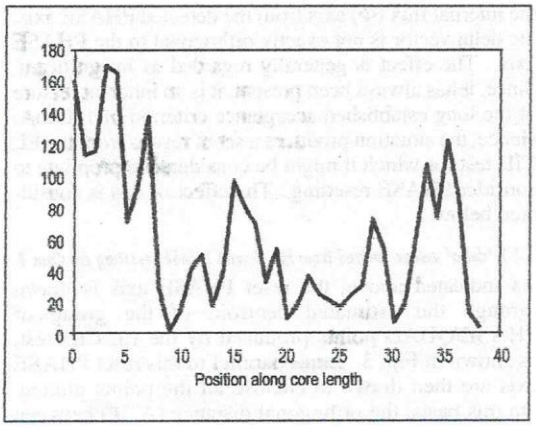

Fig. 6. The variation of delta along the core length.

Appendix 13

4.1 Evaluation of 'delta$_{max}$' without reference to basic axes

From Fig. 5, it is clear that in whatever way the results are interpreted, correct evaluation of 'delta$_{max}$' will not be achieved. The band of P, Q point values identified by lines parallel to the reset axis has a value of 295.3 mA, which is far different from the true value evaluated above.

After eliminating the PHASE reset (assuming that the plotted points had been obtained after PHASE reset), the range of QUAD values happens to be 168.3, almost the same as values evaluated above, but this is considered to be purely coincidental, and bears no real relationship to "delta$_{max}$". The conclusion is that the evaluation of delta, at any location along the core, necessitates the procedure as set out above.

4.2 Indication of the core location with the highest value of delta without reference to the basic axes

The choice of the PHASE reset angle is a matter of opinion, but would normally be where it was thought that there was least value of delta, after a preliminary scan of the slot under investigation. On this basis, Fig. 5 suggests the PHASE reset axis shown. When this choice was made, the actual values of delta along the core were not known. It so happens, however, that the chosen PHASE reset axis passes through the location along the core (position 3) where delta is maximum. This is contrary to the desired objective. The locations indicated as likely to have the largest delta values by the band of P, Q point values, identified by lines parallel to the reset axis, are locations 19 and 38. For position 19, the delta value is only 53.5 mA whilst for position 38, delta is almost zero, and is at the opposite end of the core to position 3.

Although, there are some significant delta values near to each end of the core, the higher values are in the region of position 3, which points to where an investigation should first be made.

5. Discussion

The supposition that application of PHASE reset gives approximately the same 'delta$_{max}$' value as that without PHASE reset is found to be unsafe. Although the value obtained may, in some cases, be approximately the same as the true value given by reference to the basic axes, in general this cannot be relied upon.

It has been concluded elsewhere [2010[6]] that, in the close vicinity of core joints, absolute evaluation of delta cannot always be determined reliably. Therefore, relative values along the core are important as being indicative of where the interlamination insulation is most vulnerable. It has been shown above that, for this purpose, only delta values obtained relative to the basic axes should be used.

If the QUAD signal magnitude is within the range of the EL CID equipment, there is no requirement for PHASE resetting, and it is undesirable.

If it should be desired to apply PHASE reset at locations remote from core joints, for which the results may be designated P′ and Q′, then the corresponding values of P and Q, referred to the basic axes, are quickly obtained from:

$$P = P' \cos q - Q' \sin q$$

$$Q = -\{ P' \sin q + Q' \cos q \}$$

$$\text{delta} = Q - Q_{min}$$

where: q = the PHASE reset angle and P′ and Q′ are positive values.

Attention has again been drawn to the necessity of plotting EL CID results (P and Q values) to the same scale, unless different scales are taken into account by the procedure set out in [2009 [5]].

Re-plotting QUAD values to an increased scale provides easier definition of the "zero delta line" and more accurate determination of the delta values.

Knowledge of the end points of the best "zero delta line" with equal P and Q scales permits delta values along the entire core length to be calculated rapidly, from which values of delta versus core length can be plotted, thus identifying vulnerable locations.

6. Conclusion

It has been demonstrated that PHASE resetting, unless the EL CID results are subsequently referred back to the basic axes, either distorts delta values and/or the distribution along the core is inaccurate. In general, with the latest EL CID equipment, there should be no necessity to apply PHASE resetting, whether the test location is close to a core joint or not. In the exceptional event that EL CID results have been obtained with the PHASE reset, they should be referred back to the basic PHASE and QUAD axes before being analysed to obtain delta values. It is important to plot P, Q points using the same scale for P and Q, unless the different scales are thoroughly correlated with each other. ◊

References

1. **Sutton, J.**, "EL CID: an easier way to test stator cores", *Electrical Review*, Vol. 207, No 1, 1980.
2. **Ridley, G.K.**, "EL CID – Application and Analysis", Ed.3, Adwel International Ltd. / IRIS Power LP, 2007.
3. **Ridley, G.K.**, "Evaluating interlamination circulating current at core joints in large machine stators", *The International Journal on Hydropower and Dams*, Vol. 15, Issue 6, pp 106 – 114, December 2008.
4. **Ridley, G. K.**, "Further development of the EL CID vector diagram", *The International Journal on Hydropower and Dams*, Vol. 14, Issue 4, pp 96 – 101, 2007.
5. **Ridley, G.K.**, "Increased accuracy in determining interlamination fault current at stator core joints", *The International Journal on Hydropower and Dams*, Vol. 1 5, Issue 6, December 2009.
6. **Ridley, G.K.**, "Evaluation of Interlamination circulating current at core joints in large machine stators", Proceedings of the Lisbon HYDRO 2010 conference organized by *The International Journal on Hydropower & Dams*, Paper 29.6, September 2010.

K. Ridley

Eur. Ing. G. K. Ridley retired as Design Manager for large electrical rotating machines, mainly hydrogenerators, with the British Thompson Houston Co. Ltd., England, and its successors. Since retirement in 1994, after 41 years service, his special interest has been to extend EL CID electromagnetic theory. He is a Chartered Engineer, holding the grades FIEE, FIMechE and SMIEEE, and is also a FEANI registered engineer. He has had 43 engineering papers published, plus the book "EL CID – Application and Analysis".

11 Hoskyn Close, Hillmorton, Rugby, Warwickshire CV21 4LA, UK.

Appendix 14

Correlation of EL CID Results with a Stator Core Joint Interlamination Insulation Fault

G K Ridley (Eur Ing)*

SUMMARY

An experimental study in 1998 to verify the effectiveness of the EL CID electromagnetic method for checking the adequacy of stator core interlamination insulation included some results at stator core joints. From available knowledge the original investigators considered these particular results to be useless due to the disturbed electromagnetic conditions which are produced by the small air gap inherent at a core joint. These results have now been re-appraised in light of later advances in the understanding of the EL CID technique, and it has been found that they provide good correlation with an artificial fault introduced into a stator slot at the core joint. The use of EL CID at core joints is therefore significantly affirmed, and enhances general confidence in this technique. The serviceability of vital power supply units, such as hydro generators, is thereby improved, and enhances the reliability of this increasingly important renewable energy resource. This paper describes in detail the relevant procedure for the analysis of EL CID results at stator core joints, suggesting that an earlier technique, which involved resetting the PHASE reference, is generally unecessary with modern EL CID equipment. This paper also demonstrates that the results produced can be misleading, unless referred back to the basic reference axes.

1. INTRODUCTION

In the 1970s, incidence of serious faults in large round-rotor type electrical rotating machines, due to the failure of stator core interlamination insulation, promoted the invention of an easier way to test this aspect of these machines. The solution achieved by Sutton[1] at CERL (the research branch of the CEGB in the UK) consisted of an electromagnetic method of core insulation imperfection detection. This has become widely known as EL CID, and has been successfully established for use in relation to round rotor machines for over 30 years.

When EL CID was also applied to the stator cores of large machines of the salient-pole rotor type it was found that several anomalies often arose and, initially, these sometimes prevented a useful analysis. The associated problems were gradually identified, analysed in numerous papers by the author, and ultimately incorporated into a book[2]. Since publication of the third edition of this book, a number of additional papers have been produced.

*Independent Consultant.

Appendix 14

One problem which defied solution for many years was the analysis of EL CID results in the region of joints in stator cores. Only in recent years has the required method been adequately identified.

2. GENERAL BACKGROUND PRINCIPLES

Figure 1b identifies a fault in the insulation between the adjacent laminations of a stator core built from layers of steel punchings. Such a defect completes an electrical circuit comprising the "short" across the insulation, the adjacent laminations, and the core-build (or key) bar.

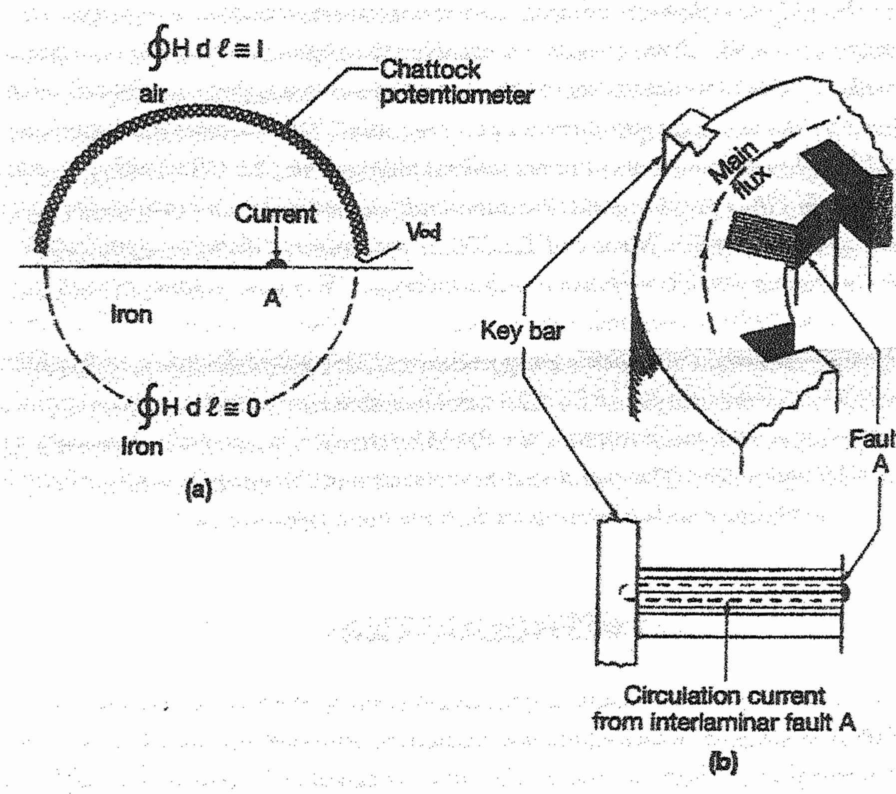

Figure 1. Basic EL CID principles (reprinted from Reference 2)

Excitation of the core, so as to induce a pulsating circumferential magnetic flux, results in flux linkage with the foregoing electrical circuit, which sets up a circulating current in accordance with Faraday's Law. At the bore of the stator core this current flows axially, i.e. at 90° to the plane of the laminations.

The circulating current is identified in Figure 1a at "A". In accordance with Ampère's Law (sometimes known as the Magnetic Circuit Law), the summation of the magnetising

Appendix 14

force (H) along any closed path around a current-carrying conductor is equal to the total current. When there are N conductors, each carrying current I, the total current is NI. Mathematically, this is stated as the line integral:

$$\oint H.dl = NI$$

Since the iron of the stator core has much greater permeance than air, the summation of H along the path in the iron is negligible, thus:

$$\oint_{iron} H.dl \approx 0$$

and the summation along the air path is effectively equal to the total current, NI, i.e.:

$$\oint_{air} H.dl \approx NI$$

This integration is conveniently achieved by the use of a special type of pick-up coil, originally devised by Chattock[3], known as a Chattock Potentiometer (so called because it measures the difference in magnetic scalar potential between its ends). The application of this device has been discussed in a further paper by Sutton[4]. The sensor comprises a long solenoid of fine wire wound on a flexible plastic former. Although the output voltage of a Chattock Potentiometer is only independent of its span for a very long current path, Sutton[5] showed that the laminar construction of stator cores caused the equipotential magnetic field lines around a relatively short current length (i.e. in an electrical short between adjacent laminations) to distort from circles to ellipses. Thus the Chattock sensor still detects a high percentage of the magnetic potential when its span is wide enough to reach the outer-most corners of adjacent teeth.

The output from the Chattock sensor is connected to an electronic package called a Signal Processor Unit (SPU). This includes a phase sensitive detector, whereby the detected signal is compared to a reference signal in order to produce an output which is readily selected to be either in phase or in quadrature with the reference signal.

Initially, it was assumed that the "in phase" component deriving from the main magnetic flux induced circumferentially around the core, and the "in quadrature" component arising from the fault current (delta), flowing in a mainly resitive circuit, substantially comprised the total signal detected by the EL CID sensor. Consequently, the simple vector diagram shown in Figure 2 was considered adequate.

Appendix 14

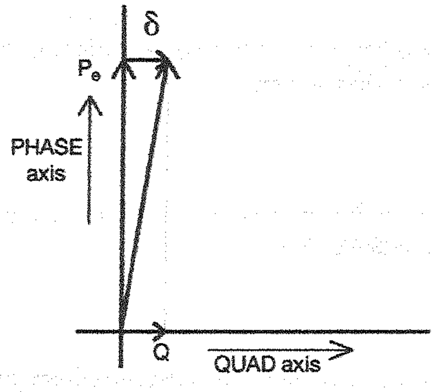

Figure 2. Basic EL CID vector diagram (reprinted from Reference 2)

3. EXTENSION OF THE EL CID VECTOR DIAGRAM

The solution of the anomalies encountered in the EL CID results from hydro generators identified a more complex electromagnetic condition at the stator bore of salient-pole electrical machines, for which it was necessary to develop a new basic vector diagram[2] (see Figure 3).

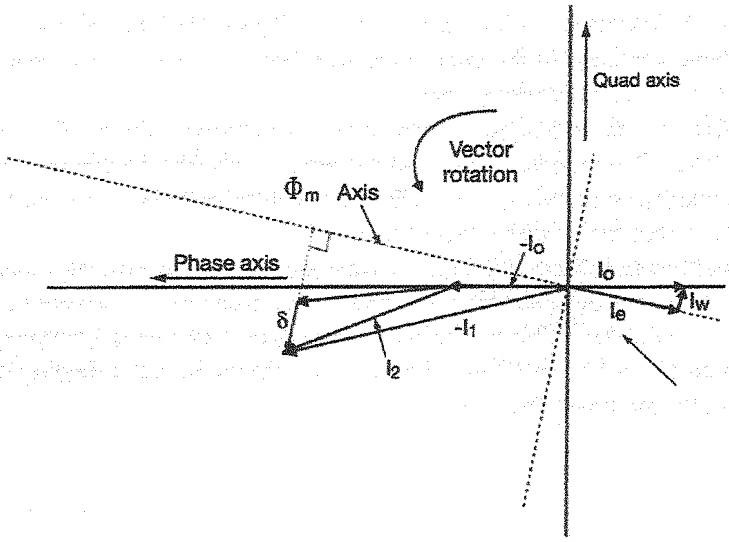

Figure 3. Extended EL CID vector diagram (reprinted from Reference 2)

Appendix 14

This extension of the vector diagram was achieved on the basis of regarding the EL CID set-up as a transformer with one, or even two, shorted secondary windings. One of these secondary windings is the circuit in which fault current is induced, as identified in Figure 1. The other secondary winding arises if the stator winding is still *in situ* and short-circuited[2].

The Chattock sensor directly detects current (i.e. delta) arising from both core interlamination degradation and the stator winding (i.e. *Ic*), which in the transformer analogy is secondary current. The subject of stator winding circulating current has been dealt with thoroughly in References 6, 7 and 8. The vector diagram is therefore drawn with reference to the secondary side of the EL CID set-up, regarded as a transformer. Thus it is necessary to reverse the phase of the primary side current, which is the excitation current (*Io*). As the EL CID phase reference is now normally set to the excitation current, there is a consequent phase shift of the vector diagram. The general direction of the stator winding circulating current (*Ic*) is that which applies for normal transformer action in a high reactance winding, but at many peripheral locations the direction will be reversed since the circulating currents must balance out throughout the winding.

It should be noted that Bertenshaw[8] subsequently published his solution to the problem, developed from a fundamental electromagnetic field point-of-view, which confirmed the aforementioned vector diagram.

4. APPLICATION OF THE EXTENDED EL CID VECTOR DIAGRAM TO CORE JOINTS

Figure 3 is the general EL CID vector diagram. This is modified to suit particular electromagnetic conditions encountered. Several of these were shown in Reference 2, and take account of virtually all the possible conditions. These included the core joint situation, which is the particular focus of this paper. The relevant form of the vector diagram is reproduced in Figure 4. Although Bertenshaw[9] also produced a version of his vector diagram with special reference to core joints, an overall resultant vector was not identified; preference being given to an understanding of the contribution to PHASE and QUAD of each component of the signal picked up by the sensor.

Support for the various forms of the EL CID vector diagram was given by the record[2] of the distribution of corresponding PHASE/QUAD values. This included results at core joints. However, derivation of the values of the circulating fault current (i.e. delta) between laminations had not been undertaken at that time. More recently the evaluation[10] of delta at the core joints of several machines was undertaken, which validates the technique, and also led to some important conclusions regarding core joint conditions generally.

In one case (Figure 5) it was possible to show the benefit of some remedial work which had been indicated as necessary from the results of both the High Flux Ring Test (HFRT) and the EL CID test, but the physical identification of the location of any particular interlamination insulation weakness was not undertaken.

Appendix 14

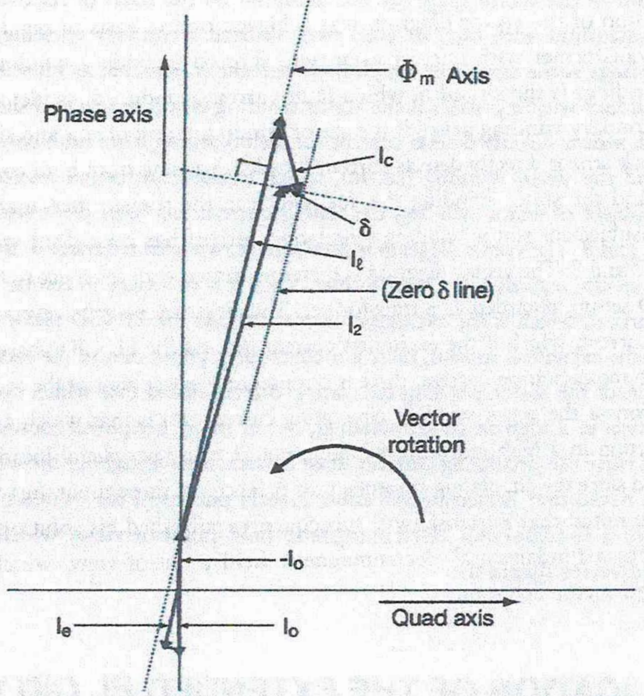

Figure 4. The EL CID vector diagram, including leakage flux from a core joint, and stator winding circulating current (reprinted from Reference 2)

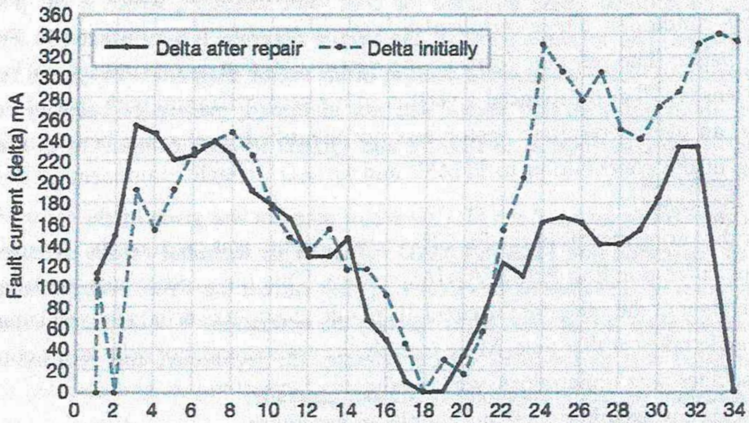

Figure 5. Comparative delta values evaluated from the results of EL CID tests before and after repair (reprinted from Reference 10)

Appendix 14

5. CORRELATION OF EL CID RESULTS WITH AN IMPOSED FAULT AT A CORE JOINT

Attention is focused in this paper on some EL CID results at a core joint published by Paley *et al*[11]. The degree of understanding at the time led to the then reasonable conclusion that the QUAD trace (Figure 6) was unusable. However, by applying Figure 4 the QUAD trace, in conjunction with the corresponding PHASE trace (Figure 6), now permits delta values along the entire length of the core at the joint to be evaluated. This leads to close identification of the location where an artificial fault had been inserted.

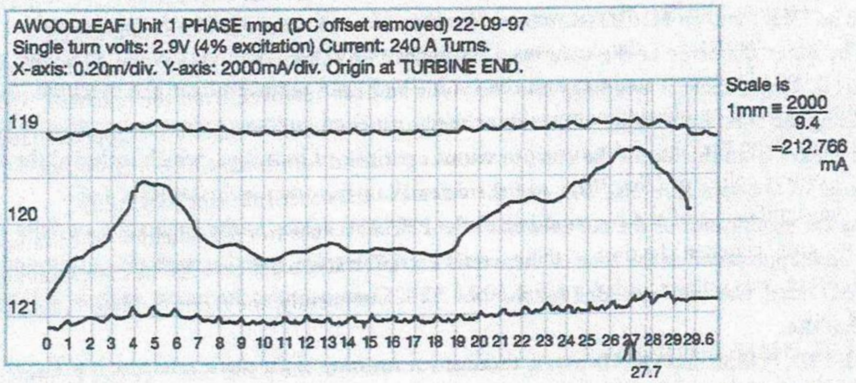

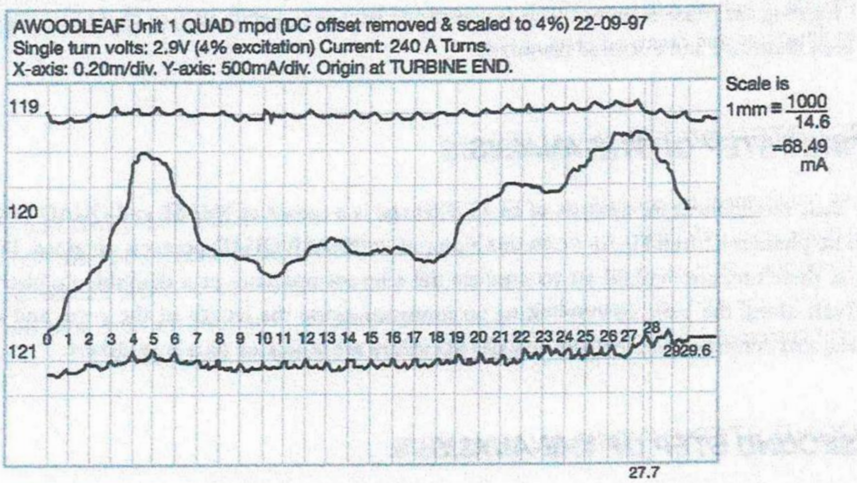

Figure 6. PHASE and QUAD traces from EL CID test at joint slot 120 after insertion of an artifical fault (reprinted from Reference 11)

Appendix 14

Details follow of the steps involved in the analysis, leading to correlation of the recorded EL CID results with the known location of the imposed fault. Hence the EL CID technique now covers every aspect of analysing stator core interlamination insulation.

6. THE GENERAL SITUATION

Prior to the EL CID test under consideration, the decision had been taken to re-stack the top two packets of one of the two sections forming the core, using some existing laminations and also some new ones. As this involved disturbing a total of about four inches at the top of the 62 inch long core, the opportunity was taken to insert artificial faults at that level before refurbishment. Both an HFRT and an EL CID test were undertaken before the remedial work commenced.

The outer diameter of the core was 190 inches (4.826m). The axis of the machine was vertical. The old stator windings and the rotor had been removed from the machine. After cleaning the core, by blasting with walnut shells, artificial faults were inserted approximately four inches from the top of the core, in various peripheral locations, which included the slot bottom of one split slot (No. 30), and the sidewall of the other split slot (No. 120).

As the significance of the contribution of the PHASE values to the evaluation of delta had not been appreciated at the time of these tests a PHASE trace, together with the corresponding QUAD trace, was only recorded for slot No. 120. Consequently, the recent analysis is limited to that slot.

EL CID, PHASE and QUAD traces, without any resetting of the phase reference (see Figure 6), were obtained and published by Paley *et al*[11]. An additional QUAD trace was also recorded after resetting the phase reference. This is considered later. The significance of phase resetting[12] has been illustrated and discussed previously.

I. FIRST STEP OF THE ANALYSIS

The basic requirement for analysis of an EL CID test is a record of PHASE and QUAD values with no phase reset (ref: Figure 6). From this a plot of PHASE/QUAD points is obtained. Both traces, therefore, are marked off to produce the relevant ordinates at a desirable number of intervals along the axis, corresponding to positions along the length of the core, and the consequent corresponding PHASE and QUAD values are tabulated on a spreadsheet.

II. SECOND STEP OF THE ANALYSIS

The next step in the analysis is to plot the PHASE/QUAD values tabulated on the spreadsheet, and to identify a line on the plot which is judged to be the reference base for delta. It is seen in Figure 4 that the signal (I_2) detected by the EL CID sensor has components arising from

Appendix 14

excitation (*Io*), flux leakage at the core split (I_ℓ), stator winding circulating current (*Ic*) and fault current (delta). At any particular slot, *Io* and *Ic* are constant along the core length. I_ℓ may vary in magnitude, but the direction is constant, being that of the main flux induced in the core. In general, delta will vary, but it will be referred to a line through the end of *Ic* and parallel to I_ℓ. This lower limit in Figure 4 defines the "zero delta line".

Determination of the location of the "zero delta line" must be done as accurately as possible. The QUAD values are relatively much smaller than the PHASE values, therefore the possibility arises of significant error when identifying the "zero delta line" from a plot with equal PHASE and QUAD scales. Consequently, an increase in the QUAD scale is desirable. For the purpose of this paper, an increase by a factor of three is convenient. To introduce an increased QUAD scale, using computer drawing facilities, the PHASE and QUAD axes have to be manipulated. First the QUAD axis is rotated clockwise through 180°, then the whole diagram is rotated through a further 90°, thus bringing the variably scaled QUAD axis vertical. For the present case, the result is shown in Figure 7.

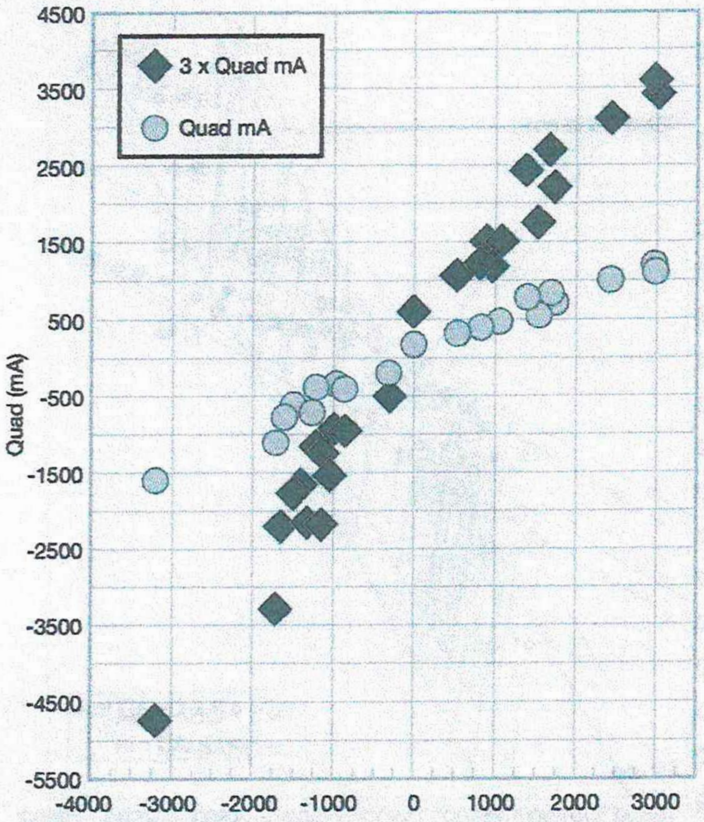

Figure 7. Spreadsheet plot of recorded PHASE and QUAD values at a core joint

Appendix 14

Figure 8 is basically a copy of Figure 7, to which has first been added the "zero delta line" for each presentation of the PHASE/QUAD plot. Due to the manipulation of the axes these "zero delta lines" now appear above the band of PHASE/QUAD values. The plot of QUAD values with an increased scale facilitates location of the "zero delta line". It can then be transferred to the original plot having equal PHASE and QUAD scales. If the fit is not considered adequate, some revision of the initial "zero delta line" location is required. In the case being considered, the fit is seen to be quite good.

After the "zero delta line" is located relative to the plot, resulting from increasing the QUAD scale (ref. Figure 8), the upper limit of delta values is a line parallel to the "zero delta line" enclosing the point, or points, of maximum delta value (ref. Figure 8).

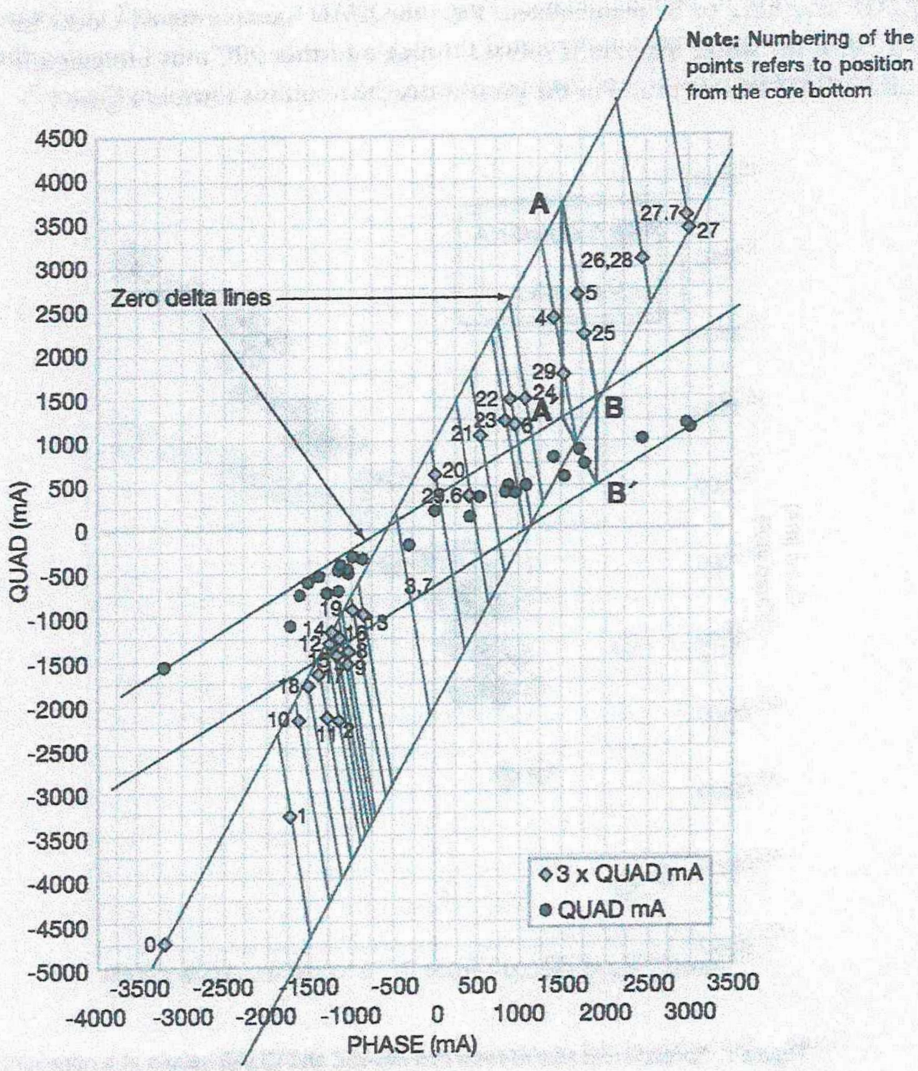

Figure 8. Plot of PHASE and QUAD values with delta lines added

III. THIRD STEP OF THE ANALYSIS

From the vector diagrams developed and reported previously[2], if the PHASE and QUAD scales are equal, the orthogonal distance between the parallel lines enclosing the PHASE and QUAD points is the maximum delta value occurring along the core length. The delta value for each point is given by the orthogonal distance to the "zero delta line".

When unequal PHASE and QUAD scales are used to maximise the accuracy of the determination of delta, the question arises as to where to draw corresponding "delta lines". The necessary relationship between the two QUAD scales has been published[13] previously, and involves construction of trapezoid *AA´B´B* (see Figure 8). Briefly, the starting point is *A* on the "zero delta line" for the *P,Q* points with the increased *Q* scale. The line *AA´* is drawn parallel to the QUAD axis, to *A´* on the "zero delta line" for *P,Q* points having equal scales. The line *A´B´* is then drawn orthogonally between the boundary lines for the *P,Q* points having equal scales. From *B´* a further line is drawn parallel to the *Q* axis to cut the boundary line of the *P,Q* points with the increased *Q* scale at *B*. The line *BA* then provides the required direction of the "delta lines", i.e. the lines from which the magnitude of delta values are derived.

IV. FOURTH STEP OF THE ANALYSIS

The appropriate delta value for each *P,Q* point is evaluated from the length of the "delta lines" drawn from each *P,Q* point, to the "zero delta line" in the direction as determined in Step 3. The delta line length was originally considered to give the delta value directly, after only a simple division by the increased QUAD scale factor (*k*, say), and application of the appropriate scale factor for converting from units of length (mm, say) to units of current (mA). If the value is determined directly with a ruler, this is the only derivation possible, but gives only an approximate delta value.

If, however, use is made of the end points of each "delta line" from the computer provided grid, followed by application of the Pythagoras theorem, it is possible to take full account of the increased QUAD scale factor (*k*). This is achieved by dividing the QUAD values by *k*, before applying the Pythagoras theorem, thus producing a length related to the original equal scales of PHASE and QUAD values, as required. Again, the length of line determined must be converted to mA by the scale factor derived by relating the equal scales to the units of the computer grid. This procedure gives the delta(3)(2nd calculation) points.

Approximate delta values were obtained as a) "delta(1)(measured)" – from direct measurement, and b) "delta(2)(1st calculation)" – by application of the increased QUAD scale factor after use of the Pythagoras theorem. Comparison of these values when plotted in Figure 9 showed that they were indistinguishable.

The delta values after proper correction for the increased QUAD scale factor are also plotted as points "delta(3)(2nd calculation)", which shows that the degree of approximation is not large. Comparison of actual values shows that there is no more than 10% error.

Appendix 14

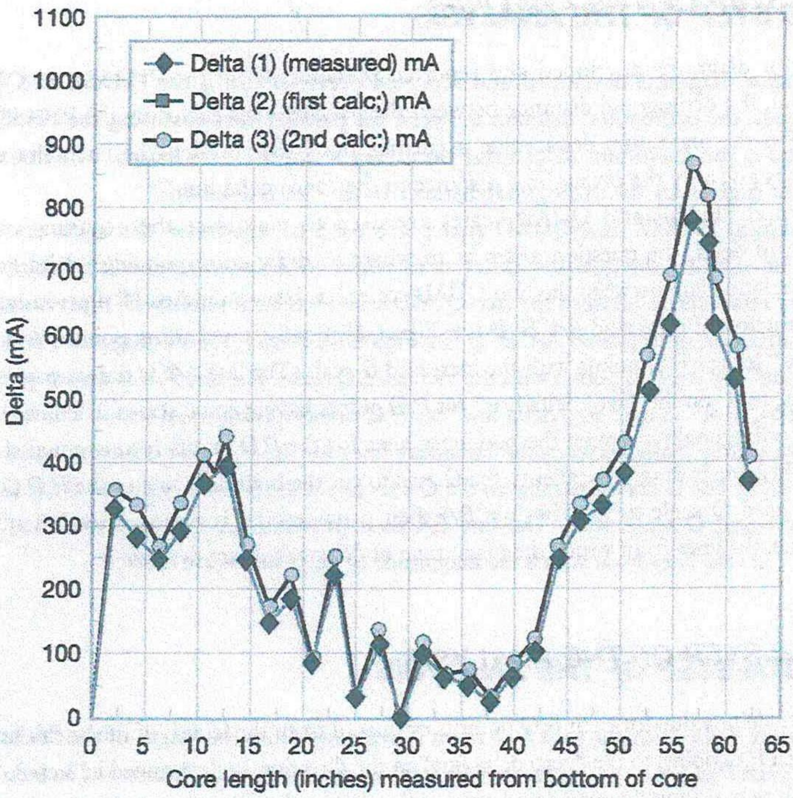

Figure 9. Variation of delta along the core length at a joint slot

V. FIFTH STEP OF THE ANALYSIS

The crucial aspect of this analysis of the EL CID results at a core joint, after an artificial fault had been applied, is the degree of correlation achieved. From Figure 9 this is shown to be remarkably good. Although the pronounced spike of delta values along the core length, from the imposed fault, appears to be not quite coincident with the reported fault location of four inches from the top of the core (position 27.7, top righthand corner in Figure 8), the difference is less than 2½% of the core length. Moreover, from other EL CID traces published by Paley *et al*[11] it is seen that there is some inconsistency in the length of the traces. This throws doubt on the length of any particular trace having exact correspondence with the core length.

Thus the exercise can be seen to have been successful in verifying the reliability of the EL CID test procedure, even when applied in the difficult magnetic field conditions arising at a core joint.

The actual values at core joints may be influenced by factors which are additional to the degree of deterioration of the interlamination insulation, such as the effect of the cut edges

Appendix 14

exposed at a core joint, as previously identified[10]. The important factor, therefore, in assessing the core condition at core joints, is the distribution of delta along the core length. The ability of EL CID to indentify this has been amply demonstrated.

7. CONSIDERATION OF EL CID RESULTS OBTAINED WITH PHASE RESET

In the paper by Paley *et al*[11], a record of the EL CID QUAD trace after resetting the Phase Reference was also included. The degree of Phase Reset is not recorded, but reference is made to there being a phase shift of about 25° at the core joints relative to the central core. An assumption of a 25° Phase Shift has therefore been made. The QUAD values relative to the reset PHASE axis are obtained by simple geometry from:

$$Q_{reset} = Q_{original}.\cos(\text{theta}) - P_{original}.\sin(\text{theta}),$$
$$\text{where theta} = \text{PHASE reset angle}$$

Figure 10 shows the calculated values of Q_{reset}, and also the values obtained by measurement on the published QUAD trace obtained after resetting the PHASE Reference. The agreement of the QUAD value characteristic along the core is generally good. Discrepancies, which occur, are probably due to several factors: a) correlation of the position along the core is difficult, due to the traces with and without Phase Reset possibly being subject to slight variations in paper stretch, b) the length of trace varies for the published recorded traces, resulting in some slight uncertainty regarding coverage of the total core length, and c) the recorded trace values fluctuate considerably over short distances along the core. Consequently a minor error in position may result in a significantly different trace value.

Appendix 14

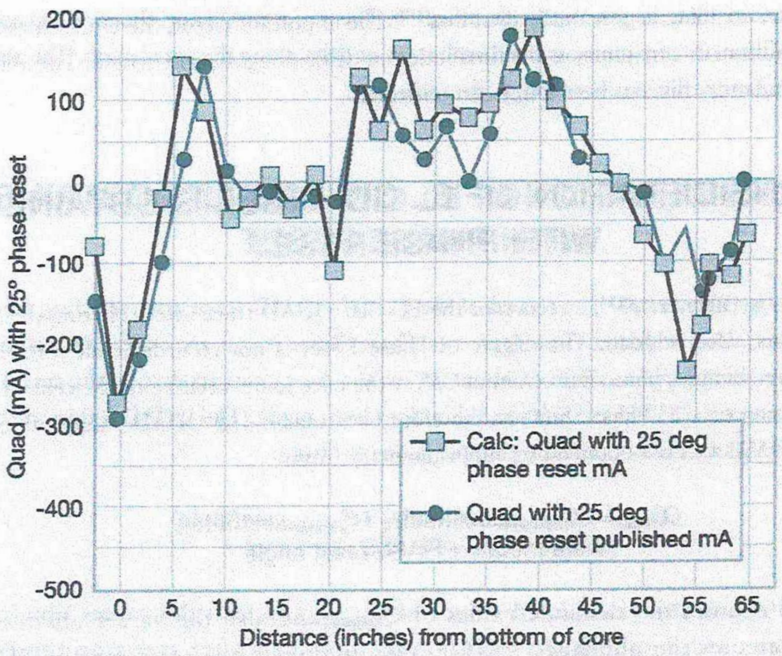

Figure 10. QUAD values with Reset PHASE axis

8. ASSESSMENT OF EL CID RESULTS OBTAINED WITH PHASE RESET

It is seen that the reset PHASE axis results in the QUAD trace being located approximately evenly each side of the new PHASE axis. This reduces considerably the magnitude of the QUAD values to be recorded. In the early days of EL CID this was an advantage as the facilities for recording the QUAD signal were limited, but this has not been a restriction for quite some time.

The recorded QUAD values along the core length with PHASE Reset do not identify the location of the artificial fault. The significance of deviations along the core is not clear from this presentation of QUAD values. From the latest EL CID vector theory[2] it is evident that QUAD values alone are insufficient for fault identification.

If QUAD and PHASE values are obtained with the PHASE axis reset then it is essential to obtain corresponding values relative to the basic axes, as previously discussed[12].

Appendix 14

9. CONCLUSION

It has been shown, by application of the procedure laid out in this paper, that EL CID results obtained at a stator core joint which were previously considered to be unusable, are now amenable to analysis, by which a fault in the interlamination insulation can be clearly identified.

The condition of the core insulation for slot 120 elsewhere than where the artifical fault was introduced is not reported by Paley *et al*[11]. It has been suggested previously[10] that the distribution of circulating interlamination fault current (delta) at a core joint is of greater significance than its actual value in the identification of defective insulation. Hence there appears to be some indication that the state of the interlamination insulation near the bottom of the core was not good. But, as also identified earlier[10], the magnitude of delta at core joints may well be exaggerated due to factors other than the insulation condition. Values of the order of 400mA at core joints have been considered as possibly acceptable, but would merit investigation. The distribution of delta in Figure 9 clearly shows, however, a focus upon the vicinity close to the imposed fault.

It is undesirable, and unecessary, to introduce resetting of the PHASE reference, which was originally undertaken as a means of reducing the QUAD signal, thereby enhancing accuracy. However, it has been shown that switching between the axes, with and without Phase resetting, can be readily achieved.

Footnote

The major references in this paper are to the author's own work. An extensive search of previous literature has failed to find any other record of EL CID tests applied to core joints in large salient-pole generators.

It is interesting to note, however, two references which relate in some measure to the work reported above. Bertenshaw & Smith[14] identified that the correlation between the temperature at an artificial fault and the EL CID signal is similar to that obtained for a situation involving core degradation. Nevertheless, it has been identified above that the EL CID detected circulating fault current (delta) at a core joint may be falsely high due to the effect of the cut edges of laminations. Consequently, the EL CID signal at core joints should be regarded with reserve, and the distribution of delta along the core length taken as the guide to the condition of the interlamination insulation.

Bertenshaw *et al*[15] refer to the EL CID QUAD readings recorded in their investigation of stator core faults in large machines as a direct indication of delta. The development of the EL CID vector diagram by the author[2] shows in Figure 11 that this is approximately true only in the specific circumstances of there being no core joints, no stator winding, and no rotor *in situ*.

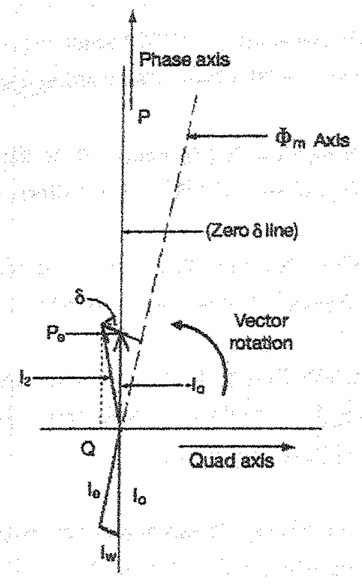

Figure 11. EL CID vector diagram in the absence of core joints, stator winding and rotor (reprinted from Reference 2)

Appendix 14

ACKNOWLEDGEMENTS

Grateful thanks are expressed to Mr D R Bertenshaw, who facilitated the search for EL CID literature.

REFERENCES

[1] Sutton, J, 'EL CID: An Easier Way to Test Stator Cores', *Electrical Review*, Vol 207, Issue 1, pp33-37 (1980).

[2] Ridley, G K, '*EL CID – Application and Analysis*', Edition 3, ADWEL International (2007).

[3] Chattock, A P, 'On a Magnetic Potentiometer', *Philosophical Magazine*, Vol 24, p94 (1887).

[4] Sutton, J, 'History of EL CID and Fundamentals', *Proceedings*, EPRI International Conference on Motor and Generator Predictive Maintenance & Refurbishment (1995).

[5] Sutton, J, 'Theory of Electromagnetic Testing of Laminated Stator Cores', *Insight*, Vol 36, Issue 4, pp246-251 (1994).

[6] Ridley, G K, 'The Impact of Stator Winding Circulating Current on EL CID Results', *International Journal on Hydropower & Dams*, Vol 11, Issue 1, pp68-73 (2004).

[7] Bertenshaw, D R & Sutton, J, 'Application of the EL CID Test with Circulating Currents in Stator Windings', *Proceedings*, Inductica, Berlin, Germany, pp128-134 (2004).

[8] Sutton, J, Chapman, B & Bertenshaw, D R, '*Effects of Stator Windings on EL CID Measurements*', EPRI, V4.3 (2004).

[9] Bertenshaw, D R, 'Analysis of Stator Core Faults – a Fresh Look at the EL CID Vector Diagram', *Proceedings*, Hydropower 2006 (on CD).

[10] Ridley, G K, 'Evaluating Interlamination Circulating Current at Core Joints in Large Machine Stators', *International Journal on Hydropower & Dams*, Vol 15, Issue 6, pp106-114 (2008).

[11] Paley, D, McNamara, B, Mottershead, G, & Onken, S C, '*Verification of the Effectiveness of EL CID on a Hydrogenerator Stator Core*', ADWEL International, Canada & UK, (1998).

Appendix 14

[12] Ridley, G K, 'Consequences of Resetting the PHASE Reference for EL CID Tests', *International Journal of Hydropower & Dams*, Vol 19, Issue 4, pp84-88 (2012).

[13] Ridley, G K, 'Increased Accuracy in Determining Interlamination Fault Current at Stator Core Joints', *International Journal on Hydropower & Dams*, Vol 16, Issue 6, pp104-107 (2009).

[14] Bertenshaw, D R, & Smith, A C, 'Field Correlation between Electromagnetic and High Flux Stator Core Tests', *Proceedings*, 6th IET International Conference on Power Electronics, Machines & Drives (PEMD) (2012).

[15] Bertenshaw, D R, Smith, A C, Ho, C W, Chan, T, & Sasic, M, 'Detection of Stator Core Faults in Large Electrical Machines', *IET Electrical Power Applications*, Vol 6, Issue 6, pp295-301 (2012).